

# The Impact of Domestic Electric Vehicle Charging on Electricity Networks



Constance Crozier  
St Hugh's College  
University of Oxford

A thesis submitted for the degree of  
*Doctor of Philosophy*  
Trinity 2019

## Acknowledgements

Firstly, I would like to express my sincere gratitude to my supervisor Prof. Malcolm McCulloch. His support and guidance throughout this research have been invaluable to me.

In addition to my formal supervisor, I would like to thank my informal mentors Dr. Dimitra Apostolopoulou and Dr. Thomas Morstyn. Dimitra, thank you for your support and guidance at the start when I didn't know what I was doing. Thomas, thank you for reading more drafts than I care to think about – your continual optimism over the past two years has really helped me.

I am indebted to Jaguar Land Rover for sponsoring this research, particularly to Nick Green who helped get the project off the ground in the first couple of years.

I am also grateful to the rest of my colleagues at EPG for making the last few years so enjoyable. Particularly to: Matt, for three years of collaboration (and/or arguments); Anna, for mix of DPhil and life advice; Liyang, for tolerating my constant distractions; Jorn, for answering my endless questions about batteries.

Last but not least, my thanks go to my friends and family for their emotional support during this process, and for not questioning my decision to stay at university.

# Abstract

This thesis investigates the impact that home charging of a large private fleet of electric vehicles would have on the power system.

A large multi-regional travel survey dataset is used to model vehicle use and charging spatially heterogeneously, and a selection of representative network models are used to assess the impact of charging on system operation. A stochastic data-driven model is proposed to model uncontrolled charging of vehicles, and convex optimisation is used to calculate the optimal smart charging strategy.

The power system is commonly broken down into the generation, transmission, and distribution systems. The operation of each of these systems will be impacted by the addition of EV charging to residential networks. A variety of objectives have been proposed for smart charging, each of which would protect the system in a different way. Existing research tends to focus on a single part of the system, and considers only the smart charging objective that most benefits that part of the system. Here, the three systems are modelled simultaneously, and a large range of smart charging objectives are investigated.

The value of explicit loss minimising smart charging is quantified, compared to a simpler and more standard load flattening algorithm. These results are used to propose a novel optimisation formulation which reduces losses without requiring extensive network information. The value of bi-directional smart charging is also quantified compared to uni-directional smart charging, in order to investigate the viability of residential vehicle-to-grid.

It is demonstrated that it is not possible to optimise the transmission level and distribution level systems simultaneously, and the penalty of only optimising for one is quantified. A method for finding a compromising solution between both system levels is proposed, which exploits the sections of the distribution where components are over-specified.

Two specific case studies are investigated. The majority of the analysis in the thesis is based on the GB power system, however the Texas system is also presented as a comparative case study.

# Contents

<b>1</b>	<b>Introduction</b>	<b>4</b>
1.1	Context . . . . .	6
1.1.1	The Energy Trilemma . . . . .	6
1.1.2	Power Systems . . . . .	7
1.1.3	Electric Vehicle Charging Infrastructure . . . . .	10
1.1.4	Smart Charging . . . . .	13
1.2	Scope . . . . .	15
1.3	Case Studies . . . . .	17
1.4	Thesis Contributions & Associated Publications . . . . .	18
1.5	Thesis Structure . . . . .	21
<b>2</b>	<b>Literature Review</b>	<b>22</b>
2.1	Overview . . . . .	22
2.1.1	Reflections . . . . .	29
2.2	Modelling Methods . . . . .	30
2.2.1	Vehicle trips and energy usage . . . . .	30
2.2.2	Vehicle charging . . . . .	32
2.2.3	Reflections . . . . .	34
2.3	Smart Charging Strategies . . . . .	35
2.3.1	Hierarchy . . . . .	35
2.3.2	Smart Charging Objectives . . . . .	37
2.3.2.1	Minimum Charging Cost . . . . .	37
2.3.2.2	Transformer Protection . . . . .	39
2.3.2.3	Power Quality . . . . .	40
2.3.3	Other Metrics . . . . .	43
2.3.4	Reflections . . . . .	43
2.4	Gap Analysis . . . . .	44
<b>3</b>	<b>Modelling Vehicle Use</b>	<b>47</b>
3.1	User Travel Behaviour . . . . .	48
3.1.1	Data sources . . . . .	48
3.1.1.1	National Travel Surveys . . . . .	49
3.1.1.2	EV Trial Data . . . . .	52
3.1.2	Cluster Analysis . . . . .	53
3.1.2.1	Algorithm . . . . .	54
3.1.2.2	Resulting Clusters . . . . .	60
3.1.3	Comparing the Electric and Conventional Fleets . . . . .	63
3.2	EV Sales Projection . . . . .	65

3.3	EV Energy Consumption . . . . .	67
3.3.1	Tank-to-wheel Model . . . . .	68
3.3.2	First-order conversion . . . . .	73
3.3.3	Concluding Remarks . . . . .	74
<b>4</b>	<b>Modelling Vehicle Charging</b>	<b>77</b>
4.1	Uncontrolled Charging . . . . .	78
4.1.1	Standard Assumption . . . . .	78
4.1.2	Stochastic Model . . . . .	79
4.1.2.1	Model Validation . . . . .	84
4.2	Controlled Charging . . . . .	87
4.2.1	Flattening Load . . . . .	87
4.2.2	Minimising Peak Load . . . . .	89
4.2.3	Multi-Phase Network Loss Minimisation . . . . .	91
4.2.3.1	Formulation Validation . . . . .	94
4.3	New Controlled Charging Strategies Considering Phase Balancing and Converter Losses . . . . .	96
4.3.1	Phase Balancing for Loss Reduction . . . . .	97
4.3.2	Incorporating Varied Charger Efficiency . . . . .	98
4.4	Concluding Remarks . . . . .	105
<b>5</b>	<b>Impacts on the Generation &amp; Transmission Systems</b>	<b>107</b>
5.1	Generation System . . . . .	108
5.1.1	Matching supply and demand . . . . .	110
5.1.2	Consumption of Renewables . . . . .	114
5.1.2.1	Maximising use of renewables . . . . .	116
5.2	Transmission System . . . . .	120
5.3	Comparative Case Study . . . . .	123
5.4	Concluding Remarks . . . . .	126
<b>6</b>	<b>Impacts on the Distribution System</b>	<b>129</b>
6.1	Network Loading . . . . .	130
6.1.1	Linear Regression Model . . . . .	133
6.2	Network Constraints . . . . .	135
6.2.1	Rochdale Case Study . . . . .	137
6.2.2	Geographic Variation . . . . .	139
6.3	Comparing smart charging objectives . . . . .	142
6.3.1	Loss minimisation . . . . .	143
6.3.1.1	IEEE European Low Voltage Test Feeder . . . . .	143
6.3.1.2	Sensitivity Analysis . . . . .	147
6.3.2	The case for bi-directional charging . . . . .	151
6.4	Comparative Case Study . . . . .	154
6.5	Concluding Remarks . . . . .	160
<b>7</b>	<b>Conflict Between System Levels</b>	<b>162</b>
7.1	Flattening at a Single Level . . . . .	163
7.2	Multi-objective smart charging . . . . .	165
7.3	Concluding Remarks . . . . .	171

<b>8</b>	<b>Conclusions</b>	<b>173</b>
8.1	Future Work . . . . .	178
<b>A</b>	<b>Line Thermal Limits</b>	<b>180</b>
A.1	Heating in overhead lines . . . . .	180
<b>B</b>	<b>Test Networks</b>	<b>184</b>
B.1	GB Representative Networks . . . . .	184
B.2	Test Feeders . . . . .	186
	<b>Bibliography</b>	<b>188</b>

# List of Figures

1.1	The number of plug-in electric vehicles in the UK with time. . . . .	5
1.2	The impacts to the power system of additional load from EV charging considered in this thesis. . . . .	10
1.3	The percentage of the UK private vehicle fleet at common locations throughout a weekday. . . . .	12
2.1	A visualisation of the literature. . . . .	24
3.1	Three example vehicle usage profiles from the NTS data. Time of day is on the horizontal axis, weekday on the right, and blue indicates that the vehicle is in use. . . . .	50
3.2	The geographic and rural-urban variation in the NTS sampled households.	51
3.3	A comparison of the driving behaviour exhibited in the two travel surveys.	52
3.4	An example vehicle usage profile from the MEA data. Date is on the horizontal axis, and time on the vertical. Red shows vehicle use and blue shows charging. . . . .	53
3.5	An example vehicle usage profile from the Texas Pecan Street data. Date is on the horizontal axis, and time on the vertical. Shaded areas shows charging. . . . .	54
3.6	(l) three days of a NTS vehicles' usage; (r) the corresponding feature vectors.	58
3.7	Three feature vectors that are equidistant, despite (a) and (b) being similar.	59
3.8	The filtered feature vectors, (a) and (b) are now much closer than (c). . .	59
3.9	The variation of sum of squares with number of clusters for both the weekday and weekend datasets. . . . .	60
3.10	The average speed profile of the vehicles in each cluster. The lines show the mean values, and the shaded areas cover the 90% confidence interval. There is no significance to the ordering of the clusters. . . . .	61
3.11	The variation in cluster composition throughout the week, and the probability a vehicle changes usage cluster the net day. U indicates the vehicle was unused. . . . .	62
3.12	The clusters found from the Texas NHTS data, analogous to Figure 3.10	62
3.13	The variation of cluster composition of the Texas vehicle with weekday. .	63
3.14	A comparison of the cluster composition of the Texas and UK clusters. .	63
3.15	A comparison of the trip frequency, distance, and timings of vehicles from the NTS and MEA data. . . . .	64
3.16	A comparison of the cluster composition of the NTS and MEA data. . .	65
3.17	Several examples of s-curves with different parameters. . . . .	66
3.18	The s-curve fitting process for one example area. . . . .	66
3.19	The projected regional penetration of EVs. . . . .	67

3.20	The two standard drive cycles used in the EPA testing. . . . .	70
3.21	A quantile-quantile plot of the vehicle model performance for 50 different EVs over the two recorded drive cycles . . . . .	71
3.22	Predicted fuel economy versus speed for three difference vehicles. The markers show the point of maximum efficiency. . . . .	72
3.23	An example use of the tank-to-wheel model from GPS data. . . . .	72
3.24	Three drive-cycles representative of European driving output from the ARTEMIS project. . . . .	74
4.1	The % probability that a charge will follow the completion of a journey, as a function of both time and SOC, for each vehicle use cluster. . . . .	81
4.2	The % probability that a charge will start independent of a journey, as a function of both time and SOC, for each vehicle use cluster. . . . .	82
4.3	A flow chart describing the charging model simulation process. . . . .	83
4.4	The starting charging probability distribution predicted from the MEA usage with both the proposed model and standard assumption, compared to the ground truth. . . . .	85
4.5	Aggregated charging of 50 households' vehicles under: (a) the assumption that charging always begins after a vehicle's final journey, and (b) the proposed model. The results are shown both using a single set of vehicles (top) and with a varied set of vehicles (bottom). The shaded area covers the 90% confidence interval. . . . .	86
4.6	Relative voltage error $\epsilon_V$ for three linearisations $\mathbf{M}_g$ , with a uniform demand $\kappa$ assigned to each residential load (with a fixed power factor). The small error shows the linear models have good accuracy. . . . .	92
4.7	A simplified 2 bus EV charging scenario. . . . .	95
4.8	Variation of the smart charging objectives in a 2-bus problem. The loss minimization plot shows both the true contours (white) and those obtained from the model (cyan). Darker colours indicate lower losses, and the minima are shown in red. . . . .	96
4.9	The variation of charger efficiency with power requested. The solid line represents the average values and the shaded area covers the range observed. . . . .	99
4.10	The power into the EV battery and drawn from the grid under three cases described in Table 4.3. . . . .	102
4.11	The total losses due to the EV charging under the three cases described in Table 4.3, broken down into distribution system and charging losses. . . . .	103
4.12	The total feeder load at 1 and 30 minute resolution under both the continuous and discrete schemes. . . . .	104
4.13	The continuous optimal profiles and discrete approximations of two random vehicles from the simulation. . . . .	105
5.1	The national demand profile on a high-use week day with no charging, controlled and uncontrolled charging of a 100% electric fleet of vehicles. For uncontrolled charging (a) shows charging after final journey, (b) shows charging using proposed model. . . . .	111
5.2	Demonstration of example curves obtained from each stage in the approximate control algorithm. . . . .	113
5.3	The accuracy with which the heuristic method proposed approximates the optimal controlled charging at the national scale. . . . .	114

5.4	The generation capacity and fuel mix in the UK on a high and low renewable production day in 2018, with fuels ordered according to preference. The line shows the national demand on that day. . . . .	115
5.5	The best and worst case percentage of electricity supplied by renewables for each charging regime in the UK. . . . .	116
5.6	The solar generation as a percentage of installed capacity throughout the year in the UK. Solid lines show average values and the shaded areas cover the 70% and 90% confidence intervals. . . . .	118
5.7	Total demand with stochastic smart charging. The dotted lines bound the demand minus solar generation covered in all scenarios, and the blue shows the total net demand once EV charging has been added in all scenarios. Solid lines show average values and the shaded areas cover the 70% and 90% confidence intervals. . . . .	119
5.8	A reduced model of the UK transmission network under uncontrolled charging peak load; (a) shows the location of the grid supply points, and the amount of EV and total demand at each; (b) shows the % of each line's rated loading being used. . . . .	121
5.9	The maximum % loading of each line high-voltage when the single largest component fails. . . . .	122
5.10	The Texas demand profile on a high-use week day with no charging, controlled and uncontrolled charging of a 100% electric fleet of vehicles. For uncontrolled charging (a) shows charging after final journey, (b) shows charging using proposed model. . . . .	124
5.11	The generation capacity and fuel mix in Texas on a high and low renewable production day in 2018, with fuels ordered according to preference. The line shows the national demand on that day. . . . .	125
5.12	The best and worst case percentage of electricity supplied by renewables for each charging regime in Texas. . . . .	126
6.1	The regional variation in ADMD (kW) predicted for each charging scenario.	132
6.2	The predicted percentage increase in ADMD in Oxfordshire as a result of 100% domestic EV charging. . . . .	136
6.3	The total power demand on the network under each charging scheme. The solid line shows the average, and the shaded area covers the 90% confidence interval. The red dotted line shows the transformer load limit. . . . .	138
6.4	The total resistive losses for each scheme. The blue line shows the median value, the box covers 50% of values, and the whiskers the total range. . .	139
6.5	The average, lowest and highest voltages in the network throughout the day under each scheme. The solid lines show the median value and the shaded area covers the 90% confidence interval. The red dotted line shows the voltage lower bound. . . . .	139
6.6	The increased likelihood of violating distribution network constraints in the UK, for charging of a 100% EV fleet and in 2030. . . . .	141
6.7	The areas most likely to require upgrades. . . . .	142
6.8	Percentage of networks expected to have violations with time. . . . .	142
6.9	The total load on the 55 bus network, without EV charging and under three different charging scenarios. The solid lines show the median load over the simulations and the shaded area covers the 90% confidence interval.	144

6.10	The energy losses per household experienced under the five scenarios. The blue line shows the median, the box covers the interquartile range, and the whiskers cover the total range. The dotted line aids comparison against the loss minimising median. . . . .	145
6.11	The test network under each EV charging regime, where the line colours show the average phase imbalance. Single phase lines are grey. . . . .	146
6.12	The average losses per length in each branch of the network under load flattening + phase balancing when compared to loss minimising. . . . .	147
6.13	The reduction in losses, per household with an EV, achieved by minimising losses rather than flattening load, against EV penetration. The solid line is the median, and the shaded area covers the inter-quartile range. . . . .	148
6.14	The reduction in losses per household achieved by each scheme compared to flattening load, for various seasons. The thick lines shows the medians, the box covers 50% of the values, and the lines the total range. . . . .	149
6.15	A comparison between the proposed smart charging schemes and load flattening for 9 different feeders, described in Table 6.3. . . . .	150
6.16	The additional reduction in peak demand achieved by bi-directional over uni-directional smart charging in the UK, varying with EV penetration. The solid lines show the average and the shaded area covers the 90% confidence interval. . . . .	153
6.17	The increase in total losses and those just in the distribution system using bi-directional charging compared to uni-directional. The lines show the average values and the shaded areas cover the 90% confidence interval. . . . .	154
6.18	The total power demand on the network under each charging scheme. The solid line shows the average, and the shaded area covers the 90% confidence interval. . . . .	156
6.19	The total resistive losses for each scheme. The blue line shows the median value, the box covers 50% of values, and the whiskers the total range. . . . .	157
6.20	The average, lowest and highest voltages in the network throughout the day under each scheme. The solid lines show the median value and the shaded area covers the 90% confidence interval. . . . .	157
6.21	The additional reduction in peak demand achieved by bi-directional over uni-directional smart charging in Texas, varying with EV penetration. The solid lines show the average and the shaded area covers the 90% confidence interval. . . . .	158
6.22	An example of total feeder load under both charging schemes. The dotted line shows the demand before EV charging was added, the solid line shows the total load with optimal G2V charging, and the dotted line shows optimal V2G charging. . . . .	159
6.23	The increase in total losses and those just in the distribution system using bi-directional charging compared to uni-directional. The lines show the average values and the shaded areas cover the 90% confidence interval. . . . .	159
7.1	The GB national demand profile throughout the year with uncontrolled charging, and controlled charging if load is flattened in residential distribution networks. . . . .	164

7.2	The LV network loading from the case study section 6.2.1, but where the controlled charging scenario represents flattening load at the transmission level. . . . .	165
7.3	The expected number of distribution constraint violations with uncontrolled charging, and charging controlled at either the distribution (D) or transmission (T) level. . . . .	165
7.4	The cumulative allowable increase in LV network peak demand without transformer violations. . . . .	167
7.5	The heuristic algorithm steps. . . . .	168
7.6	The total residential load in three example local authorities with and without the proposed controlled charging. The percentage of allowable overshoot in peak demand is shown in brackets in the title of each subfigure. . . . .	170
7.7	The national load profile under the proposed controlled charging scheme, broken down into domestic, industry, and charging load. . . . .	170
A.1	A diagram of the idealised overhead line. . . . .	180
A.2	The relationship between cable parameters that determines whether a voltage or thermal limit occurs first. The shaded area shows lines for which voltage limits are the constraints. The red dashed lines show the range of available cable diameters that are used in LV distribution networks. . . . .	183
B.1	The test networks used. Blue markers show the household locations and the black marker shows the substation position. . . . .	185
B.2	The transformer ratings of networks with varying numbers of households.. . . .	186
B.3	The test feeders considered. Blue markers show the household locations and the black marker shows the substation position. . . . .	187

# List of Tables

1.1	The energy security and overall trilemma ranks of 26 European countries, ordered by their 2018 EV sales. . . . .	7
1.2	Voltage classifications used in this thesis. . . . .	8
1.3	A description of the types of charger currently available in the UK. *Approximate time taken to charge a 30 kWh battery from 0-80%. . . . .	11
1.4	A selection of typical modern household appliance loads, compared with EV charging loads. . . . .	13
2.1	A summary of the referenced smart charging algorithms. C = minimum cost, P = minimum peak load, F = flattened load, L = minimum losses, B = balanced phases, E = maximum charging. . . . .	36
3.1	Example vehicle-day from data and corresponding un-normalised features. . . . .	57
3.2	The average distance travelled by each cluster (miles) . . . . .	65
3.3	Nissan Leaf Model Parameters . . . . .	71
3.4	Consumption per mile of common EV models for each drive-cycle. . . . .	75
4.1	The efficiency values assumed for each power. . . . .	100
4.2	Calculated distribution losses for each charging power. $L$ uses $\eta_c$ from Table 4.1, while $L_0$ assumes a $\eta_c=90\%$ . . . . .	101
4.3	A summary of the three cases considered. . . . .	102
5.1	The GB nameplate generation capacity . . . . .	112
5.2	The scenarios created for the stochastic optimisation. . . . .	119
5.3	The nameplate generation capacity in Texas. . . . .	124
6.1	A summary of the variables used. . . . .	133
6.2	The mean and standard deviation of the variables, used to normalise. . . . .	134
6.3	The daily losses in each of the networks considered. . . . .	150
7.1	A summary of the effects of each charging scheme assuming that all EV demand is met. . . . .	171

# Nomenclature

<b>a</b>	Linear power flow model bias (V)
$c_j$	Binary random variable modelling whether an after journey charge begins
$c_i$	Binary random variable modelling whether an independent charge begins
$d$	Binary random variable modelling whether it is a weekday or weekend
$E$	Charging energy requirement (Wh)
$f_0$	Constant coast-down coefficient (N)
$f_1$	Linear coast-down coefficient ( $\text{Nsm}^{-1}$ )
$f_2$	Squared coast-down coefficient ( $\text{Ns}^2\text{m}^{-2}$ )
<b>h</b>	Household load (W)
$\mathcal{H}_x$	The set of households on phase $x$
<b>i</b>	Node currents (A)
$k$	Random variable modelling vehicle usage cluster
$K$	Total number of clusters
$L$	Total energy lost (Wh)
$m$	Mass of the vehicle (kg)
$\mathbf{M}_y$	Linear power flow model load weights ( $\text{VW}^{-1}$ )
$N_b$	Total number of buses on the network
$N_h$	Total number of households
<b>p</b>	Real power injected (W)
$P_{max}$	Maximum allowable charging power (W)
$P_0$	Constant drive-train losses (kW)
<b>q</b>	Reactive power injected (VAR)
<b>s</b>	Power injections into the nodes (VA)

$s$	Random variable modelling vehicle state of charge
$t$	Random variable modelling time
$T$	Total number of time intervals
$\mathbf{v}$	Node voltages (V)
$\mathbf{x}$	Vehicle load (kW)
$\mathbf{Y}$	Admittance matrix ( $\Omega^{-1}$ )
$\Delta t$	Size of each time interval (mins)
$\eta_c$	Charging efficiency
$\eta_d$	Discharging efficiency
$\eta_v$	Drivetrain efficiency
$\bar{\tau}$	Time interval in which the vehicle departs
$\underline{\tau}$	Time interval in which the vehicle arrives

## Notation

$\cdot^*$	Complex conjugate
$\cdot^{(j)}$	Belonging to household $j$
$\cdot^{(k)}$	Quantity at node $k$
$\cdot_{\mathbf{t}}$	Quantity at time interval $t$
$p(a   b)$	Probability of $a$ given $b$

# Abbreviations

ADMD	After diversity maximum demand
DNO	Distribution network operator
EV	Electric vehicle
G2V	Grid-to-vehicle
GPS	Global positioning system
LF	Load flattening
LM	Loss minimising
LV	Low voltage
PB	Phase balancing
PDF	Probability distribution function
PV	Photovoltaics
QP	Quadratic program
MEA	My electric avenue
MV	Medium voltage
NHTS	National household travel survey
NTS	National travel survey
SOC	State of charge
TOU	Time of use
TSO	Transmission system operator
V2G	Vehicle-to-grid

# Chapter 1

## Introduction

This thesis aims to answer the research question:

*As we move towards a 100% penetration of electric vehicles, how will this affect the steady state operation of the electricity network?*

There are two components to this question. First, what would be the impact of uncontrolled charging of a large fleet of electric vehicles on the electrical power system? Second, what would be an appropriate strategy to reduce this impact? This thesis addresses these questions using stochastic simulations of two case study power systems based on large datasets. In order to construct these simulations, novel data-driven modelling techniques and optimisation formulations are proposed.

Globally, transport accounts for 11% of CO<sub>2</sub> emissions [1], however in highly developed countries the share is even larger; for example, in the UK transport accounted for 33% of CO<sub>2</sub> emissions in 2018 [2]. Therefore, the decarbonisation of transport has been identified as one of the key objectives that must be met if we are to meet the targets set out in the Paris Climate Change Agreement [3]. Several alternative fuel vehicles have been developed that could replace traditional internal combustion engine vehicles, including biomass vehicles, hydrogen fuel cell vehicles, and electric vehicles (EVs). Of these technologies, EVs are the most mature – and the only one so far to be widely

commercially available.

Compared to conventional petrol vehicles, EVs reduce emissions in several ways. Firstly, they do not produce tail-pipe emissions, thereby moving emissions away from cities (where high levels of pollution have been linked with health concerns [4]). Secondly, the tank-to-wheel efficiency of EVs is about four times higher than conventional vehicles [5]. This means that, provided electricity generation is not coal-generated, CO<sub>2</sub> emissions will be reduced [6]. Finally, while petrol can not be decarbonised, low-carbon electricity generation is possible – meaning the total emissions attributed to EVs will reduce as the fuel mix becomes lower carbon.

Government incentives and falling battery prices have triggered a rapid increase of EV sales in high-income countries; Figure 1.1 shows the number of progression of the number of plug-in EVs in the UK over the last eight years. As of Q2 2019, there are 217,000 plug in EVs on the roads [7], and this number is forecast to rise to 36,000,000 by 2040 [8]. This transition will significantly reduce carbon emissions. However, the private vehicle fleet consumes a large amount of energy, so EV charging will add significant load to the power system, and it is important to understand how this will affect operation.

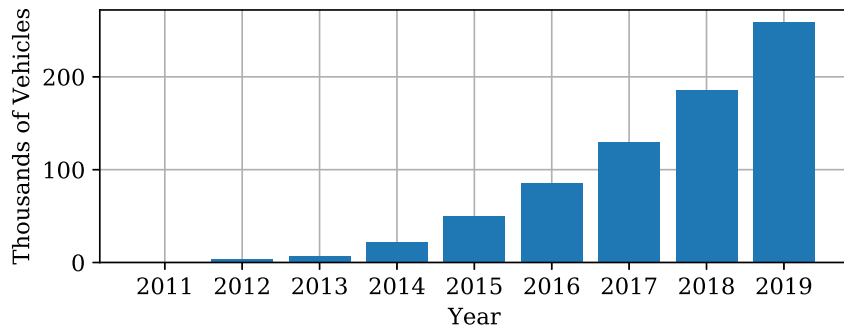


Figure 1.1: The number of plug-in electric vehicles in the UK with time.

There are several levels of electrification that are possible for vehicles. At the lowest level are mild hybrids, which have a small battery that is charged using excess energy created by the internal combustion engine, resulting in a reduced fuel consumption. Next comes plug-in hybrids, which have a larger battery that is charged externally, but also have an internal combustion engine to be used when the battery is empty. Since April 2019, these vehicles are no longer eligible for the UK’s plug-in vehicle grant, following

reports that users were not charging their vehicles – negating the decarbonising benefits of the technology [9]. Finally, there are fully electric vehicles (often called battery electric vehicles) which do not have an internal combustion engine, and are powered exclusively by a large battery. For the remains of this thesis, unless otherwise specified, EV refers to a fully electric vehicle.

## 1.1 Context

### 1.1.1 The Energy Trilemma

The World Energy Council has defined three core dimensions of sustainability for energy systems: energy security, energy equity, and environmental sustainability [10]. Combining these three objectives results in an index which is used to assess the sustainability of an energy system as it undergoes the transition to lower carbon fuels. Energy security describes a system’s ability to ensure a supply of electricity throughout the energy transition, energy equity describes the ability of the system to provide low cost electricity to consumers, and environmental sustainability describes the quality of the pathway to decarbonisation.

The electrification of vehicles aids in environmental sustainability, but puts strains onto security of supply; this demonstrates why these dimensions are described as a trilemma. This affect can already be seen in the council’s rankings of energy systems – the UK is ranked 4th overall, but only 28th in energy security. This pattern is repeated across Europe, where many of the countries leading on EV sales have a relatively low rank when it comes to energy security; Table 1.1 lists a number European countries, ordered by the percentage of their vehicles sold in 2018 which were pure electric or plug-in hybrid, and their World Energy Council rankings. This thesis will therefore focus on the impact of EV charging on the energy security of a power system. Although EV charging will affect the other two dimensions of sustainability, these are not analysed further in this thesis.

Country	EV Sales	Overall Rank	Energy Security Rank
Norway	49%	11	73
Sweden	8.1%	2	1
Netherlands	5.7%	14	39
Finland	4.8%	5	3
Portugal	3.5%	29	54
Switzerland	3.2%	1	11
United Kingdom	2.5%	4	28
Austria	2.5%	7	18
Belgium	2.5%	24	68
Denmark	2.1%	3	2
France	2.1%	6	27
Germany	2.0%	9	16
Ireland	1.6%	25	96
Hungary	1.5%	19	12
Slovenia	0.91%	12	9
Spain	0.91%	18	36
Italy	0.56%	20	37
Bulgaria	0.55%	41	33
Latvia	0.53%	22	4
Romania	0.47%	26	8
Lithuania	0.44%	36	74
Czech Republic	0.38%	16	10
Estonia	0.36%	30	31
Greece	0.31%	47	99
Slovakia	0.50%	23	26
Poland	0.25%	53	70

Table 1.1: The energy security and overall trilemma ranks of 26 European countries, ordered by their 2018 EV sales.

### 1.1.2 Power Systems

Electricity supply is commonly broken down into three stages: generation, transmission, and distribution [11]. The power generation system’s primary function is to ensure that there is a national match between supply and demand. At all times there must be a similar amount of power flowing into and out of the grid; a mismatch in supply and demand will result in the national frequency deviating from its allowable range, resulting in damage to steam turbines and over-currents in constant power loads. In order for the system to operate successfully, national power demand must be forecast and allocated between producers. Historically, allocating demand meant selecting the traditional generators

that can provide the cheapest power. However, the recent rise in renewable generation has complicated the task of supply-demand matching, because solar and wind generation are difficult to forecast and can not be directly controlled [12].

The transmission system transports power from generators to grid supply points (which each service a portion of the distribution system) using a network of high voltage transmission lines. Throughout the thesis high, medium, and low voltage are defined according to IEC 60038 [13], the ranges of which are displayed in Table 1.2. High voltage is used for transmission because it results in small currents, and therefore low resistive losses during transmission. Each line is designed to tolerate a certain maximum current. Successful operation of the transmission system involves ensuring that the proposed generation mix does not result in any lines carrying currents above their limit, and maintaining security of supply in the event of a fault in the network. Typically, transmission networks are fully meshed, meaning that there are at least two paths connecting each pair of nodes. Therefore, most systems are designed to be able to operate if any single line failed. In the UK, the government has set an objective for the system to be 100% operational in the event of a single failure, referred to as N-1 secure [14]. The generation and transmission systems are often grouped, as they are both concerned with operation at a national level and are governed by the transmission system operator (TSO).

Voltage Level	Rating
Low Voltage	< 1 kV
Medium Voltage	1 – 35 kV
High Voltage	> 35 kV

Table 1.2: Voltage classifications used in this thesis.

The distribution system connects homes to their nearest grid supply point using a large number of low and medium voltage circuits. Low voltage residential networks service a small number of households, each of which are typically connected as a single phase load. These networks are connected to the medium voltage system using 3-phase transformers, and nodes are connected using either underground or overhead cables. The topology of networks varies [15] – for example the US favours radial networks, while

European networks tend to be more meshed. Successful operation of the distribution network involves ensuring that the system is operating in a safe region, and that the power quality delivered to loads remains acceptable. Power quality encompasses both the bounds on magnitude and the harmonics of the AC signal.

In terms of increasing load in distribution networks, both the voltage and thermal limits in the network are of concern. Voltage limits refer to the bounds on the voltage supplied to households that ensure household device safety. Thermal limits occur when the current through a component results in a temperature that would damage it. Both the transformer and the cables in a network have thermal limits. However, it is shown in Appendix A that, for low voltage distribution network cables, under-voltages will typically occur before the line reaches its thermal limit. Therefore, thermal limits of the lines are not considered further here; thermal limit is assumed to refer only to the transformer.

Each transformer that connects a residential network to the higher-voltage grid (often called a distribution transformer) is rated to a certain maximum demand. Once the power through the transformer exceeds this value it is deemed to be overloaded, which may result in degradation of the insulating layers in the core, and therefore a reduced lifespan. The operation and maintenance of these circuits is carried out by a distribution network operator (DNO). Typically the distribution network is split into discrete sections which are each managed by a separate entity.

A summary of the impacts to each subsystem that are considered in this thesis is presented in Figure 1.2. For the generation system, the national peak demand is likely to increase, which could violate the system's supply constraints – meaning that, even with the maximum possible power generation, the demand could not be met. This would necessitate installing additional generation capacity, which is an expensive and inefficient solution – as the additional capacity would likely only be used for a small portion of the day. A change in the national demand profile would also affect the mix of fuels that are used, especially if charging occurs at times when renewable generation is not available.

While the generation system is concerned only with the aggregate load, the impact on the transmission and distribution systems will depend on the locations of the addi-

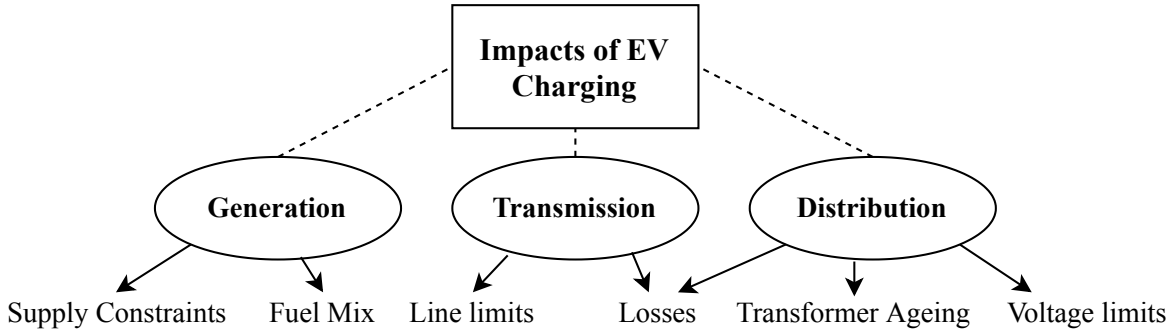


Figure 1.2: The impacts to the power system of additional load from EV charging considered in this thesis.

tional loads. The worst case scenario for the transmission system occurs when the EV load is concentrated in areas far away from the generation, requiring the high voltage transmission lines to carry significantly increased loads. Each line is rated to a maximum load, and if this is exceeded the line would have to be upgraded. Additionally, increased currents in high-voltage transmission lines result in additional system losses which would have to be accounted for. It should be noted that the effect of EV charging on voltages in the transmission system has not been considered, as these are routinely managed using tap-changes. The transmission system is designed be able to operate after the failure of a single component. Therefore, these metrics need to be investigated under both normal operation and in the N-1 case. If there are violations in the latter case, then the security of supply will have been impacted.

The worst case scenario for the distribution network is where many EVs charge simultaneously in a single residential network. The large individual loads will increase resistive losses, causing the voltage at nodes further down the network to drop. Additionally, the large aggregated load may cause the peak demand in the residential network to violate the transformer’s thermal limit. Violation of either of these limits would necessitate reconfiguration or upgrades to the network.

### 1.1.3 Electric Vehicle Charging Infrastructure

The infrastructure used will influence the impact that EV charging has on the system. This is because the style of charger dictates the size of the load and its position in the

network. The different types of charger available in the UK at the time of writing are described in Table 1.3, using the speed definitions from [16].

Speed	Power (kW)	Mode	Connector	Charging Time*
Slow	3.5	AC	Type 1/Type 2	8 hrs
Fast	7	AC	Type 1/Type 2	4 hrs
Fast	22	AC	Type 2	80 mins
Rapid	43	AC	Type 2	35 mins
Rapid	50	DC	CHAdEMO	30 mins
Rapid	50	DC	CCS	30 mins
Rapid	120	DC	Type 2	12.5 mins

Table 1.3: A description of the types of charger currently available in the UK. \*Approximate time taken to charge a 30 kWh battery from 0-80%.

The connector on a charge point restricts the vehicles that can use it; Type 1 connectors are standard in the US, and Type 2 connectors are standard in Europe; CCS chargers fit BMW and VW vehicles, while CHAdEMO chargers fit the other mainstream models; only Tesla vehicles can use the 120 kW rapid chargers. The speed (and hence power rating) of a charger dictates where in the network it can be positioned. Slow and fast chargers can be installed into low voltage residential networks (although 22 kW chargers have to be wired to all three phases), while rapid chargers need to be connected to the medium voltage network.

There are four broad locations where charge points are installed: service stations, shopping centres, work places, and residential areas [17]. With the exception of service station charge points, charger locations are chosen to maximise convenience, allowing users to charge without disrupting their normal routine. Figure 1.3 shows the percentage of the UK fleet that is parked at home, work, or shopping car parks throughout a normal weekday. Home and work are the most dominant location for vehicles to be parked, suggesting that these locations would be the most convenient to charge. Note that this figure does not show the percentage of vehicles that visited the shops, just those that are there at any one time; parking duration at shopping centres is likely to be significantly shorter than that at work places. While there are public charging points installed in residential areas, many users choose to install their own private charge point outside

their home. This guarantees charging availability, and likely reduces the users' charging costs.

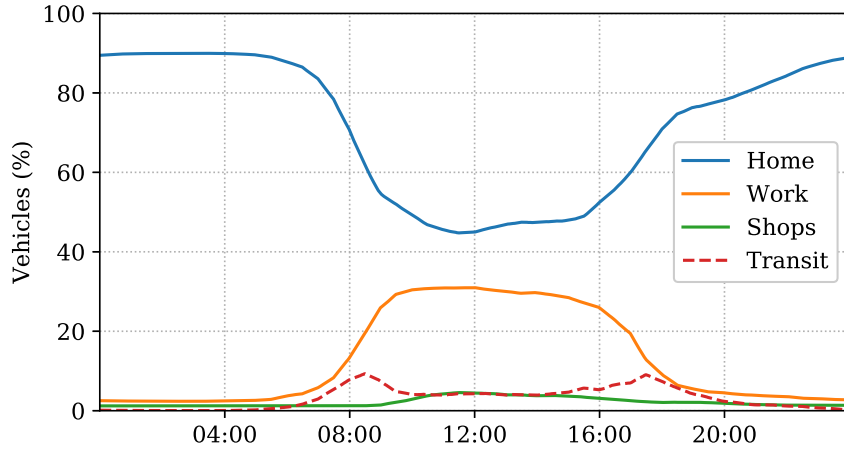


Figure 1.3: The percentage of the UK private vehicle fleet at common locations throughout a weekday.

Each charging location presents different challenges to the power system, depending on the position of the chargers in the network and the way that they are operated. Rapid chargers represent very large loads, so national supply-demand balancing problems may occur if a large number of vehicles begin charging at once. However, they are connected to a higher voltage network, which is designed to tolerate larger loads, so local problems are unlikely. On the other hand, slow chargers are less likely to cause problems for the transmission network, but are typically placed in low voltage networks, which were not designed to support loads of this size. Table 1.4 compares the load of a residential EV charger to other modern household appliances. Even the slowest rated EV charger has a higher power rating than the upper limit of the other devices listed. Additionally, the existing large loads (microwaves and kettles) are appliances that are only used for several minutes, meaning it is unlikely that a large number of them will be on at the same time in a network. Whereas, EV chargers are on for hours at a time, making the probability of an overlap between charger loads on the same network much more likely.

Typically, once a charge has been started, EV batteries are charged using a constant current, constant voltage (CC-CV) profile. This involves a period of charging at maximum current, followed by a period of charging at decreasing current but maintaining a constant voltage. Battery manufacturers recommend this cycle to minimise charging time given

Appliance	Min Power (W)	Max Power (W)
Single lightbulb	12	60
LCD television	20	150
Refrigerator	100	200
Microwave	850	1 800
Kettle	1 500	3 000
Residential EV charger	3 500	22 000

Table 1.4: A selection of typical modern household appliance loads, compared with EV charging loads.

a particular current and voltage limit [18]. Although this is regarded as the optimal profile, other charging profiles are considered safe, provided they stay below a 1C rate (the current that would charge the battery in an hour).

In terms of power, CC-CV results in the charger operating at approximately rated power until the battery is around 80% charged, after which the power consumed decays exponentially (e.g. [19]). There are losses in the charger, which mean that more power is drawn from the grid than delivered to the battery. Note that the charger efficiency drops as the power decreases [20], so near the end of charging there may still be significant load drawn from the grid.

### 1.1.4 Smart Charging

EV charging is a flexible demand; it does not matter to users when exactly their vehicle is charging, provided it has accrued sufficient charge by the time they next need it. This makes EVs' charging a good candidate for providing demand response, where loads are reduced or increased in order to protect the power system operation. The practice of co-ordinating EV charging to improve system operation is typically referred to as smart charging.

It is expected that smart charging will play a role in the successful integration of EV charging into the system; the UK government now requires EV chargers to be 'smart enabled' in order to receive a government subsidy [21]. Charging load can be manipulated by either shifting the load in time (i.e. delaying charging until off-peak) or by scaling the power of the individual charging loads. The amount by which charging can be shifted

therefore depends on the total energy demand of the EV, the time it is available to charge, and the rating of the charger. Domestic charging offers the greatest flexibility compared to other charging locations, as vehicles remain parked at home for the majority of the day. On the other hand, users of public charge points are only parked at the charge point for a short time, and extending the charging duration may prevent others from using the charger.

There have been some trials of EV domestic smart charging, most notably *Electric Nation* which investigated 673 EV users' response to having their charging controlled in return for financial incentives [22]. However, no market platform currently exists that allows users to charge their vehicles smartly. This means that, while it is possible to start chargers on a timer so that charging begins off-peak, there is no wide-spread financial reward for doing this, and no coordinator to determine the optimal charging of vehicles. Therefore, the way that the flexibility of EV charging will be used has yet to be determined; this decision will affect the impact that charging has on the power system.

From the power system's perspective there are several ways smart charging could be used. At the transmission level system, smart charging could be used to keep the national peak demand as low as possible, thereby minimising the amount of generation capacity required to ensure supply (e.g. [23]). Alternatively, charging could be shifted in order to make the best use of renewable generation, optimising the fuel mix (e.g. [24]). If real-time control of vehicles were possible, EV charging could be increased or decreased in order to maintain stability of the national frequency.

At the distribution level, smart charging could be used to protect components and therefore postpone required upgrades. This could either be done by reducing the total demand through the secondary transformer (e.g. [25]), or by reducing losses in the network (e.g. [26]) – thereby protecting the cables and reducing voltage drops.

In recent years there has been interest in making smart chargers bi-directional, so that they can send power back to the grid – or provide vehicle-to-grid (V2G) services. For example, the vehicle could inject power into the system if the frequency became too low. The main interest in these has been for DC rapid V2G chargers, but there have also

been AC fast V2G chargers developed.

Once the desired co-ordination of EV charging has been decided, users need to be incentivised to participate. Electricity suppliers buy power in the whole-sale electricity market, and prices are higher at off peak times. This means that shifting demand to off-peak saves the supplier money, but consumers typically pay a flat rate to the supplier, so they receive none of this saving. In *Electric Nation* consumers were retrospectively reimbursed when their EV's charging was controlled, so this is one possibility. A potentially more lucrative scenario is where EVs act as service providers and bid for up/down balancing or frequency reserve contracts. However, currently these contracts are only available to very large loads, so it is difficult to say how financially viable this option would be in a reformed electricity market. In order to understand the value that smart charging would generate, it is necessary to understand the costs associated with EV charging both with and without co-ordination.

## 1.2 Scope

This thesis will focus only on domestic charging, and investigates the scenario where the majority of vehicles' charging occurs at home. This is consistent with the behaviour of the early adopters, as it is estimated that 87% of charging is currently happening at the owners' homes [27]. The assumption of mass home charging sometimes receives criticism due to the 43% of households that do not have access to off-street parking [28]. While it is currently only possible to install residential vehicle chargers outside households with a private parking spot, here the assumption of mass home charging is defended for the following reasons. First, the 43% figure takes no account of vehicle ownership – many of the households that do not have off-street parking do not own a vehicle. Second, public chargers are sometimes installed into parking bays in residential networks, and charging using these can be modelled in the same way as home charging. Third, that lamp post chargers and extension leads allow similar (although less desirable) charging opportunities outside of users' homes.

It is clear that the impact that EV charging will have on the power system will depend on the number of EVs using the infrastructure. Two scenarios for EV propagation are considered in this research. The first focuses on a 100% penetration scenario, where the total number of private vehicles remains the same, but they are all fully electrified. It is useful to consider the 100% scenario because it represents the upper bound of the possible EV charging load. However, EVs are likely to become prevalent in some areas much earlier than others, and it would be useful to know which areas of the system need to be prioritised when it comes to reinforcements. Therefore, a 2030 scenario is also considered, where the total number of private vehicles still remains the same, but the percentage of those that are electric is extrapolated for each region.

Both scenarios assume no change in driving behaviour or vehicle ownership compared to current vehicle use. While some research assumes that electrification will change travel patterns, this is normally to incorporate the use of charging infrastructure, which would not be necessary with mass home charging. The effects of autonomous vehicles, and mobility-as-a-service have also not been incorporated. Either of these changes would drastically alter the fleet behaviour and energy consumption, introducing a large number of modelling parameters that would be difficult to choose meaningfully. Therefore, this analysis is outside of the scope of this research.

Here the only change assumed to domestic electricity demand is the addition of electric vehicle charging. This means that the electrification of heating and the increase in embedded generation are out of the scope of this research. It should be noted that some electric heating and solar generation are included in the power demand data, but an increase in the penetration of these technologies is not considered.

This thesis only investigates the system under steady state normal operation. This means that the effects on harmonic distortion and fault levels are considered outside of scope, as they require faster dynamic models.

This thesis focuses on the impact of EV charging purely from the network's perspective. This means that costs and benefits of charging to EV owners, aggregators, and policy makers are not considered. Furthermore, in the smart charging scenarios

the optimal charging is calculated using optimisation with perfect knowledge of the EV and existing electricity demand. Once the co-ordination strategy has been chosen for smart charging, research will need to be done to develop a mechanism by which EVs are controlled and rewarded.

### 1.3 Case Studies

In order to address the identified research question, this thesis will use two specific power systems as case studies. Here, a brief background to each system is provided.

**Great Britain (GB)** The first case study, which the majority of the results will focus on, is the GB power system. This was chosen because of the large amount of additional information available to UK research institutions, allowing a more detailed analysis to be carried out. The GB grid covers England, Wales, and Scotland, and runs at a frequency of 50 Hz. It is connected via undersea interconnections to France, Ireland, the Isle of Man, and the Netherlands. The transmission system is operated by National Grid PLC. The distribution system operation is split into 14 licenses, which are held by a total of six companies.

Relative to comparable countries, the UK has been a faster adopter of EVs; the government has subsidised the purchase of new EVs since 2011, and has committed to ban petrol and diesel vehicle sales by 2040. In 2018, 2.5% of vehicles sold in the UK were plug in electric vehicles [7]. In general, private vehicle use is relatively high; there are 0.58 registered vehicles per capita. However these are very unevenly distributed – 22% of households do not have access to a vehicle, while 42% have more than one [29].

Domestic electricity use in the UK is comparatively low when compared to other developed countries. The largest single uses of domestic electricity and lighting (19%) and heating (17%) [30]. This means that the electricity demand is largest in the winter, when the temperatures are coldest and the daylight hours are shortest. The last decade has seen a reduction in electricity demand due to improvements in device efficiency. However, 87% of dwellings are currently connected to the gas network as well as the electricity network,

and the majority of these use gas as their primary source of heating [31]. This means that, as heating is decarbonised, GB is likely to see an increase in electricity demand.

**Texas, US** A second case study of Texas, US is used, to demonstrate how the results presented may change for other systems. This case study is not analysed as extensively, because not all of the required data was available. However, Texas was chosen for the case study due to a relatively large amount of public access data being available. Texas is one of the only US states whose grid is managed independently (the North American grid is split into nine operating regions). The Texan grid is operated by the Electric Reliability Council of Texas (ERCOT). The system has two connections to the Eastern grid, and one to Mexico.

Texas does provide an EV incentive program which adds to the US federal tax credits available [32], however EV penetration remains comparatively low; in 2018, 0.58% of vehicles sold were electric [33]. Vehicle ownership is very high, with 0.797 registered vehicles per capita (this is actually below the US average) and only 5.5% of households do not have access to a vehicle.

Texas is the largest electricity consumer out of the US States, and has been since at least 1960 (when records began) [34]. The hotter temperatures mean air conditioning makes up 18% of electricity demand, and therefore the demand is largest in the summer months [35]. Unlike GB, in Texas 60.5% of homes already use electricity for heating [36]. Given that electric heaters are large individual loads, this suggests that the Texan grid may be built to withstand larger loads. It also means that a transition away from gas heating would not result in as significant an increase in electricity demand.

## 1.4 Thesis Contributions & Associated Publications

Specifically, this thesis makes the following contributions to the existing literature.

1. *Vehicle load is modelled as spatially heterogeneous.* Previously, when the impact of vehicle charging was modelled on a large system a spatially homogenous fleet of EVs was assumed. In reality travel behaviour varies regionally, so making this

assumption has a smoothing effect on the charging load, and risks underestimating the impact on the network. Here raw travel survey data is used that is broken down according to local authority level – allowing the variation in vehicle use to be accurately captured.

2. *A stochastic model is proposed for uncontrolled charging which incorporates variability in both vehicle use and charging behaviour.* The stochastic models for uncontrolled charging present in the literature either incorporate uncertainty into charging behaviour or vehicle use, but not both. This means that these models can not be applied to a non-homogenous set of vehicle use to produce meaningful results. In this thesis a model is developed which incorporates variability into both, allowing uncontrolled charging of a varied group of vehicles to be more accurately modelled.
3. *The action of various smart charging objectives are qualitatively compared, using realistic stochastic simulations of residential charging.* While a variety of objectives for smart charging have been proposed in the literature, their action has not been compared in simulations representative of domestic EV charging. Specifically, this thesis investigates the benefits and costs of load flattening and loss minimising objectives for protecting the local distribution network, and the case for bi-directional charging in low voltage networks.
4. *The conflicts between the optimal charging scenarios of the transmission level and distribution level systems is investigated.* The case for smart charging has predominately been discussed in respect to individual parts of the network in isolation. However, it is not possible to simultaneously optimise charging for all parts of the network simultaneously. Specifically there is likely to be a conflict between protecting local network components and optimising the system nationally. In this thesis, the scale of this conflict is quantified, and the degree to which compromise can be achieved is investigated.

Several papers have been published based off the content in this thesis. The table below lists these papers, along with the section of the thesis and contribution that they corre-

spond to.

<b>Paper</b>	<b>Thesis Section</b>	<b>Cont.</b>
C. Crozier, M. Deakin, T. Morstyn & M. McCulloch (2019), The Case for Bi-directional Charging of Electric Vehicles in Low Voltage Distribution Networks, <i>Applied Energy</i>	Section 6.3.2	3
C. Crozier, D. Apostolopoulou & M. McCulloch (2018), Mitigating the impact of personal vehicle electrification: A power generation perspective, <i>Energy Policy</i>	Section 5.1.1	1
C. Crozier, M. Deakin, T. Morstyn & M. McCulloch (2019), Incorporating Charger Efficiency into Electric Vehicle Charging Optimization, <i>Proceedings of Innovation in Smart Grid Technologies (ISGT) Europe</i>	Section 4.3.2	4
C. Crozier, D. Apostolopoulou & M. McCulloch (2018), Numerical analysis of national travel data to assess the impact of UK fleet electrification, <i>Proceedings of the 20th Power Systems Computation Conference (PSCC)</i>	Section 3.2	1
C. Crozier, D. Apostolopoulou & M. McCulloch (2018), Clustering of usage profiles for electric vehicle behaviour analysis, <i>Proceedings of Innovation in Smart Grid Technologies (ISGT) Europe</i>	Section 3.1.2	2

In addition, the following papers are under review:

<b>Paper</b>	<b>Thesis Section</b>	<b>Cont.</b>
C. Crozier, T. Morstyn & M. McCulloch (Under Review), A stochastic model for uncontrolled charging of electric vehicles using cluster analysis, <i>IEEE Transactions on Transport Electrification</i>	Section 4.1.2	2
C. Crozier, M. Deakin, T. Morstyn & M. McCulloch (Under Review), Controlled charging with Reduced Network Information, <i>IET Smart Grid</i>	Section 4.3.1	3
C. Crozier, T. Morstyn & M. McCulloch (Under Review), The Impact of Domestic Electric Vehicle Charging on the GB Power System, <i>Applied Energy</i>	Chapter 7	4

## 1.5 Thesis Structure

The remainder of this thesis is structured as follows. In order to contextualise the contributions of this thesis, a review of the existing literature is presented in Chapter 2. The impact of EVs will depend strongly on how the vehicles are used, so Chapter 3 discusses and proposes methodology for modelling EV vehicle use. This includes a novel method of predicting electricity consumption using conventional vehicle data, and clustering of vehicle usage. The timing of vehicle charging will also have a large effect on the impact on the power system, so Chapter 4 outlines methodology for modelling vehicle charging. Two sections are included: one proposing a stochastic model for the uncontrolled charging of vehicles, the other setting up formal optimisation problems which compute the optimal smart charging strategy.

The impact of EV charging on the transmission level and distribution level power systems is likely to be significantly different. Therefore, Chapter 5 investigates the impacts and mitigations of charging on the generation and transmission systems, while Chapter 6 does the same for the distribution system. In each case both the uncontrolled charging scenario, and the optimal controlled charging is investigated – for both the 2030 and 100% EV scenarios. The main findings from these chapters use the GB system, but in each case a section is included comparing the results for the Texas system. Chapter 7 then investigates the conflict between the optimal scenarios for the transmission and distribution systems, and evaluates the feasibility of finding a solution that is near-optimal for both systems.

Finally, Chapter 8 concludes the thesis. Appendix A contains the reasoning for disregarding thermal limits of lines from the analysis. A full description of the test networks used in the analysis is also presented in Appendix B.

# Chapter 2

## Literature Review

The impact of EV charging on power systems was considered as early as 1983 [37], and there is now a large amount of existing literature covering this topic. In this chapter, the existing research and modelling methodologies are explored. First, the existing literature is structured according to the level of EV control and system fidelity considered. Second, the modelling methodologies and charging strategies that have been previously proposed are discussed. Finally, the identified gaps in the literature is described.

### 2.1 Overview

Here previous electric vehicle modelling studies are classified according to the level of EV control and the fidelity with which the impact on the system is modelled. For both of these metrics several categories are defined, such that each study falls into at least one. The categories considered are explained briefly below.

**Level of Control** This determines the extent to which vehicle charging is shifted in order to improve the system operation (or the complexity of the smart charging strategy). The levels considered (from lowest to highest control) are as follows:

1. Uncontrolled: EVs charge without intervention.
2. Centralised Control: One central actor has direct control over the charging of a group of EVs.

3. Decentralised control: Each EV's charging is optimised individually to suit the owner's preferences in the presence of a price signal. Although a central controller may be able to change the price signal, they do not have control of how the vehicles will respond to it.

**System Impact Fidelity** This describes the aspect of the power system operation that is investigated. In general, when a smaller number of aggregated vehicles are being considered, higher fidelity modelling is required. The levels considered here are listed below, in order of complexity.

1. No Impact: The paper includes only a methodology.
2. National Energy: The total energy demand of an EV fleet is estimated.
3. National Power: The aggregated power demand profile of a fleet of charging EVs is estimated.
4. Distribution Loading Case Study: Loading of an example network with EV charging is modelled, and the impact on the transformer is investigated.
5. Distribution Power Flow Case Study: Power flow analysis of an example network with EV charging demand added, allowing the impact on losses and voltages to be investigated.
6. Transmission Operation: The impact of EV charging on a transmission system, taking into account geographic variation in travel behaviour and electricity use.
7. Distribution Operation: The effect of EV charging on a distribution system, taking into account geographic variation in travel behaviour, electricity use, and circuitry.

The reviewed literature can be visualised according to these breakdowns in Figure 2.1, where the size of the markers is proportional to the number of papers which fall into that category. The red markers show the percentage of the papers which include stochasticity. For uncontrolled charging papers, this means capturing the likely variability in vehicle

usage and/or charging. For controlled charging papers, this means the optimal solution can be found even if the problem constraints are not known with certainty.

Note that some papers contribute to more than one area, for example many papers compare the action of controlled and uncontrolled charging on the system; in these cases the papers are accounted for twice on the graph. The groups of existing research are described with more detail in the remains of this section, in order of increasing modelling fidelity.

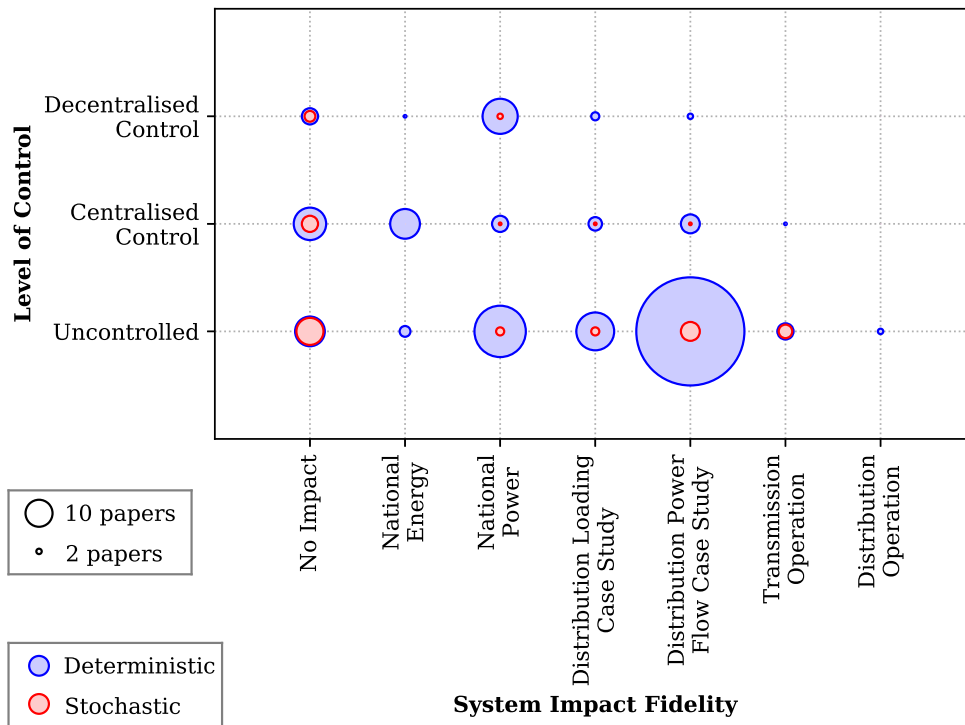


Figure 2.1: A visualisation of the literature.

**No Impact** These are papers that do not include any network simulations or case studies, but contain only methodological contributions. The majority of these propose methodologies for control of EV charging [38–53]. The breadth of this field is due to the large number of possible objectives and potential implementations, which are further broken down and described in Section 2.3. Some papers propose basic frameworks that allow EVs to provide V2G services by direct market participation [54], or acting as part of virtual power plants [55]. Another large group of papers propose methods for modelling

uncontrolled EV charging [53, 56–66]. This group in particular is dominated by newer research, as the availability of battery data has allowed charging to be more accurately modelled. These methods, along with other modelling techniques, are expanded upon in Section 2.2.

**National Energy** These papers estimate the aggregated energy demand profile of a large fleet of vehicles. These often have an economic focus, estimating the change in energy costs [67], or average household bill [68]. Controlling vehicle charging does not affect the total energy consumption of vehicles, but can affect the amount of energy drawn from the grid – due to varied losses in the charger and network. Therefore, some studies estimate the reduction in costs to the utility [69, 70] and household bill payer [71] as a result of smart charging.

The largest group of research in this area investigates the financial viability of EVs as service providers. Specifically, participating in the whole sale market [72, 73], committing to up/down balancing [74], or providing frequency response [75, 76]. Additionally, the energy demand estimates are used to estimate potential of EV charging to offset uncertainty in intermittent solar [24] or wind [77, 78] generation.

**National Power** These papers estimate the aggregated charging demand profile of a large fleet of vehicles – mostly at the scale of a country’s entire vehicle fleet. There is a general consensus around the future energy consumption of EVs, however the same can not be said for their charging profile. This is because the location, timing, and frequency of charging all affect the aggregated power demand profile. This gives rise to a large range of possible modelling approaches, and thus a large number of studies model the aggregated charging of a large fleet of EVs [23, 79–94].

The reviewed studies quantify the potential changes to the national power demand in several countries, including: the UK [79], Netherlands [80], the US [81–84], Canada [85], Portugal [86], Germany [87], Sweden [88], and Greece [23]. These give a wide range of results, with the increase in peak demand ranging from 0.12–2.7 kW per EV; this difference can be attributed to the range of modelling assumptions, as well as national

variation in travel.

Several studies investigate the variance of demand with charging location, most commonly comparing home with work charging [84,85,90], but also home with public [89,92], and home with uniformly distributed [83]. The majority of these studies superimpose their result onto the existing national demand profile to quantify the change in national peak demand, which dictates the country’s required generation capacity. Some studies also use the altered demand profile to quantify the changes to system reliability [91,92], and fuel mix [86].

In some ways, predicting the national power demand with smart charging is easier than with uncontrolled charging, because human decision plays a smaller role in the result. Some papers investigate the effect of tariff pricing on national demand, however the success of this strategy is disputed; while [90] concludes that a dual tariff would reduce the peak demand compared to uncontrolled charging, [95] finds that it would create a new peak higher than that seen in uncontrolled charging.

Other research predicts the national demand if vehicles were allowed to provide ancillary services, such as V2G trading [83,96], frequency response [97], and participation in a ramp market (where the ability to turn up or down at speed is traded) [98]. These market mechanisms result in a lower national peak demand compared with uncontrolled charging, but not the optimal loading case. Whereas, a number of studies show that directly controlling charging can avoid any increase in peak demand [93,95,99–101], as well as improving system reliability [91], and the fuel mix [94,102].

**Distribution Loading Case Study** These papers estimate the aggregated charging demand profile of a smaller fleet of vehicles – typical of the level of aggregation seen in residential networks. When considering the aggregated national fleet, individual variation in vehicle use is unimportant; the number of vehicles is sufficient to consider only average use. However, in residential networks only a small number of vehicles are aggregated, so individual vehicle use and variability becomes much more important. Therefore, several studies investigate the loading of an example residential network with a large penetration of uncontrolled EV charging. Some focus only on the aggregate charging load [103,104],

however most evaluate the change in total load, including household demand [105–110].

The peak demand on a residential network affects the distribution transformer, so some studies also look at the change to transformer losses [111], efficiency [112], temperature [113, 114], and ageing [84, 104, 115, 116]. Some papers demonstrate the potential benefit of smart charging on residential network loading, either by: ensuring demand is below the transformer limit [114, 117], flattening the load [118], or (for residential micro-grids) minimising mismatch between supply and demand [119, 120]. The results of all of these studies vary significantly according to the load modelling methodology, and source of vehicle data.

**Distribution Power Flow Case Study** These papers model the aggregated charging of a small fleet of vehicles, then load a test network with the resulting load and perform power flow analysis. The transformer is only one of the components in a distribution network that may be affected by EV charging, however more extensive analysis requires solving for the currents and voltages in the network. Therefore, a large number of studies use power flow analysis to investigate the impacts of EV charging on voltages [121–135], losses [26, 136–146], line loading [147–151], phase imbalance [152–154], and harmonic distortion [155–161] in example networks.

The majority of these use medium voltage (MV) networks, typically rated at 11 kV or 23 kV, where low voltage networks are treated as single point loads. Some use IEEE test feeders, specifically the 13-bus [147], 30-bus [134, 155], 31-bus [122, 140], 33-bus [139], 43-bus [123], and 69-bus [124, 137, 138] networks; some use real network data from DNOs [121, 136, 141, 143, 157, 162]; some use idealised single line networks [26, 135, 142, 144, 149, 152, 156, 158, 159]. Analysis of MV networks is easier, due to the (typically) smaller number of buses and the larger number of available test networks.

As EVs contribute a larger share of the load in low-voltage (LV) networks, the impact of charging is likely to be more severe in these networks; it is shown in [136] that the proportional increase in losses will be largest in LV networks, compared to the medium and high voltage networks. Some studies use 2-bus [146, 151] or single line [126–128, 132, 153, 160] LV networks to investigate the impact of EV charging, but these are not

representative of real residential networks. There are two LV standard feeders which have been investigated under EV charging – the IEEE 34 bus network [125, 133, 145], and the 19-bus standard network [129, 161]. However, these are both US-style networks and in [163] it is shown that the impact of EV charging will be worse in European-style networks. Finally, some studies have used real LV networks from Manchester [130, 131], Belgium [132, 154], and Bosnia [150]. The results of these studies varied hugely with network, but even those which use the same network conclude different results.

Some studies use distribution network case studies to demonstrate the effectiveness of controlled charging for protecting network operation. In [164, 165] cable loading in a single line network is optimised, [166, 167] maximise charging without violating voltage constraints in the IEEE 123-bus network, [168] optimise harmonics in the IEEE 31-bus, and [169] performs security constrained optimal power flow in the IEEE 24 and 118-bus networks. Case studies using real networks are used to optimise losses [170], voltages [171], and phase balance [172]. These all show that controlling charging can significantly improve operation of the system, with a variety of objectives and network topologies.

Distribution power flow case studies are the largest body of research reviewed, presumably due to the wide range of potential network styles, and metrics to be investigated. The main problem with all of the case studies is that the results are highly sensitive to the network circuitry and modelling assumptions used. The standard networks, while useful for testing and comparing new methodologies, can not be assumed to represent all networks.

**Transmission Operation** These are papers which estimate the change to loading on a transmission system, taking into account spatial-heterogeneity of EV charging. A small amount of research has attempted to capture geographic variation in EV charging demand, with the aim to assess changes to the transmission system operation. Previously, local travel data has been used to investigate changes to the regional system demand in China [173], the San Francisco Bay Area [174] and Queensland, Australia [175]. In the first case only the very high level system is included, and in the latter two only a small

geographic area is considered; this demonstrates the trade off between spatial resolution and geographic breadth when it comes to data collection. In [176] high rate motorway charging is predicted using GPS data from long journeys across the UK, forecasting this type of charging is important but this method is not applicable to domestic charging.

Some papers propose models which include coupling of the transport and power networks [177–180]. A fuzzy logic model is used in [177] to translate trip chains into location specific charging demand. In [178] the transport network is defined as a directional graph, where each node has a charging facility whose demand is a function of the traffic flow through the node. A large example network with a mix of commercial, industrial, and residential properties is investigated in [179], and origin-destination pairs are used to estimate the likely regions of high EV charging demand. In [180] node specific pricing is used to encourage vehicle to charge in less congested locations. None of these models could be scaled to simulate a national transmission network.

**Distribution Operation** These are papers which estimate the change to loading on a distribution system, taking into account spatial-heterogeneity of EV charging. Investigation into geographic variation in distribution system operation is difficult, due to the scarcity of mobility data and the lack of network visibility. Network operators have published some guidance concerning the regional impact on the network; in [181] it is estimated that 32% of the UK’s MV networks will require intervention due to EV charging, and [182] predicts that the average distribution network can support 33 EV chargers – rising to 102 if smart charging is employed. However, this research does not include regional mobility data, only local circuit information is used. Also, the charging assumptions used are very simplistic – it is assumed that all charging is coincident.

### 2.1.1 Reflections

Based on this overview, several broad observations can be made. It is clear that power flow case studies on test distribution systems are vastly overstudied. Although these examples were useful for a preliminary assessment of the impacts of EV charging on

distribution networks, they can not be extrapolated to represent a larger system. On the other hand, barely any work has been done on the operation of the transmission and distribution systems that includes geographic variation in vehicle use. The lack of network visibility and difficulty in spatially modelling vehicles makes this analysis much more difficult than single network case studies, however this research is vital in understanding the impact that EV charging will have. This thesis will supplement the research in these areas, investigating both uncontrolled and controlled charging of vehicles.

Another area which clearly requires further investigation is the effect on networks of ancillary service provision. Thus far the research on ancillary services has focused only on the value it can provide to the national system, not the effects it will have on low voltage networks. However, this is left as further work – to be completed if ancillary service provision by EVs is to be pursued.

## **2.2 Modelling Methods**

The results of existing impact studies vary significantly, and this is partly down to the wide range of methodologies used to model EV use and charging. This section details the common approaches used for modelling both the use and charging of a future EV fleet.

### **2.2.1 Vehicle trips and energy usage**

A variety of approaches have been used to estimate the energy demand of EVs, using a varying level of modelling fidelity. Predicting vehicles' energy demand is the first step in determining the impact that EV charging will have on the power system, as the total electricity demand of the fleet can be quantified.

For studies involving hybrid vehicles, it is sometimes assumed that all batteries will be emptied everyday (e.g. [110]), however for purely electric vehicles this is not reasonable. A number of studies directly model the state-of-charge (SOC) of vehicles at the end of the day, for example using a uniform [99], Normal [147], or discrete [183] distribution. However these approaches have two significant drawbacks. Firstly, it is difficult to

intelligently choose the form of the distributions, due to the limited amount of charging data available. Secondly, the interdependence between SOC and availability can not be taken into account – vehicles that have travelled further are likely to be available to charge for a shorter period of time.

The most common approach is to convert distance travelled into a predicted energy consumption (e.g. [184]). This is advantageous because distance travelled is well measured, both directly and indirectly using fuel consumption. The simplest of these models uses a constant coefficient to map distance to energy (e.g. [103]), however the coefficient chosen will have a large impact on the results – values in the literature vary between 0.23 and 0.4 kWh/mile. In reality a vehicle’s energy consumption is highly dependant on its physical parameters [185], meaning no single coefficient is likely to fit all vehicles well. As a result, some studies extend the linear model by defining separate coefficients for different vehicle types [186].

High fidelity models have been developed which model the full drivetrain in an EV (e.g. [187]), and these allow more accurate predictions of energy consumption to be made. The required modelling fidelity depends on the number of vehicles’ being aggregated, because the variability decreases as the number of agents being summed increases – meaning that the total consumption will converge towards the average. Therefore, when estimating a country’s annual EV energy expenditure a linear coefficient is likely appropriate, whereas for estimating an individual vehicle’s required battery capacity a high fidelity model is necessary. For the applications in this thesis, it is likely that a linear coefficient – if appropriately chosen – is sufficient, as the focus is on the average impact of a large fleet of vehicles.

In addition to the energy consumption of the EVs, it is also important to estimate the availability of the vehicle to charge. A vehicle’s availability determines when it is likely to charge, but also the flexibility it could achieve with smart charging.

If individual usage data is available, then the actual time when the vehicle was parked at home may be known. If only aggregate data is available, then availability must be modelled. The most popular approach for modelling availability is to define probability

distributions for arrival and departure times (e.g. [99]) which are sampled for modelling individual vehicles. The main limitation of this approach is that the relationship between vehicle use and availability is not taken into account; clearly in reality, vehicles which are used more are available for less time. There are some studies which model both use and charging simultaneously, for example [88] uses Markov chains to model movement of an EV between locations, however these models tend to have a large number of parameters that are difficult to find accurate values for.

### 2.2.2 Vehicle charging

In terms of power system operation, the timing of vehicle charging is extremely important. Therefore, the method chosen for modelling EV owners' decision to charge has a large effect on the simulation results. Modelling techniques from the literature can be broadly divided into deterministic and stochastic.

**Deterministic** The simplest form of models are deterministic, meaning charging and vehicle usage are modelled with a one-to-one relationship – such that two vehicles with identical usage will necessarily have the same charging pattern. This is not a realistic representation of the way EVs are charged. However, given that a large amount of this research took place before any real EV charging was recorded, the majority of literature surveyed uses deterministic assumptions. The most common assumption is that charging begins immediately following the completion of the final journey of the day (e.g. [82]). However, a number of other assumptions are present: [26] assumes all EVs begin charging simultaneously, [149] assumes charging begins at one of a discrete number of times, and [175] assumes that vehicles charge whenever they are parked. The power system currently relies on diversity between consumers, as this results in a smoothing effect when demand is aggregated. Assuming that all EVs charge with the same deterministic rule results in very little diversity between vehicles, so a one-to-one model for EV charging is likely to overestimate peak charging demand of a group of vehicles.

**Stochastic** Power systems are designed to operate under uncertain loading, with some degree of confidence. Therefore, when planning for the future, it is insufficient to estimate the average load due to EV charging – the variability also needs to be considered. This is especially important when considering the aggregate charging of small numbers of vehicles, such as in residential networks. Stochastic load models output a probability distribution of power demand, rather than a single estimate. In the case of EV charging, there are two main sources of variability: the vehicle use, and the charging behaviour. The first describes variations in travel behaviour, both between users and day-to-day. The second describes variations in the circumstances under which a user will charge their vehicle. These must both be modelled in order to fully capture the variability in charging. Stochastic models for EV charging can be broadly decomposed into three groups: deterministic models applied to stochastic vehicle use [59, 61, 82, 89, 103, 147, 152, 176, 188, 189], stochastic models applied to deterministic vehicle use [85, 104], and top down stochastic charging models [57, 58, 60, 62, 88, 190].

The first group encompasses the majority of the early research in this area. In these models simple assumptions are made for charging – e.g. that it begins after completion of the final journey of the day, or anytime the vehicle is home. Variation in predicted charging is then due only to varied vehicle use, which is captured by sampling either raw vehicle data (e.g. [89]), or probability distribution functions (PDFs) for energy use and arrival times (e.g. [59, 61, 82, 103, 147, 152, 176, 188, 189]). Providing the data source is large and representative, these models will capture variability in vehicle use. However, they do not include variability introduced by users’ charging decisions – all variability will be due to the distribution of arrival times.

The second group of models take a given vehicle use, and produce a stochastic estimate of charging. Creating these generally requires data recording both the use and charging of EVs. Fuzzy logic models are used in [85, 104], where certain combinations of input parameters result in a low, medium or high probability of charging. In [85] the vehicles’ SOC and length of parking time are assumed to impact the users’ decision to charge, while [104] also incorporates the distance from home. Considering only three probability

states limits the accuracy of these models, however further states introduce additional parameters, which require a large amount of data to set confidently.

The third group directly models charging, rather than the relationship between vehicle use and charging. In other words, these are top-down models for EV charging. Sometimes standard probabilistic models are used: Gaussian Mixture Models are used in [58, 190], and [57, 88] use Markov Processes. In [60, 62] random point processes are used to describe EV arrivals, and queueing theory is used to model EV charging. However, this approach is perhaps better suited to public charging, where the availability of the charger is a limiting factor. In general, these top down models likely capture the variability from their constituent datasets, but also any sources of bias present in the data. Additionally, since their parameters do not have a physical interpretation, they are hard to generalise to a different set of vehicle usage.

### 2.2.3 Reflections

Although a variety of modelling techniques are available in the literature, some further models will need to be developed in order to accurately estimate the impact of EV charging on the power system.

In terms of energy consumption, it is likely that a first order conversion from distance to energy will be sufficient for estimating the impact of EV charging on the national scale. However, the coefficient used for the conversion will have a large influence on the simulation results. Additionally, the energy consumption of a vehicle will depend largely on the vehicle parameters and the user's driving patterns. Therefore, a higher fidelity model should be developed which can be used in order to accurately estimate conversion factors for various vehicles and driving styles.

For vehicle charging, incorporating stochasticity is important – particularly when considering the impact of charging small numbers of vehicles in distribution networks. If regional variation in vehicle use is to be taken into account, it is necessary to use a model that map vehicle use to charging (i.e. models from the second group identified). The existing models which fall into this category are very simplistic – in fact, they both

assume that charging is independent of time of day. Therefore, it is necessary to develop a higher fidelity model that falls into this category in order to accurately assess the impact of uncontrolled charging on the power system.

## 2.3 Smart Charging Strategies

A large amount of research proposes methodologies for determining the optimal charging profiles of vehicles. In this section, a survey of the existing smart charging formulations from the literature is presented, which is summarised in Table 2.1. Schemes are categorised according to their objective, hierarchy, convexity, whether they incorporate network constraints, and whether the formulation holds for V2G. In the following sections, these metrics and the studies which fall within them are discussed in more detail. One criteria which has not been included in this breakdown is the incorporation of battery degradation into the smart charging algorithm. Battery degradation can increase the costs to the EV owner of charging their vehicle, so its incorporation can significantly affect the optimal results. However, as the focus of this analysis is on the costs to the network operator, it has not been included here.

### 2.3.1 Hierarchy

Smart charging strategies can be broken down according to their control hierarchy, which effectively describes the way the strategy is implemented. In [163] smart charging strategies are broken down into time-of-use and direct control, and in [194] the latter is broken down into centralised and decentralised. Therefore, in this review these three categories are considered.

**Time-of-use** The simplest method of smart charging is using a straightforward economic incentive. So called time-of-use (TOU) strategies involve multiple tariff prices which make charging at off-peak times cheaper. The main benefit of TOU strategies are that they are cheap to implement, as no sophisticated communication or control equipment is required – the shifting of demand is left up to the individual user. This

	Objective	Centralised?	Convex?	Network Constraints?	V2G?
[38]	C	×	✓	×	×
[48]	C	×	×	×	✓
[49]	C	✓	✓	×	✓
[44]	C	✓	×	×	✓
[102]	C	×	×	×	×
[46]	C	✓	×	×	✓
[45]	C	✓	×	×	✓
[43]	C	✓	×	×	×
[96]	C	✓	×	×	✓
[51]	C	✓	×	×	✓
[50]	C	✓	×	×	✓
[99]	C	✓	✓	×	✓
[47]	C	×	×	×	×
[100]	P	✓	✓	×	×
[140]	P	✓	×	✓	×
[42]	F	×	×	×	×
[41]	F	×	×	✓	×
[26]	L	✓	×	✓	×
[140]	L	✓	×	✓	×
[191]	L	✓	×	✓	×
[141]	L	✓	×	×	×
[192]	L	✓	✓	×	✓
[139]	L	✓	×	✓	×
[146]	L	✓	✓	✓	×
[154]	B	✓	✓	×	×
[172]	B	×	×	✓	×
[153]	B	✓	×	✓	×
[118]	B	×	✓	✓	×
[193]	E	✓	×	×	×
[170]	E	✓	×	✓	×
[164]	E	✓	×	✓	×
[165]	E	×	×	✓	×
[171]	E	✓	×	✓	✓
[117]	E	✓	×	✓	×

Table 2.1: A summary of the referenced smart charging algorithms. C = minimum cost, P = minimum peak load, F = flattened load, L = minimum losses, B = balanced phases, E = maximum charging.

is advantageous because if the implementation costs are too high it may be more cost-effective to upgrade the network; [195] concludes that TOU is financially viable, while more sophisticated control strategies are not. However many users do not respond to varied price signals [196], and this can make it difficult to intelligently set the price; In [197] individuals were surveyed to assess their willingness to change their behaviour in response to various price signals, however it has been demonstrated that stated preference methods (when individuals are asked to hypothesise their response to a scenario)

can give inaccurate results [198].

**Centralised** In centralised schemes, one actor has direct control of a group of EVs' charging. Aggregating EVs allows an actor to obtain sufficient demand to participate in the wholesale market [199] or to influence system operation [200]. Centralised control typically involves solving a single optimisation problem, and optimality is guaranteed as the actor has direct control over the vehicles. However, this single problem may become intractably large as the number of vehicles to be controlled grows. Additionally, there are some data privacy concerns around this type of control, due to the sensitivity of vehicle use and availability information [201].

**Decentralised** In decentralised schemes, each vehicle optimises its own charging in response to price signals broadcast by a central actor. Computationally this scales much better than centralised control, as the individual optimisation problems have a fixed size [202]. Additionally, vehicles' individual requirements do not need to be broadcast, which resolves the data security concern. However, bi-directional communication infrastructure between all vehicles and the price setter is required, and convergence to the optimal solution can be slow.

## 2.3.2 Smart Charging Objectives

Various objectives have been proposed for the optimisation of EV charging. All seek to move charging demand away from peak times, however they vary according to the modelling approach and the incentives that the charge co-ordinator uses. Smart charging formulations allow the optimal controlled charging scenarios to be calculated, however it is important to be able to compare the action of the various schemes.

### 2.3.2.1 Minimum Charging Cost

A large number of proposed smart charging algorithms aim to minimise the cost of electricity used to charge the vehicle, i.e. costs to the customer. The focus of this thesis is on cost to the system, rather than cost to the consumer; in [162] it is demonstrated that

strategies which minimise charging costs without taking the network into account may not result in an optimal situation from the perspective of the entire electricity delivery system. However, these strategies are included in the literature section because it is likely that the practical implementation of smart charging will involve a market mechanism.

**Static Price Curve** The simplest method of optimising charging takes a fixed time-varying price signal (e.g. a dual tariff pricing structure such as Economy 7) and optimises charging to reduce cost [38,48]. The price signal is set offline, and therefore does not adapt to the actual demand on the system. This is computationally cheap to implement, as each vehicle optimises its charging independently. Both of these papers assume TOU tariff style prices, but [48] incorporates uncertainty in household demand and bi-directional charging. This method reduces the direct costs to the EV owner, but the TOU prices may not reflect the demand on the system, so the cost to the system is not necessarily reduced. Additionally, as vehicle charging is not co-ordinated, this strategy may end up creating a new peak demand at a different time.

**Uncertain Price** Some studies assume that the price is variable, and the vehicles minimise their cost in the presence of an uncertain price signal [44–46, 49, 102]. These all consider an aggregator with centralised control of a fleet of vehicles. In [44, 49, 102] the price uncertainty is due explicitly to renewable generation, while [45, 46, 102] consider market uncertainties. The majority of these studies use two-stage linear stochastic programming, where price estimates are obtained in the first stage. However, [46] uses mixed-integer programming and [45] uses information gap-theory.

**Market Participation** Other studies assume that participation in various electricity markets is possible, and optimise charging within this framework [43, 50, 51, 96]. This allows aggregators to directly profit from vehicle charging in addition to reducing costs. The problem is that this relies on market reform, as the existing frequency market requires a minimum of 3 MW capacity and guaranteed availability [203]. Additionally only long-term contracts are currently available, whereas the studies include participation in the

day-ahead [43], intra-day [96], and real-time [50,51] markets. In [43] only uni-directional charging is considered, while the others all include bi-directional charging.

**Real Time Pricing** Finally, some studies assume a real-time electricity price, which incorporates the effect that vehicle charging will have on the price [47,99]. This is distinct from a time-varying fixed price because the price is set online, so the price is guaranteed to be high when demand is high. In [99] it is assumed that price is a linear function of load, such that the total cost can be expressed as a quadratic function of load. While [47] assumes a predicted spot price which is iteratively updated based on the intentions of the vehicles. Unlike the other cost minimising algorithms, these guarantee optimality from the perspective of the system. However, real time pricing would require a large amount of communication infrastructure and market reform, so can not realistically be seen as a short term solution.

### 2.3.2.2 Transformer Protection

Low voltage networks are connected to the medium voltage system via a distribution transformer. These all have a rated apparent power (in kVA) which represents the maximum power that should flow through the transformer. If the total power demand of the network is above this, then the transformer needs to be upgraded to avoid accelerated ageing. Therefore, several smart charging formulations aim to protect the transformer by preventing violation of this demand limit [41,42,100,140].

**Minimum Peak Load** Some formulations directly minimise the peak of the total demand on the network [100,140]. The formulation in [100] is a convex linear program, while [140] incorporates constraints on the line flows and bus voltages – thus sacrificing convexity. The problem with this objective is that the peak demand depends on the time resolution used, meaning if a coarse time resolution is used then an increase in system demand could still be observed. For example, you could avoid increasing the peak demand at 1 min resolution while increasing the peak at 30 min. The thermal time constant of a transformer means that the load at 30 min dictates whether the transformer

will overheat, while voltage problems occur at much faster time scales. This means that there is no one time resolution which is appropriate; in order to protect the whole system a smart charging strategy should be invariant to time resolution.

**Flattened Load** Some formulations propose using smart charging to flatten load [41, 42]. This minimises the peak demand at all time resolutions, and reduces the network losses when compared to merely minimising peak demand – although the objective becomes quadratic rather than linear. In [42] the algorithm is network invariant, while [41] includes constraints on the network voltages – therefore requiring a full network model.

### 2.3.2.3 Power Quality

Appliance safety requires that voltages in the network be kept within strict bounds, which vary according to country. Adding load to the network will result in an increase in the resistive losses, and therefore voltage drops along the network. Therefore, unless there is also additional generation in the network, it is the lower bound that is likely to be of concern. Here, the smart charging formulations that reduce voltage drop across the network are described.

**Minimum Losses** Minimising the resistive losses in distribution networks with EV charging has been proposed [26, 139–141, 146, 191, 192]. Low voltage distribution networks currently account for 29% of electrical losses in the UK power system [204], and EV charging is expected to increase this share [125]. Losses not only waste electricity, but generate heat in the cables and transformer – leading to degradation of the cables’ insulation [205], and a reduction in the transformer’s lifespan [113]. Additionally, losses in a cable result in a potential difference between its two ends, meaning an increase in losses will increase the voltage drop across the network. Therefore, minimising system losses can reduce both operating and fixed costs as well as the voltage drop across the network. Loss minimisation in distribution networks is a mature research topic; solutions have focused on network reconfiguration, placement of capacitors, and adding distributed generation [206, 207]. However, the flexibility of EV charging demand means that losses

can be reduced by controlling charging.

Flattening load is often assumed to be equivalent to minimising losses (e.g. [208]), and distribution network operators (DNOs) are predominately focusing on shifting load to off-peak times in order to reduce losses [204]. Losses vary quadratically with current, so higher peak loads result in larger losses, and in [111] it was found that flattening EV charging load reduced losses by 20% compared to uncontrolled charging. However, minimising losses is only strictly equivalent to flattening load if all loads are drawn from a single bus on the network [26].

Explicitly minimising losses with EV charging is the theoretically optimal solution for distribution network operators (DNOs). However, it requires a complete model of the network impedances, which can be difficult to calculate, and would have to be updated every time the network is reconfigured. Additionally, the problem is NP hard and non-convex, meaning the computation time of the problem scales poorly with the number of loads and time resolution [209]. This is largely because calculating the losses requires solving the power flow equations, which are non-linear, resulting in a non-convex problem. Nevertheless, several studies have proposed smart charging algorithms that minimise losses using the full equations [140, 141, 191]. However, the computational burden necessitates simplifications in the problem set up; [140] uses a time resolution of 1 hour and treats EVs as homogenous, [191] assumes a flat voltage profile, and [141] only considers reactive power for reducing losses. Further examples of non-convex loss minimisation can be found in micro-grid optimal power flow problems [210, 211]; these are also limited to small networks at coarse time resolutions.

Alternatively, it is possible to formulate approximate loss minimisation problems that can be solved in polynomial time. Typically, these involve simplification of the power flow equations, in order to obtain a convex formulation. For example [192, 212] use a DC approximate power flow in order to minimise losses in a micro-grid. In [139] a relaxation of the power flow equations is used to formulate active power loss minimisation as a second-order cone programming problem, however it is mixed-integer so still non-convex and thus scales poorly. Local problems that do not require solving the power flow equations

can also be formulated (e.g. [146]) – although there is no guarantee that the global optima is found.

It should be noted that while minimising losses will minimise the voltage drop across the network, it does not ensure that the voltage stays within bounds – if too much load is added under-voltages will occur regardless.

**Balanced Phases** In 3-phase networks, load imbalance between the phases increases losses, so reducing phase imbalance has also been suggested as a smart charging objective [118, 153, 154, 172]. Phase imbalance is caused by both systemic imbalance in the network, and imbalance in load [213]. While the former can not be easily changed, the latter can be reduced by shifting demand. In the case of 3-phase smart chargers, load can be shifted in real-time from one phase to another (e.g. [154, 172]). For single phase chargers, it is necessary to co-ordinate the fleet of vehicles, and the resulting problem is non-convex and requires a full network model (e.g. [118, 153]). While imbalance between phases results in additional losses, the minimum losses do not occur at the minimum phase imbalance. This is because phase imbalance does not take account of the size of the load, so well-balanced large loads result in high losses. For this reason, phase imbalance alone is not considered as a smart charging objective in this thesis.

**Maximum Charging** Minimising losses does not ensure that the network voltages actually stay within bounds, in some cases it will be impossible to achieve the required charging without violating the voltage limits. Therefore, some formulations aim to maximise the amount of charging given some network constraints [117, 164, 165, 170, 171, 193]. The constraints considered vary: [193] defines a constraint on the network peak demand, [170, 171] directly limits voltages, and [164, 165] includes both voltage and thermal constraints. In [117] the MV distribution network was considered (as opposed to the LV residential network) and total charging is maximised, assuming that each MV node connects to a LV network.

This approach has the advantage of ensuring that constraints are not violated, but does not seek to optimise the loading beyond this. It is possible to incorporate network

performance as a secondary objective, however none of the surveyed methods took this approach. It should be noted that some of the formulations mentioned in other sections include constraints for both network limits and total charging, but these result in an infeasible problem if loading is too heavy – i.e. it may be impossible to meet both the charging and the network constraints.

### 2.3.3 Other Metrics

In addition to the objective and hierarchy, here the surveyed literature is categorised according to the following metrics:

**Convexity** Convex optimisation problems are those with a convex objective, and a convex feasible set. These problems are computationally significantly easier to solve than non-convex problems, as they have a unique minimum value and only one local minima.

**Network Constraints** Regardless of the objective, some smart charging algorithms incorporate the constraints of the network into the problem constraints. Most commonly, these are voltage constraints, but current and transformer limits are also possible. Incorporating the constraints ensures the safety of the network, however can result in infeasible optimisation problems and typically sacrifices convexity.

**Bi-directional Charging** Finally, strategies can be broken down according to whether they allow bi-directional charging (V2G). Incorporating V2G increases the flexibility of EV smart charging, and hence the potential benefit to the network. However, round-trip losses mean that discharging can not be treated as negative charging, so incorporating this functionality is non-trivial and typically increases problem complexity.

### 2.3.4 Reflections

A large number of smart charging formulations have been proposed in the literature. In order to address the identified research question, the impact of optimally controlled

charging on the power system must be quantified, and this will require a scheme for optimising charging. Broadly speaking, schemes adopt one of six objectives, and it would be useful to compare how each of these affect the power system operation. However, in order to directly compare the results of these schemes they must be computationally comparable.

In terms of calculating an offline optimal scenario, convex problems are computationally superior. This means that they can be used to calculate the optimal charging of a larger number of vehicles, at a higher time resolution. This means that they are likely to out-perform non-convex schemes for which a lower resolution is necessary. If formulations are to be compared, then a consistent time resolution and number of vehicles needs to be used, meaning the formulations must be computationally comparable.

Therefore, although a variety of formulations are available, these may have to be modified in order to create directly comparable schemes – particularly for the case of loss minimisation, for which an accurate convex formulation has not been proposed.

## 2.4 Gap Analysis

As a result of the literature review, the following gaps were identified:

(A) *Spatial heterogeneity of EVs* The majority of surveyed research assumed a spatially homogenous fleet of EVs, meaning there were no significant differences in simulated vehicle use on different geographic sections of the system. This is unrealistic, as travel behaviour varies regionally; assuming a homogenous fleet effectively applies the average vehicle load to all points in the network. This has two implications for analysis of the impact of charging on the power system. First, for the transmission system analysis, the load flow analysis will be inaccurate, as in reality some parts of the network are likely to be disproportionately loaded by EV charging. Second, some distribution systems are likely to be more severely affected by EV charging than others, so assuming homogenous EVs will underestimate the impact on these systems.

*(B) Stochastic modelling of charging* EV charging in residential networks is highly stochastic, due to the high variability when a small number of vehicles are aggregated. However, the majority of analysis in the literature used very limited methods to capture stochasticity. In general, models either incorporated stochasticity in vehicle use (through travel survey data) or stochasticity in plugging-in (using EV trial data) but not both. This limits the reliability of results, because diversity between consumers plays a vital role in power system operation, and not fully capturing stochasticity will underestimate diversity.

*(C) Comparison of EV smart charging objectives* While a wide variety of smart charging strategies and formulations have been proposed, there has been very little research comparing the action of different smart charging objectives. Typically, papers that propose a charging scheme only compare the action of their algorithm versus uncontrolled charging, not to other smart charging objectives. For example, many papers propose using smart charging to minimising losses, but do not quantify the size of the additional loss reduction compared to a simpler scheme such as flattening load. Another example is studies that propose bi-directional smart charging (V2G), and quantify the benefit compared to uncontrolled charging, but not to smart uni-directional charging (which would require less infrastructure). This lack of comparison makes it difficult to assess the value of various schemes, which is important when deciding what technology to pursue.

*(D) Integrated analysis of the transmission and distribution level systems* Most of the surveyed literature focused on one level of the power system, either the low, medium, or high voltage networks. This makes it difficult to compare the impacts of EV charging on different parts of the system as studies use differing sets of assumptions and data sources. Additionally, all work quantifying the benefit of smart charging optimises for the level of the system considered. However, the optimal charging for the distribution network is not the same as the optimal charging for the transmission system, and this potential conflict

has not yet been explored.

# Chapter 3

## Modelling Vehicle Use

The impact that EV charging will have on power systems depends largely on the size of the EV energy demand, with respect to the existing electricity demand. Therefore, it is necessary to anticipate the number of EVs that will be charging on the system, where they are located, and how often they will require charging. This chapter focuses on the data sources and modelling methodology required to estimate these parameters.

Section 3.1 focuses on analysis of user travel behaviour. Clustering is used to identify typical usage modes of vehicles, and these results are used to qualitatively compare the use of vehicles from various datasets. This analysis is useful because the times that vehicles are being used and the distances that they are travelling dictate when they are able to charge and how much energy they are likely to require.

In Section 3.2 a technology transition forecasting technique is applied to regional sales of electric vehicles. Therefore the number of EVs in each area at various points in the future can be estimated. This will allow required infrastructure upgrades to be ordered in terms of urgency, and areas where high EV penetration will occur earliest to be identified.

Section 3.3 proposes a novel model for predicting the energy consumption of an EV from conventional vehicle driving data. The model allows conventional vehicle behaviour to be used in simulations of EV charging, rather than relying purely on data concerning EVs. This is valuable because the current EV fleet is very small and biased – under a high penetration scenario the future EV fleet usage is more likely to resemble the current

conventional fleet usage.

Although none of this content maps directly to one of the contributions, the clustering analysis and the energy consumption model are novel, while the s-curve modelling is not.

## **3.1 User Travel Behaviour**

This section includes analysis of both conventional vehicle and EV usage. First, the sources of data used are described. Then, clustering is used to identify typical modes of vehicle use. Finally, the differences in the use between the conventional and electric vehicles are quantified.

### **3.1.1 Data sources**

Due to the novelty of EVs, data concerning their usage is currently scarce. In the short term, it is likely that EVs will represent a biased set of drivers – meaning the average EV driving pattern will be different than the average conventional vehicle driving pattern. However, this research focuses on a scenario with a large penetration of EVs, at which point the behaviour of the fleet of electric vehicles is likely to more closely mirror the current conventional vehicle fleet.

Therefore, both electric and conventional vehicle usage data is utilised in this thesis. Existing EV data results from research trials, where the usage and charging of a small number of vehicles is carefully monitored. Typically this data is accurate and high-resolution, but represents a biased set of vehicles – due to trials often being opt-in. Conventional vehicle data has been collected for decades, and so there is a much larger selection available. This allows analysis of the dependence of vehicle use on location and socio-economical factors. In general, these datasets tend to be lower quality, however the low cost of acquiring such data means that the sample size is much larger. This section further describes the two data types, and the exact sources for the UK and Texas case studies in this thesis.

### 3.1.1.1 National Travel Surveys

Travel surveys are carried out routinely by many countries and local authorities, in order to understand the travel behaviour of their citizens. Households are randomly selected and asked to record all of their trips that were undertaken during a trial period. Data is recorded by hand, and therefore subject to human errors and rounding. However, providing the respondents are numerate and well sampled, the behaviour captured should be representative of the population as a whole. These surveys typically record all modes of transport, but filtering by mode of transport and grouping according to vehicle ID allows the usage of individual vehicles to be extracted.

The predominant data source used in this research was the UK National Travel Survey (NTS) [214], which has been carried out annually since 2002. Participants record all of their journeys for a week, and the trial periods are staggered throughout the year. The full data set includes the time, distance, purpose and mode of transport of nearly 2 million journeys – from which more than 100,000 private vehicles’ usage can be extracted.

Figure 3.1 shows three example week-long vehicle usage profiles extracted from the NTS data. Each vehicle is shown on a separate subplot, the time of day is shown on the horizontal axis, the weekday on the vertical, and shaded areas show times that the vehicle was in use. It can be seen that the second vehicle has a regular commute on the weekdays, while the other two show sporadic use.

Households are randomly invited to complete the travel survey based on post-code, however there is some participation bias introduced by non-respondents (in general those living in the most urban areas are less likely to respond to the invitation). The geographic and rural-urban variation in participants and shown in Figure 3.2. There are four rural-urban categories used in the NTS: ‘urban conurbation’, ‘urban city & town’, ‘rural town’, and ‘rural villages, hamlets & isolated dwellings’ (listed in order of increasing sparsity). Areas are classified based on population density and sparsity of dwellings, and the government publishes the classification of each census area in the UK [215]. It can be seen that the percentage of households within a local authority included in the NTS sample vary between 0.3% and 1.2%, meaning some areas are sampled four times more rigorously

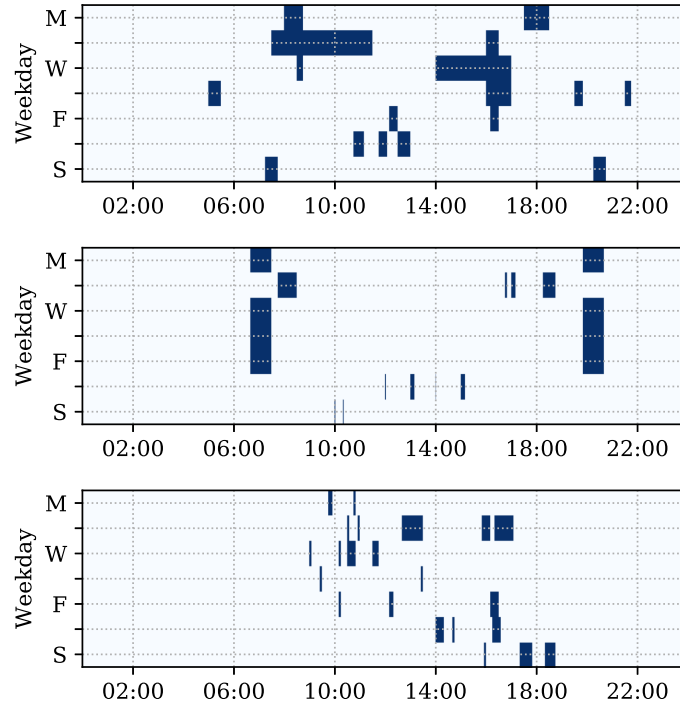
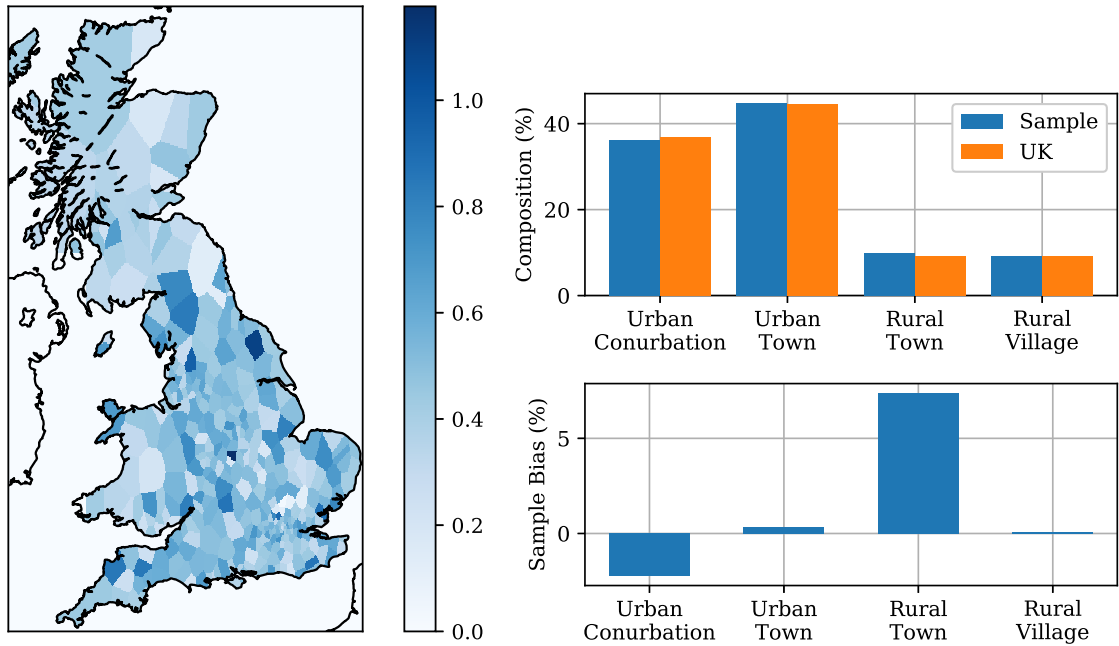


Figure 3.1: Three example vehicle usage profiles from the NTS data. Time of day is on the horizontal axis, weekday on the right, and blue indicates that the vehicle is in use.

than others. The figure also shows the percentage difference between the proportion of NTS respondents from each classification and the national proportion. The rural-urban skew of the overall sample is less significant than the geographic skew, however cities are notably under-sampled, and rural towns over-sampled. The urban-rural bias should be corrected for when simulating the national vehicle demand, because vehicle usage is significantly higher in rural areas.

For the Texas case study the US National Household Travel Survey (NHTS) was used [216]. This was carried out in both 2009 and 2017, at staggered periods throughout the year. In this case, households only recorded a single day’s travel behaviour, but there was a larger number of participating households. Similar parameters were recorded to the NTS, and the dataset included just under 60,000 vehicles from Texas. Due to non-affiliation with a US research institution, it was not possible to get a geographic breakdown of the NHTS data beyond the resident State.

The most relevant information when it comes to predicting the future charging behaviour of a vehicle are the distance it has travelled and the times it is available to charge. The focus of this thesis is on home charging, and it is possible to infer from the purpose



(a) % of households sampled by location

(b) Rural-urban composition of sample

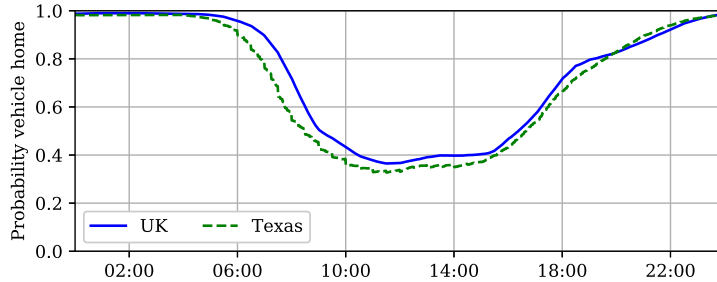
Figure 3.2: The geographic and rural-urban variation in the NTS sampled households.

of the recorded journeys when the vehicles are at home. Figure 3.3 shows the probability distribution function of daily mileage and probability of a vehicle being home with time, for both the UK and Texas datasets. The average distance travelled by the Texas vehicles was significantly higher, although this could be in part attributed to the fact that the trial period was shorter and unused vehicles are not declared – meaning vehicles that are not used every day may be excluded from the data. The probability of being at home is similar for both datasets, although Texan vehicles are slightly more likely to be away from home in the middle of the day. In both cases a large percentage of the fleet are home at any given time, so home charging is likely to offer a large amount of flexibility.

In this thesis, the travel survey data will be used to predict the energy demand of vehicles at high levels of aggregation – e.g. nationally, or at the transmission system level. Where possible, it also will be used to estimate the geographic variation in future charging demands.



(a) Distribution of daily driven distance.



(b) Probability of a vehicle being at home throughout a weekday.

Figure 3.3: A comparison of the driving behaviour exhibited in the two travel surveys.

### 3.1.1.2 EV Trial Data

Early scale EV trials have started to record the way consumers are actually charging. These trials provide valuable information about charging behaviour, but are small and typically opt-in – meaning that a sample bias is likely.

This research uses data from My Electric Avenue (MEA) [217], a UK trial which finished in 2016. During the 18 month trial period 213 Nissan Leafs were loaned out to households, with the caveat that all of their vehicle use and charging would be recorded and available for research purposes. The households were located in geographic clusters, and the trial was opt-in. This means that the behaviour captured is likely to represent early-adopters of EV technology and those living in the trial areas, but not the national as a whole. A rigorous analysis of the data from this trial is presented in [131].

In the vehicle usage data, the distance, time, and energy consumption of each journey are recorded. In the charging data, the time and SOC of the EV at the start and end of each charge are logged. All the vehicles had a 24 kWh battery so it was possible to infer the SOC of the vehicle at all times. An example usage profile from the data is shown in Figure 3.4. The date is shown on the horizontal axis, time of day on the vertical, blue

areas show charging, and red areas show vehicle use. The vehicle takes one of three states at any time: driving (red), charging (blue), or not in use (white). It can be seen that in this case, the vehicle has a regular weekday morning journey, along with shorter sporadic journeys throughout the day, and charging occurs almost exclusively at night.

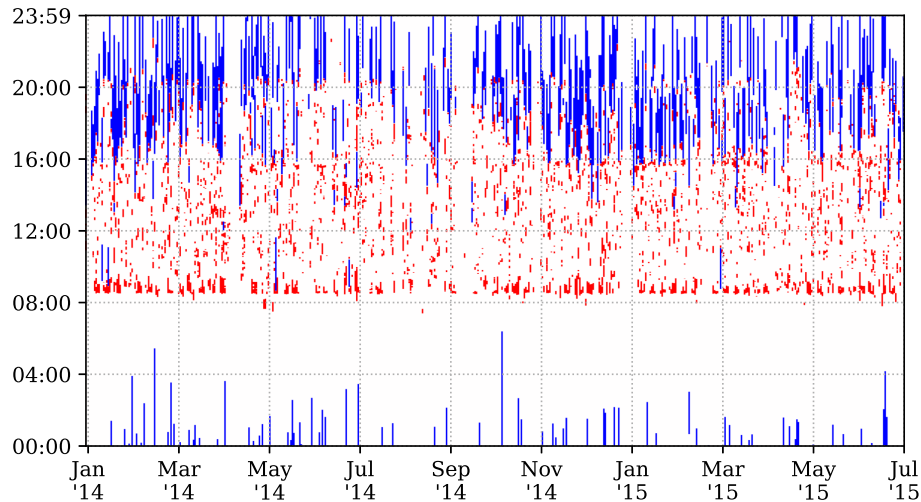


Figure 3.4: An example vehicle usage profile from the MEA data. Date is on the horizontal axis, and time on the vertical. Red shows vehicle use and blue shows charging.

For the Texas case charging data was used from a US smart metering trial, Pecan Street [218]. This study included metering at the charge point, but not any within the vehicle. This means that the power demand of the charge point at 1 minute resolution was available, but no details about the vehicle SOC or driving schedule – also, it is worth noting that there could be more than one vehicle using the charge point. An example household’s charging profile is shown in Figure 3.5, where charging is shown in dark blue but driving data is unavailable. The length of recording period and the time resolution are similar to the MEA data, however only the charging data is available.

In this thesis, EV trial data will be used to perform case studies on single residential networks, and to parameterise the model for uncontrolled charging that is developed in Section 4.1.2.

### 3.1.2 Cluster Analysis

Clustering is a method of identifying patterns in large datasets. There are several advantages to applying clustering algorithms to the vehicle usage data: firstly, it allows

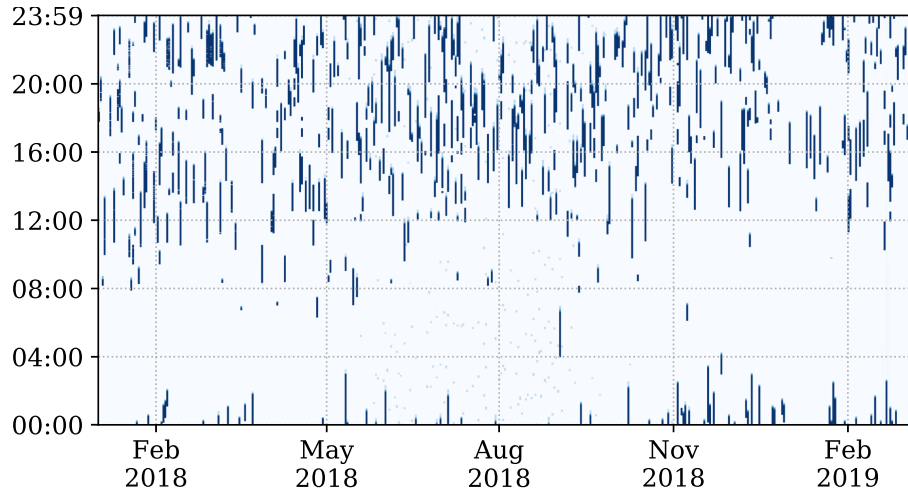


Figure 3.5: An example vehicle usage profile from the Texas Pecan Street data. Date is on the horizontal axis, and time on the vertical. Shaded areas shows charging.

visualisation of the way the fleet of vehicles is being used, which is not otherwise possible for very large datasets; secondly, more insightful comparisons can be made between the vehicle use described in the various datasets; finally, it allows vehicle use to be reduced to a one-dimensional parameter, which is later used as a model input.

In this section clustering is performed on both the UK and Texas travel survey data, and the resulting clusters are analysed and compared.

### 3.1.2.1 Algorithm

Every point in the data to be clustered is defined by a feature vector, which contains a collection of variables that distinguish the data points. The variables can have different units, but are normally scaled across the dataset to prevent one variable from having a proportionally larger impact on the result. Clustering groups the data according to similarity of feature vectors, as defined by some distance metric. Any function  $d$  can be used as a distance metric, providing that it is symmetric and strictly non-negative, such that it satisfies:

$$d(x_1, x_2) = d(x_2, x_1) \quad (3.1)$$

$$d(x_1, x_2) \geq 0, \quad (3.2)$$

for all  $x_1, x_2$ . In addition to the choice of feature vector and distance metric, the clustering algorithm used will affect the chosen clusters.

Clustering algorithms can be split into: connectivity-based, centroid-based, distribution-based, and density-based. In connectivity-based, points that are close to each other are successively joined, until clusters are formed. In centroid-based, clusters are defined by centroids (a representative point within the group), and points added to the cluster whose centroid they are closest to. In distribution-based, clusters are defined by probability distributions, and points are assigned according to maximum likelihood. In density-based, clusters are created in areas with a high density of points, and low density areas are assumed to be noise.

While each of these subsets have their own advantages and disadvantages, here centroid-based clustering was chosen due to its relative computational simplicity. The travel survey data is very large – both in number of points, and the amount of information attached to a single point. This means that computational complexity was the most important consideration for this exercise.

K-means clustering is a special case of centroid-based, where the number of clusters is known and Euclidean distance is used as the distance metric. The K clusters are each defined by a centroid, given by:

$$\mathbf{y}^{(c')} = \frac{1}{N_{c'}} \sum_i^{N_{c'}} \mathbf{x}_i^{(c')}, \quad (3.3)$$

where  $\mathbf{y}^{(c')}$  is the centroid of cluster  $c'$ ,  $\mathbf{x}_i^{(c')}$  is the feature vector of the  $i$ th point belonging to cluster  $c'$ , and  $N_{c'}$  are the total number of points in that cluster. The clusters are chosen so as to minimise the average distance of a point from its centroid, and the quadratic form of the distance metric means that this is equivalent to minimising the inter-cluster variance. The standard algorithm for applying K-means is as follows:

1. Initialise cluster centroids as randomly chosen points.
2. Add each point to the cluster whose centroid is closest to it.
3. Update the centroids as the mean of the points assigned to it.

4. Repeat 2-3 until convergence is achieved.

To begin,  $K$  points are selected at random, and these are used as the initial cluster centroids. Then another point from the data is chosen at random and the euclidean distance of that point to each of the centroids is calculated. The point is assigned to the cluster whose centroid is the smallest distance away. This process is then repeated until all points have been assigned to a cluster. The cluster centroids are then updated so that they become the average of the points in that cluster and all points are removed from all clusters. Points are then added to the cluster whose centroid they are now nearest to, which may have changed following the update. This algorithm is repeated until the cluster centroids stop changing – i.e. until there is an iteration where none of the points move cluster.

Convergence of this algorithm is guaranteed, however it is not guaranteed to find the global optima – the final result may depend on the initialisation chosen. Therefore, it is common to test the algorithm with several starting points. In general k-means can be solved in time  $\mathcal{O}(ns^{dk+1})$ , where  $n$  is the number of points,  $d$  is the length of the feature vector, and  $k$  is the number of clusters [219]. Thus, heuristic algorithms are normally used instead – such as Lloyd’s algorithm which has running time  $\mathcal{O}(ndki)$ , where  $i$  is the number of iterations needed for convergence. Typically  $i$  is small, but at worst case the algorithm becomes super-polynomial [220].

The main drawback of K-means is that, in order to retain the computational advantage, the number of clusters  $K$  must be chosen in advance. While there exist metrics for quantifying the performance of clustering algorithms, here only K-means is explored as it produced useful results. This follows the practice outlined in [221], which states that clustering is an art as well as a science, and the success of a clustering exercise can not be measured by simple metrics – it depends on the reason for clustering and the way the results are to be used.

In this case, the data to be clustered is the usage of vehicles recorded in the NTS. The objective of this exercise is to identify vehicles that could be grouped during modelling of charging. In order to model and optimise a vehicle’s charging, it is important to know

how much and when the vehicle is being used. Here, each vehicle-day is considered as a separate data point, as vehicles may be used in different ways on different days. The data is split into weekday and weekend driving, as driver behaviour is observed to be significantly different between the two [222].

In this case 48 features were chosen, each quantifying the distance travelled by the vehicle in a 30 minute time period. This time resolution was chosen because it was considered to be a compromise between computational cost and precision. Additionally, due to human rounding, the travel survey data was assumed to be inaccurate at any lower time resolution. The feature vector was then normalised – so that the features of an individual vehicle sum to 1. Normalising is a normal choice with profiles to prevent high use vehicles from being a large distance from all other points. Normalising sacrifices the precise total distance travelled, however vehicles travelling further are likely to be used for longer, so this information is still captured. As an example, Table 3.1 shows the raw data and corresponding feature vector corresponding to one vehicle-day. In this case the vehicle has an outward and return journey of equal length, but the return journey takes longer due to congestion. The majority of the features are zero (indicating that the vehicle is unused for the majority of the day) and the features corresponding to the trips take different values, representing the different speeds. Further examples can be seen in Figure 3.6, which shows the feature vectors created from one vehicle one three consecutive days.

Trip	Start time	End time	Distance (miles)
1	07:20	07:59	20
2	16:00	16:59	20

Feature	Value (mph)
1-14	0
15	10
16	30
17-32	0
33-34	20
35-48	0

Table 3.1: Example vehicle-day from data and corresponding un-normalised features.

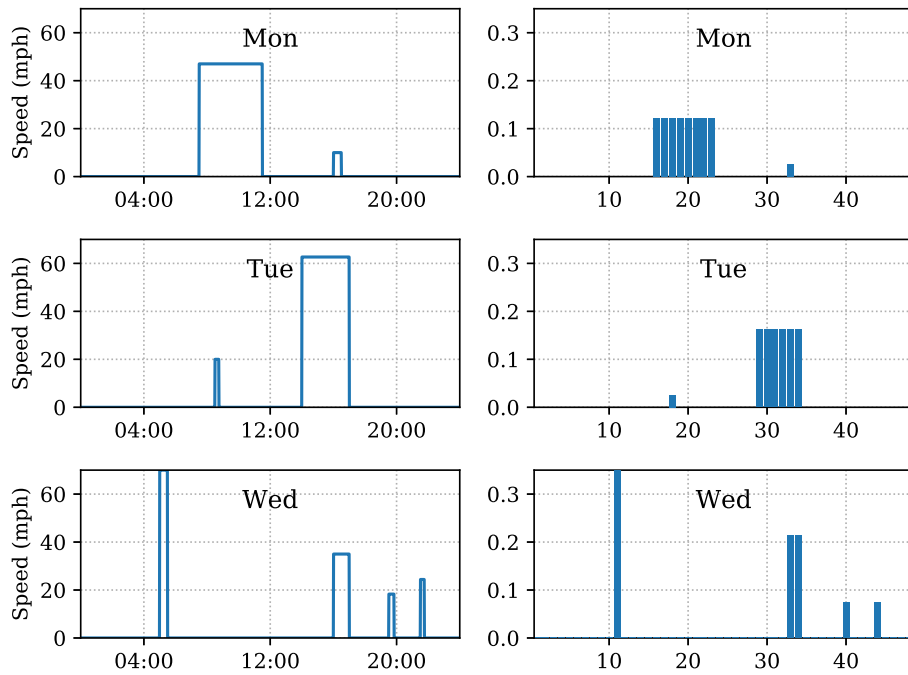


Figure 3.6: (l) three days of a NTS vehicles' usage; (r) the corresponding feature vectors.

The main drawback of this approach is that the time periods are treated as independent by the distance metric. Figure 3.7 illustrates this problem using three example feature vectors. The left figure shows the three feature vectors superimposed; vectors (a) and (b) were created from the same vehicle usage, but with one shifted by 30 minutes, while vector (c) was created from a vehicle exhibiting entirely different behaviour. The second two figures show the absolute difference between (a)-(b) and (a)-(c) respectively. Euclidean distance defines the total distance between two points as the resultant of the absolute difference components. This means that the Euclidean distance between (a)-(b) and (a)-(c) will be the same, despite (a) and (b) seeming much more closely related. More complex methods are available for time series clustering (e.g. [223]), however the size of the NTS data size made these intractable.

One potential solution to this problem is to apply a smoothing filter to the feature vectors before clustering. As with all averaging, this results in some loss of information, but also links features that are next to each other in time. Figure 3.8 shows the same three feature vectors, but with Gaussian filters applied to them. It is clear that using Euclidean distance (a) and (b) will now be much closer than (c) even though the features are considered independently. If this method is used the width of the smoothing filter

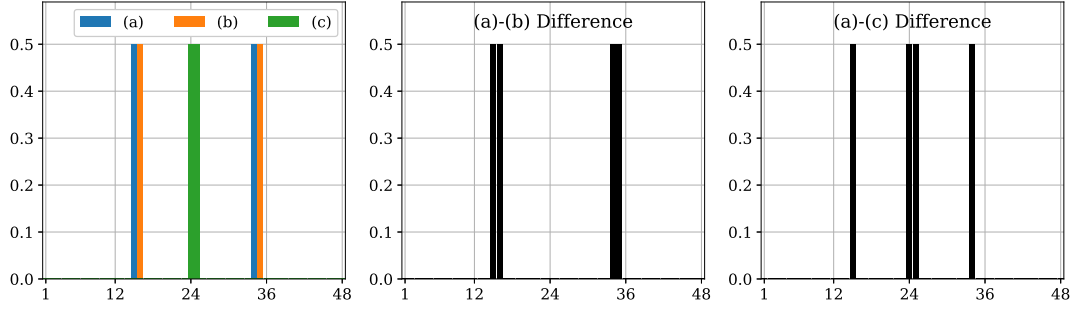


Figure 3.7: Three feature vectors that are equidistant, despite (a) and (b) being similar.

must be chosen carefully, as there is a trade-off between linking related times and losing information.

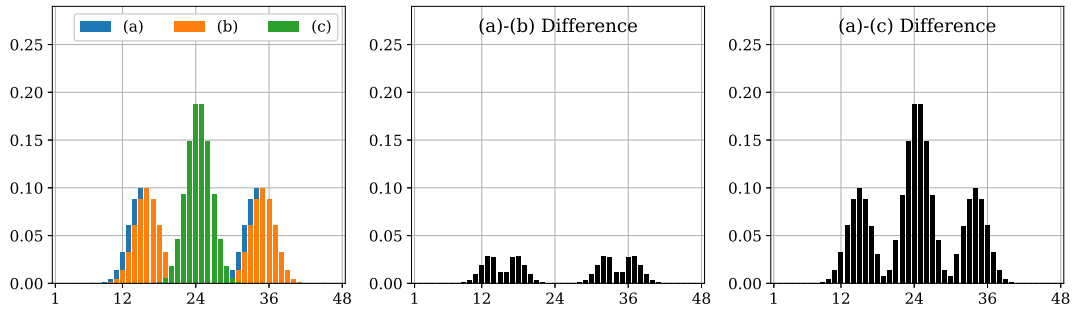


Figure 3.8: The filtered feature vectors, (a) and (b) are now much closer than (c).

In order to run the K-means algorithm the number of clusters,  $K$ , needs to be defined. Various heuristic methods have been proposed to do this, and here the elbow method is followed (e.g. [224]). This method dictates that  $K$  is found by plotting the variation of *sum of squares* with number of clusters. Sum of squares is defined as:

$$SoS = \sum_i^N \left\| \mathbf{x}_i^{(c)} - \mathbf{y}^{(c)} \right\|^2, \quad (3.4)$$

where  $N$  is the total number of data points across all of the clusters. This is a measure of inter-cluster variance, and will necessarily decrease as  $K$  is increased.  $K$  is then chosen at the *elbow* (or the corner point) of this curve, where the reduction in variance achieved by an additional cluster is no longer significant. Typically, this point is determined by eye. Figure 3.9 shows the curve for both the weekday and weekend data, in both cases  $K=3$  was selected. Implicitly there is an extra cluster containing vehicles which are not used in that day; these all have zero feature vectors and are removed before the clustering

process. It is worth noting that the sum of squares is higher for the weekend data than the weekday, even though there are fewer weekend days. This shows that weekend driving behaviour is more variable, meaning it is likely harder to predict and model.

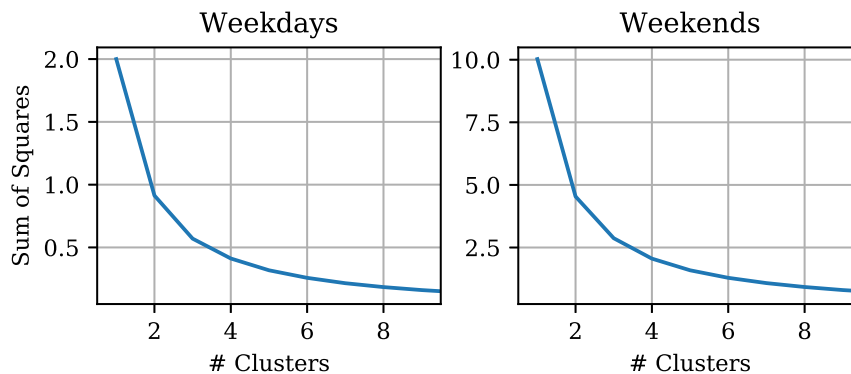


Figure 3.9: The variation of sum of squares with number of clusters for both the weekday and weekend datasets.

### 3.1.2.2 Resulting Clusters

Figure 3.10 shows the representative speed profile of vehicles from each cluster. The solid lines shows the average values and the shaded area covers 90% of the values in the cluster. These are not the same as the cluster centroids, because the points are not normalised before averaging. This allows the average speed information to be visualised, which is lost in the centroid. For the weekdays: cluster 1 is dominated by evening use, 2 by morning use, and 3 follows a typical commuting pattern – these will hereafter be referred to as evening drivers, morning drivers, and commuters. In the weekends: clusters 1 and 3 suggest a single short journey at different times, while 2 shows more distributed use throughout the day – hereafter these will be referred to as morning single use, midday single user, and high use respectively.

Further insight can be gained by analysing the relative size of the clusters, and how likely an individual vehicle is to belong to the same cluster on consecutive days. Figure 3.11a shows the cluster composition by weekday, where U indicates the vehicle which were unused on that day. Across the weekdays vehicle use is fairly consistent, although there are slightly fewer commuting vehicles on Mondays and Fridays. Saturday and Sunday

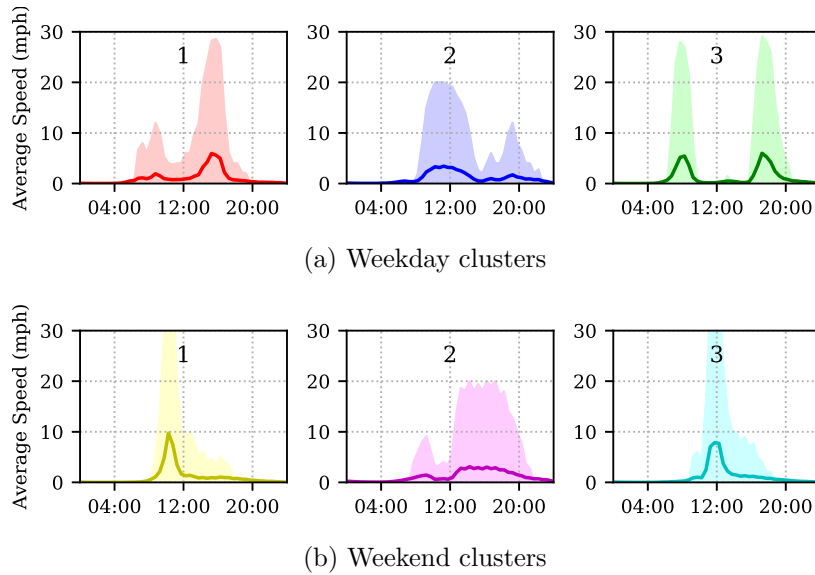


Figure 3.10: The average speed profile of the vehicles in each cluster. The lines show the mean values, and the shaded areas cover the 90% confidence interval. There is no significance to the ordering of the clusters.

use differs more drastically, with all modes of vehicle use being less common on Sundays, particularly high use vehicles. Given that the average use of vehicles is much lower at weekends, the majority of simulations in the results chapters will focus on weekdays. The cluster transition probabilities are shown in Figure 3.11b, these give the probability of a vehicle in any weekday cluster belonging to each cluster on the next day. The most likely estimate in each case is that the vehicle remains in the same cluster, particularly commuting vehicles which have a 62% chance of also commuting the next day. However, in all cases there is a significant chance that vehicle use will be different on consecutive days – in fact, for the morning and evening drivers it is more likely that they will change cluster than not. This result demonstrates that there is variation in individual vehicle use, as well as between vehicles – meaning that uncertainty in vehicle use is likely to be high, even once historical data is collected.

The clustering exercise was repeated using the Texas travel survey, and the resulting clusters are shown in Figure 3.12. These clusters map directly to the ones found from the UK travel survey, although there are some notable differences. The confidence intervals cover higher speeds for all clusters (note the different y axis limit), and the peaks are wider (suggesting longer journey times). These differences makes sense, given the mileage

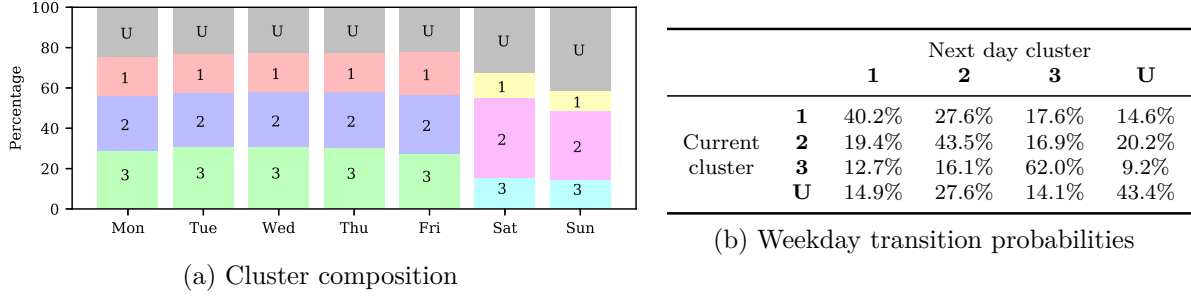


Figure 3.11: The variation in cluster composition throughout the week, and the probability a vehicle changes usage cluster the net day. U indicates the vehicle was unused.

was shown to be higher in the Texas travel survey.

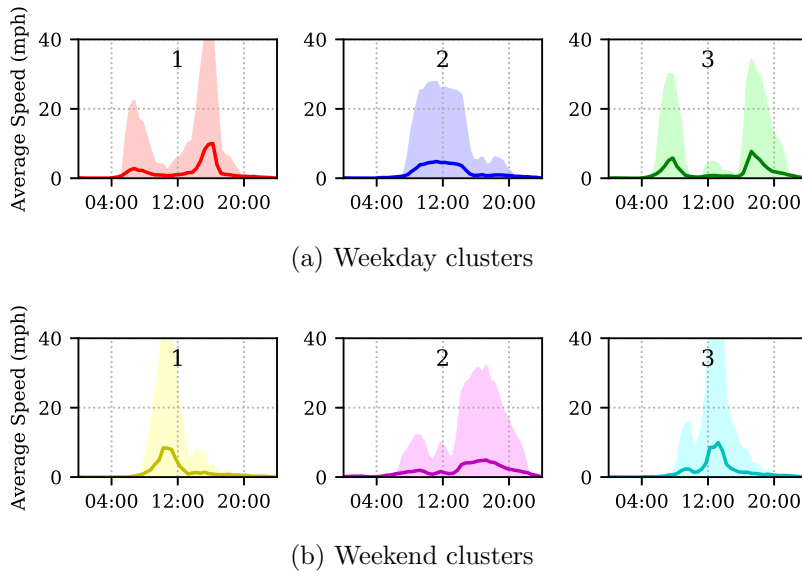


Figure 3.12: The clusters found from the Texas NHTS data, analogous to Figure 3.10

The weekday breakdown of the observed cluster are shown in Figure 3.13. Note that as each vehicle in the travel survey is recorded for only one day, it is not possible to investigate the unused vehicles or transition probabilities. Again, usage across weekdays is fairly consistent, and more notably different between weekend days. However, in this case it is hard to make meaningful comparisons between Saturday and Sunday driving without knowing the percentage of vehicles that are unused. Also, the comparisons are less reliable because each day includes a different set of vehicles.

It is not possible to compare Figure 3.13 to the UK cluster breakdown, not only due to the effect of the unused vehicles, but because the cluster centroids are not identical. In order to make a more precise comparison between the two datasets, the Texas vehicles

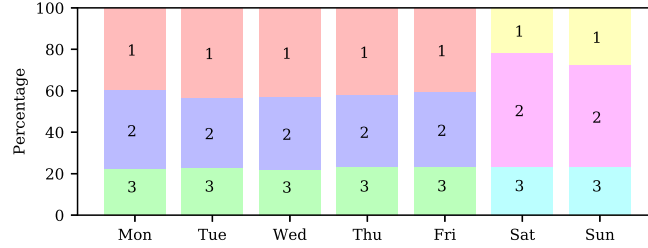


Figure 3.13: The variation of cluster composition of the Texas vehicle with weekday.

were reclustered using the centroids from the UK clustering. This means an iterative process was not necessary, for each Texan datapoint the nearest UK cluster centroid was identified. Figure 3.14 shows the comparison between cluster composition of the two fleets. During weekdays there were comparatively fewer commuting vehicles in the Texas data, and high use vehicles were significantly more common at the weekends.

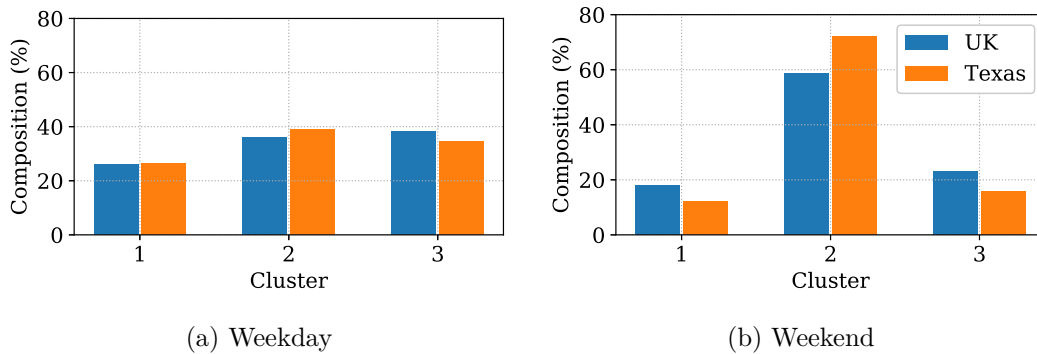


Figure 3.14: A comparison of the cluster composition of the Texas and UK clusters.

### 3.1.3 Comparing the Electric and Conventional Fleets

In addition to comparing the UK and Texas vehicle usage captured in the respective travel surveys, we can also compare the usage captured in the EV trial (MEA) with the UK travel survey (NTS). MEA provides the best available evidence for EV user residential charging behaviour in the UK. However, the vehicle use exhibited represents a biased set of drivers – 67.3% of participants were male, and 41% were within the 40-49 age bracket. Quantifying this bias allows the likely error from extrapolating this trial data to represent a large fleet of vehicles to be predicted.

Some direct comparisons from the raw vehicle usage data are shown in Figure 3.15.

The MEA vehicles are used more frequently at both weekdays and weekends, and travel further on weekdays. The vehicles show relatively similar usage profiles – note that the saw tooth shape in the NTS data in Figure 3.15c is likely due to the fact that the NTS data is recorded by hand, and participants have the tendency to round to the nearest whole hour.

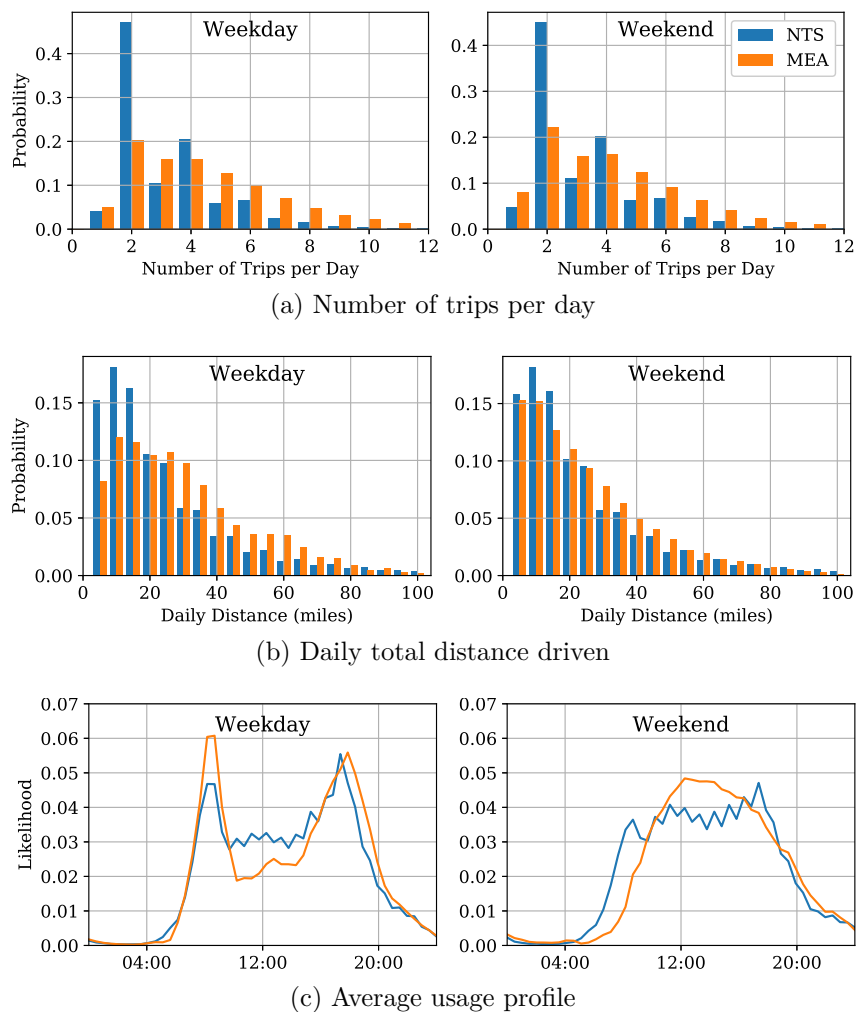


Figure 3.15: A comparison of the trip frequency, distance, and timings of vehicles from the NTS and MEA data.

We can further compare the usage of the vehicles by creating equivalent feature vectors from the MEA data and classifying points according to the clusters defined in Section 3.1.2.2. By comparing the cluster composition of the datasets, modes of vehicle use that are over represented in the trial data can be identified. Figure 3.16 shows the distribution of clusters for both datasets, and Table 3.2 shows the average daily distance travelled by vehicles in each cluster.

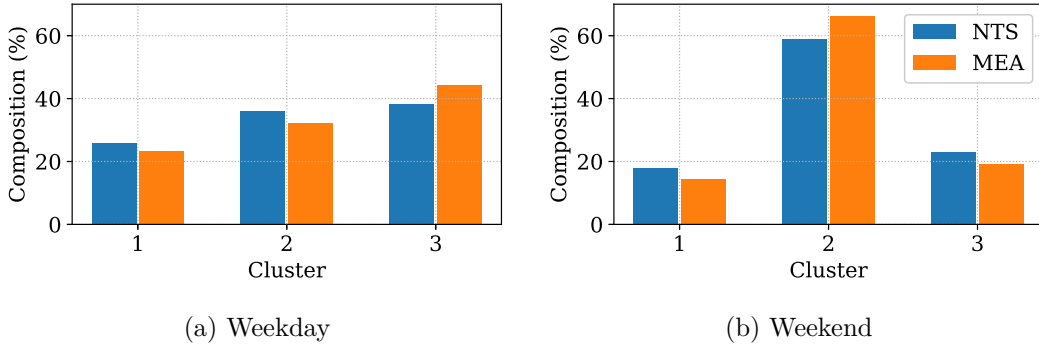


Figure 3.16: A comparison of the cluster composition of the NTS and MEA data.

	NTS Cluster			MEA Cluster		
	1	2	3	1	2	3
Weekday	25.4	25.4	27.2	28.8	29.3	29.7
Weekend	23.9	28.1	25.2	22.5	26.5	24.6

Table 3.2: The average distance travelled by each cluster (miles)

The cluster composition is broadly similar, although there is a slight bias in the MEA data towards weekday commuters. However, distance travelled varies more significantly – all weekday clusters travel further than average and all weekend clusters travel shorter distances. Overall the average MEA driver travels 12% further than the average NTS driver on a weekday. Therefore, using the MEA data to directly forecast future charging will overestimate the energy requirement, and likely also the peak demand.

## 3.2 EV Sales Projection

EV sales are currently unevenly distributed across the UK, and this means that some areas of the power system will be impacted earlier than others. Therefore it is useful to consider which areas are likely to see high penetrations of EVs first, and estimate when these levels might be achieved. Technical transitions are often modelled using s-curves [225], which are described by the equation:

$$y(t) = \frac{1}{1 + \alpha e^{-\beta t}}, \tag{3.5}$$

where  $t$  is time, and  $\alpha, \beta$  are parameters which determine the speed and shape of transition. The limits of the equation are 0 and 1, which is one of the reasons it is suited for describing transitions. Several example s-curves with different vales of  $\alpha$  and  $\beta$  are shown in Figure 3.17. In general,  $\alpha$  governs the shape of the curve, and  $\beta$  the scale.

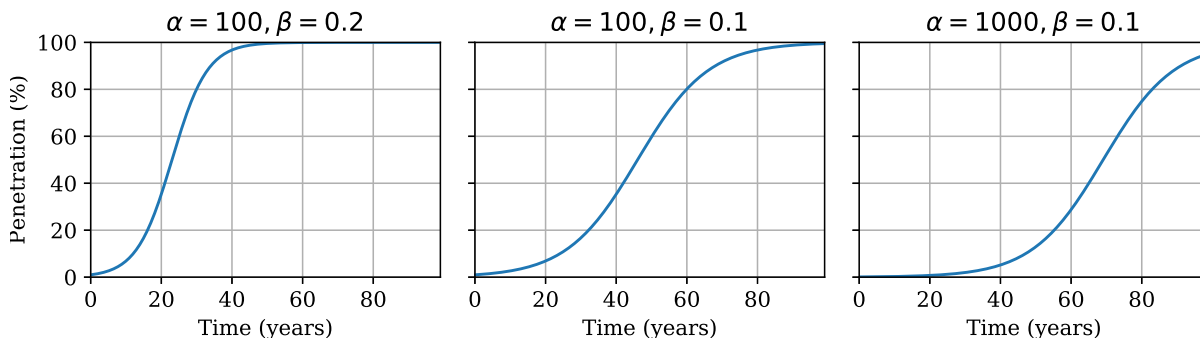


Figure 3.17: Several examples of s-curves with different parameters.

The Driver and Vehicle Licensing Agency in the UK publish quarterly vehicle registration figures, which give historic values for the number of vehicles in each local authority. The number of these vehicles that qualify as ‘ultra low emission’ are also published, from which the local EV penetration can be inferred. Fig 3.18 illustrates the process of finding the best fit s-curve for one of the regions. Finding the least-square values for  $\alpha, \beta$  is equivalent to finding the the best fit line on a set of log axis. This allows standard linear regression algorithms to be used, such as the *numpy polyfit* module.

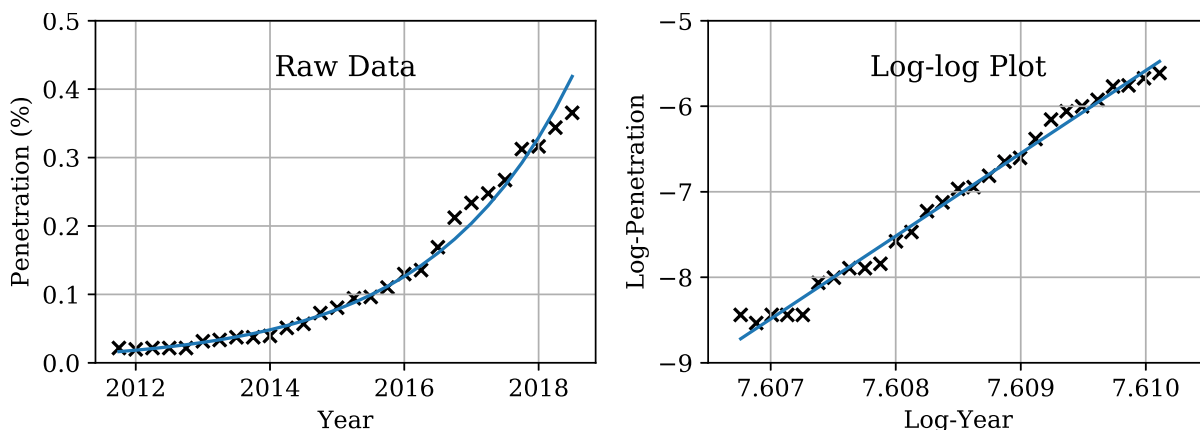


Figure 3.18: The s-curve fitting process for one example area.

Once separate s-curve parameters have been obtained for each local authority the penetration of EVs can be estimated for some point in the future. Figure 3.19 shows the geographic variation in EV penetration in 2020, 2025, and 2030. The fastest penetration

is observed in Peterborough, which is estimated to reach nearly 100% penetration by 2025, while there are many areas projected to still be below 20% penetration in 2030. Although extrapolations of these kind can not be taken with any serious confidence, it does allow meaningful comparison between local rates of adoption.

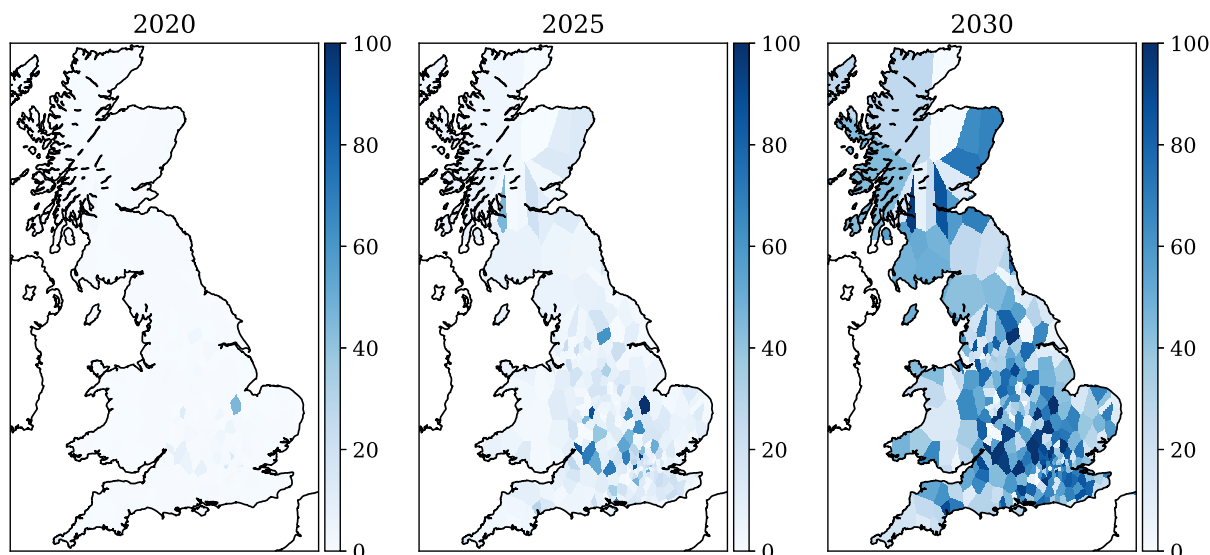


Figure 3.19: The projected regional penetration of EVs.

While it is important to consider the impacts of EV charging on the power system at 100% penetration, for short-term planning it is also important to know when these impacts are likely to be felt. Therefore, in the distribution system analysis in Chapter 6, both a 100% and the projected 2030 scenario are considered.

### 3.3 EV Energy Consumption

In order to use travel data from conventional vehicles to estimate EV demand, a method is required for predicting the energy consumption of each vehicle if it were electric. The consumption of a vehicle depends not only on its driving pattern, but on the vehicle shape, mass and drivetrain.

In this section, methods of estimating vehicles' energy consumption from their driving patterns are discussed. First, a detailed tank-to-wheel model is proposed, then a first order approximation is given for a variety of vehicles.

### 3.3.1 Tank-to-wheel Model

A tank-to-wheel model is a model which predicts the energy consumption of vehicles over a given drive-cycle. A drive-cycle is essentially a trace of the vehicle's velocity. For conventional vehicles, very high fidelity models have been developed – which individually model the physical components in the drivetrain. However, for EVs there are much fewer components in the drivetrain so it is suggested that a lower fidelity model can achieve a good performance.

Such a model would have two useful applications. First, it would allow the energy consumption of a vehicle to be estimated using GPS data – meaning users could predict the battery size they would require if they switched to an EV. Second, the model could be fit to more representative drive-cycles to give a more accurate set of consumption per mile numbers.

In order to estimate the energy a vehicle requires, first consider the force which the wheels must overcome at a given time  $t$ , which can be expressed as:

$$F_t = ma_t + mg \sin(\theta_t) + F_t^{res}, \quad (3.6)$$

where  $m$  is the vehicle's mass,  $g$  is the gravitation constant,  $a_t$  is the vehicle's acceleration,  $\theta_t$  is the slope of the road, and  $F_t^{res}$  is the resistive force. Resistive force is commonly broken down into a constant term, one proportional to velocity and one to velocity squared [226]. It is therefore assumed that the resistive force at time  $t$  is given by:

$$F_t^{res} = f_0 + f_1 v_t + f_2 v_t^2, \quad (3.7)$$

where  $v_t$  is the velocity at time  $t$  and  $f_0$ ,  $f_1$ , and  $f_2$  are called the coast-down coefficients. Overcoming this force requires a power of

$$P_t = F_t v_t \quad (3.8)$$

at the wheel-axle. Substituting (3.7) and (3.6) into (3.8) and utilising a backwards-

difference approximation (e.g. [227]) for the acceleration term we arrive at:

$$P_t = f_0 v_t + f_1 v_t^2 + f_2 v_t^3 + m \frac{v_t - v_{t-1}}{\Delta t} v_t + mg \sin(\theta_t), \quad (3.9)$$

where  $\Delta t$  is the size of the time-step. The power required from the vehicle's battery will not be equal to the power required at the wheel-axle; there will be some losses in the drivetrain which must be accounted for. The amount of power lost will depend largely on the vehicle, but also on the drive cycle and external conditions. Here we make the simplifying assumption that the power required from the 'tank' at time  $t$ ,  $P_t^{req}$ , is given by:

$$P_t^{req} = \begin{cases} P_0 + \eta P_t & \text{for } a_t < 0 \\ P_0 + \frac{1}{\eta} P_t & \text{for } a_t > 0 \end{cases} \quad (3.10)$$

where  $P_0$  is a constant power loss, and  $\eta_v$  is an efficiency specific to the vehicle. This is a significant simplification, however, by learning this value from real-world data, unmodelled complexities can be absorbed. For example, EVs will often use regenerative braking, which isn't explicitly modelled here, but this will be reflected by higher values of  $\eta_v$ . This first order model for losses was chosen in order to reduce the number of introduced parameters, if a large amount of data were available, a higher fidelity model could be used. The total energy expenditure requirement,  $E$ , of a journey will then be given by the area under the power requirement curve, such that:

$$E = \sum_{t=1}^T P_t^{req} \Delta t. \quad (3.11)$$

There are several parameters in this model, which must be chosen before the model can be applied. Here these are fit using data published by the Environmental Protection Agency (EPA), who carry out standard testing on every vehicle available for sale in the US [228]. The testing is geared towards conventional vehicles, so many of the recorded parameters (e.g. engine size) are not valid for vehicles without an internal combustion

engine. However, some fuel consumption results are included for EVs and these will form the basis of the proposed energy consumption model.

Empirical values for the coast-down coefficients,  $f_{0,1,2}$  are included in the dataset. These are determined from a coast-down test, where a vehicle is brought up to a specific speed and allowed to decelerate with the engine turned off [229]. It should be noted that the effect of weather and road surface on resistive force is implicitly ignored in this relationship.

In addition to the coast down test, the energy consumption of the vehicle over two standard drive cycles are recorded. The drive cycles used in this testing are shown in Figure 3.20; one represents urban style driving and one represents highway driving. While these consumption figures give an idea about the relative fuel consumption of vehicles, there has long been concern about whether these tests are representative of consumer driving behaviour. In [230] it is reported that 55% of hybrid vehicles missed their EPA fuel economy rating by more than 10% using real-world driving. However, by using the results to parameterise the tank-to-wheel model, a vehicle’s consumption using other drive-cycles can be predicted.

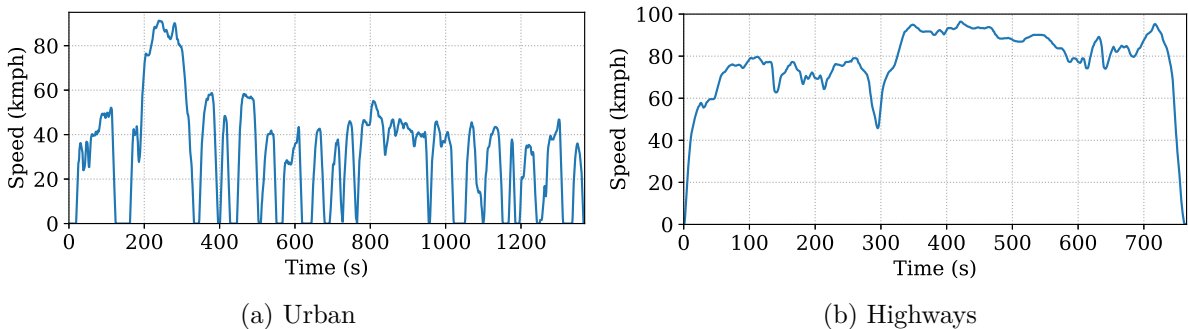


Figure 3.20: The two standard drive cycles used in the EPA testing.

The EPA data includes  $2n$  known energy consumptions, where  $n$  is the number of EVs in the dataset, one for each of the standard drivecycles. As of 2019, there were 50 different EVs in the dataset, although many of them are different versions of the same car – e.g. Teslas with different battery capacities. This means a maximum of  $2n - 1$  parameters can be learned from the data while preventing overfitting. Therefore, it was decided to assume that  $P_0$  is constant for all vehicles, while  $\eta$  is unique to the vehicle. If

this model were fitted to more data, then this assumption could be relaxed.

Parameters were chosen so as to minimise the mean square error of the model on the observed data. The resulting errors are shown on a quantile-quantile plot in Figure 3.21. The  $y=x$  line demonstrates where the points would lie if zero-error were achieved, note that this plot has a false origin. The model achieves a reasonable fit over both drive-cycles, with an root mean square error of 0.15 kWh. As an example, the parameters of the model chosen for the Nissan Leaf are shown in Table 3.3.

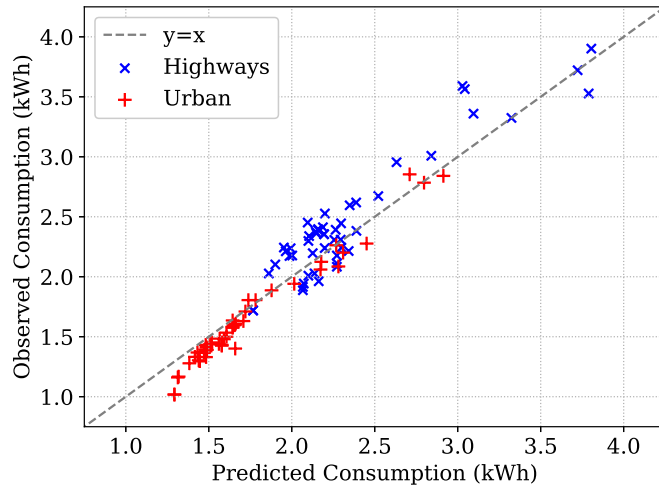


Figure 3.21: A quantile-quantile plot of the vehicle model performance for 50 different EVs over the two recorded drive cycles

$m$ (kg)	$f_0$ (N)	$f_1$ (Nsm <sup>-1</sup> )	$f_2$ (Ns <sup>2</sup> m <sup>-2</sup> )	$P_0$ (kW)	$\eta_v$
1704	150	0.615	0.508	1.31	92.0%

Table 3.3: Nissan Leaf Model Parameters

To illustrate the difference that the vehicle-specific coefficients have on the energy consumption, Figure 3.22 shows the predicted fuel economy versus speed for three different EVs. This was produced assuming zero acceleration and slope, such that the consumption depends only on the resistive force and the internal losses. While the three curves show similar shapes and all have maximum efficiency points around 40 kmph, there are significant differences. The BMW I3 out-performs the other two vehicles for all speeds considered, the Tesla performs badly at low speeds, whereas the Nissan Leaf performs badly at high speeds. Note that constant speed driving does not take into account the

mass, so the vehicles' relative performance may change once acceleration or slope is included.

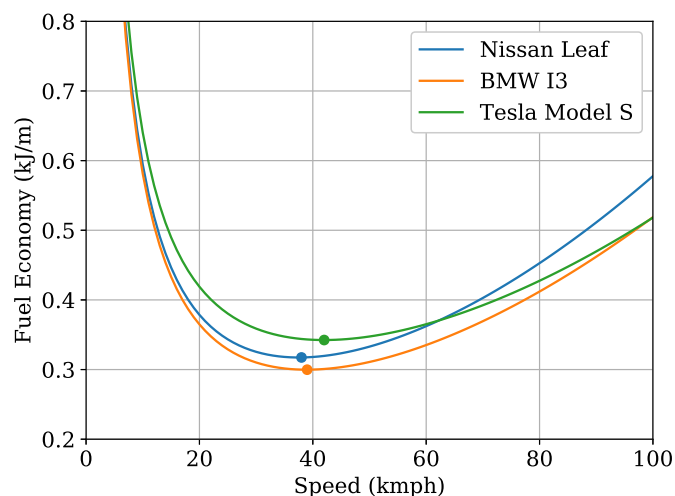


Figure 3.22: Predicted fuel economy versus speed for three different vehicles. The markers show the point of maximum efficiency.

If GPS vehicle data is available, real drive-cycles can be derived. Figure 3.23a shows the path travelled over a day by a goods delivery van (with co-ordinates removed), where the colour shows the elevation (from which the slope can be inferred). The consumption over the day was estimated using the model for the Ford Focus, and assuming a 60 kWh battery. Figure 3.23b shows the drive-cycle and predicted state-of-charge profile of the vehicle. In this case, the vehicle was in use for around half of the day, and only 40% of the battery capacity was used.

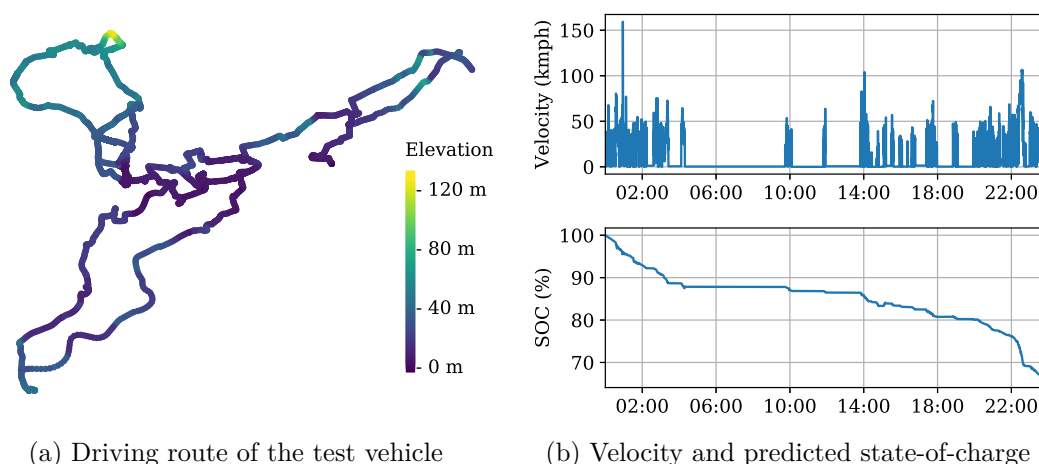


Figure 3.23: An example use of the tank-to-wheel model from GPS data.

This type of simulation is useful for small scale studies, where the behaviour of a small number of individual vehicles is to be analyzed. However, for prediction of the behaviour of a large fleet of vehicles this level of detail is unnecessary, and potentially infeasible (if the data is not available).

### 3.3.2 First-order conversion

In large scale analysis (where a very large number of vehicles is being aggregated) we need only be concerned with average behaviour; the law of large numbers says that when a large number of independent agents are aggregated the variance becomes very low. This means that average drive-cycles can be used to derive appropriate conversion factors which map driven distance directly to an energy consumption. While individual vehicles' consumption will not be accurately predicted, the fleet total consumption should be.

In 2004 a European research project, ARTEMIS, was completed [231]. The objective was to derive a common set of reference real-world driving cycles which are representative of real-world driving in Europe. Three drive-cycles were derived which represent rural, urban, and motorway driving respectively. The three profiles are shown in Figure 3.24. The proposed model is run for each of these cycles for every vehicle available in the EPA dataset, and the energy consumption per distance travelled is calculated in each case.

The conversion factors predicted for the most common EVs in the UK for each representative cycle are given in Table 3.4. Values ranging from 0.21 to 0.55 kWh/mile were observed, depending on vehicle and driving style. Rural driving was the consistently the most efficient driving style across all vehicles, while similar values were observed for urban and motorway driving – the urban drive-cycle was penalised by its frequent stopping, and the motorway drive-cycle by its speed. In general, vehicles with larger  $f_2$  terms performed worse on the motorway drive-cycle.

For the analysis in Chapters 5-7, unless otherwise specified, the conversion factors of a Nissan Leaf are used – as this is currently the most prevalent EV in the UK. It is worth noting that the model as it stands does not include the *accessory load* resulting from on-board electronics. While lights and entertainment could justifiably be neglected,

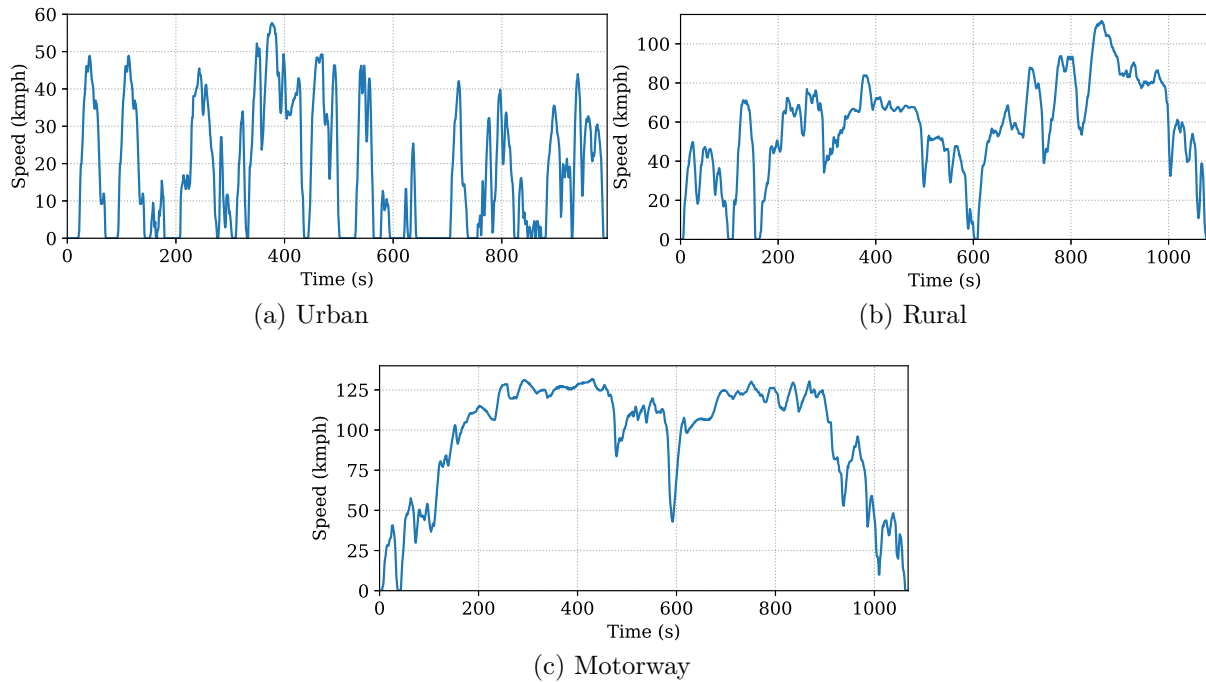


Figure 3.24: Three drive-cycles representative of European driving output from the ARTEMIS project.

heating and air conditioning do contribute a significant amount the overall consumption. Therefore, depending on the simulation being carried out, it may be appropriate to increase  $P_0$  by up to 1.2 kW to account for this load. It also should be noted that there are seasonal variations in road surface which may cause the energy consumption to be higher in the winter, and these are not accounted for here.

### 3.3.3 Concluding Remarks

In this chapter, methods for modelling vehicle use and predicted the future energy consumption of EVs were discussed.

Three distinct modes of weekday vehicle use were identified: morning drivers, evening drivers, and commuters. Similar proportions of these types of driver were found in the UK and Texas conventional vehicle data, but the EV trial data contained a disproportionately large number of commuting vehicles. This has implications when it comes to modelling charging, because the charging behaviour of commuters is likely to be significantly different from vehicles which remain at home all day.

S-curves were used to forecast the future EV population in different parts of the UK.

Model	Year	Consumption per Mile (kWh)		
		Rural	Urban	Motorway
Bluecar	2016	0.34	0.46	0.48
BMW I3	2016	0.21	0.29	0.29
BYD e6	2012	0.41	0.51	0.55
	2016	0.34	0.42	0.48
Chevrolet Spark	2016	0.21	0.31	0.30
Coda	2013	0.36	0.50	0.47
Fiat 500e	2015	0.22	0.32	0.30
Ford Focus	2016	0.25	0.34	0.35
Nissan Leaf	2012	0.26	0.35	0.37
	2016	0.22	0.30	0.33
Toyota Scion iQ	2013	0.20	0.27	0.28
Honda Fit	2014	0.21	0.30	0.29
Kia Soul	2016	0.23	0.30	0.35
Mercedes-Benz B-class	2016	0.32	0.46	0.41
Mercedes-Benz Smart	2016	0.23	0.30	0.37
Mitsubishi i-MiEV	2016	0.22	0.31	0.32
Tesla Model S 60R	2016	0.25	0.31	0.32
Tesla Model S 60D	2016	0.21	0.24	0.28
Tesla Model S 85D	2014	0.29	0.42	0.37
	2016	0.26	0.38	0.34
Toyota RAV4	2014	0.32	0.45	0.45
Volkswagen e-Golf	2016	0.24	0.33	0.31

Table 3.4: Consumption per mile of common EV models for each drive-cycle.

It is clear that some areas are going to reach high levels of EV penetration much earlier than others. This is particularly significant when it comes to predicting the impact of EV charging on the distribution system, because it is likely that some residential networks will see an EV penetration of 100% many years before this level is reached nationally.

A method was proposed for modelling the energy consumption of each commercially available EV, based on GPS trip data. For cases where this data is not available, linear coefficients were proposed to convert distance travelled into an energy consumption. Separate coefficients were found for different vehicle models and driving styles – ranging from 0.20-0.55 kWh/mile.

While energy consumption is useful for battery sizing, understanding the impact that charging will have on the power system requires demand profiles for EV charging. In

order to convert the predicted EV energy consumption into power demand profiles, the charging behaviour of the individual vehicles must be modelled.

# Chapter 4

## Modelling Vehicle Charging

Once the energy demand of a vehicle fleet has been predicted, the vehicles' charging behaviour must be modelled in order to assess the impact of charging on the power system. The timing and distribution of the charging demand relative to the existing demand will have a large effect on the impact of EV charging; if all vehicle charging is concentrated around the existing peak demand, the impact will be much worse than if charging is distributed throughout the day. This section therefore focuses on methods for estimating vehicles' charging demand profile.

Section 4.1 focuses on modelling uncontrolled charging. It is important that the impact that an uncontrolled fleet of vehicles would have on the system be quantified, so that the cost to the system of not implementing smart charging is understood. Two methods for modelling uncontrolled charging are described, and both are used in the analysis in Chapter 5. First the dominant model from the reviewed literature is explained; this is used so that the results in this thesis can be directly compared to existing results from other studies. Then, a novel method is proposed which stochastically models a vehicle's charging from its usage data.

In Section 4.2 methods for calculating the optimal controlled charging strategy are discussed. By comparing the impacts of uncontrolled and optimally controlled charging, the potential value that smart charging could provide is quantified. Standard optimisation problems from the literature are formulated for flattening load and minimising peak

demand, which are the simplest objectives for smart charging. Then, three novel strategies are proposed for co-ordinating EV charging. The first is a convex formulation for loss minimisation in multiphase networks, which is computationally comparable to flattening load, but requires detailed network information to formulate. The second is a modification to the standard load flattening problem to incorporate phase balancing, such that losses are reduced. Finally, a method for considering the relationship between converter losses and charging power is proposed. A wide range of objectives are required in order to address gap (*C*) from the literature review – a lack of comparison between smart charging strategies. All optimisation problems formulated in this section are convex, and this is important because the formulations need to have similar computational complexities to compare their action.

## 4.1 Uncontrolled Charging

Uncontrolled charging describes the way that vehicles will be charged without the presence of any demand shifting incentives. As the focus of this thesis is on domestic charging, it was assumed that access to a charger was not a limiting factor. Although it is not necessary to be able to correctly predict the charging of individual vehicles, the model needs to produce representative results at both small and large levels of aggregation.

Here two methods are presented; the first is taken from the first group of models described in section 2.2.2 of the literature review, and is used as a comparison to the standard practice; the second is a novel model which would fall within the second group of models.

### 4.1.1 Standard Assumption

The most common method of predicting charging from vehicle usage is assuming that charging begins immediately after the completion of the final journey of the day (e.g. [59, 61, 82, 103, 152, 188, 189]). This assumption was proposed before any domestic EV charging was observed, using the reasoning that this option would offer the most flexibility and

convenience to users.

There are two main problems with this method for modelling charging. First, that the natural diversity in users' charging is ignored. This is important because, diversity in behaviour results in a cancellation effect when demand is aggregated – meaning that the peak demand per vehicle of a large group of vehicles is likely to be lower than for a small group. Second, the domestic charging that has now been observed does not support this assumption; only 41% of charges recorded in the MEA data begun within 10 minutes of finishing their final journey, and only 70% of charging events were within 10 minutes of the completion of any journey.

In Section 4.1.2, a more complex model is formulated using the observed charging from MEA. However, there is a danger of overfitting the behaviour of a small group of drivers, when predictions are based on the charging observations from one study. Therefore, this method is kept as a means of comparison – with the understanding that it likely represents an overestimate of the peak charging power demand.

#### **4.1.2 Stochastic Model**

In this section a stochastic model for EV charging is presented, which is parameterised by EV trial data but can be applied to conventional vehicle travel survey data – thus combining the benefits of both sources of data. The success of a model like this can be quantified by the accuracy with which it predicts the observed trial data. Providing the model performance is good, insight on the likely regional variation in EV charging can be gained by applying it to the trial data.

The model presented here uses random variables to model both charging and vehicle use, allowing the conditional relationship between the two to be modelled using Bayesian statistics. In order to model vehicle use as a single variable, the clustering results from Section 3.1.2 are used.

The majority of charging observed in the MEA data immediately follows a journey. This means that, as there are only a small number of journey end times compared to the total number of time instances, the probability of a charge beginning at the end of a

journey is substantially higher than at another time. In order to tackle this, here charging after a journey is modelled with a separate variable than charging at an independent time. Hereafter, these types of charging will be referred to as *after journey* and *independent* charges and will be modelled using the random variables  $c_j$  and  $c_i$  respectively.

The variables considered to influence charging decision are: the vehicle's SOC, the time, and the usage cluster that the vehicle belongs to. Due to the quality and amount of data available, SOC is discretised into 6 states, and time is discretised into 48 half hour states. Formally, we therefore define the following random variables:

$$c_j \in \mathbb{Z}_2, \quad c_i \in \mathbb{Z}_2, \quad d \in \mathbb{Z}_2, \quad k \in \mathbb{Z}_3, \quad t \in \mathbb{Z}_{48}, \quad s \in \mathbb{Z}_6,$$

where  $\mathbb{Z}_x$  denotes the integer set from 1 to  $x$ ,  $c_j$  is the binary variable determining whether an after journey charge begins,  $c_i$  the binary variable determining whether an independent charge begins,  $d$  states whether it is a weekday or weekend,  $k$  is the cluster the vehicle belongs to that day,  $t$  is the time, and  $s$  is the SOC. Now, instead of considering only the probability that a charge will occur, the *joint distribution* of all variables must be considered. Every possible scenario is described by a combination of these variables, meaning that:

$$\sum_{c_j, c_i, d, k, t, s} P(c_j, c_i, d, k, t, s) = 1, \quad (4.1)$$

where  $P$  is the probability distribution function. The prediction problem becomes calculating the *posterior* probability that each type of charge begins, given the known values for the other variables. For after journey charging this is written as:

$$P(c_j = \text{True} \mid c_i, d, t, k, s), \quad (4.2)$$

where  $\mid x$  implies that the value of  $x$  is known. The total probability of a charge beginning will be the sum of this conditional probability and an equivalent expression for  $c_i$ . From the definitions of  $c_i$  and  $c_j$  it can be seen that it is impossible for both variables to be true

simultaneously, as they are describing the same phenomena under different circumstances. Therefore we can exclude  $c_i$  from (4.2) because if  $c_j$  is true, then  $c_i$  is necessarily false (however they could both be false, so still need to be considered separately in (4.1)). The expression therefore reduces to:

$$P(c_j = \text{True} \mid d, t, k, s), \quad (4.3)$$

which is defined over  $2 \times 48 \times 3 \times 6 = 1728$  possible scenarios. This discrete distribution can be populated using the observed charging events from the MEA data. For each possible value of  $(d, t, k, s)$  (4.3) is approximated using discrete observations from the data; in other words the probability is the percentage of observations of that combination of  $(d, t, k, s)$  which occurred at the start of a charge. This probability is then calculated for each combination of variables to build the full distribution. Note that only times when a journey had just ended are considered. A Gaussian filter was used to smooth the distributions in order to compensate for areas in state space where data was scarce. Figure 4.1 illustrates (4.3) using heatmaps, one for each possible  $k$  and  $d$  combination, with  $t$  on the horizontal axis and  $s$  on the vertical.

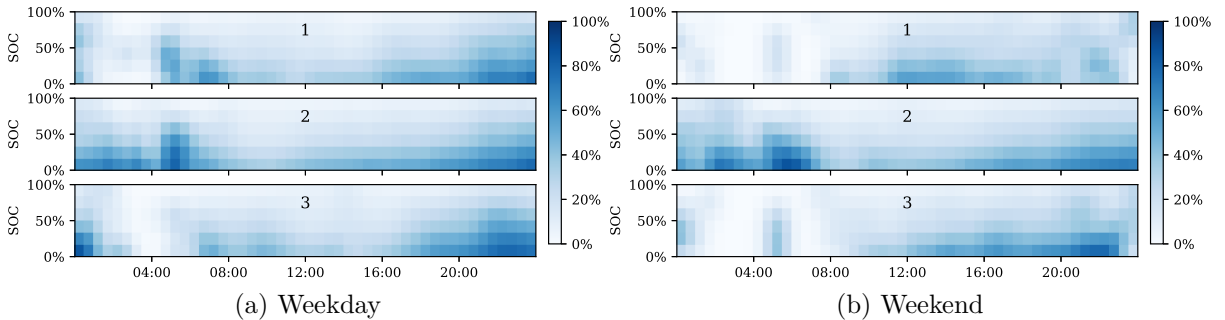


Figure 4.1: The % probability that a charge will follow the completion of a journey, as a function of both time and SOC, for each vehicle use cluster.

The fact that the distributions vary significantly with  $k$  supports its incorporation as a parameter; if EVs' charging were independent of usage cluster, then the three heatmaps would be identical. During weekday use, morning and evening drivers are likely to charge after journeys in either the morning or evening, and plug in with relatively high SOC. Whereas, commuters plug in almost exclusively after evening journeys and often have

very low SOC. During weekend use, single use vehicles (clusters 1 and 3) were most likely to charge after journeys ending in the early afternoon, while high use vehicles charged at either ends of the day. Overall, the peaks in the probability distribution occur at low values of SOC (as expected), in both the evening and early morning. Note that this does not mean that all vehicles are likely to charge in the early hours, just that vehicles that complete journeys at this time are likely to charge afterwards.

For independent charging, it was found that the vehicle usage had a negligible effect on whether or not a charge was started. In fact, often these events occurred on days where there was no vehicle use – and as a result no value of  $k$ . Therefore it was assumed that if  $c_i = \text{True}$ , then  $P$  is independent of  $k$ , such that the posterior distribution to be estimated becomes:

$$P(c_i = \text{True} \mid t, d, s), \quad (4.4)$$

Figure 4.2 illustrates this distribution. In this case there is not a significant difference between weekend and weekdays, suggesting that  $d$  could also be excluded from (4.4). However, as minor differences are observed in the early evening (which is the time of greatest interest) the variable was kept in this analysis. Here the distribution peak occurs shortly after midnight, and it is suggested that this is the results of timers set to coincides with the start of Economy 7 cheaper pricing (the UK’s dual tariff scheme).

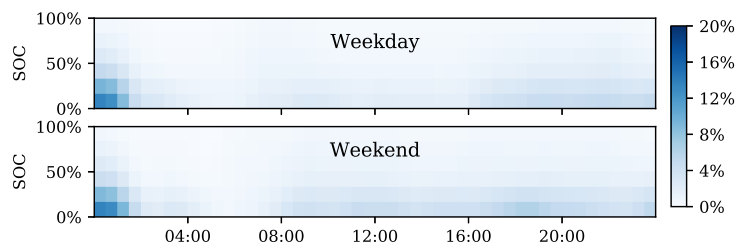


Figure 4.2: The % probability that a charge will start independent of a journey, as a function of both time and SOC, for each vehicle use cluster.

These distributions can then be applied to the NTS data, as  $(d, t, k)$  are all known and  $s$  can be estimated by assuming a battery capacity and a relationship between energy consumption and distance. The simplest method is to use a linear relationship, such that

a constant coefficient is defined which maps the distance to an energy consumption. If additional information were available, the relationship of consumption on driving style and vehicle parameters could be incorporated by altering the parameter according to the information. This allows a Monte Carlo simulation to be set up, which is described by the flow chart in Figure 4.3.

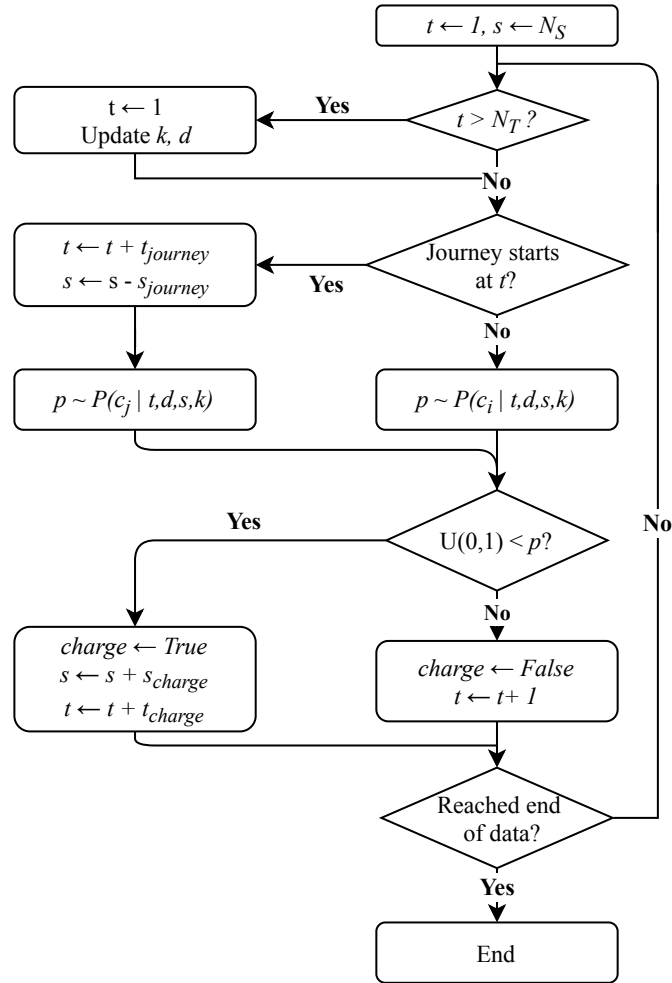


Figure 4.3: A flow chart describing the charging model simulation process.

Initially it is assumed that the vehicle is fully charged ( $s = 6$ ) and that it is the beginning of the day ( $t = 1$ ), then the day of week type and vehicle usage cluster are calculated. The simulation then steps forward in time, if a journey ends at that time-step then the SOC is reduced and the probability of an after journey charge is calculated, if not then the probability of an independent charge is calculated. Once a probability of a charge beginning has been calculated, a random number between 0 and 1 is generated. If this number is less than the probability calculated, then a charge begins, ending either

when the battery is full or when the vehicle is next used. The SOC and time are also updated accordingly. If a charge does not begin, the time is increased by one and the process is repeated until the end of the dataset is reached. Once the end of a day is reached ( $t = 48$ ) the type of day  $d$  and usage cluster  $k$  need to be updated, and  $t$  is set back to 1.

Stepping through the data once will result in a single estimate of charging. Stochasticity is captured by repeating the simulation, resulting in a distribution of predicted charging. Variation in both charging and vehicle use can be incorporated by running further Monte Carlo simulations where the input vehicles are randomly sampled from the whole travel survey dataset.

#### 4.1.2.1 Model Validation

The accuracy of the model proposed in Section 4.1.2 can be quantified by predicting the charging of the MEA vehicles from their usage data. It is important to use different data to train and test the accuracy of a model; otherwise the model may be overfit – meaning it fits the training data with very high accuracy, but performs badly on unseen data. Given the limited amount of data collected in MEA, significantly reducing the size of the training data is likely to degrade the performance of the model. Therefore the whole dataset is used as testing data, but the model is re-trained for each vehicle with the data from all vehicles except that one. For an individual vehicle-day the model predictions will vary significantly between runs. However, when considering the prediction of the whole dataset the law of large numbers says the variance should become very small. Therefore, an overall PDF of predicted charging start times can be produced by running the model a small number of times over the entire dataset.

For charging after final journey there is no stochasticity in the model, so the PDF of starting charging will equal the PDF of final journey end times. Figure 4.4 shows both estimated PDFs, compared to the distribution of times when charging is observed to have started. It can be seen that assuming charging starts immediately after the last journey overestimates charging between 16:00 and 23:00 by up to 70%. This is especially

problematic for peak demand prediction, as the existing peak occurs within this window. The new charging model achieves within 25% error across all times. Weekday observations are fit with greater accuracy, which is unsurprising given the larger variability in weekend vehicle use. It could be argued that, as the weekday vehicle use is higher, these days are of greater concern. It is worth noting that these metrics only show the expected error; the error on individual predictions will vary case-by-case.

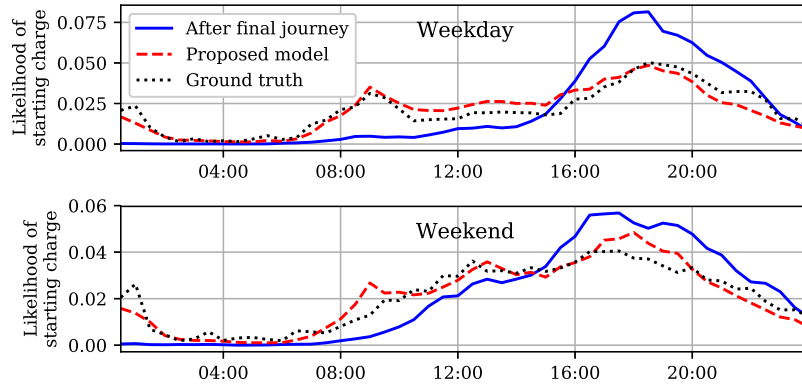


Figure 4.4: The starting charging probability distribution predicted from the MEA usage with both the proposed model and standard assumption, compared to the ground truth.

The difference in performance between this model and the standard assumption described in Section 4.1.1 can be further explored using a case study. Here we consider the aggregated charging of 50 households' vehicles. This is representative of charging in a LV distribution network, where 100% of vehicles are electric. Simulations of this kind are important, because we need to understand how diversity between vehicles is likely to manifest at low levels of aggregation. Likely, if 50 vehicles charged simultaneously on a single feeder, then network limits would be violated. However there are existing appliances (e.g. kettles or showers) which would cause overload if all households used them simultaneously; in reality natural diversity between users renders this situation extremely unlikely. As EV adoption increases, accurately modelling the diversity of EV charging will be crucial in predicting the peak demand.

For this case study, vehicle data was taken from NTS households in North Lincolnshire (a county in the North East of England) on a Wednesday. These parameters were fixed in order to remove geographic and weekday variations in vehicle use. It was assumed that

chargers were rated at 3.5 kW and had an efficiency of 90%. Monte Carlo simulations were constructed to estimate the average and variance of the vehicles' aggregate charging profile. Two simulations were carried out, one considering only variation in charging, and one considering both variation in vehicle use and charging. In the first, a single set of 50 vehicles was chosen from the data, and in the second, the 50 vehicles were allowed to varied between runs of the Monte Carlo simulation.

The simulation results are shown in Figure 4.5 for both the proposed stochastic model, and the assumption that vehicles charge after their final journey. In the single set simulation there is no variation in the latter as the model is deterministic. Whereas, when the set of vehicles is varied, stochasticity is introduced via the vehicle use. In both simulations the peak demand predicted under the new model is lower than that predicted by assuming charging begins after the final journey. This is significant because it supports the hypothesis that using the standard assumption produces overestimates.

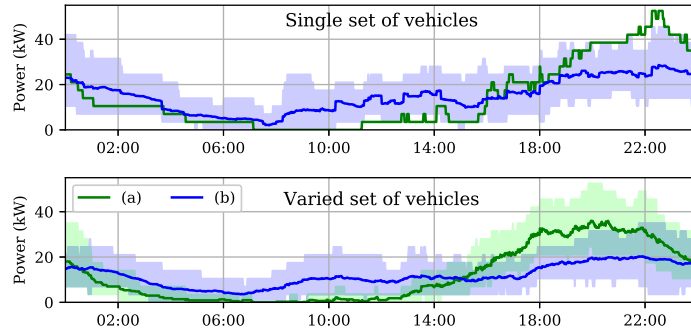


Figure 4.5: Aggregated charging of 50 households' vehicles under: (a) the assumption that charging always begins after a vehicle's final journey, and (b) the proposed model. The results are shown both using a single set of vehicles (top) and with a varied set of vehicles (bottom). The shaded area covers the 90% confidence interval.

It should be noted that the variability demonstrated is due to variations in populations and use. The derived bounds can not be directly translated into a forecast uncertainty, as this will depend on the prior information that is available about the vehicle fleet.

## 4.2 Controlled Charging

Quantifying the optimal action of smart charging strategies allows the value of controlling charging to be estimated, and any unavoidable network upgrades to be identified.

Several objectives have been proposed for smart charging. Flattening load or minimising peak demand are the two most common objectives, however, the most economic strategy for network operators may be to minimise losses. In this section, each of these objectives are formulated as a formal convex optimization problem. The convexity means that the problem has a unique global optima, and can be solved for a relatively high time resolution and large number of vehicles. These all assume centralised control with accurate predictions are available – meaning that all vehicles’ charging is controlled by one central actor who has deterministic values of future vehicle use and electricity demand. These assumptions mean that the optimal solution could not be calculated in real-time, however calculating the offline optimal solution is useful in assessing the maximum technical potential of smart charging. In reality, vehicle behaviour and existing demand would need to be forecast and a predictive optimisation strategy would be required, however these are beyond the scope of this thesis.

### 4.2.1 Flattening Load

Load flattening schemes aim to smooth some aggregated load profile, including both existing and vehicle charging demand. The level of aggregation used dictates the benefit of smoothing the load; if an individual with an EV, solar panel and home energy storage system flattens their load, they will maximise their self-consumption (and thus minimise their electricity bill); if vehicles flatten the load in their residential network, the peak demand at the distribution transformer will be minimised.; if vehicles flatten the national load, the total power generation capacity required will be minimised. These results would all be useful, but the beneficiary is different in each case. Mathematically, these problems have the same formulation, and this is described below.

Consider a fleet of  $N$  vehicles and  $N$  associated inelastic loads (typically household

loads) over  $T$  discrete intervals of duration  $\Delta t$ . The charging power of the vehicle at node  $j$  during time interval  $t$  is given by  $x_t^{(j)}$ . The vector  $\mathbf{x}^{(j)} \in \mathbb{R}^T$  then represents the proposed charging profile of that vehicle over the whole time period, and  $\mathbf{h}^{(j)}$  is the household load (or inelastic load) profile at node  $j$ . Note that  $x$  are the loads seen from the grid side, any losses in charging need to be taken into account before the energy demand of the vehicle is met. The load flattening objective function to be minimised is then:

$$f(\mathbf{x}) = \left\| \sum_{j=1}^{N_h} (\mathbf{h} + \mathbf{x})^{(j)} \right\|_2^2. \quad (4.5)$$

The 2-norm is used here because when the energy demand is fixed, the flattest load will minimise the sum of the square components. Additionally, unlike other norms, this function is convex, which improves the computational performance of the optimisation. The individual EV energy requirements and limit of the chargers are encoded in the problem constraints. Every time a vehicle  $j$  is plugged in a new set of constraints are generated, which are defined by: the time interval in which the vehicle arrives,  $\underline{t}$ , the time it is needed by,  $\bar{t}$ , and the energy it requires,  $E^{(j)}$ . Mathematically these constraints can be described as:

$$\eta_c \sum_{t=\underline{t}}^{\bar{t}} x_t^{(j)} \Delta t = E^{(j)}, \quad (4.6a)$$

$$0 \leq x_t^{(j)} \leq P_{max} \quad \forall t \in [\underline{t}, \bar{t}], \quad (4.6b)$$

where  $\eta_c$  is the charging efficiency, such that (4.6a) ensures that the vehicle has received the right amount of energy before it is required, and (4.6b) limits each charging power to be non-negative and below a maximum value. Finally, the optimisation can be described as:

$$\underset{\mathbf{x}}{\text{minimise}} \quad (4.5) \quad \text{subject to} \quad (4.6),$$

which takes the form of a quadratic program (QP). These are convex problems, providing the matrix of the quadratic component is positive definite [232], and can be solved in

polynomial time using standard software packages, such as *cvxopt* [233]. Charging cost minimising optimisations with a dynamic prices would also result in the load flattening solution, so from a system perspective these objectives can be seen as equivalent.

## 4.2.2 Minimising Peak Load

While flattening load will minimise the peak demand at all time resolutions greater than  $\Delta t$ , it is not possible to formulate a convex problem for flattening load with bi-directional charging. This is because if  $x$  can take negative values then the function (4.5) can equal zero, meaning that the objective is no longer positive definite. This means that, in order to consider the effect of V2G charging, a different problem formulation must be used. This can be formulated as a linear program, meaning it is computationally less intensive than flattening load. However, peak load is dependant on the time resolution used, so careful consideration needs to be given to the desired time resolution. For example, avoiding increasing the peak demand at the 1 minute resolution does not guarantee that the 30 min peak demand does not increase. Contrastingly, if the load is flat at 1 minute resolution, it is also flat at 30 min. Here separate problems are defined for uni-directional and bi-directional charging. Both take the form of convex linear programs, which are computationally simpler than QPs.

First, the case where only uni-directional charging is allowed is considered. In order to minimize peak load, an additional variable  $z$  is defined so that:

$$p_t + \sum_{j=1}^N x_t^{(j)} \leq z \quad \forall t, \quad (4.7)$$

where  $p_t$  is the existing feeder load at time  $t$ . The objective of the optimization is then described by:

$$\underset{\mathbf{x}, z}{\text{minimise}} \quad z \quad \text{subject to} \quad (4.6)(4.7).$$

The value of  $z$  changes throughout the optimisation, however as it is minimised, it will always reach the equality constraint in (4.7) – meaning it equals the peak demand once vehicle charging has been added.

In order to allow bi-directional charging it is insufficient to merely remove the positive constraint on vehicle charging, as the charger round-trip efficiency must be taken into account (losses in the charger mean that energy is wasted when power is transferred in either direction). Therefore if  $x$  were allowed to be negative, the constraint (4.6a) would no longer capture all of the losses, and any vehicles providing V2G would not receive enough power.

Here two sets of variables are defined,  $x_t^{(j)}$  for the power flow to EV  $j$  at time  $t$ , and  $y_t^{(j)}$  for the power from EV  $j$  at time  $t$ . This means the constraint (4.7) can be rewritten as:

$$p_t + \sum_{j=1}^N x_t^{(j)} - \sum_{j=1}^N y_t^{(j)} \leq z \quad \forall t, \quad (4.8)$$

and (4.6a) as:

$$\sum_{t=1}^T \left( \eta_c x_t^{(j)} - \frac{y_t^{(j)}}{\eta_d} \right) \Delta t = E^{(j)}. \quad (4.9)$$

An additional constraint is also required to ensure that the SOC of the vehicles remains between 0 and 100% for all time instances. Mathematically this can be written as:

$$0 \leq E^{(j)} + \sum_{t=1}^{\tau} \left( \eta_c x_t^{(j)} - \frac{y_t^{(j)}}{\eta_d} \right) \leq C^{(j)} \quad \forall \tau, \quad (4.10)$$

where  $C^{(j)}$  is the capacity of vehicle  $j$ 's battery. The constraint (4.6b) still holds, along with a similar constraint on  $y$ :

$$0 \leq y_t^{(j)} \leq P_{max} \quad \forall t \in [\underline{t}, \bar{t}]. \quad (4.11)$$

Finally, the problem can be described as:

$$\underset{\mathbf{x}, \mathbf{y}, \mathbf{z}}{\text{minimise}} \quad z \quad \text{subject to} \quad (4.6b)(4.9)(4.10)(4.11).$$

This formulation will implicitly prioritise charging over discharging for minimising peak

demand due to the efficiency terms. In other words  $y_t^{(j)}$  will be necessarily zero if  $x_t^{(j)}$  is non-zero. This is because any non-zero  $y$  will increase the total energy demand, so it will only be increased when it directly reduces the objective – i.e. at peak demand time. This means that there will no times when there is both charging and discharging. For both uni-directional and bi-directional formulations the resulting problem is a linear program.

### 4.2.3 Multi-Phase Network Loss Minimisation

Here a linearisation of the power flow equations is used to formulate approximate loss minimisation as a convex QP problem. In the case of a three phase, unbalanced, star-connected distribution network with  $N_b$  3-phase buses, we can write down the power flow equations as:

$$\mathbf{s} = \text{diag}(\mathbf{v})\mathbf{i}^*, \quad (4.12a)$$

$$\mathbf{i} = \mathbf{Y}\mathbf{v}, \quad (4.12b)$$

where  $\mathbf{s}, \mathbf{i} \in \mathbb{C}^{3N_b}$  are vectors of the complex power and current injections at each bus,  $\mathbf{Y} \in \mathbb{C}^{3N_b \times 3N_b}$  is the network admittance matrix and  $\mathbf{v} \in \mathbb{C}^{N_b}$  is the vector of bus voltages. The admittance matrix and voltages can be decomposed as:

$$\mathbf{Y} = \begin{bmatrix} \mathbf{Y}_{00} & \mathbf{Y}_{0L} \\ \mathbf{Y}_{0L} & \mathbf{Y}_{LL} \end{bmatrix} \quad \mathbf{v} = \begin{bmatrix} \mathbf{v}_0 \\ \mathbf{v}_L \end{bmatrix}, \quad (4.13)$$

where  $\mathbf{Y}_{00} \in \mathbb{C}^{3 \times 3}, \mathbf{v}_0 \in \mathbb{C}^3$  describe the slack bus (which is set to nominal voltage in order to create a solvable set of equations). The linearisation described in [234] is followed, such that the bus voltages are approximated as:

$$\mathbf{v} = \mathbf{M}_y \begin{bmatrix} \mathbf{p} \\ \mathbf{q} \end{bmatrix} + \mathbf{a}, \quad (4.14)$$

where  $\mathbf{p}, \mathbf{q}$  contain the real and reactive load injections respectively, and

$$\mathbf{M}_y = \begin{bmatrix} \mathbf{Y}_{LL}^{-1} \text{diag}(\bar{\mathbf{v}}_L)^{-1} & -j\mathbf{Y}_{LL}^{-1} \text{diag}(\bar{\mathbf{v}}_L)^{-1} \end{bmatrix} \quad (4.15a)$$

$$\mathbf{a} = -\mathbf{Y}_{LL}^{-1} \mathbf{Y}_{L0} \mathbf{v}_0, \quad (4.15b)$$

which is calculated around a known power flow solution  $\bar{\mathbf{v}}$  (the linearisation point). Given that there will only be loads placed on a subset of the buses on the network, we can remove columns from  $\mathbf{M}_y$  which correspond to buses without loads on. This means that  $\mathbf{M}_y \in \mathbb{C}^{3N_b \times 2N_h}$ , where  $N_h$  is the number of households (or applied loads) on the network.

To validate the linear models (prior to optimisation), we consider a *relative voltage error*,  $\epsilon_V$ , given by

$$\epsilon_V = \frac{\|\mathbf{v} - \bar{\mathbf{v}}\|_2}{\|\bar{\mathbf{v}}\|_2}. \quad (4.16)$$

Power flow solutions and the admittance matrix are both obtained using OpenDSS [235]. We study the error  $\epsilon_V$  for three linearisations: one linearisation  $\mathbf{M}_{0.3}$  with all loads at 0.3 kW, then  $\mathbf{M}_{0.6}, \mathbf{M}_{1.0}$  likewise at 0.6 kW and 1.0 kW respectively. For each of these models, a uniform demand  $\kappa$  is applied to all loads, and the error calculated by comparison to the true power flow solution (see Figure 4.6). There is zero error at the linearisation and no-load points, as expected [234], and less than 0.02% error within  $\pm 50\%$  of the linearisation point. The observed mean load of a large series of household smart meter data was approximately 0.6 kW, and so the model  $\mathbf{M} = \mathbf{M}_{0.6}$  is used subsequently.

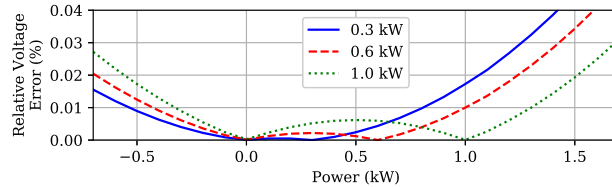


Figure 4.6: Relative voltage error  $\epsilon_V$  for three linearisations  $\mathbf{M}_{\bar{s}}$ , with a uniform demand  $\kappa$  assigned to each residential load (with a fixed power factor). The small error shows the linear models have good accuracy.

The complex power injection at a given node  $k$  is given by:

$$s^{(k)} = v^{(k)} i^{*(k)} = v^{(k)} [\mathbf{Y}\mathbf{v}]^{*(k)}, \quad (4.17)$$

where  $v^{(k)}$  is the node voltage,  $i^{(k)}$  is the current injection at the node. The losses can then be written as:

$$\sum_{k=1}^{N_b} Re\{s^{(k)}\} = Re\{\mathbf{v}^\top \mathbf{Y}^* \mathbf{v}^*\}. \quad (4.18)$$

In order to convert this expression from voltages to applied loads we need to substitute in (4.14). In this case, only one type of load is considered (EV chargers) so it is reasonable to assume a fixed power factor, meaning the reactive applied load can be expressed as:

$$\mathbf{q} = \alpha \mathbf{p}, \quad (4.19)$$

where  $\alpha \in \mathbb{R}$  is some constant. If each load had a different power factor, then  $\alpha$  would be a diagonal matrix. Considering:

$$\mathbf{M} = \begin{bmatrix} \mathbf{M}_p & \mathbf{M}_q \end{bmatrix}. \quad (4.20)$$

and substituting in (4.19), (4.14) is reduced to  $\hat{\mathbf{M}}\mathbf{p} + \mathbf{a}$ , where:

$$\hat{\mathbf{M}} = \mathbf{M}_p + \alpha \mathbf{M}_q. \quad (4.21)$$

Finally, the losses can be expressed as a quadratic function of the applied real power:

$$\sum_{k=1}^{N_b} Re\{s^{(k)}\} = \mathbf{p}^\top \mathbf{\Lambda} \mathbf{p} + \boldsymbol{\gamma}^\top \mathbf{p} + c, \quad (4.22)$$

where:

$$\begin{aligned}\mathbf{\Lambda} &= Re\{\hat{\mathbf{M}}^\top \mathbf{Y}^* \hat{\mathbf{M}}^*\}, \quad \boldsymbol{\gamma} = Re\{2\mathbf{a}^\top \mathbf{Y}^* \hat{\mathbf{M}}^*\}, \\ &\text{and } c = Re\{\mathbf{a}^\top \mathbf{Y}^* \mathbf{a}^*\}.\end{aligned}\tag{4.23}$$

In order to minimise real power losses due to EV charging we need to consider the total energy lost over  $T$  time intervals:

$$\mathbf{L} = \Delta t \sum_{t=1}^T \sum_{k=1}^{N_b} Re\{s_t^{(k)}\}.\tag{4.24}$$

By considering  $\hat{\mathbf{p}} = [\mathbf{p}_1 \dots \mathbf{p}_T]^\top$ , the concatenation of the applied loads at all time instances, we can express:

$$\mathbf{L} = \Delta t \hat{\mathbf{p}}^\top \hat{\mathbf{\Lambda}} \hat{\mathbf{p}} + \Delta t \hat{\boldsymbol{\gamma}}^\top \hat{\mathbf{p}} + cT\Delta t,\tag{4.25}$$

where  $\hat{\mathbf{\Lambda}} \in \mathbb{R}^{N_h T \times N_h T}$  is a block diagonal matrix of  $\mathbf{\Lambda}$ , and  $\hat{\boldsymbol{\gamma}} \in \mathbb{R}^{N_h T}$  contains  $T$  concatenated copies of  $\boldsymbol{\gamma}$ . The real power load,  $\hat{\mathbf{p}}$ , can be decomposed into the uncontrollable household load,  $\mathbf{h}$ , and the controllable EV load,  $\mathbf{x}$ . The total losses can then be expressed as:

$$\begin{aligned}\mathbf{L} &= \mathbf{x}^\top \hat{\mathbf{\Lambda}} \mathbf{x} + [(\hat{\mathbf{\Lambda}} + \hat{\mathbf{\Lambda}}^\top) \mathbf{h} + \hat{\boldsymbol{\gamma}}]^\top \mathbf{x} + \\ &\quad \mathbf{h}^\top \hat{\mathbf{\Lambda}} \mathbf{h} + \hat{\boldsymbol{\gamma}}^\top \mathbf{h} + cT\Delta t,\end{aligned}\tag{4.26}$$

which finally allows the problem to be expressed as the QP:

$$\underset{\mathbf{x}}{\text{minimise}} \quad (4.26) \quad \text{subject to} \quad (4.6).$$

#### 4.2.3.1 Formulation Validation

Due to the non-convexity of the true problem, it is impossible to quantify the accuracy of the approximate optimisation when applied to a full problem. However, for small problems it is possible to search for the optimum point empirically, by calculating the

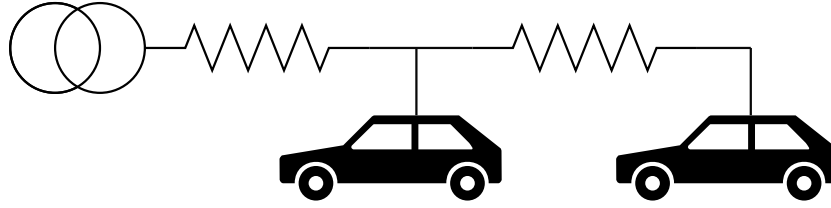


Figure 4.7: A simplified 2 bus EV charging scenario.

value of the objective at a fine grid of points. In this case the problem does not need to be convex, as the objective will be evaluated at all points - so there is no danger of finding a local minima. This means that the full non-linear power flow equations could be incorporated.

Consider two vehicles charging: one at the top of the feeder and one at the bottom, as shown in Figure 4.7. The second vehicle is a greater electrical distance from the substation so its charging will result in larger losses. We consider two time instances during which there is no base load, and each vehicle must receive an average of 0.5 kW. The maximum charging power they can receive in one time instant is 1 kW. There are only two decision variables in this problem - the charging power of each vehicle at the first time instant. The charging powers of the vehicles in the second time instant are then determined by the total energy that they need to receive over the time range. It is therefore possible to visualise how the simplified and true objective functions vary throughout the decision space using a heat map. This subproblem was constructed in openDSS, a power flow solver, and the actual losses were calculated using a full mesh of decision variables.

Figure 4.8 shows heat maps of both loss minimising objective functions, and the load flattening objective for comparison. For the loss minimising heat plot the contours of the true objective are shown in white, and the proposed model contours are shown in dashed cyan. Both plots are scaled to have a maximum value of 1 and the contours show increments of 0.1. In this case the approximate algorithm has matched the true function well, and the correct minima was identified. Although a promising result, it is impossible to determine whether this level of accuracy is maintained for the full sized problem.

The load flattening heat map is included because it helps visualise key differences between the objectives. While the loss minimising problem has a unique minima, the

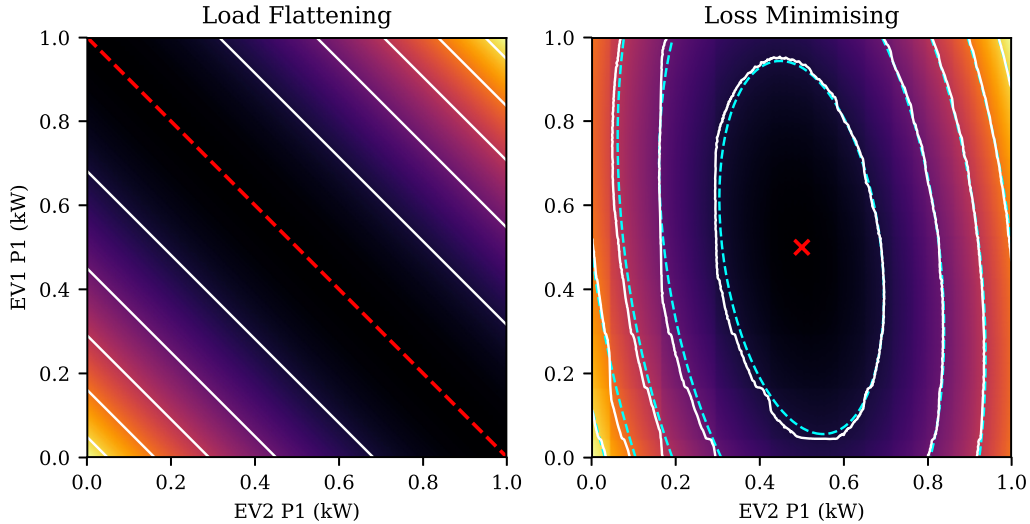


Figure 4.8: Variation of the smart charging objectives in a 2-bus problem. The loss minimization plot shows both the true contours (white) and those obtained from the model (cyan). Darker colours indicate lower losses, and the minima are shown in red.

load flattening problem has an infinite number of solutions which produce an equally flat load. Additionally, the load flattening problem treats the buses as homogenous, whereas you can see that the loss minimising objectives skew towards smoother charging at the bus further down the network.

Although this formulation allows losses to be directly minimised without sacrificing convexity, it has several disadvantages. Firstly, it requires exact information about the entire network topology and impedances, which may be unknown and difficult to determine accurately. Secondly, the peak load at the transformer is not explicitly minimised – so the transformer may suffer larger peak loads in return for the reduced losses. Thirdly, the quadratic matrix is more densely populated than in the load flattening case, so the problem will take longer to solve.

### 4.3 New Controlled Charging Strategies Considering Phase Balancing and Converter Losses

The previous section detailed controlled charging formulations that compute the optimal solution for various objectives. These formulations are non-causal, centralised, and require extensive information. Additionally, they rely on the assumption of a constant charger

efficiency, which is not accurate for the full range of operating powers. While a causal, decentralised implementation of these strategies is outside of the scope of this thesis, this section details some simplifications that can be made to the problems in order to address some of these issues.

First, an extension to the load flattening problem is proposed so that the loss minimising solution is better approximated. Then, the effect of varied charger efficiency on smart charging optimality is discussed, and a method is proposed to mitigate the problem.

### 4.3.1 Phase Balancing for Loss Reduction

The load flattening problem is ill-posed, as a unique solution does not exist. This is because all vehicles are treated as homogenous, meaning that charging can be shifted from one vehicle to another without affecting the objective function. It follows that there are a set of solutions that flatten load optimally, and the solver will just pick the one closest to its starting point – typically solvers initialise all variables as equal, so the resulting profiles tend to be slow and flat. Tikhonov regularization is a method of creating a unique solution which is in some way preferable. A second function is added to the objective, weighted by a very small number  $\lambda$ , such that the function only becomes significant once the minima of the primary function has been found.

In this case, it is desirable to select a load flattening solution which results in lower losses. Phase imbalance is one cause of losses, and can be quantified using the ratio  $|I_2|/|I_1|$  [236], where  $I_{0,1,2}$  are the zero, positive, and negative sequence currents. These are calculated by:

$$\begin{bmatrix} I_0 \\ I_1 \\ I_2 \end{bmatrix} = \frac{1}{3} \begin{bmatrix} 1 & 1 & 1 \\ 1 & a & a^2 \\ 1 & a^2 & a \end{bmatrix} \begin{bmatrix} I_A \\ I_B \\ I_C \end{bmatrix}, \quad (4.27)$$

where  $a = e^{j\frac{2\pi}{3}}$ , and  $I_{A,B,C}$  are the currents in phases  $A, B$  and  $C$  [237]. Minimising this ratio across the network is a non-convex problem and requires the full network model to be known. However, the branch currents are driven by the applied loads, so it follows that

the average phase imbalance in the network could be reduced by balancing the applied load across the phases. Therefore, here the following convex objective is considered:

$$\begin{aligned}
g(\mathbf{x}) = & \left\| \sum_{j \in \mathcal{H}_A} (\mathbf{h} + \mathbf{x})^{(j)} - \sum_{j \in \mathcal{H}_B} (\mathbf{h} + \mathbf{x})^{(j)} \right\|_2^2 + \\
& \left\| \sum_{j \in \mathcal{H}_A} (\mathbf{h} + \mathbf{x})^{(j)} - \sum_{j \in \mathcal{H}_C} (\mathbf{h} + \mathbf{x})^{(j)} \right\|_2^2 + \\
& \left\| \sum_{j \in \mathcal{H}_B} (\mathbf{h} + \mathbf{x})^{(j)} - \sum_{j \in \mathcal{H}_C} (\mathbf{h} + \mathbf{x})^{(j)} \right\|_2^2,
\end{aligned} \tag{4.28}$$

where the set  $\mathcal{H}_i$  contains the households in the networks on phase  $i$ , such that each household belongs to exactly one set. While calculating losses requires all of the network impedances to be known,  $g(\mathbf{x})$  requires only each load's phase. This is easier for DNOs to determine, and would likely only need to be found once (unlike network topology, which regularly changes as a result of network reconfiguration). It is shown in Chapter 6 that incorporating this function as a secondary objective to the load flattening problem has the effect of reducing  $|I_2|/|I_1|$  across the network. The proposed optimisation can be described as:

$$\underset{\mathbf{x}}{\text{minimise}} \quad f(\mathbf{x}) + \lambda g(\mathbf{x}) \quad \text{subject to} \quad (4.6)$$

where  $\lambda \ll 1$ . The resulting problem remains a QP, however the computational complexity is larger than for the standard load flattening problem due to the increased density of the quadratic matrix.

### 4.3.2 Incorporating Varied Charger Efficiency

In order to guarantee convexity, the smart charging formulations in Section 3.2 all assumed a constant charging efficiency. Charger efficiency is defined by the ratio of the DC power into the battery to the AC power drawn from the grid. The difference between the two is caused by losses in the converter, and assuming a constant efficiency is equivalent to assuming that converter losses are linearly related to power. In reality there are two components to losses: conductive losses which vary approximately with the square of load, and switching losses which are approximately constant (see Section 2.4.3 [238]).

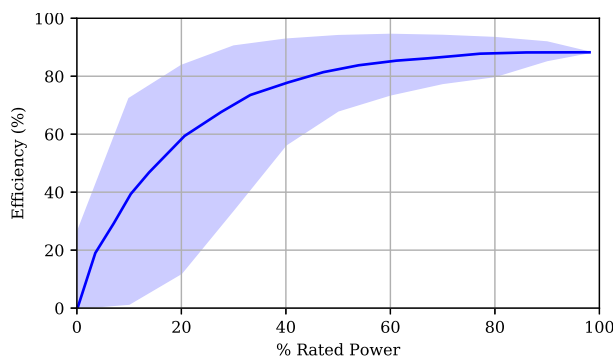


Figure 4.9: The variation of charger efficiency with power requested. The solid line represents the average values and the shaded area covers the range observed.

This means that when the charging power is low, the efficiency becomes poor as the switching losses make up a proportionally bigger proportion of the load. Therefore, if a vehicle uses a charging profile which includes low powers, it will not receive the intended amount of energy.

The amount of losses will vary between chargers, and only a limited amount of data was found recording the efficiency of EV chargers. Some lab based measurements of efficiency are available (e.g. [239]) but there is a shortage of data from operational EV chargers operated at various powers. In [20] a bi-directional EV charger was operated at various power levels and the efficiency was recorded in each case. Hundreds of data points were gathered and there was a large amount of variation in efficiency experienced, Figure 4.9 shows the average and variation in efficiency recorded at each power. Some of the variation was due to a delay between the recordings, meaning the efficiency was also dependant on the previous power. However, this is the most relevant set of efficiency data that could be found in the literature.

In this section, a simple example is used to quantify how drastically incorporating varied efficiency effects the result; the example problem has to be small in order to retain tractability of the non-convex optimisation. Then, a heuristic method of altering the results of the optimisation problems in Section 3.2 to avoid operating at low efficiencies is presented.

Consider a single vehicle charging at the lossiest node on the IEEE European Test Feeder [240], aiming to optimise its charging so as to minimise losses in the presence of a

constant base load. In this case the decision variable  $x_t$  is defined as the power on the DC side of the converter at time  $t$  (in Section 3.2 the power on the grid side was used). This change is necessary in order to express the energy requirement of the vehicle as a linear constraint. In order to reduce the size of the problem, charging power is also discretised such that:

$$x_t \in [0, 0.5, 1.0, 1.25, 1.5, 1.75, 2.0, 2.25, 2.5, 2.75, 3.0]. \quad (4.29)$$

Each possible charging power has an associated constant efficiency, derived from the data in [20], which are described in Table 4.1. In this case it is assumed that the vehicle is charging over 20 half hour intervals, during which it requires 10 kWh of charge. The problem size is further reduced by discretising charging power, such that:

$$\frac{1}{2} \sum_{t=1}^{20} x_t = 10. \quad (4.30)$$

The problem is further reduced using the assumption that the base load is constant

$x$ (kW)	0.0	0.5	1.0	1.25	1.5	1.75	2.0	2.25	2.5	2.75	3.0
$\eta_c(x)$ (%)	0	50	70	79	82	85	87	88	89	90	90

Table 4.1: The efficiency values assumed for each power.

– meaning the order that a sequence of charging powers are carried out won't affect the losses. With the chosen time and power resolution there are 39 916 800 points (or potential charging profiles) in the solution space. However, only 29 903 satisfy the constraint (4.30), and this number can feasibly be checked exhaustively. The power flow equations do not need to be calculated each time, as each charging power will have an associated distribution loss. The loss associated with each charging power can be found using the following steps:

1. Use the efficiency to calculate the equivalent power drawn from the network.
2. Add the load to the appropriate point in the network and run a power flow.

$x$ (kW)	0.0	0.5	1.0	1.25	1.5	1.75	2	2.25	2.5	2.75	3.0
$L(x)$ (W)	0	47	69	77	90	104	118	133	149	165	183
$L_0(x)$ (W)	0	25	52	66	81	97	113	130	147	165	183

Table 4.2: Calculated distribution losses for each charging power.  $L$  uses  $\eta_c$  from Table 4.1, while  $L_0$  assumes a  $\eta_c=90\%$ .

3. Calculate the increase in total load into the feeder minus the power into the battery.

Assuming all base loads on the network are set at 1 kW, the resulting distribution system losses from each charging power are shown in Table 4.2.  $L$  describes the losses calculated including the varied efficiency, while  $L_0$  are the losses calculated assuming a constant 90% efficiency. You can see that at high charging powers the values are identical, while at low charging powers  $L$  is nearly twice the size of  $L_0$ . Here three objectives are considered. The first aims to minimize the total losses in the distribution system over the time period, such that:

$$f(\mathbf{x}) = \sum_{t=1}^{20} L(x_t). \quad (4.31)$$

The second aims to consider the total energy losses, including both the distribution losses and those in the vehicle charger. This is considered separately because distribution system losses cause heating and degradation in the network, so minimising them is optimal for the network, whereas minimising total losses is economically optimal. The total losses can be expressed as the function:

$$f(\mathbf{x}) = \sum_{t=1}^{20} L(x_t) + \sum_{t=1}^{20} [1 - \eta_c(x_t)]x_t. \quad (4.32)$$

Finally, the distribution system losses using the assumption of constant efficiency is used as an objective:

$$f(\mathbf{x}) = \sum_{t=1}^{20} L_0(x_t). \quad (4.33)$$

This allows the impact of ignoring the relationship between charging and efficiency to

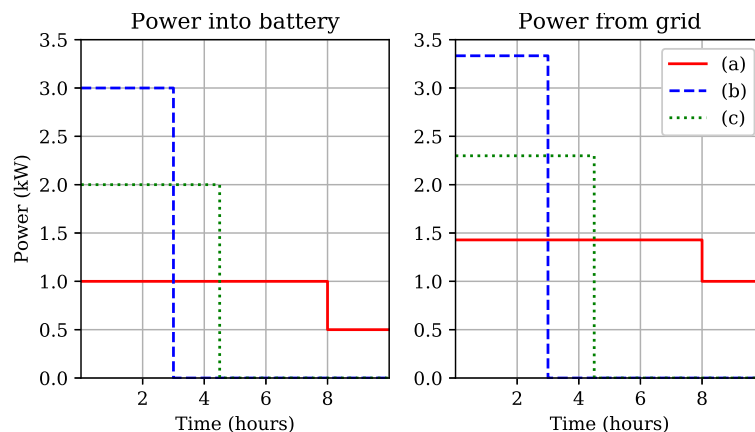


Figure 4.10: The power into the EV battery and drawn from the grid under three cases described in Table 4.3.

be quantified for this case. A summary of the three problems is presented in Table 4.3, and the optimal charging profiles found are shown in Figure 4.10. The left graph shows the power into the battery, which is what is being controlled. The right shows the power drawn from the grid, which includes charger losses.

Case	Objective	Include Charging Losses
(a)	Minimise distribution system losses	×
(b)	Minimise distribution + charger losses	✓
(c)	Minimise distribution system losses	✓

Table 4.3: A summary of the three cases considered.

In case (a) where efficiency was ignored the slowest charging profile possible is selected (as expected). When total losses were minimized in case (b) the vehicle charged as fast as possible, running at full power. In the final case, considering only distribution losses a medium rate was selected. The losses associated with these profiles are shown in Fig 4.11, broken down into charger and distribution losses. It is clear that the charger losses are much more significant than the distribution losses in this example, which is surprising given that the feeder is quite heavily loaded. In fact, the variation in distribution losses in each case is minimal when compared to the variation in charger losses. It is also worth noting that the distribution losses are actually highest in case (a), where they were explicitly minimised but varied charger efficiency was not taken into account. This demonstrates the importance of using a higher fidelity vehicle charger model.

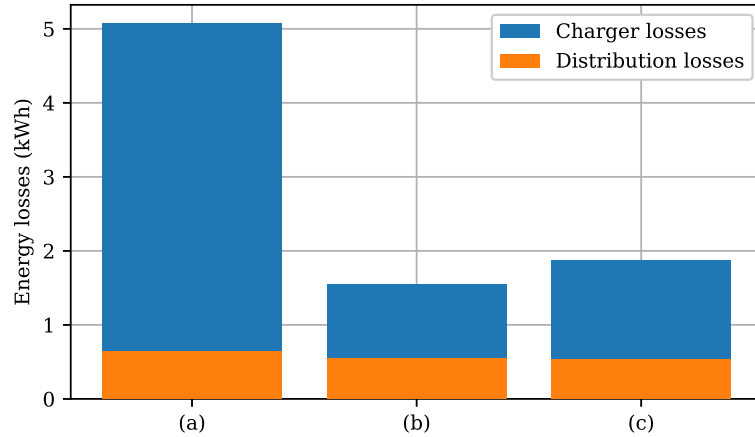


Figure 4.11: The total losses due to the EV charging under the three cases described in Table 4.3, broken down into distribution system and charging losses.

It should be noted that none of the optimisation strategies discussed consider the impact of the charging profile on the battery. CC-CV profiles are typically used to protect the battery’s state of health, but incorporation of the requirements of the battery is left as further work.

There is no way to incorporate varied charger efficiency into the optimisation without sacrificing convexity. However, the assumption that  $\eta_c$  is constant is reasonable above certain charging powers. If the fleet of EVs being controlled is large, it is possible that the same level of load flattening could be achieved by switching vehicles on and off at full power, however this would require reformulation as a mixed integer program (e.g. [241]). These are non-convex and therefore scale badly, meaning they are unlikely to be suitable for control of a network containing many vehicles.

Due to the time constant of the transformer and cables, network operators are primarily concerned with loading at a 30 minute resolution. This is significant because at a 30 minute resolution there is no difference between charging at 1.5 kW for 30 minutes, and charging at 3 kW for 15 minutes. Therefore the 30 minute resolution load can be maintained while charging losses are reduced by charging at full power for a subset of the 30 minutes. This means that the EVs are effectively operating with a duty cycle, where they are on for a certain percentage of the time period.

If each vehicle charges in this way then the optimal behaviour at a 30 minute resolution is guaranteed. It should be noted that while network operators are primarily concerned

with the 30 minute resolution, large peak loads at 1 minute resolution are still undesirable. While the transformer overheating is unlikely to be a problem, losses will be increased and this may cause voltage limits to be violated. Therefore, some thought needs to be given to how each vehicle is allocated the subset of the 30 minutes which it charges for.

Here a simple approach is proposed, where each EV  $j$  is allocated a number of minutes past the half-hour when it begins charging,  $\phi^{(j)}$ . Therefore, optimal charging profiles can be found using the methods in Section 3.2 and altered using the following method. For each  $x_t^{(j)}$  calculate the equivalent time at which the vehicle would charge at full power to receive the same energy  $t_{\text{req}}$ . The vehicle then charges from  $\phi^{(j)}$  to  $\phi^{(j)} + t_{\text{req}}$ , wrapping round the half hour if necessary.

As an illustrative example, consider 50 vehicles on a 50 household network trying to flatten the total demand. The vehicles are controlled at 1 minute resolution but the load only needs to be flattened at 30 minute resolution. Figure 4.12 shows the total feeder load at both 1 and 30 minute resolutions resulting from both methods. At the 1 minute resolution the peak demand is much higher in the discrete than continuous case, however at the 30 minute resolution the two schemes are identical.

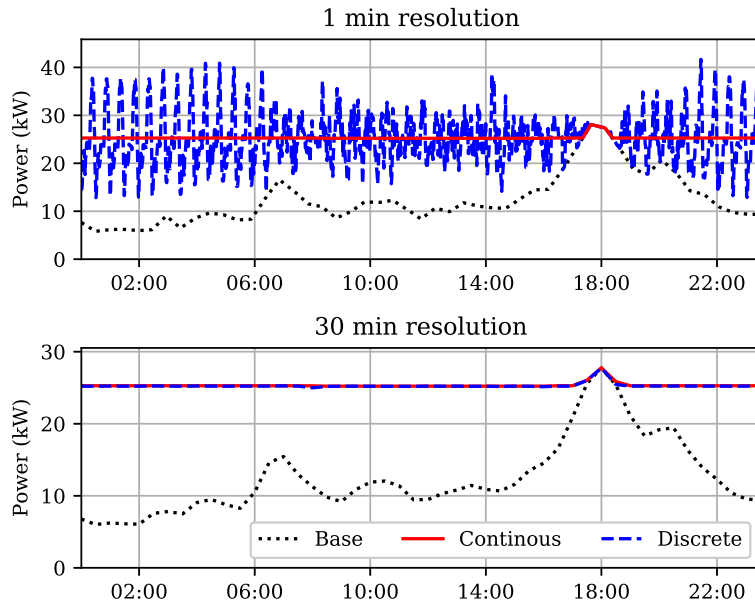


Figure 4.12: The total feeder load at 1 and 30 minute resolution under both the continuous and discrete schemes.

The differences between the schemes are demonstrated by looking at individual charg-

ing profiles, and Figure 4.13 shows two example vehicle charging profiles from the simulation; (a) shows the full 24 hours of charging, and (b) zooms in on the 8PM to midnight window. The availability restrictions are the same under both schemes, but while the continuous case results in a constant slow charge, the discrete case resulted in bursts of charging at full power.

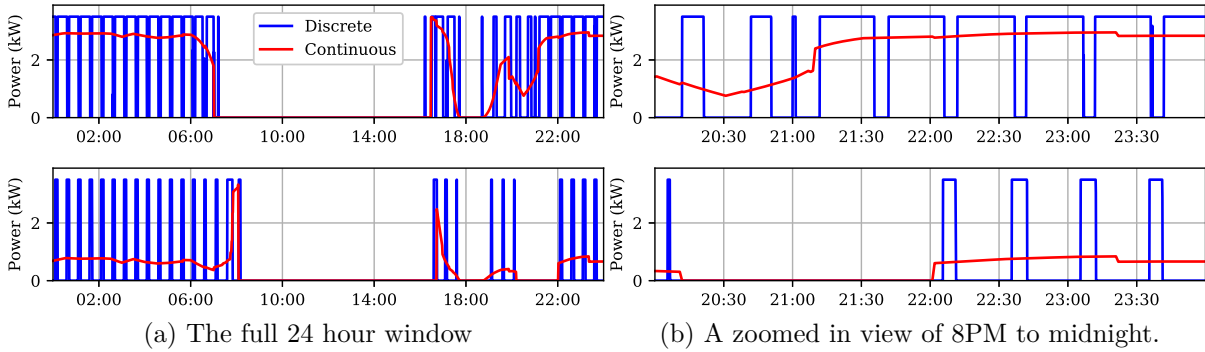


Figure 4.13: The continuous optimal profiles and discrete approximations of two random vehicles from the simulation.

This algorithm will not achieve the optimal behaviour, but adds diversity between the profiles, such that the higher resolution behaviour is improved. It is possible that more optimal behaviour could be achieved using a hierarchical optimization approach, where individual mixed integer problems are set up for each 30 min period to determine the optimal time for each vehicle to charge within the interval. Each mixed integer problem would be small and could be solved in parallel, meaning the computational complexity may no longer be a limiting factor. However, this is left as further work.

## 4.4 Concluding Remarks

In this chapter methods for modelling charging of electric vehicles, given their energy consumption and availability, are discussed.

A model for uncontrolled charging of electric vehicle is proposed which incorporates stochasticity in both vehicle use and charging behaviour. This means that variability of EV charging can be quantified at small levels of aggregation, and different charging behaviour will be forecast according to the EVs' usage.

Several optimisation problems are formulated for controlled charging, using a variety of objective functions: load flattening, peak demand minimising, loss minimising, load flattening with phase balancing, and load flattening with varied charger efficiency. All formulations are convex, taking the form of linear or quadratic programs. This means that the optimal smart charging strategies can be calculated for a range of schemes – allowing the action of different schemes to be directly compared.

Using the modelling methodology presented in this chapter, it is possible to estimate the power demand created by EV charging at a variety of levels of aggregation. This will allow changes in power demand to be quantified at both the residential network level, and the national scale. Once the new power demand has been attained, changes to the operation of the system can be investigated.

# Chapter 5

## Impacts on the Generation & Transmission Systems

This chapter investigates the effect that EV charging will have on the transmission level power system, which encompasses the generation and transmission systems.

The transmission level system is concerned with the aggregated demand of a national fleet of EVs. Energy demand from EVs is predicted using the linear conversion factors described in Section 3.2.2. The uncontrolled charging scenarios are calculated using both methods in Section 4.1, and the smart charging scenarios are determined using the load flattening optimisation from Section 4.2.1.

Section 5.1 focuses on the impacts of the additional charging load on the GB generation system operation. First, the change to the national demand profile is investigated at various times of year, which allows the required installed generation capacity to be quantified. Second, the implications of the change in profile on the use of renewable energy is discussed – as part of this, a method for using EV charging to maximise renewable consumption is proposed.

In Section 5.2 the impact of the additional demand on the GB transmission system operation is investigated. The line loading in the high-voltage network is calculated with uncontrolled charging, both under normal operation and in the case where the single largest component has failed. The change to network losses is also investigated.

Section 5.3 repeats the results from Section 5.1 but for the Texas case study. This gives an example of how the results are likely to change for a different power system and travel behaviour.

## 5.1 Generation System

In order to maintain the system frequency, at all times there must be a match between the power demand and supply across the system. While high voltage interconnections allow power to be bought from neighbouring systems, the bulk is generated internally – in 2018 93% of GB’s electricity demand was met with power generated in GB. Each fuel source has different benefits and costs – for example gas is very easily controlled, while solar and wind power have zero-marginal cost, and zero carbon emissions. The mix of fuels used is determined by an economic dispatch which incorporates the availability, cost, and location of the potential supply sources.

A change to the aggregate demand profile could have two significant impacts. Firstly, if the peak demand exceeded the total generation capacity, then additional power stations would need to be built. Traditional power stations are expensive to build and operate, so this should be avoided if possible. Secondly, depending on the time of the additional demand, the mix of fuels that is utilised may change.

Here the generation level system is considered exclusively from the demand perspective. This means that the implications of EV charging on the electricity market have not been considered, and system dynamics are not analysed. This narrower scope was selected because the system at this level has been comparatively well studied in the literature. It should be noted that none of the thesis contributions outlined in Section 1.4 relate to this material.

In order to simulate the charging of a 100% EV fleet, vehicle usage from the travel survey datasets were used. Distances were converted into energy consumptions using the conversion factors for the Nissan Leaf given in Table 3.4 – ‘motorway’ for journeys over 10 miles, otherwise ‘rural’ or ‘urban’ depending on the location of the sampled household.

It was assumed that all EVs had a battery size of 30 kWh, which is consistent with the Nissan Leaf. If a journey was estimated to use more than 30 kWh the consumption of the vehicle was capped at that point. Although this does mean that some energy used by the vehicles is unaccounted for, the vehicles in question were those driving over 100 miles, and would likely charge at a motorway charging station – meaning it is unrealistic to assume that these vehicles would charge in residential distribution networks. It should also be noted that, even in terms of energy, these vehicles represented a very small percentage of the fleet demand. Increasing the assumed size of EV battery would likely reduce the peak charging demand, as vehicles would be on charge for longer but less often. However, it is possible that the charging behaviour captured in MEA would be different with a larger battery. Therefore, the mid-range battery size was chosen in order to maximise relevance of the charging data.

A scaling factor is then calculated for each of the four rural-urban classifications. This is done by dividing the GB population living in areas with that classification to the population included in the travel survey sample living in areas with that classification. Note that it is important to include households without vehicles in this calculation. Then the predicted energy demand of all vehicles from the survey is scaled using the relevant weighting factor. The decision to scale by population rather than by number of vehicles was based on two points. Firstly, there may have been vehicles owned by the travel survey households which were not captured in the dataset, because vehicle IDs were only recorded if they were used during that week. Secondly, the amount of travel is likely to be more closely linked to population size than number of vehicles – households with two vehicles do not necessarily travel twice as far as those with one.

The uncontrolled and controlled charging power demands of the vehicles are then calculated using the methodology described in Chapter 4. For the uncontrolled charging scenario chargers were assumed to be rated at 3.5 kW and have an efficiency of 90%, as similar values have been measured in domestic charging [242]. For the controlled charging the load flattening formulation in section 4.2.1 was used – as flattening load results in the minimum peak demand. The existing demand that was associated with vehicle  $j$  was

a scaled down version of the total load, such that  $\mathbf{h}^{(j)} = \frac{1}{N_h} \mathbf{P}_{\text{tot}} \quad \forall j$ , where  $\mathbf{P}_{\text{tot}}$  is the aggregate demand before any vehicle charging is added. Note that, in the optimisation, the maximum charging power has to be scaled with the energy demand.

A full economic dispatch model is outside of the scope of this thesis, meaning the changes to the fuel mix can not be accurately calculated. However, analysis of historic wind and solar generation alongside the modelled demand profiles are used to set bounds on the percentage of energy demand which could be met using zero-carbon sources.

In later chapters, the case for bi-directional smart charging (V2G) is considered. However, at the transmission system level V2G has not been included in the analysis. This is because the effect of V2G on a national system has been quite thoroughly studied in the literature. Additionally, for a high penetration of EVs it will be shown that the controlled load profile is relatively flat – meaning that V2G would not have a significant additional advantage.

### 5.1.1 Matching supply and demand

Due to the dominance of heating and lighting in the UK’s electricity demand, loads vary significantly throughout the year. Therefore, here the power demand on a high-use day from each season is investigated. Weekdays were chosen as vehicle use is much higher during the week, so the impact of charging is likely to be worse. Figure 5.1 shows the national power demand under each charging scenario. Two versions of uncontrolled charging are shown: Figure 5.1(a) shows the predicted national demand under the assumption that all vehicles charge immediately following completion of their final journey, and Figure 5.1(b) shows the predicted demand using the stochastic model proposed in Section 4.1.2. Note that, although the charging model is stochastic, no uncertainty is seen at this level of aggregation due to cancelling between vehicles – this was verified using stochastic simulations. Note that there will be uncertainty in the existing load, however the highest demand deterministic day is used here in order to investigate the upper bound. In all cases the peak demand in scenario (a) is higher than (b), which aligns with the assertions in the previous chapter that assuming immediate after journey charging overestimates

the peak demand. The remaining analysis only considers the stochastic charging model in (b), however scenario (a) is left here as a form of upper bound. This is useful because there is some danger that the proposed charging model still captures the biases of the EV trial data that was used to parameterise it.

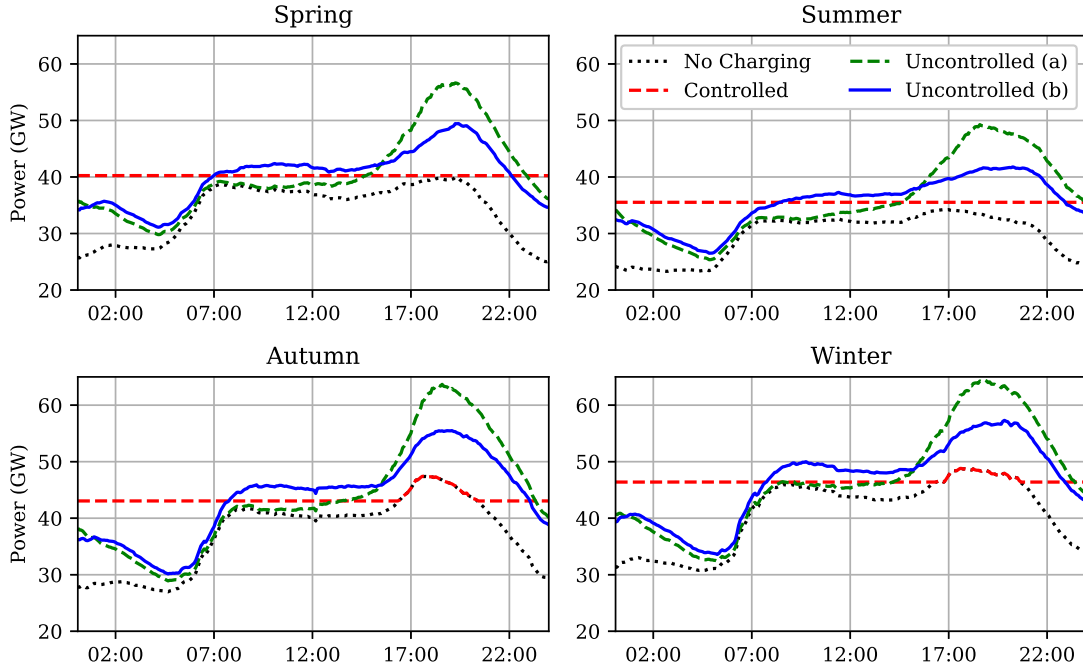


Figure 5.1: The national demand profile on a high-use week day with no charging, controlled and uncontrolled charging of a 100% electric fleet of vehicles. For uncontrolled charging (a) shows charging after final journey, (b) shows charging using proposed model.

Uncontrolled charging increases the peak demand by around 10 GW across all seasons. This will have the greatest impact in the winter when the existing load is highest. Whereas, controlling charging can mostly avoid any increase in peak demand. Table 5.1 shows the total existing generation capacity in GB, and the amount of this that is solar and wind generation. It can be seen that, even if there is no solar or wind available, there is sufficient capacity to meet the uncontrolled charging demand. This is partly because the past decade has seen a decline in electricity demand, due to increased efficiency, so the system was designed to operate under a higher load. However, it is also important for GB to have some redundancy in its capacity, because there are only a small number of inter-connectors which allow purchase of power from neighbouring countries – the surplus allows power stations to be switched off for refurbishment without relying on foreign imports. Additionally, the UK has a 100% decarbonisation objective by 2050, so reducing

peak demand will reduce the challenge of replacing with renewable capacity.

Total (GW)	Solar (GW)	Wind (GW)
91.9	12.8	8.5

Table 5.1: The GB nameplate generation capacity

**Approximate Control of a Large Fleet** At low levels of aggregation, variability is high and load prediction is very difficult. However, the load at substation level is routinely forecast within 1-2% accuracy [243], and national demand is forecast with even greater success [244]. Additionally, when the number of vehicles is high, the load flattening optimisation tends to result in the majority of vehicles following similar profiles. It stands to reason that, in this case, an algorithm could be created which approximates these optimal profiles.

Here, an example method is proposed for approximately flattening load with a large fleet of vehicles which does not require communication between vehicles, and requires only a forecast of the aggregate demand. The proposed algorithm is described below:

1. Forecast the base load at the suitable level of aggregation.
2. Invert prediction by subtracting each time step from the maximum value.
3. Isolate the period during which the vehicle is available to charge and calculate the energy (area under curve) of the resulting signal.
4. Scale the signal to the required energy, ensuring that the resulting profile does not exceed the limit of the charger.

These stages are demonstrated for an example vehicle in Figure 5.2.

First, the existing load that is to be flattened is forecast. Second, this load is inverted, resulting in the power demand that the aggregated EV fleet would follow if the final load were to be perfectly flat. Third, the vehicle constrains the signal to be zero at times it is unavailable to charge. Finally, the remaining signal is scaled such that the area under

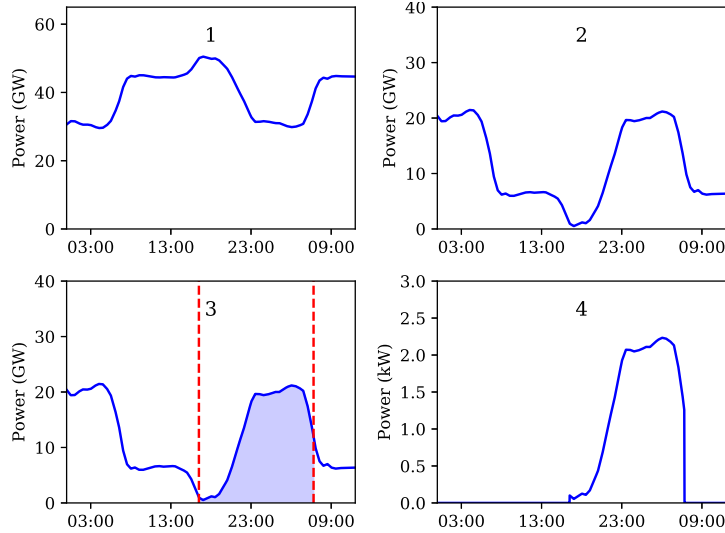


Figure 5.2: Demonstration of example curves obtained from each stage in the approximate control algorithm.

the curve matches the vehicle’s energy requirement. A limit on the individual power that a vehicle can charge at is set at the rate of slow charging (3.5 kW). This means that if a user plugs in their vehicle saying they need it again in an hour it will not fully charge, but charge at 3.5 kW for the duration of time it is plugged in. This prevents individual profiles from being scaled to unrealistic powers. It is noted that in some cases this algorithm will result in low power charging, so the heuristic method from Section 4.3.2 would need to be implemented to avoid issues with charger efficiency.

This algorithm means that all EVs follow partial scaled versions of the same charging profile. In order for this algorithm to achieve optimal flattening all EVs would need to be available for the full 24 hours, which is infeasible. Figure 5.3 shows the accuracy that is achieved with the heuristic charging metric for each of the simulations shown above. In the winter and autumn simulations the approximate method avoids any increase in peak demand, despite not perfectly flattening the load. Whereas, in the spring and summer increases in peak demand of up to 2 GW are seen. This disparity occurs because the algorithm tends to underestimate the optimal case in the middle of the day, due to limited availability of EVs. In the colder seasons the majority of the optimal charging occurs overnight, so this shortcoming has less of an influence. However, in all cases this demonstrates that at the national level heuristic methods can easily achieve near-optimal

smart charging results.

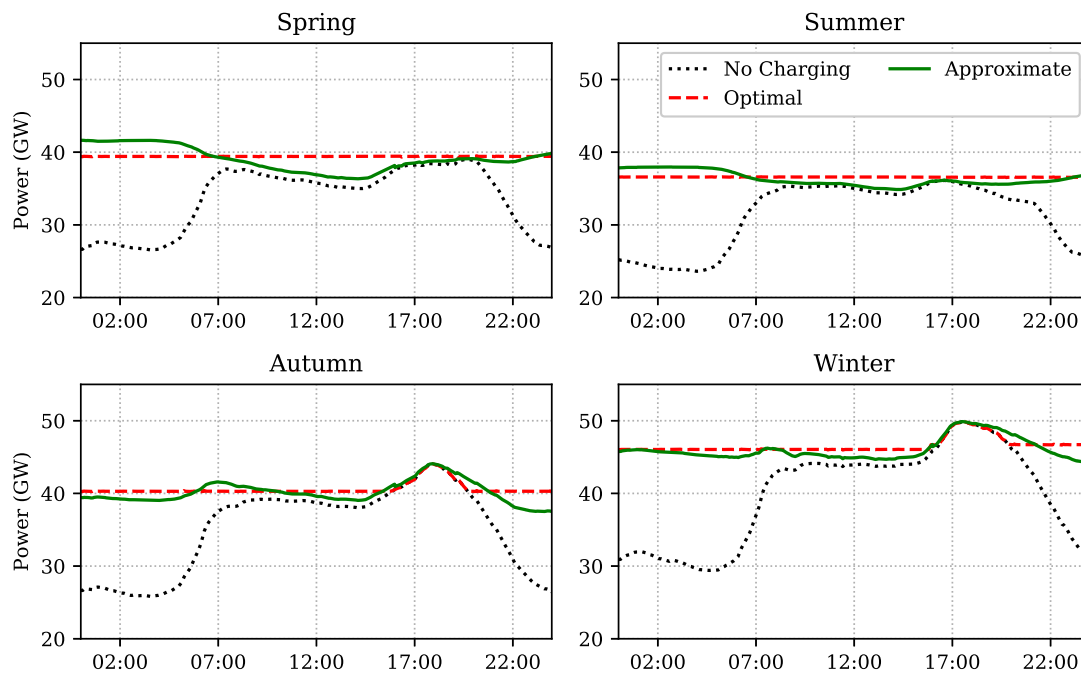


Figure 5.3: The accuracy with which the heuristic method proposed approximates the optimal controlled charging at the national scale.

### 5.1.2 Consumption of Renewables

The fuel mix describes the make-up of sources used to generate a country's electricity. The UK has made commitments to increase the percentage of its electricity that is generated using low carbon sources, which means reducing the amount of coal and gas on the system. The transmission system operator decides the sources of generation used for each time period, based on the cost and location of available producers.

Figure 5.4 shows the available capacity by fuel source on the single best and worst day for renewable generation in 2018, and the associated demand. The solar, wind, and other renewables are taken from historic generation data and the nuclear and fossil capacity are assumed to be constant throughout the day. By assuming that the renewable fuels were used first, followed by nuclear, and finally fossil fuels the upper limit of renewable penetration can be calculated. It is likely that this bound would not be achieved in practice, due to local transmission constraints and system inertia.

The maximum possible percentage of electricity generated by renewables is shown in

the middle of each plot. On days with low renewable generation the electricity demand tends to be higher, due to the worse weather. Note that this plot confirms that, even with the worst renewable generation and the highest demand, a 10 GW increase in peak demand is within the UK generation capacity.

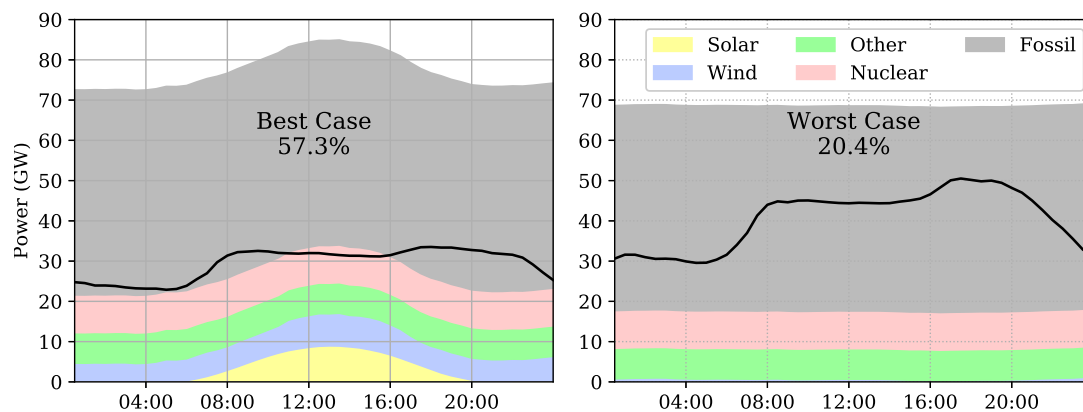


Figure 5.4: The generation capacity and fuel mix in the UK on a high and low renewable production day in 2018, with fuels ordered according to preference. The line shows the national demand on that day.

It can be seen that, even with the maximum possible renewable generation, the demand always exceeds the renewable generation. In fact, in 2018 the peak renewables generation in the UK was 18.0 GW, at which time there was a demand of 35.2 GW – so renewables currently only need to be curtailed if there are local network constraints. This means that, with the UK’s current generation portfolio, the additional electricity demand from any charging regime, would be supplied by fossil fuels. Therefore, both uncontrolled and controlled charging would decrease the percentage of electricity supplied by low carbon sources by the same amount.

To illustrate this Figure 5.5 shows the seasonal variation in 2018 of the maximum and minimum renewables fuel mix under each charging scheme. In all cases the best renewables mix was seen in the no charging case. The fuel mix was slightly better in the controlled case, but due only to the reduction in resistive losses that occurs due to the reduced peak load.

In the future, if there were a significant increase in installed solar power then flattening the demand may prevent all solar power from being used. In this scenario, smart charging of electric vehicles could be used to offset the uncertainty in renewable production

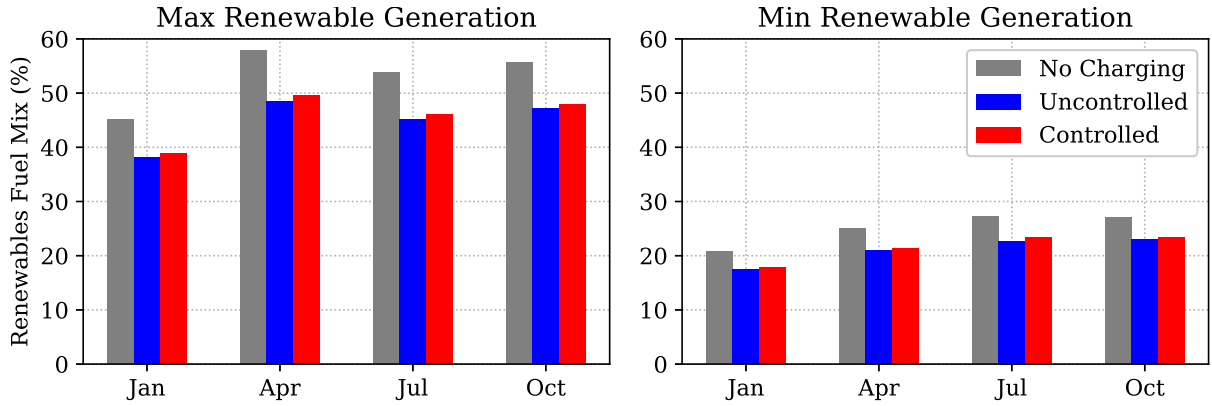


Figure 5.5: The best and worst case percentage of electricity supplied by renewables for each charging regime in the UK.

(rather than to flatten the load). This would mean that the controlled charging scenario would result in a significantly higher percentage of electricity generated from low carbon sources. The next section demonstrates the feasibility of this proposal, and suggest a way in which it could be implemented.

### 5.1.2.1 Maximising use of renewables

Although with the UK's current generation mix renewables rarely need to be curtailed, this will not always be the case. As the penetration of solar and wind increases, so does supply uncertainty – due to the dependence of these technologies on weather. This complicates the problem of supply-demand matching because there is uncertainty in both the supply and demand, as opposed to just the demand. Under this scenario it would make sense to use the flexibility of EV charging demand to offset the uncertainty in supply. If real-time control of EVs is possible then this could be achieved through participation in a balancing market. However, smart charging could also be used to optimise behaviour using offline forecasts of solar generation, and this is what is proposed in this section.

Deterministic optimisation involves finding the value  $\mathbf{x} \in \mathcal{X}$  that minimises some function  $f(\mathbf{x})$ , where  $\mathcal{X}$  is the set of solutions that satisfy some constraints. For the case of flattening an uncertain load, the function  $f$  is not known with certainty. Stochastic optimisation aims to find the optimal decision over a set of uncertain circumstances. In the literature section several reference papers considered stochastic optimisation of EV charging over an uncertain price. These were all two-stage problems, meaning the

problem objective function takes the form:

$$f(\mathbf{x}) = g(\mathbf{x}) + E_{\eta}[Q(\mathbf{x}, \eta)], \quad (5.1)$$

where  $g(\mathbf{x})$  is a deterministic objective and  $Q(\mathbf{x}, \eta)$  is the optimal solution to the separate problem:

$$\underset{y}{\text{minimise}} \quad q(\eta, y) \quad \text{subject to} \quad y \in \mathcal{Y}(\eta).$$

This formulation describes a decision maker taking some action, after which a random event  $\eta$  occurs which affects the outcome of the first-stage decision. A second decision can then be made in the second stage which compensates for bad first-stage decisions. The reason this formulation is popular in smart charging is that it allows both the day-ahead and intra-day markets to be modelled simultaneously. Therefore, if power was bought in the day-ahead market and the price forecast is increased, it can be sold back in the intra-day market. However, this formulation is computationally very complex, and for flattening an uncertain load, a single-stage problem is sufficient.

Single-stage stochastic optimisation problems seek the optimal action over a range of scenarios  $s$ , each of which has a function  $f_s$  and an associated probability  $p(s)$ . The objective is formulated as the weighted sum of the objective for each scenario such that:

$$f(\mathbf{x}) = \sum_s p(s) f_s(\mathbf{x}), \quad (5.2)$$

so that  $f$  is the expected value of  $f_s$ . In this case, each scenario has an associated existing load, such that the objective function (4.5) becomes:

$$f_s(\mathbf{x}) = \left\| \sum_{j=1}^{N_h} (\mathbf{h}_s + \mathbf{x})^{(j)} \right\|_2^2, \quad (5.3)$$

where  $\mathbf{h}_s$  is the net demand associated with each household under scenario  $s$ . The uncertainty is technically in the generation not the demand, however as the objective is to flatten the net demand (after the solar has been used) the solar generation is considered as a negative existing demand.

In order to form a realistic set of scenarios, historic UK solar generation was analysed. Figure 5.6 shows the average and variation in solar generation as a percentage of the installed capacity throughout the year. The solid lines show the average yield for each month, and the shaded areas cover the 70% and 90% confidence intervals. The large size of the bounds demonstrates that solar generation varies significantly day-to-day as well as seasonally. These distributions can be discretised to create a finite number of scenarios.

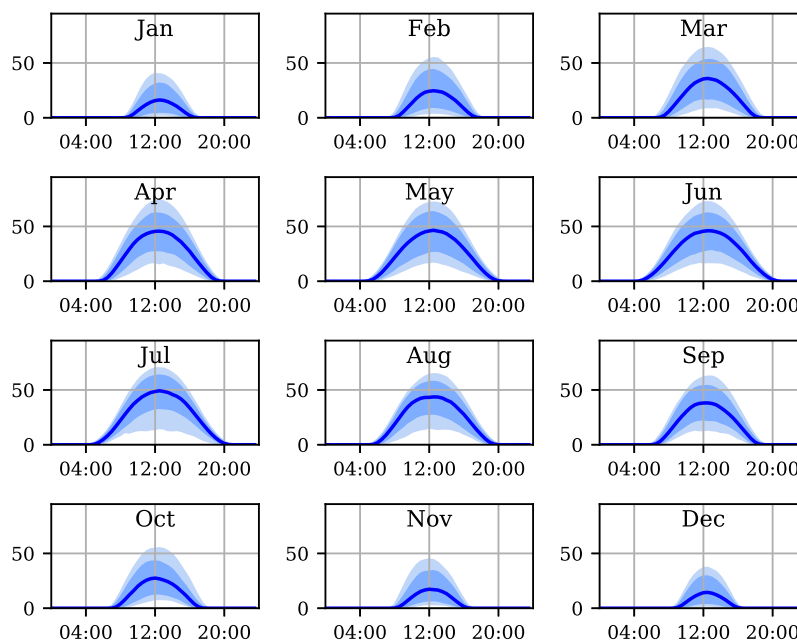


Figure 5.6: The solar generation as a percentage of installed capacity throughout the year in the UK. Solid lines show average values and the shaded areas cover the 70% and 90% confidence intervals.

Here a case study of Cornwall was considered, purposefully chosen because there is already more than 1 kW of solar installed per capita. The scenarios were generated by scaling the data from Figure 5.6 to the installed capacity of solar, and matching historic demand with the historic solar generation. For each month, the days of solar generation were ordered according to their total energy production. Then the 2.5<sup>th</sup>, 7.5<sup>th</sup>, 22.5<sup>th</sup>, 50<sup>th</sup>, 67.5<sup>th</sup>, 92.5<sup>th</sup>, and 97.5<sup>th</sup> percentile days were extracted as scenarios, and assigned probabilities according to the percentage of days closest to that percentile; the resulting values are summarised in Table 5.2.

Cornish vehicles were extracted from the NTS and their demand was scaled to represent a fleet of 100% EVs. Then the stochastic optimisation was performed, where the

No.	1	2	3	4	5	6	7
<b>Percentile</b>	2.5	7.5	22.5	50	67.5	92.5	97.5
<b>Probability</b>	0.05	0.1	0.2125	0.275	0.2125	0.1	0.05

Table 5.2: The scenarios created for the stochastic optimisation.

constraints matched those in Section 4.2.1 but the objective is (5.2). Figure 5.7 shows the net demand after the solar generation had been subtracted. The dotted lines show the bounds on net demand before the EV charging is added. It can be seen that in summer months there is sometimes more generation than demand in Cornwall. The blue area shows the net demand once the EV demand is added, with the line showing the most likely scenario and the shaded area covering the 70% and 90% confidence intervals. The 70% confidence interval in this case is equivalent to covering the range of scenarios 3-5, and the 90% covers scenarios 2-6.

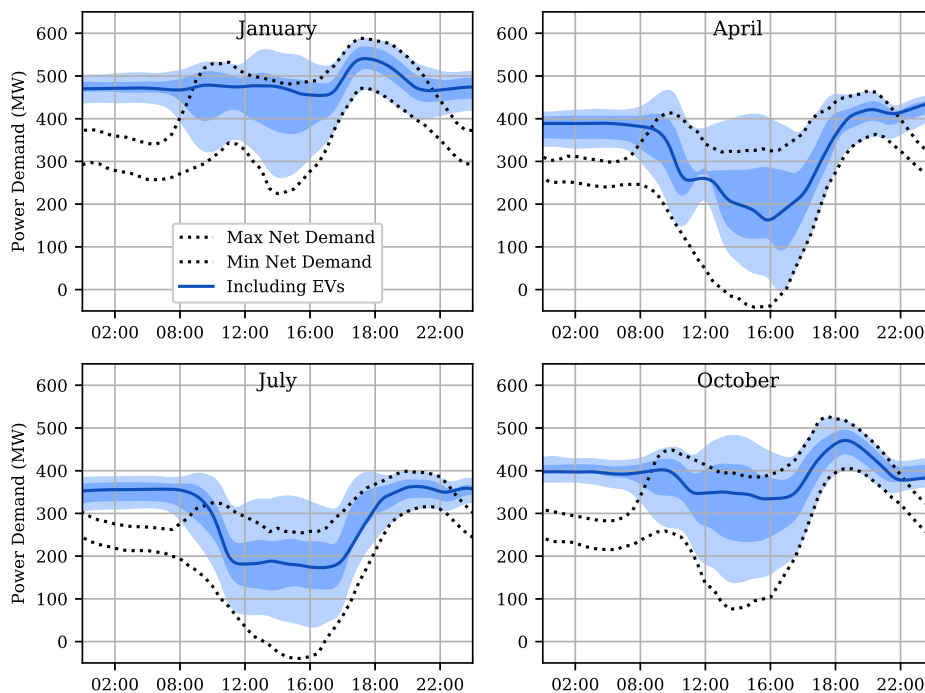


Figure 5.7: Total demand with stochastic smart charging. The dotted lines bound the demand minus solar generation covered in all scenarios, and the blue shows the total net demand once EV charging has been added in all scenarios. Solid lines show average values and the shaded areas cover the 70% and 90% confidence intervals.

As the stochastic optimisation finds a unique value of  $\mathbf{x}$ , the EV charging is the same

in all scenarios – all variation is due to the net existing demand variability. It can be seen that there is no scenario where perfect load flattening is achieved, However, in the confidence intervals shown, the peak demand is kept within the range seen before EV charging was added.

This case study demonstrates that smart charging could be used effectively to offset renewables uncertainty without real-time control of vehicles. It is worth noting that the range of scenarios considered in this example were very varied, as no prior information was assumed apart from the time of year. In reality an EV aggregator is at least likely to have day-ahead forecasts of solar generation, resulting in a smaller range of scenarios and a flatter optimised load.

In the short term there is not sufficient solar generation to significantly affect the stability of the system in GB, so this mechanism would not be necessary. However, as the penetration of low-carbon technologies increases, supply intermittency will become a larger problem, and smart charging of EVs could be a viable solution.

## 5.2 Transmission System

As far as the generation system is concerned, the location of power production and loads within the UK is unimportant. However, in reality the power needs to be transported from a small number of power plants to a large number of houses, and this is primarily done using the high-voltage transmission system. The GB distribution network is sectioned into discrete areas, each connected to the high-voltage system via a grid supply point.

In this section, the transmission system is simulated under uncontrolled charging of a 100% electric fleet. The highest loading case was considered – at the peak time on the coldest winter day. The impact is quantified in terms of the loading in the individual lines and the increase in losses in this part of the system.

A reduced version of the GB transmission system is published in [245], which includes the grid supply points and installed controllable generation. Scaled data from the NTS was used to construct uncontrolled charging load for each grid supply point, making the

simplifying assumption that everyone is connected to their nearest grid supply point. A peak load optimal power flow was then run in *Pandapower* [246].

**Line limits** Figure 5.8 shows the reduced version of the GB transmission system under the peak loading from uncontrolled charging of a 100% electric fleet. On the left map, the grid supply points are marked with bubbles whose size show the total load connected to that part of the network. The red bubbles show the percentage of that load that is EV charging. The map on the right shows the resultant loading of the high voltage transmission lines, as a percentage of their rated maximum current. None of the lines exceed their rated limit, and the majority of the lines are well within their design specifications.

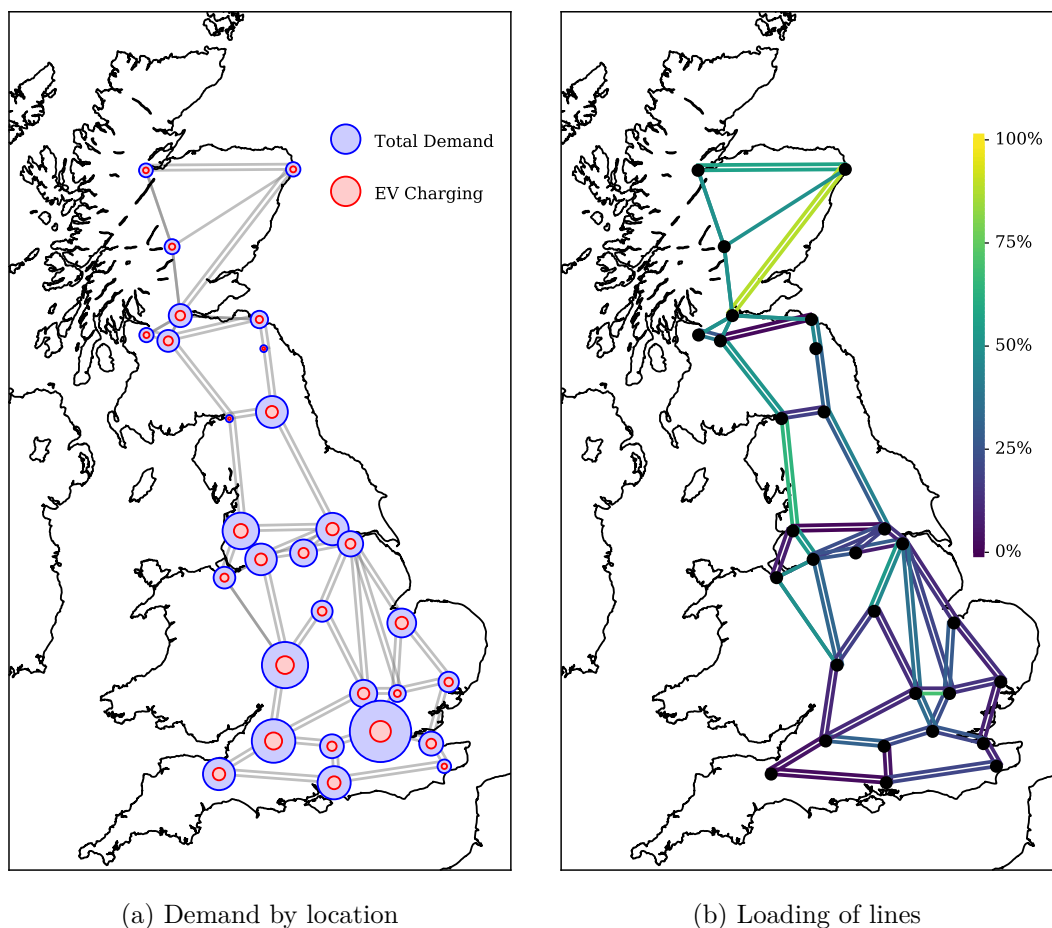


Figure 5.8: A reduced model of the UK transmission network under uncontrolled charging peak load; (a) shows the location of the grid supply points, and the amount of EV and total demand at each; (b) shows the % of each line's rated loading being used.

Part of the reason that the system is operating well below its limit is that the UK

has a target of 100% N-1 supply security, which means the demand could always be met if the single largest piece of infrastructure fails [247]. The transmission network is fully meshed, meaning there are at least two routes connecting every pair of nodes, so all grid supply points can still be serviced with a single line down. However, with one line down the others will have to carry an increased current, and this may result in violation of their constraints. Therefore, here the line limits are also investigated under the scenario that a single line in the network is down.

In order to perform this analysis, one-by-one the lines were removed from the network and the optimal power flow re-run. Figure 5.9 shows the maximum load in each cable over all simulations, with and without the uncontrolled charging load. Where lines are loaded at over 100% they are capped there, and marked with a red circle. Two scenarios of uncontrolled charging are included: 100% penetration, and the 2030 projection of EV penetration.

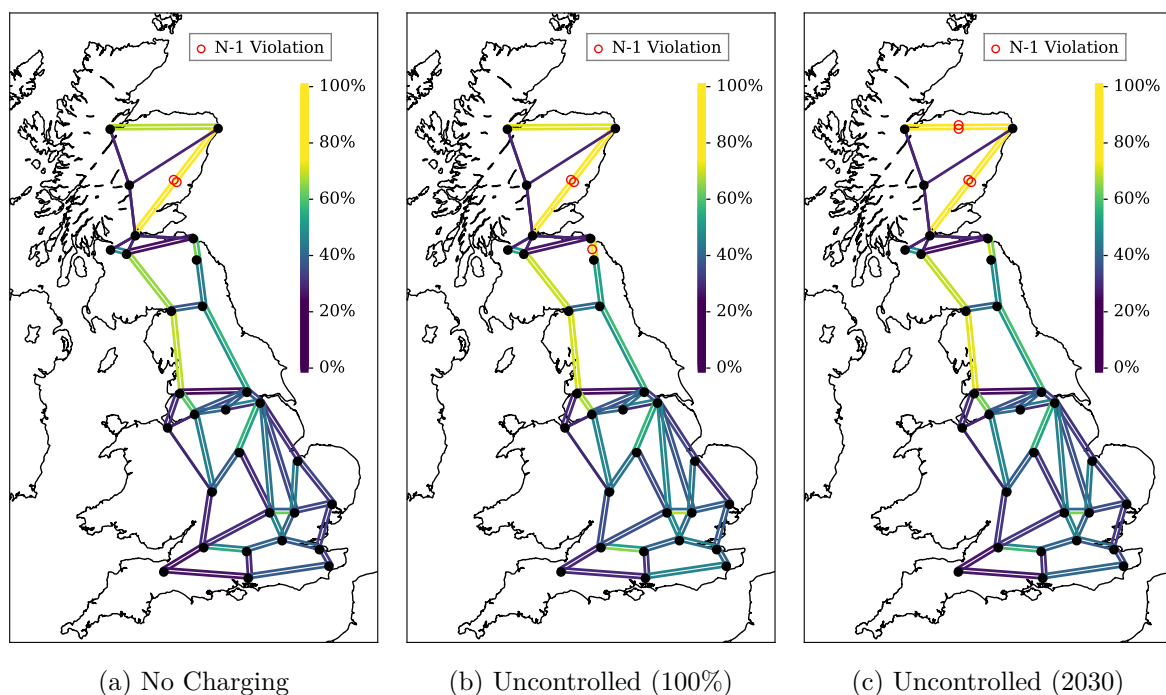


Figure 5.9: The maximum % loading of each line high-voltage when the single largest component fails.

It can be seen that, compared to the loading when all lines are operational (Figure 5.8b), the system is operating much closer to its limit in all charging scenarios. In the

no charging scenario there are two lines with violations, but this number rises with the addition of uncontrolled charging; there is one additional violation in the 2030 scenario and two in the 100% scenario.

In all cases it is the northern part of the network which is near its limit – the majority of the southern network is below 50% capacity, even under N-1 security. This is partly because the southern network is better meshed, and partly because the Scottish system is at a lower voltage than the rest of GB. Note that the effect of storage and HVDC interconnections have not been considered, so it is possible that the demand could still be met without violations by utilising these resources.

**Network Losses** Despite the line currents being within operating limits, the increased load will result in higher system losses. At peak load in the no charging scenario 0.51% of the power put into the transmission system was dissipated as resistive losses. As losses vary quadratically with current, this number will be lower at other times of day. The addition of uncontrolled EV charging increases this share to 0.56%. Losses are uneconomical, but in this case their size is not sufficient to warrant optimising vehicle charging for this part of the system; in Chapter 6 it is shown that compared to the distribution system losses this change is insignificant. The controlled charging scenario is not considered separately, as it has already been shown that the controlled charging peak load is identical to the no charging peak load.

### 5.3 Comparative Case Study

As a comparison to the GB case, a similar simulation was constructed for Texas, US. A transmission system model for Texas was not available, so this section deals only with the aggregated demand and fuel mix.

**Supply-Demand Matching** Figure 5.10 shows the aggregate demand in Texas with charging of a 100% electric fleet, analogous to Figure 5.3. Due to the hotter temperatures, the base electricity demand in Texas varies conversely to the UK; the load is highest in

the summer, due largely to air-conditioning loads. Uncontrolled charging of a 100% fleet of electric vehicle is projected to increase the peak demand by around 8 GW. This is a proportionally smaller increase than in the GB case, however Texas has much lower redundancy in its generation capacity – as would be expected given that GB is an island, while the Texas grid is well connected to its neighbouring states’ systems. The nameplate total, solar, and wind generation capacity in Texas are shown in Table 5.3. It can be seen that, even with perfect renewable generation, the summer uncontrolled charging scenario will exceed the generation limit.

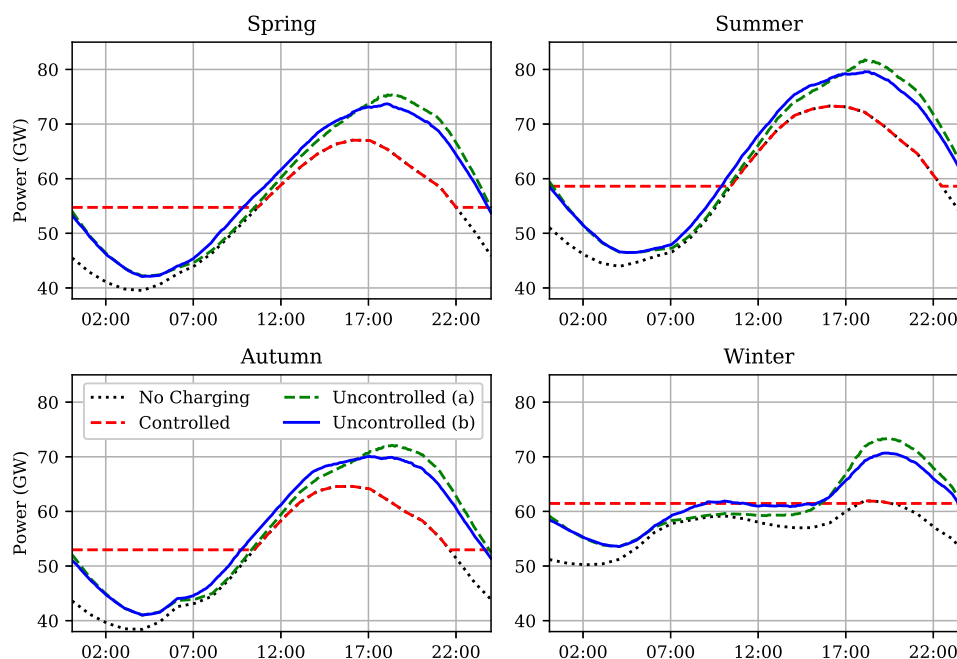


Figure 5.10: The Texas demand profile on a high-use week day with no charging, controlled and uncontrolled charging of a 100% electric fleet of vehicles. For uncontrolled charging (a) shows charging after final journey, (b) shows charging using proposed model.

<b>Total (GW)</b>	<b>Solar (GW)</b>	<b>Wind (GW)</b>
77.2	2.9	22.6

Table 5.3: The nameplate generation capacity in Texas.

In all seasons controlled charging can avoid any increase in peak demand, and in the warmer seasons there is additional room for flexible demand; despite vehicle usage being higher in Texas, the ratio of vehicle to existing energy consumption is lower. Another point of interest is the smaller difference between the uncontrolled charging scenarios (a)

and (b); in the UK case after-journey charging overestimated the proposed model by 100%, while in this case there was only around a 20% increase. This may be due to the smaller percentage of vehicles being at home in the middle of the day, such that in both cases most of the charging occurred overnight. It could also be due to the larger daily vehicle consumption, meaning vehicles have a lower SOC in the evening and are less likely to delay charging until the next day.

**Fuel Mix** The generation mix in Texas is markedly different from the GB mix. The renewable generation is heavily dominated by wind power and the Texan generation system operates much closer to its capacity limit. Figure 5.11 shows the generation capacity and fuel mix in Texas on the best and worst day for renewable generation in 2018. In the best case up to 20 GW of wind power are produced, resulting in almost 50% of electricity supplied by renewables. However, the nature of wind generation is that on still days the output becomes very low, so on the worst case day there is insufficient generation to meet the demand – power will have to be imported from a neighbouring state.

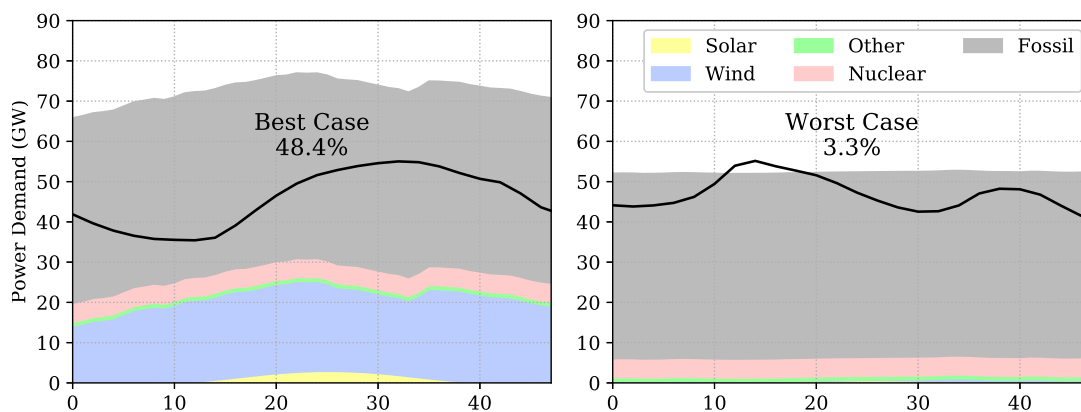


Figure 5.11: The generation capacity and fuel mix in Texas on a high and low renewable production day in 2018, with fuels ordered according to preference. The line shows the national demand on that day.

In one aspect the UK and Texas are similar: any increase in demand would need to come from fossil fuels. Figure 5.12 shows the best and worst case renewables fuel mix, under each charging regime. In every scenario, the addition of charging reduces the percentage of electricity demand met by renewables, and controlled charging is only

marginally better than uncontrolled.

The difference between the best and worst case fuel mix is much larger at all times of year, highlighting the drawbacks of using a single source of renewables. There is quite a large variation between seasons in the best case, however wind generation is less seasonal than solar so this may well be down to the specific weather or electricity demand in 2018.

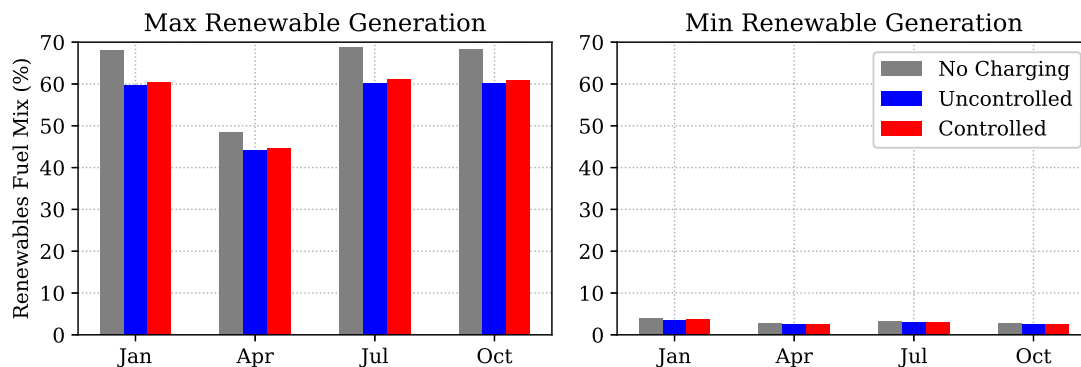


Figure 5.12: The best and worst case percentage of electricity supplied by renewables for each charging regime in Texas.

## 5.4 Concluding Remarks

In this chapter the impact of electric vehicle charging on generation and transmission systems was explored, using case studies from GB and Texas.

Uncontrolled charging of 100% EVs would increase the GB peak demand by 8 GW, or 16%. While this increase is within the existing installed capacity, it exacerbates the difficulty of switching towards a lower carbon system. In Texas there would also be an increase of 8 GW, representing a smaller increase of 11%. However, Texas does not have sufficient installed capacity to meet this increase, so (regardless of low carbon ambitions) additional generation would need to be installed. In both GB and Texas, any increase in peak demand could be completely avoided by using smart charging to flatten demand nationally.

There is currently insufficient renewable generation to meet the existing demand in either Texas or GB. This means that, in the short term, any additional increase in electricity demand will come from fossil fuel sources – regardless of whether EV charging

was controlled or not. Currently the only difference in fuel mix between uncontrolled and smart charging is that there are fewer electrical losses associated with smart charging, so the additional fossil fuel requirement would be slightly lower. However, system dynamics have not been considered in this thesis, and it is possible that the flexibility of EV charging could be used to provide system inertia at times when renewables would otherwise need to be curtailed. Additionally, it was demonstrated that in the future, if a large amount of intermittent renewables were installed onto the system, EV charging could be controlled stochastically to mitigate uncertainty in the renewable generation.

Uncontrolled charging of a 100% EV fleet would not significantly impact the GB transmission system under normal operation; all lines remain within their limits, and losses are only marginally increased from the no charging case. However, the UK government aims for the system to be able to operate in the event of the failure of any single line. The addition of EV charging load means that some lines may suffer limit violations in the event of the failure of another line, so these areas would require reinforcement to meet the system's security target. Flattening load at the transmission level would mitigate this increased risk.

The difference between the GB and Texas case studies demonstrates that these results can not be extrapolated to represent other power systems, however some generalised statements can be made. Firstly, uncontrolled charging of EVs is likely to increase peak demand (particularly if the existing peak occurs in the early evening), but this increase can be reduced by flattening load at the national level. Secondly, unless there is an existing surplus of renewables, the addition of EV charging will reduce the percentage of electricity generated from low carbon sources (regardless of charging strategy). Thirdly, with uncontrolled charging the transmission system will be forced to carry larger currents, which will increase losses and may violate line limits (in either normal operation or the N-1 case). Flattening load at the transmission level will reduce or mitigate the increases in currents, and hence these negative effects.

These results have focused on the national loading of the system, which deals with the aggregated charging of a large number of vehicles. Different challenges are faced when

the number of vehicles being aggregated is lower, as is the case in the distribution system.

# Chapter 6

## Impacts on the Distribution System

Analysis of the distribution system operation is more complex than analysis of the generation and transmission system operation. While the transmission system is one large high-voltage network, the distribution system is made up of thousands of low voltage circuits. The topology of these networks varies according to the road layout and the date the networks were constructed. The load on the networks is also likely to vary regionally, according to the lifestyle of local residents and whether the households are also connected to the gas network. The structure of the full distribution network is not available for research purposes; in fact, no organisation holds the full dataset, as the network is sectioned into discrete areas each owned by a different distribution network operator (DNO). Therefore, it is difficult to accurately assess which portions of the network are currently the closest to their operating limit.

However, it is possible to assess the regional variation in loading of the network. Within distribution networks load is highly stochastic, as the variability of individual consumers is not negligible relative to the total load. In contrast, the national system mainly experiences seasonal and weather related variation, so it is sufficient to investigate the deterministic usage on the coldest winter day. Stochasticity complicates analysis because we require the networks to operate with some degree of confidence, not just in the average case. Therefore, a larger amount of data, and more complex modelling methods are required to assess loading at this level.

In this chapter, the impact of domestic EV charging on the distribution system is investigated. Section 6.1 focuses on the changes to distribution network loading across GB. This does not require knowledge of the network, and allows the areas which will experience the largest proportional increase in residential load to be identified. These results are presented at local authority resolution for the whole country, and at a higher geographic resolution for Oxfordshire.

Section 6.2 estimates the impact of the additional EV load on network operation in the GB system. Although transformer data and example networks were available, a number of simplifying assumptions have to be made to investigate this. Therefore, the results from this section are less reliable than the loading simulations.

In Section 6.3 the use of various alternative smart charging objectives (presented in Section 4.2 and 4.3) are investigated. The first two sections only use load flattening as an objective, so this section determines whether an alternative objective can achieve a better result.

Finally, Section 6.4 presents a comparative case study to demonstrate how the results may vary for systems other than GB.

## 6.1 Network Loading

In this section, the change to distribution network loading as a result of charging a 100% electric fleet is forecast. Load is network invariant, meaning it is not affected by the structure of the network. Given the full GB network model is not available, this means the results are subject to fewer modelling assumptions than operation analysis (and thus more accurate).

In the UK, distribution networks are designed to tolerate a certain after diversity maximum demand (ADMD) [248]. This is the peak demand per household at a 30-min resolution averaged over the network. The ADMD that a network is designed to depends on the size of the households on the network, and whether it has dual-tariff electricity meters. Dual-tariff meters are the only established demand response mechanism in the

UK; they apply time-of-use pricing using two electricity tariffs, such that there are seven off-peak hours where electricity is cheaper. According to the design specifications in [248], electricity networks in single-tariff areas are designed to tolerate an ADMD of 1.2-2.4 kW, depending on the size of the houses.

EV charging is likely to increase ADMD everywhere, but some areas may be worse affected than others due to: larger travel distances, higher vehicle ownership, lower variability between local vehicles, or a lower existing peak load. Simulations were completed to estimate the increase in ADMD due to charging of a 100% EV fleet in each local authority in the UK. This required both the existing ADMD and the peak EV charging demand at 30 minute resolution to be predicted.

The regional break down in the NTS makes it possible to separately simulate charging of electric vehicles in each local authority, using Monte Carlo simulations. These simulations are the simplest way to capture the effect of stochastic input parameters; a large number of simulations are run with the input parameters randomly sampled from predetermined probability distributions each time, which results in a probability distribution of output parameters. In each simulation run, 50 households were randomly selected from the subset of the NTS data that was recorded in the chosen area, and their vehicles' charging was predicted using the model described in Section 4.1.2. 50 was chosen for the number of vehicles to be representative of a standard UK low voltage residential network with 100% of households having an EV (e.g. see European Low Voltage Test Feeder [240]). Monte Carlo simulations were repeated until the average charging demand of the simulations converged. The controlled charging scenario was calculated using a similar methodology, except that, instead of applying the uncontrolled charging model, the load flattening strategy in section 4.2.1 was used to determine charging.

Existing ADMD depends on a number of factors, including: the energy efficiency of buildings, the number of residents per dwelling, the affluence of the area, and whether or not the homes are connected to the gas network. The UK government publishes the annual electricity consumption of households within each local authority, as well as the number of households on each tariff structure [249]. In the UK there are two commonly

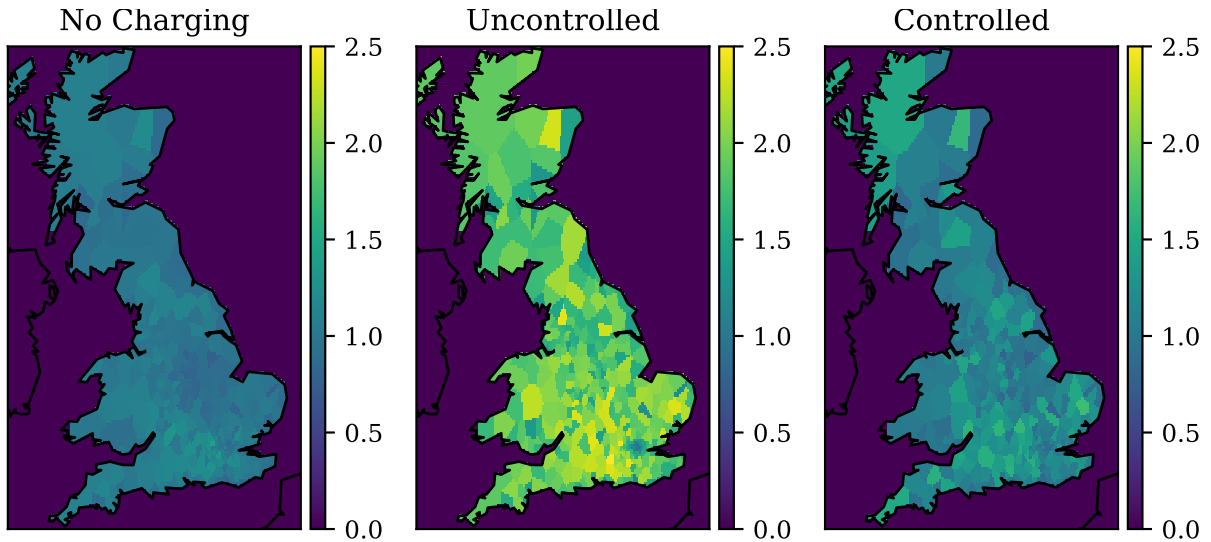


Figure 6.1: The regional variation in ADMD (kW) predicted for each charging scenario.

available structures: a flat rate, and dual tariff (where there are 7 hours at a lower rate). Elexon produce demand profiles representing the average user from each structure, on weekdays/weekends and in different seasons [250]. Here, the existing power demand for each area is estimated by averaging the two tariff structures weighted according to the percentage of homes on each meter type. The resultant profile is then scaled to match the recorded area-specific energy consumption. Daily energy consumption was estimated by scaling the annual consumption figures, assuming that winter usage is 20% higher than average – as shown in the Elexon profiles. The predicted charging is then superimposed onto this demand, and the percentage change in ADMD is calculated.

Figure 6.1 shows the predicted ADMD in each local authority across GB, under each charging scheme. In the no charging case all areas are below 1.2 kW, while uncontrolled charging increases the demand in several areas to 2.5 kW. Controlled charging reduces the ADMD compared to uncontrolled charging, but (unlike in the national loading case) there are many areas which will see increases in demand despite smart charging. Many of the highest loaded areas are suburban areas to the west of London, where both existing electricity demand and vehicle use is high. Areas with the lowest uncontrolled ADMD were those where private vehicle use is lowest, most notably: central London, Oxford, and Cambridge.

It should be noted that these are average results – there will be high-use days where the

ADMD will be larger than that shown on the map. Additionally, the results are averaged geographically (as only one result is presented for each local authority); in reality there will be residential networks within the area whose loading is both higher and lower than that shown.

### 6.1.1 Linear Regression Model

When the NTS is broken down to the local authority level there are some areas where the sample size becomes quite small. This means that outliers will have a heavier impact on results; for example, if there is a vehicle in the travel survey with a 100 mile commute this may skew the results for that area. One way to investigate this is to fit a regression model that maps travel parameters to the predicted charging demand. This is useful because there are several statistics recorded in the NTS that are also measured in the national census [29]. The census collects a much smaller set of data per sample, but surveys the entire country. Therefore, its statistics are more accurate and can be broken down to a much lower geographic resolution – lower super output area (LSOA) level. As of 2011, LSOAs in the UK contained between 983 and 8300 residents. The existing electricity demand used in the analysis is also available at the LSOA level, published by the UK government as part of the Digest of UK Energy Statistics (DUKES) report [249]. A model that maps these statistics to the results would remove bias created from small samples, and allow the results to be predicted at a much lower geographic resolution.

Variable	Description	NTS	Census	DUKES
$f_1$	Average commuting distance by private car	✓	✓	
$f_2$	Percentage of households commuting by car	✓	✓	
$f_3$	Number of vehicles owned per household	✓	✓	
$f_4$	Number of residents per household	✓	✓	
$f_5$	Annual electricity demand			✓
$f_6$	% of households with dual-tariff meters			✓

Table 6.1: A summary of the variables used.

A linear regression model was built which maps the variables described in Table 6.1 to some output  $y$ . It is standard practice to normalise both the features  $f$  and the target

$y$ . This normalised variable,  $\hat{f}_i$ , is given by the calculation:

$$\hat{f}_i = \frac{f_i - \mu_{f_i}}{\sigma_{f_i}}, \quad (6.1)$$

where  $\mu_{f_i}$  is the mean of the feature  $f_i$ , and  $\sigma_{f_i}$  is its standard deviation. In this example, the target is to predict the percentage increase in ADMD as a result of uncontrolled EV charging. Given that the addition of EV charging can not decrease the peak demand, the change in ADMD must be a positive number. Therefore, it was decided to use the natural log of the percentage increase as the target variable, such that:

$$y = \log_e \left[ \frac{\max(\mathbf{x} + \mathbf{h})}{\max(\mathbf{h})} \right], \quad (6.2)$$

where  $\max$  finds the largest value of the vector with time, and recalling that  $\mathbf{h}$  represents household demand and  $\mathbf{x}$  is vehicle charging. Using the logarithm means that there is no combination of input parameters which can result in a decrease in peak demand being predicted, and reduces the training error of the model.

As the model is linear, the final function will have the form:

$$\hat{y} = \sum_{i=1}^6 c_i \hat{f}_i, \quad (6.3)$$

where  $c_i$  are the model parameters to be found. These parameters are found by fitting the local authority simulation results to the variables recorded from NTS for each area. The features from both datasets are normalised using the mean and standard deviation from the census data – given it is the larger data set. Table 6.2 lists the mean and standard deviation, allowing readers to apply this model if desired.

	$f_1$	$f_2$	$f_3$	$f_4$	$f_5$	$f_6$	$y$
$\mu$	7.5 miles	41%	1.0	2.3	3000 kWh	15%	-1.2
$\sigma$	1.9 miles	13%	0.17	0.38	610 kWh	12%	0.52

Table 6.2: The mean and standard deviation of the variables, used to normalise.

The maximum likelihood parameters were found for the function using a standard linear regression package, resulting in the equation:

$$\hat{y} = 0.079\hat{f}_1 + 0.258\hat{f}_2 + 0.163\hat{f}_3 + 0.020\hat{f}_4 + 0.152\hat{f}_5 - 0.139\hat{f}_6. \quad (6.4)$$

The size and sign of the coefficients give interesting insight into the weighting of each parameter on the result. The most significant predictor for large increases in ADMD is the percentage of households that use private vehicles as their primary commuting mechanism, followed by the number of vehicles owned. Contrastingly, the commuting distance and number of residents per household have only a small effect.

This equation allows the results from Figure 6.1 to be repeated at a lower geographic resolution. It is difficult to extract meaning from the entire GB map at this resolution, so Figure 6.2 shows the results zoomed in to Oxfordshire. Each LSOA is shown by a shaded region, whose colour shows the predicted percentage increase in ADMD. The county boundary is shown in black, and salient locations are marked. The shaded shapes show the LSOAs and their colour shows the percentage increase in ADMD in that area. In the city centre, where average commuting-by-car distance and vehicle ownership is very low, there is almost no increase in ADMD. Whereas, in some of the rural areas there is a 40% increase. It should be noted that a 40% increase is relatively low compared to the national average; this agrees with the previous assertion that load in Oxfordshire Oxfordshire will be only moderately affected by electric vehicle charging.

## 6.2 Network Constraints

In order to evaluate the likelihood of the distribution network constraints being violated, a network model is required. Here, a set of representative networks are used to estimate the effect of EV charging on system operation. Three networks are used, representing urban, suburban and rural network styles respectively. The networks are described in detail in section B.1 of the appendix.

Monte Carlo simulations were again constructed for each local authority. However this

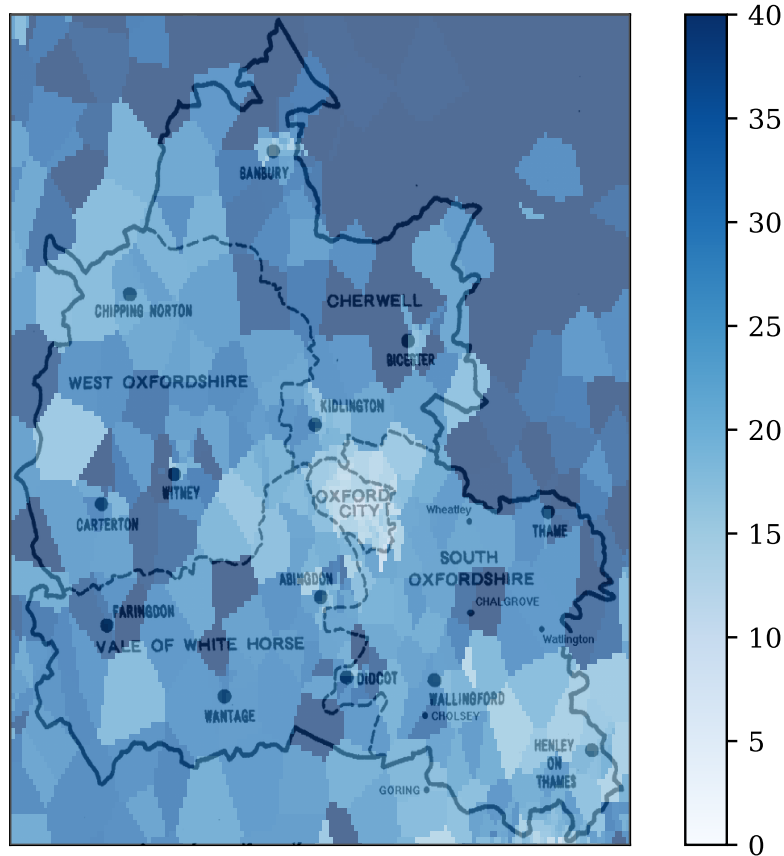


Figure 6.2: The predicted percentage increase in ADMD in Oxfordshire as a result of 100% domestic EV charging.

time 1 minute resolution household loads from [251] were used, and scaled according to the electricity demand data from the area. The higher time resolution loads were chosen because 30 minute resolution is not sufficient to properly estimate network losses. The relevant test network was selected according to the population density of the area. In each run of the simulation, household and vehicle loads were randomly assigned and a power flow simulation was carried out. The resulting voltage profiles and losses were stored and then the process was repeated. It is important that a full probability distribution of results be obtained, because we want to quantify the probability of a violation occurring – not just whether there is a violation in the average case.

Here we consider two potential network violations: violation of transformer limit, and violation of voltage bounds. Residential networks are connected to the higher voltage system using a secondary transformer, which is rated to a certain maximum load. If the total load passing through the transformer exceeds this then overheating will occur,

decreasing its life expectancy. Therefore a transformer overload is defined as a case where the total load on the residential network exceeds this design limit.

Appliance safety in GB requires bus voltages to stay within  $\pm 10\%$  of 230 V [252]. Resistive losses cause voltage drops, so parts of the network a large electrical distance from the transformer are likely to be at a lower voltage. As the load in the network increases, so do the line currents, and hence the losses – meaning under-voltages become more likely. A voltage violation is therefore defined as a case where the voltage falls below this threshold at some point in the network.

In this section, first a single area is used as a case study to visualise the effect of EV charging on the system operation. Then the probability of a constraint violation is estimated for each local authority in GB.

### 6.2.1 Rochdale Case Study

The local authority of Rochdale was randomly selected as a case study, to demonstrate the impacts of EV charging on network peak demand, losses, and voltages. Rochdale is a suburban town 10 miles outside of Manchester which has relatively low vehicle ownership.

**Power demand** Figure 6.3 shows the demand of the example distribution network at 1 min resolution with no EV charging, and with uncontrolled and controlled charging of a 100% electric fleet. The household and vehicle load data came from a network metering trial [251]. The solid line shows the average profile, and the shaded area covers the 90% confidence interval. At this level of aggregation, there is a large variance in the power demand, so it is important that not only the average case is considered. Uncontrolled charging more than doubles peak demand, due to the most popular charging time being in the early evening (when the existing demand is already highest). The transformer limit in this case was 315 kVA which, assuming a 0.95 power factor, translates to a rough demand limit of 300 kW. In the no charging case, demand is always below this limit, while uncontrolled charging violates the limit more than 50% of the time. Controlling charging can likely prevent a violation, although there is a slightly increased risk compared to the

no charging case.

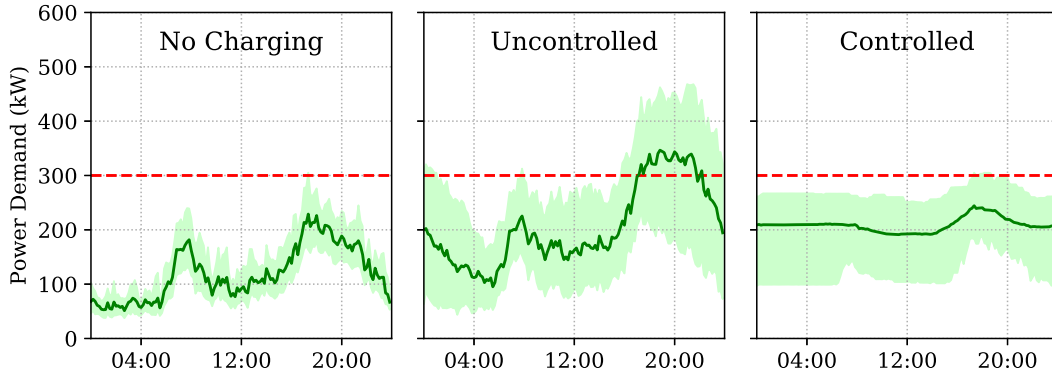


Figure 6.3: The total power demand on the network under each charging scheme. The solid line shows the average, and the shaded area covers the 90% confidence interval. The red dotted line shows the transformer load limit.

**Network losses** LV distribution networks currently account for 29% of total losses in the power system [204]. Losses not only waste energy, but generate heat in cables, and increase voltage drops across the network. Figure 6.4 shows the total resistive losses in the distribution network before charging, with uncontrolled charging, and with smart charging. The blue line shows the average value, the box covers 50% of the values and the vertical lines cover the full range of values. Uncontrolled charging triples the average resistive losses in the network, which would significantly increase the total wasted energy in the system. Flattening load can avoid some of this increase, but the losses are still more than twice what they were without the EV charging – some increase in losses is unavoidable with a larger energy demand. Therefore, without system reinforcements, EV charging will likely increase the low-voltage share of system losses.

**Voltages** The increase in resistive losses will result in voltage drops, potentially leading to unsafe operating conditions for household devices. Figure 6.5 shows the average, lowest, and highest bus voltage in the network under each scheme. Solid lines show median values, and the shaded area covers the 90% confidence interval. The voltage lower bound is shown as a red dotted line. In all cases there is minimal variation in the highest voltage, this is because it normally occurs in the node at the top of the feeder, whose voltage changes very little with network loading. However, occasionally phase imbalance

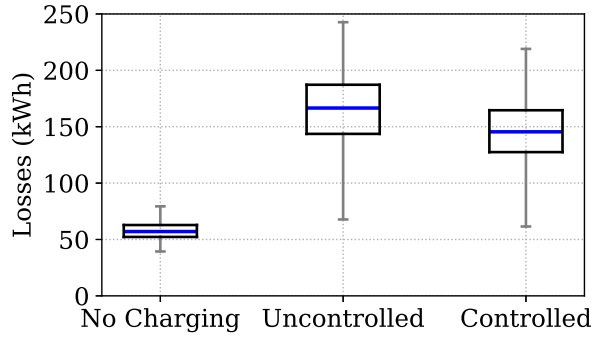


Figure 6.4: The total resistive losses for each scheme. The blue line shows the median value, the box covers 50% of values, and the whiskers the total range.

leads to spurious high voltages further down the network. The lowest voltage experiences much greater variance, and significantly lower values are observed in the uncontrolled case than the controlled case. As with losses, a reduction in voltages is unavoidable with the additional vehicle load (without network reconfiguration), but the flatter load results in less extreme low values. In the no charging case there are no violations of the lower voltage limit, while there are in both the charging scenarios; the risk is reduced, but not avoided, by controlling charging.

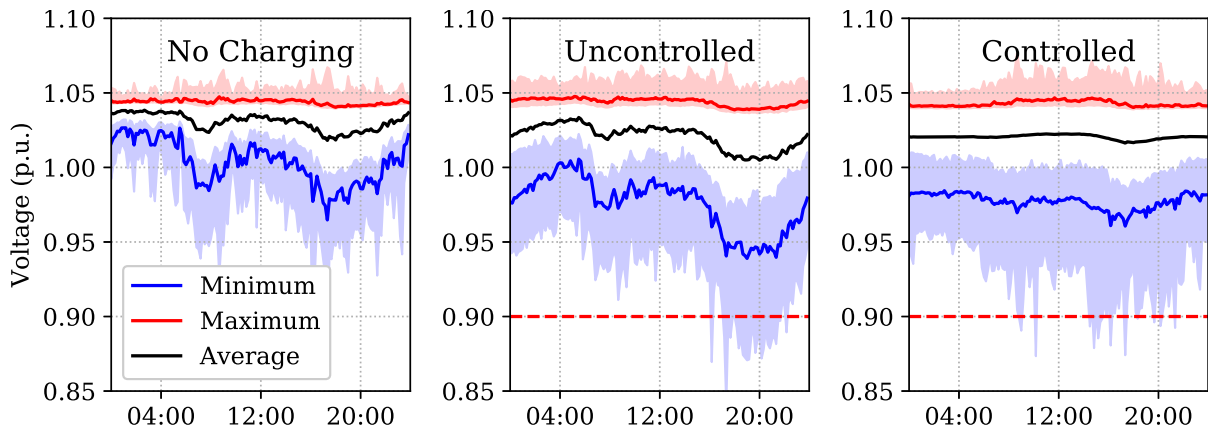


Figure 6.5: The average, lowest and highest voltages in the network throughout the day under each scheme. The solid lines show the median value and the shaded area covers the 90% confidence interval. The red dotted line shows the voltage lower bound.

## 6.2.2 Geographic Variation

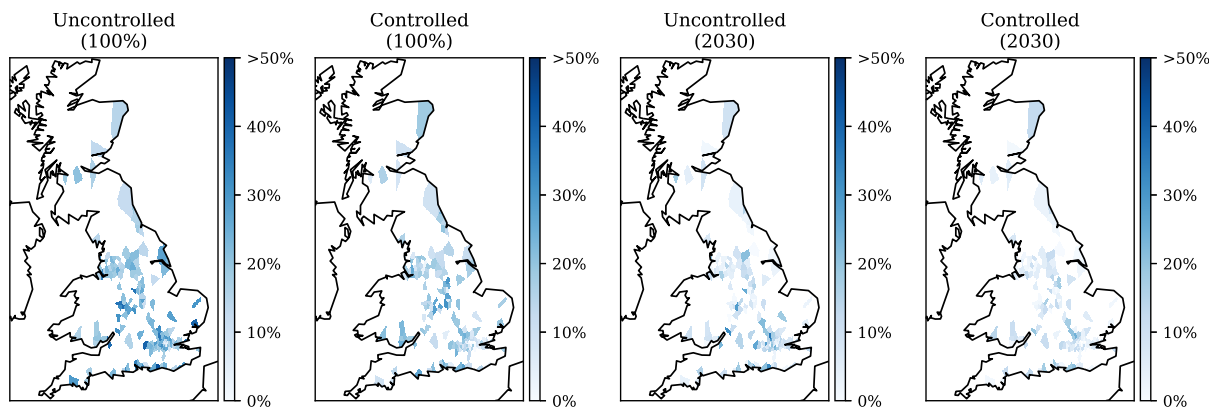
For the Rochdale case, it appears that uncontrolled charging of a 100% EV fleet will likely result in transformer violations, and possibly also voltage violations. It also showed that

smart charging was very effective at avoiding transformer limits, but only slightly superior when it came to voltage violations. However, these results are specific to Rochdale, and can not be used to make broader statements about the impact of EV charging in the UK. Individually analysing the results for every local authority would be exhausting for both the author and the reader. However, the results can be summarised by considering the probability of either a voltage or transformer violation for each area. Here this is calculated as the percentage of the Monte Carlo runs which experienced a violation. For the Rochdale case study, this results in transformer and voltage violation probabilities of 75% and 13% respectively.

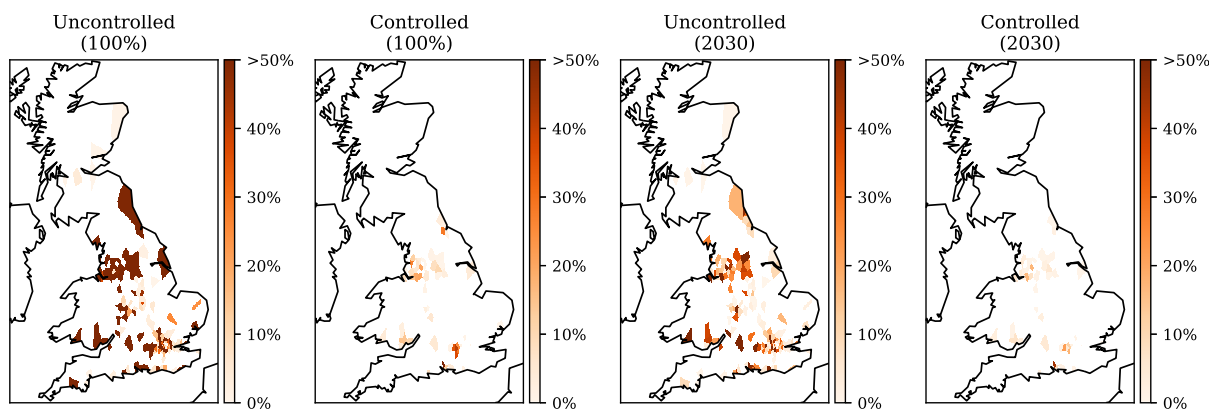
Figure 6.6 shows the increased likelihood of violating either constraint under both uncontrolled and controlled charging for each local authority in the UK, compared to the no charging case. Both the 100% case and the projected 2030 scenario from section 3.2 are presented. Note that the scale has been capped at 50% in order to see more detail (any areas with risks above 50% would definitely require upgrades anyway). It can be seen that there are many areas which do not experience either type of violation in any scenario, while there are some areas which have a significantly increased risk of violation. This suggests that there are many parts of the network which are designed to tolerate a significantly higher loading than they are currently experiencing. This could be because of the recent decrease in UK household electricity demand, or because of the difficulty in forecasting household load before the network has been built. It is also worth noting that it may be worthwhile for DNOs to over-specify networks, because the cost of fitting or upgrading the underground network exceeds the costs of components.

Where they occur, transformer violations have greater certainty than voltage violations. However, they are also reduced with much greater success using controlled charging. By comparing the uncontrolled 100% and 2030 scenarios it can be seen that many of the areas which are most likely to experience violations, are not projected to have large numbers of EVs in the immediate future. This demonstrates that, in the short term, it is important to look at the local population of EVs in addition to the operation forecasts.

Figure 6.7 displays the areas most likely to experience either violation under uncon-



(a) Increased Probability of Voltage Violation (%)



(b) Increased Probability of Transformer Violation (%)

Figure 6.6: The increased likelihood of violating distribution network constraints in the UK, for charging of a 100% EV fleet and in 2030.

trolled charging in both the 100% and 2030 scenarios. There was a strong correlation between voltage and transformer violations, however voltages violations were more strongly correlated with population density, while transformer violations were negatively correlated with the percentage of meters that are dual-tariff. Overall, areas most likely to experience transformer overloads were suburban areas outside of larger cities, and voltage violations were most likely in bigger cities with less public transport infrastructure. In the 2030 scenario there is a stronger correlation between voltage and transformer violations than in the 100% case. This demonstrates that, in the short term, the size of the EV population is more important than the network or local travel behaviour.

Figure 6.8 shows how the overall percentage of networks expected to experience violations changes with time. Under uncontrolled charging transformer violations are much more likely than voltage violations, while under controlled charging the converse is true.

Transformer		Voltage		Transformer		Voltage	
Stockton	91%	Reading	51%	Watford	84%	Watford	37%
Eastleigh	90%	Worthing	49%	Slough	79%	Worthing	33%
Cannock	89%	Sandwell	47%	Gloucester	75%	Gloucester	33%
Dudley	89%	Bristol	46%	Swindon	74%	Birmingham	29%

(a) Worst affected in 100%                      (b) Worst affected in 2030

Figure 6.7: The areas most likely to require upgrades.

If a 100% electric fleet were allowed to charge without intervention, then 20% of networks would experience transformer violations and 10% voltage violations. These numbers reduce to 2% and 6% respectively with controlled charging. It is clear that, on average, flattening load is much more effective in preventing transformer violations than voltage violations.

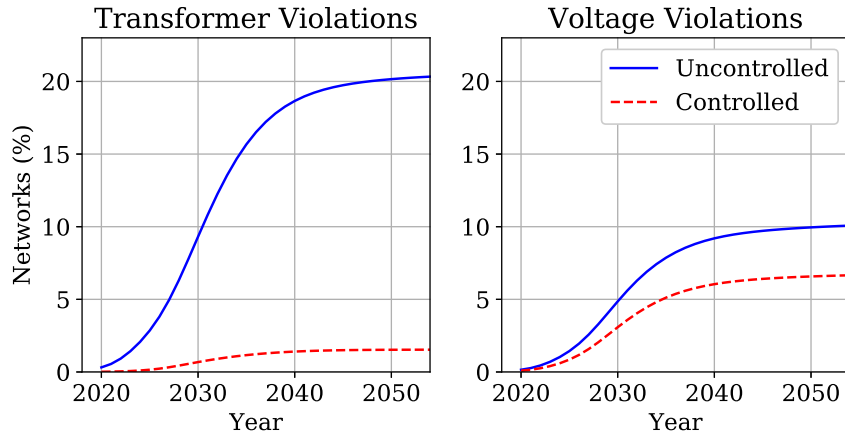


Figure 6.8: Percentage of networks expected to have violations with time.

These results all need to be taken with caution due to the simplifying network assumptions made. However, even if the absolute figures are untrustworthy, the comparison of results from different areas in GB is still valid.

### 6.3 Comparing smart charging objectives

Thus far, only load flattening has been considered as a controlled charging strategy. However, there are several possible objectives for smart charging. For the generation and transmission systems it is clear that flattening load is the optimal scenario, as it minimises the required generation capacity. However, at the distribution level we are

concerned about both transformer and voltage violations. Flattening load will minimise transformer violations, but not explicitly voltage violations – which could partially explain the smaller improvement in voltage violations seen in Figure 6.8.

This section investigates the possibility of using other smart charging objective in low voltage residential networks. First, explicit loss minimisation is considered. Then, the potential of vehicle-to-grid (V2G) to further flatten load is considered.

### **6.3.1 Loss minimisation**

In a purely resistive network, minimising losses will minimise voltage drops. Therefore, when the voltage lower bound is of concern and the R/X ratio is high, minimising losses can be treated as equivalent to minimising voltage violations. It is also economical because any resistive losses have to be accounted for by the generation system. Flattening load is often used in order to minimise losses, however these objectives are not identical, so some of the losses incurred under load flattening schemes could be avoided. In this section, case studies are used to estimate the relative size of the avoidable losses in simulations of EVs smart charging in residential networks. Then the effect of incorporating phase balancing as a secondary objective (as proposed in Section 4.3.1) is evaluated.

#### **6.3.1.1 IEEE European Low Voltage Test Feeder**

Monte Carlo simulations were constructed on the 55 household IEEE European Low Voltage Test Feeder (shown in Appendix B.2). The network was loaded using 1 minute resolution winter load data, and EV charging data from MEA. Five charging scenarios were considered:

- No EVs – only the household loads were included.
- Uncontrolled charging – EVs charge as observed.
- Loss minimising (LM) – EVs charge according to Section 4.2.3.
- Load flattening (LF) – EVs charge according to Section 4.2.1.

- Load flattening with phase balancing (LF+PB) – EVs charge as proposed in Section 4.3.1.

All optimisation problems were formulated at 1 minute resolution, with a maximum vehicle charging power of 3.5 kW. The total load profiles resulting from the scenarios are shown in Figure 6.9. Note that load flattening with phase balancing is not included, as the load profile is identical to load flattening.

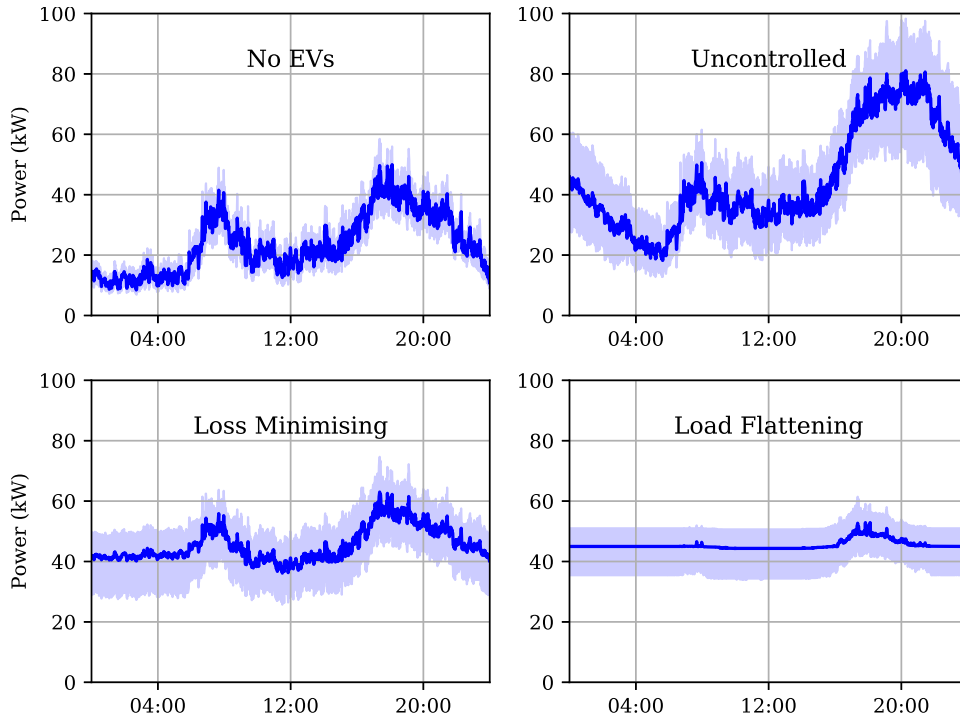


Figure 6.9: The total load on the 55 bus network, without EV charging and under three different charging scenarios. The solid lines show the median load over the simulations and the shaded area covers the 90% confidence interval.

While the load flattening algorithm nearly perfectly flattens the load and avoids an increase in peak demand, minimising losses incurs up to 20% increase in peak demand. This is perhaps surprising, as large peak loads induce large currents (and hence losses). However the total load on the feeder only determines the current at the top of the network, so the difference in load profiles between load flattening and loss minimising is dictated by the dominance of the losses in the top of the network. In other words, if only the losses at the top of the network are significant, then flattening load and minimising losses are approximately equivalent. However, if the losses at the end of the network are dominant then the solutions are likely to be very different.

The losses experienced in each scenario are shown in Figure 6.10, where the blue lines show the median values, the boxes cover 50% of the values, and the whiskers show the range. Flattening load reduces the losses by 18% compared to uncontrolled charging, while minimising losses achieves a 24% reduction. However, the increase in peak load seen in Figure 6.9 means that the reduced probability of voltage violation may be offset by an increased probability of transformer overload. The load flattening with phase balancing achieves approximately half of the possible reduction without increasing peak demand.

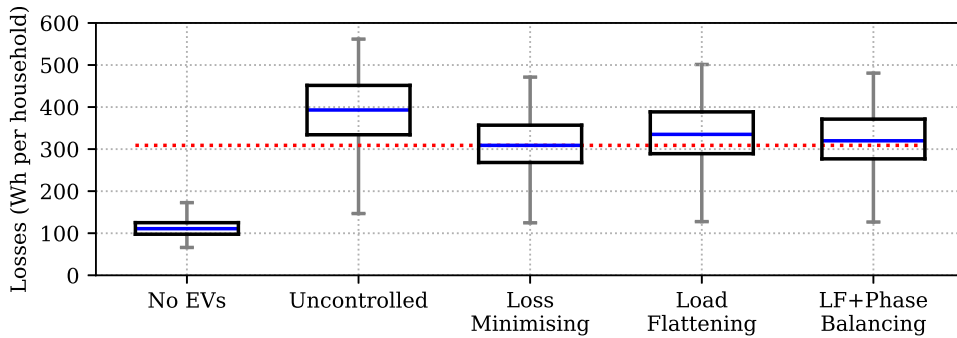


Figure 6.10: The energy losses per household experienced under the five scenarios. The blue line shows the median, the box covers the interquartile range, and the whiskers cover the total range. The dotted line aids comparison against the loss minimising median.

Based on these results, minimising losses may be worthwhile, but only if the network is near its voltage bounds and not near its transformer limit. If the network is also near its transformer limit, or the full network model is not available, then using the load flattening with phase balancing (LF+PB) scheme proposed in section 4.3.1 provides some benefit. However, it should be remembered that the potential reduction in losses is only small, so voltage violations would only be marginally improved.

To understand how the LF+PB scheme achieves lower losses, it is useful to visualise the phase imbalance in each case. Figure 6.11 shows the average phase imbalance throughout the simulation in all 3-phase lines, for each EV charging scenario. The values are capped at 15% and 55%, and the coloured markers show the phase that each household is on. Under all scenarios the phase imbalance is worse further down the network, which is unsurprising as the systemic imbalance will be greater at lower levels of aggregation. All the smart charging schemes exacerbated the imbalance at the bottom of the network compared to uncontrolled charging, potentially because in the uncontrolled case the EVs

broadly follow similar charging profiles (predominantly overnight). This demonstrates the fact that phase imbalance does not take account of the size of the load, so would not necessarily reduce losses if used as the primary objective. LF+PB has the smallest phase imbalance at the top of the network. This is unsurprising, as the phase balancing objective (4.28) considers the imbalance of all of loads summed – which is analogous to the load at the top of the network.

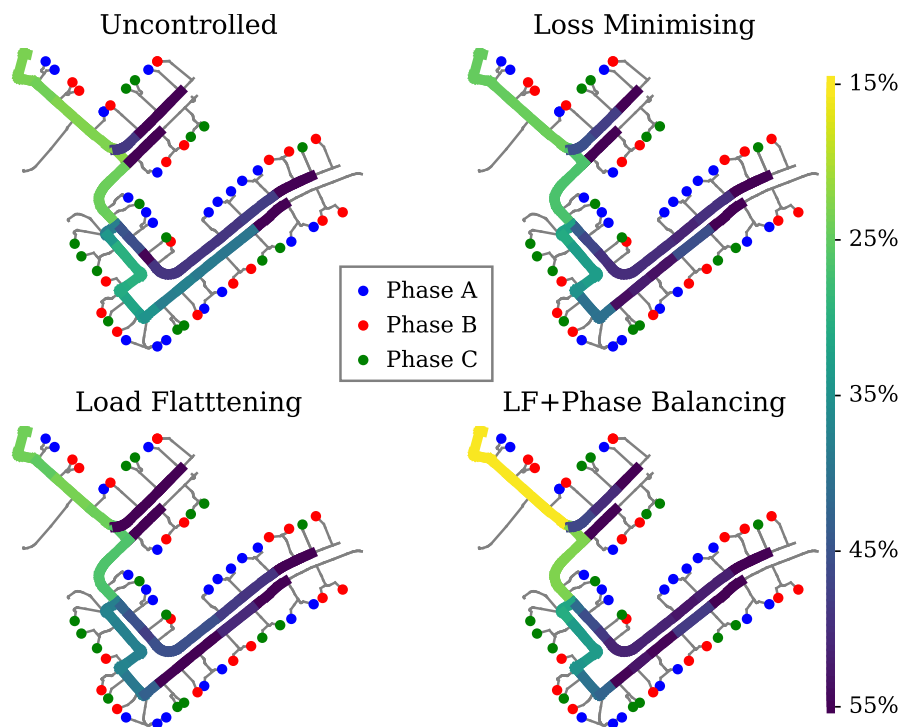


Figure 6.11: The test network under each EV charging regime, where the line colours show the average phase imbalance. Single phase lines are grey.

It is interesting that the loss minimising solution has only marginally better balanced phase than the load flattening case. This suggests that phase imbalance is less significant than prioritising high impedance lines. However, losses can be heuristically reduced by reducing the phase imbalance. The reason that loss minimising results in lower losses despite the phase imbalance can be understood by comparing the location of the losses in the network under both smart charging scenarios. Figure 6.12 shows the difference in average losses per meter over the day between phase balancing and loss minimising, for each line in the network. At the top of the network, where the load is flattest and better balanced, the losses are lower in the load flattening with phase balancing case, while further down the network the losses are lower in the loss minimising case.

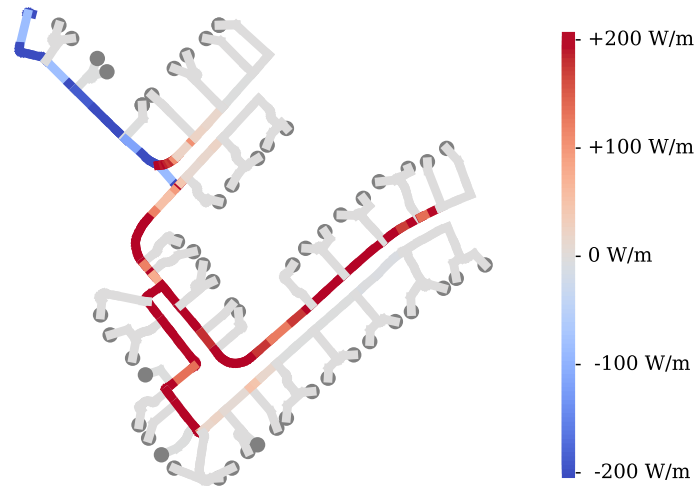


Figure 6.12: The average losses per length in each branch of the network under load flattening + phase balancing when compared to loss minimising.

This confirms that flattening the load and reducing the phase imbalance at the top of the network does result in lower losses in that section of the network. However, the losses in the branches further down the network are more significant when it comes to reducing the total losses. This will not be true in all networks, and sensitivity to the network structure is studied in the next section.

### 6.3.1.2 Sensitivity Analysis

The results in the previous section suggest that explicitly minimising losses can achieve only a moderate reduction in losses compared to flattening total load, and comes at the expense an increase in peak load. Whereas, a lot of the benefit can be achieved by incorporating phase balancing as a secondary objective to load flattening – which avoids the increase in peak demand. However, these simulations all consider winter loading of a 100% EV population on the IEEE European LV Test Network. It is not clear whether these results will carry across to other networks or loading conditions. Therefore, this section investigates the sensitivity of this result to the modelling parameters.

**EV Population** Thus far, it has been assumed that there is one EV at each household. However, smart charging is likely to be implemented before this penetration level is reached. It is therefore important to consider how the difference between these algorithms

changes for lower levels of penetration. The simulation from section 6.3.1.1 was repeated 55 times, where the number of EVs is changed each time. 55 was chosen because this was the number of households on the network, so every possible number of EVs was trialled. The position of the EVs in the network was chosen at random in each run of the Monte Carlo simulation. This meant that, as the numbers of EVs was increased, a varied number of Monte Carlo runs were required, because the the number of possible combinations for EV locations changes.

Figure 6.13 shows the additional loss reduction achieved by the loss minimising and LF+PB algorithms when compared with load flattening. The solid lines show the median value, and the shaded area covers the interquartile range. It can be seen that, regardless of penetration level, phase balancing achieves an average of 50% of the possible reduction in losses, and that there is an approximately linear relationship between EV population and loss reduction. This means that with fewer EVs on a network, the additional benefit of minimising losses is lower than that shown in Section 6.3.1.1. The relative performance of the LF+PB scheme was approximately constant with EV penetration; around 60-70% of the avoidable losses were reduced for each level.

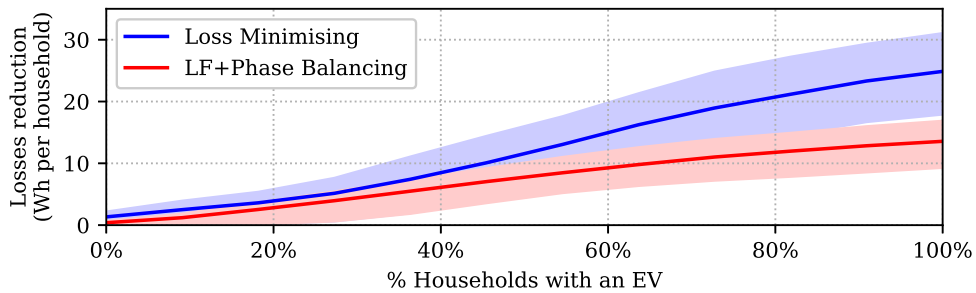


Figure 6.13: The reduction in losses, per household with an EV, achieved by minimising losses rather than flattening load, against EV penetration. The solid line is the median, and the shaded area covers the inter-quartile range.

**Season** In the UK, heating and lighting contribute significantly to household electricity demand. Throughout the year there is a 12.7 °C change in average temperature and an 8.8 hours change in daylight length. This means that the shape and size of household demand varies significantly with the time of year. To quantify the effect this has on the difference between the algorithms the simulation was repeated using load and vehicle data

from different times of year. Figure 6.14 shows the additional reduction in losses achieved by the more advanced smart charging schemes, compared with load flattening for each of the seasons. There was minimal difference in the results, although slightly larger values were observed in the winter simulation (where the feeder was the most heavily loaded).

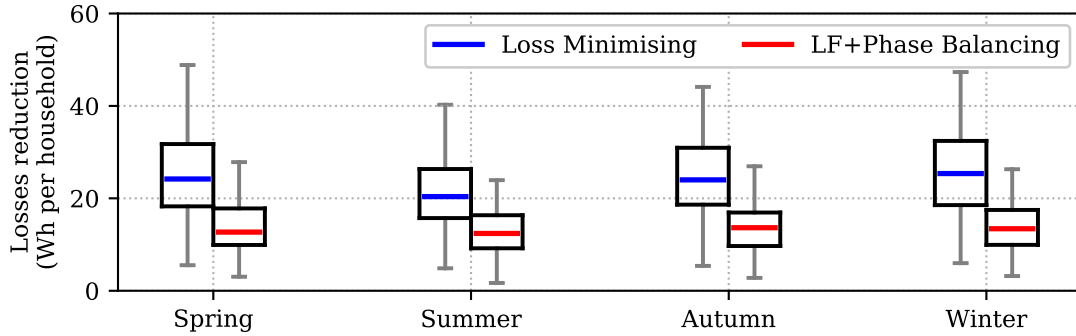
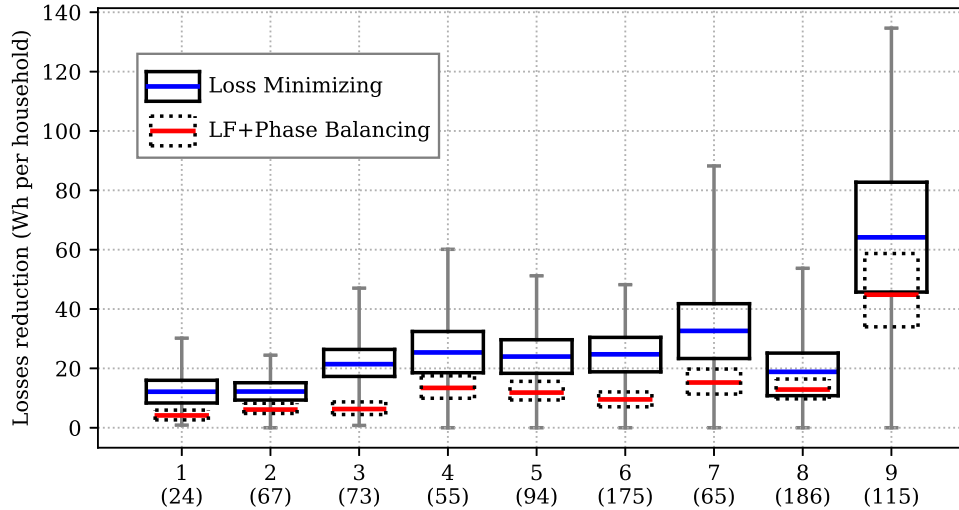


Figure 6.14: The reduction in losses per household achieved by each scheme compared to flattening load, for various seasons. The thick lines shows the medians, the box covers 50% of the values, and the lines the total range.

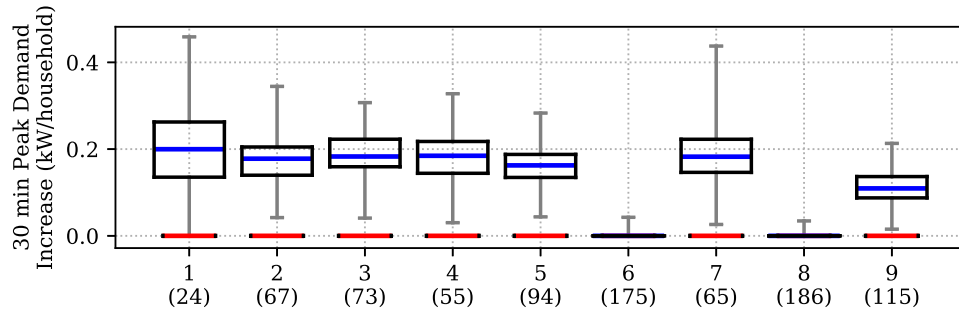
**Network Structure** Thus far, the results have focused on the IEEE European Low Voltage Test Feeder. However, network topology and the phase distribution of loads have a large effect on the losses in a distribution network. Therefore, the simulation described in Section 6.3.1.1 is repeated for 8 other feeders from [253]. Figure 6.15 shows the additional loss reduction and associated increase in peak demand for the two algorithms, compared with flattening load, for each network.

As expected, load flattening with phase balancing does not increase peak demand compared with load flattening. The networks are ordered by their losses per household before EV charging is added, and the number of households on the network is shown in brackets. Network 4 is the IEEE European Low Voltage Test Feeder; a mapping of the feeders to those in [253] is presented in section B.2 of the Appendix. The full results are displayed in Table 6.3.

For all of the feeders considered, flattening load resulted in a small but noticeable amount of avoidable losses. In general, this was larger for lossier feeders. For most of the feeders, the reduction in losses came at the expense of around a 0.2 kW increase in peak 30 minute demand per household. On average, balancing phase reduced between 30%



(a) Reduction in losses per household.



(b) Increase in peak demand per household at 30 min resolution.

Figure 6.15: A comparison between the proposed smart charging schemes and load flattening for 9 different feeders, described in Table 6.3.

#	Loads	Losses (Wh per household)				
		No EVs	Uncontr.	LM	LF	LF+PB
1	24	40	133	102	114	110
2	67	57	199	160	172	166
3	73	106	378	308	329	323
4	55	111	385	306	332	318
5	94	138	479	392	416	404
6	175	164	576	475	500	490
7	65	179	632	515	548	532
8	186	384	1344	1153	1171	1157
9	115	481	1664	1379	1442	1396

Table 6.3: The daily losses in each of the networks considered.

and 70% of the avoidable losses, without an increase in peak demand. It's worth bearing in mind that the relative reduction in losses is still small, compared to the no charging case. Therefore, smart charging can not be used to mitigate voltage violations with the

same success as it mitigates transformer overloads.

### 6.3.2 The case for bi-directional charging

We have seen in Figure 6.1 that in some cases smart charging will not be able to mitigate an increase in network peak demand. It is possible that the addition of vehicle-to-grid (V2G) charging will be able to prevent this increase. Furthermore, V2G may allow peak demand to be reduced beyond the no charging case, reducing the resistive losses in the network.

As of Q1 2019, the majority of commercially available V2G chargers are DC fast chargers – designed to be connected directly to the medium voltage network. However, trials have been taking place using AC slow V2G chargers [254], which could be connected into residential networks. The technology required for bi-directional charging is more complex and expensive than that for uni-directional charging. Additionally, in order for users to provide power to the network, a market framework must be set up. Therefore, careful consideration needs to be given to the value that V2G adds to the local system before this technology is pursued.

The hardware expense is not the only additional cost incurred from V2G. Round-trip losses in the charger mean that the households' total net energy consumption will increase – which, depending on the buy and sell price, may make the service unprofitable. Additionally, the total throughput of EVs' batteries will be increased, potentially accelerating their ageing. An EV's battery accounts for 15-35% of its total cost, and batteries must be replaced once their capacity has reached below roughly 80% of its initial capacity. There is a lack of consensus around the impact of V2G on battery degradation; [255] concludes that battery degradation will significantly reduce the revenue for V2G and [256] found that it made V2G unviable, whereas [257] suggests that V2G may increase the lifetime of batteries. This presents a problem when analysing the financial case of V2G, as the financial benefit is highly dependant on the degradation costs. Therefore, here the costs are considered in terms of the increase in battery throughput, which is used as a first order model for cycle ageing [258].

Also of concern are the energy losses in the network. Although peak demand reduction is assumed to reduce losses, we have seen in the previous section that the current in the lower branches of the network has a large effect on the total losses. While V2G will likely reduce the current through the transformer, it may significantly increase the currents further down the network, as power is transferred from vehicles to households elsewhere in the network. On top of these losses, there are also losses in the charger which occur in both charging and discharging. This will increase the total energy demand of the vehicles which raises total cost and the required generation.

Therefore, this section quantifies the additional benefits, and associated costs, that V2G provides, compared to uni-directional smart charging – or grid-to-vehicle (G2V). The simulations still focus on the IEEE LV Test Feeder, however the household load data was taken from [259] and the vehicle data from the NTS. This load data was 30 min smart meter data from 14,000 households distributed across the UK, meaning it included a diverse range of consumers. Using data at this resolution likely underestimates the resistive losses (which is why it wasn't used in the previous section), however for this simulation, accurately capturing diversity is more important than calculating precise values for the losses.

When V2G is incorporated the load flattening optimisation proposed in 4.2.1 is no longer valid, therefore both the bi-directional and uni-directional smart charging scenarios were calculated using the peak demand minimisation proposed in 4.2.2. The losses were calculated using the commercial power flow software, *OpenDSS* [235].

**Peak Demand** Figure 6.16 shows the percentage reduction in peak demand achieved by bi-directional over uni-directional smart charging, and the associated increase in battery throughput of the EVs, against the percentage of households on the network which had an EV. The percentage increase in throughput describes the increase relative to throughput of the battery with only uni-directional charging – so a 100% increase means that the V2G EV has two times the throughput that it had with only G2V. The solid line shows the average values over the Monte Carlo simulations, and the shaded area covers the 90% confidence interval.

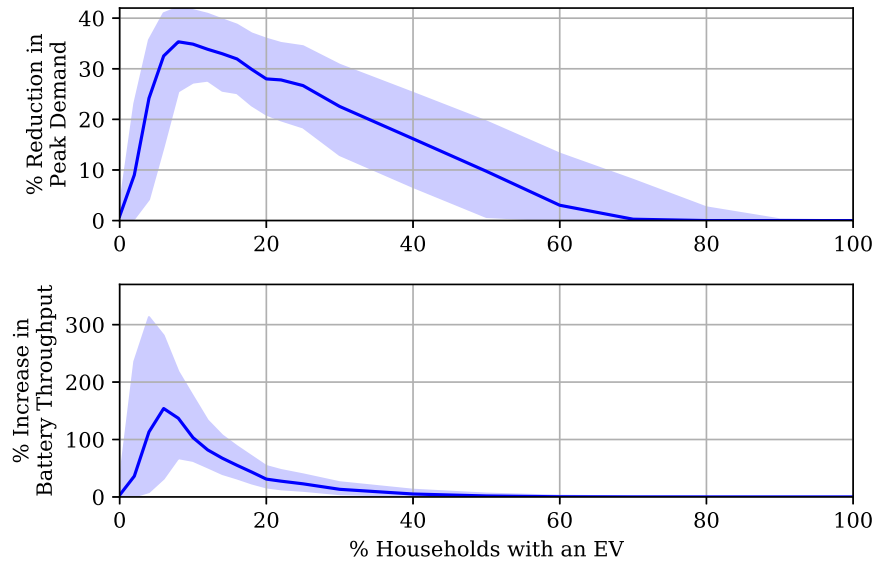


Figure 6.16: The additional reduction in peak demand achieved by bi-directional over uni-directional smart charging in the UK, varying with EV penetration. The solid lines show the average and the shaded area covers the 90% confidence interval.

With a very small number of electric vehicles, the average reduction is low, and the variance is high. This is because there is a significant chance that there will be no vehicles available to discharge at peak times. The additional reduction in peak demand is largest when approximately 10% of the households have EVs, with an average of 35% reduction possible. Once the EV population grows beyond this point the additional reduction shrinks, leaving no additional reduction possible when 100% of households have an EV. This is because additional vehicles add load, as well as flexibility, to the network; at 100% EV penetration the load can be perfectly flattened using uni-directional charging. The increase in battery throughput is closely related to the reduction in peak demand, which is intuitive as both are dictated by the amount of V2G deployed. At the point of maximum service provision, vehicles' throughput is increased by an average of 150%. The variance in battery throughput is larger than in peak demand reduction, as it is dependant on the distance travelled by the vehicles as well as the amount of V2G provided.

**Losses** Figure 6.17 shows the change in losses for the same set of simulations. The solid line shows the total losses, and the dotted line shows the distribution losses – the charging losses account for the difference between the two. The lines show the average

value and the shaded area covers the 90% confidence interval.

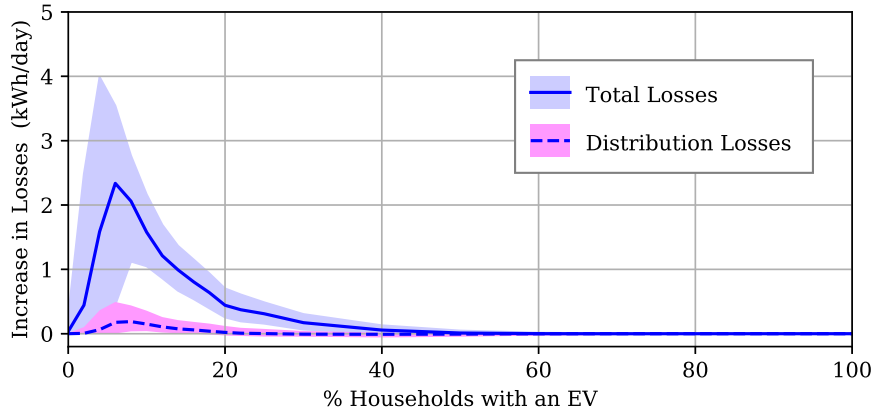


Figure 6.17: The increase in total losses and those just in the distribution system using bi-directional charging compared to uni-directional. The lines show the average values and the shaded areas cover the 90% confidence interval.

Both charging and resistive losses were always increased by the addition of V2G, despite the reduction in peak demand. This is because the peak load dictates the current at the top of the feeder, but not elsewhere in the network; vehicles providing power for other households will likely increase currents elsewhere in the network. In this example the charging losses are much more significant than the distribution losses. Therefore, the majority of the increased cost is borne by the household owner – who is already suffering an increase in battery degradation. These results suggest that, although AC V2G charging of a small number of EVs has the potential to provide significant benefit to residential network operation, the costs are significant. These means that serious thought needs to be given to the financial value or reducing network peak demand before this technology is pursued.

## 6.4 Comparative Case Study

The results in this section have so far been specific to the UK. It was not possible to analyse the spatial change in loading to the Texas distribution network, as the geographic break down of the NHTS is not available to UK researchers. However, household electricity demand and a representative network were available, so this section includes some

comparative case studies for Texas. Unlike the previous chapter, these results can not be used to directly compare Texas and GB, because the networks and data used are not directly equivalent. Therefore, these results should just be treated as an example of how different household loads, vehicles, and networks can change the results.

First, the loading, losses, and voltages in a representative network are studied. Then, the additional benefits and costs of incorporating V2G technology are quantified. Measured Texas household and electric vehicle charging data was taken from [218]. A significant number of households from this dataset had solar generation, which was left in the profile. Hot summer days were chosen for the simulation, meaning the both domestic loads and solar generation were high. The EV charging was uncoupled from the household loads so that both could be varied independently in the Monte Carlo simulation. The network was the EPRI K1 test feeder (shown in section B.2 of the appendix). This network supplies 311 residential loads and 13 industrial loads, only the residential loads were varied in this simulation.

**Peak Demand with 100% EVs** The total residential load profile on the test network for each charging case is shown in Figure 6.18. The solid line shows the median load over the Monte Carlo simulation and the shaded area covers the 90% confidence interval. It can be seen that before the EV charging is added the households are net exporters in the middle of the day, due to solar generation. Compared to the GB case, the EV charging has a much smaller impact on the network loading. This is largely due to the household loads being significantly higher in the Texas case – the UK households used an average of 10.4 kWh per day, while the Texas households used average of 26.7 kWh. Therefore, the uncontrolled charging only increases the residential peak demand by 7%. This network has a 12 MVA transformer as the industrial loads are nearly 8 MVA, so the network is not near its loading limit, meaning the addition of EV charging will not result in an overload.

The solar generation has a large effect on the loading; in both the uncontrolled and controlled charging scenarios the network becomes a net exporter in the middle of the day. The controlled charging scenario avoids increasing the peak in demand, and prevents

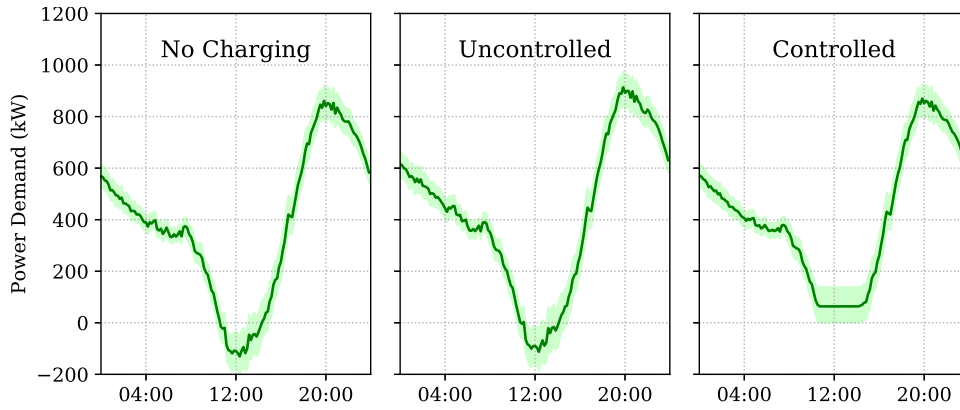


Figure 6.18: The total power demand on the network under each charging scheme. The solid line shows the average, and the shaded area covers the 90% confidence interval.

the demand from going negative. Compared to the GB case, the variance between Monte Carlo runs is small. It is possible that this is due to a narrower set of behaviour captured in the Texas trial compared to the GB one, but could also demonstrate a lower variance in vehicle charging behaviour.

**Losses** The total losses in the network are shown in Figure 6.19. Note that there is a false origin on the plot, so that the differences between the charging schemes can be seen. In this simulation the increase in losses due to charging is very small in both relative and absolute terms; the daily losses per EV are around 0.25 kWh, while in the Rochdale simulation they are 5.5 kWh. This difference further illustrates the importance of network structure on electrical losses. There is a very minor reduction in losses achieved with controlled charging, however it is less substantive than in the Rochdale case. The final notable difference between the simulations is in the variance of losses observed; in the previous case there is very little variance in the no charging case, but a large variance in both charging scenarios; whereas in this case, there is a large variance in all scenarios.

**Voltages** In the US, appliance safety requires that voltages must be kept within  $\pm 5\%$  of unitary voltage in normal operation. Figure 6.20 shows the highest and lowest voltages in the network under each charging scenario. As would be expected given the similar losses, there is very little variation between charging regimes in voltage profiles. The lower bound of 0.95 is some distance from the lowest voltage in the network. The highest

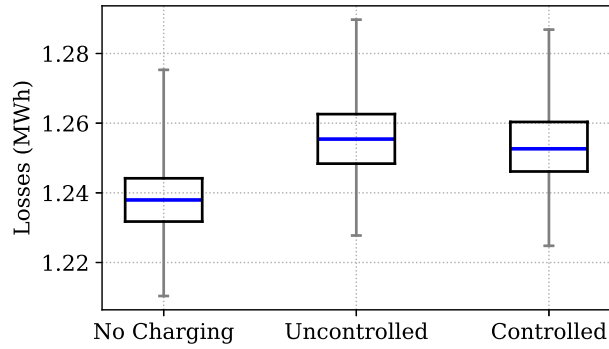


Figure 6.19: The total resistive losses for each scheme. The blue line shows the median value, the box covers 50% of values, and the whiskers the total range.

voltages are much nearer the 1.05 limit. This is likely due to the voltage rise caused by exporting solar power to the grid. However, the highest voltages are slightly lower in the controlled charging case, because the charging offsets the voltage rise at the time of maximum export. However, neither upper or lower voltage limit is violated in any charging scenario.

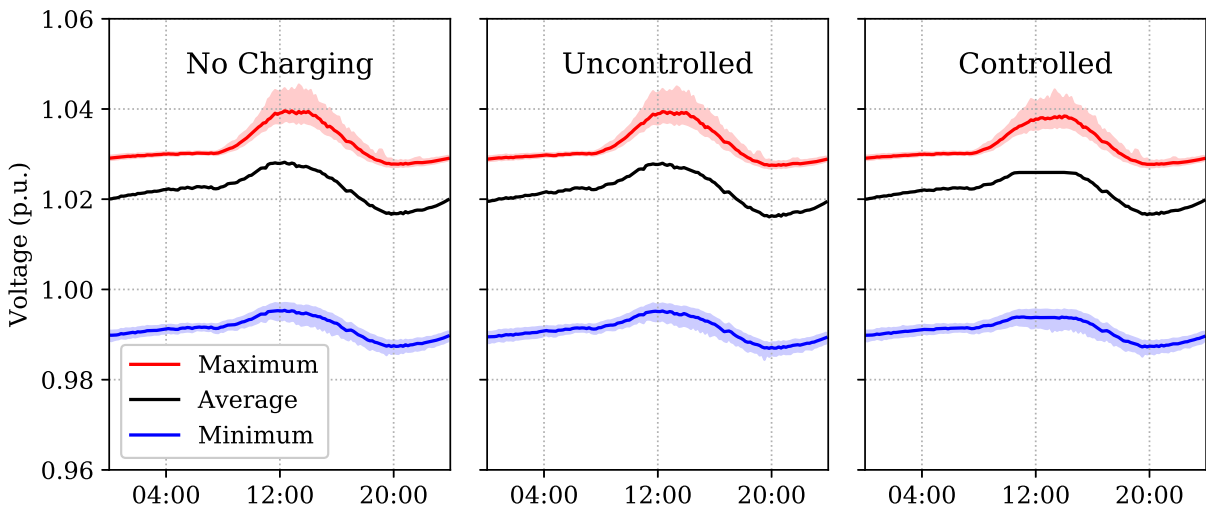


Figure 6.20: The average, lowest and highest voltages in the network throughout the day under each scheme. The solid lines show the median value and the shaded area covers the 90% confidence interval.

**Vehicle-to-grid** A second simulation was constructed, analogous to that in Section 6.3.2, which investigates the case for bi-directional charging using the Texas load data and network. Figure 6.21 shows the additional reduction in peak demand possible with bi-directional smart charging compared to uni-directional case, and the increase in EV battery throughput, for varying levels of EV penetration. Similar to the GB case, when

the number of EVs is small, availability limits the potential reduction. However, unlike the GB case, there is still additional value to bi-directional charging when 100% of households have vehicles. When more than 25% of households have an EV, a 15-20% reduction in peak demand is possible. While the peak demand reduction does not taper away significantly for high penetration levels, the increase in EV battery throughput does. This is because the power requirement is being split between a larger number of vehicles.

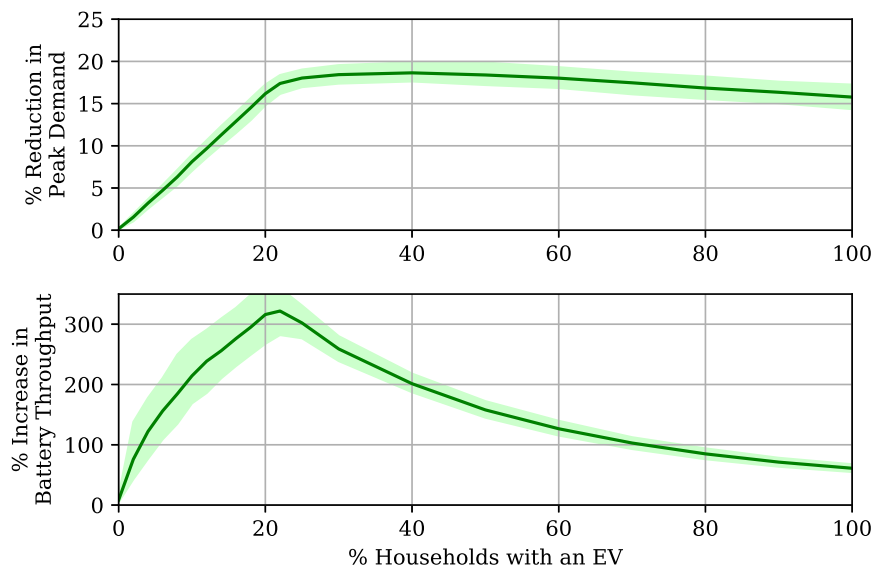


Figure 6.21: The additional reduction in peak demand achieved by bi-directional over uni-directional smart charging in Texas, varying with EV penetration. The solid lines show the average and the shaded area covers the 90% confidence interval.

The difference between the two simulations is largely due to the solar generation and higher household loads, resulting in a much larger difference between peak and trough demand; this means that the EV load is not large enough to flatten the load with only uni-directional charging. This is demonstrated in Figure 6.22, which shows examples of the total feeder load profiles when 100% of households had an EV. The dotted line shows the demand before EV charging was added, the solid line shows the total load with optimal G2V charging, and the dashed line shows optimal V2G charging. In the GB case the optimal profiles are identical, because the EV load is large enough to completely flatten the profile without V2G. Whereas, in the Texas case the EV load was not sufficient to completely flatten load with G2V, so the peak demand can be reduced by using V2G to flatten total load.

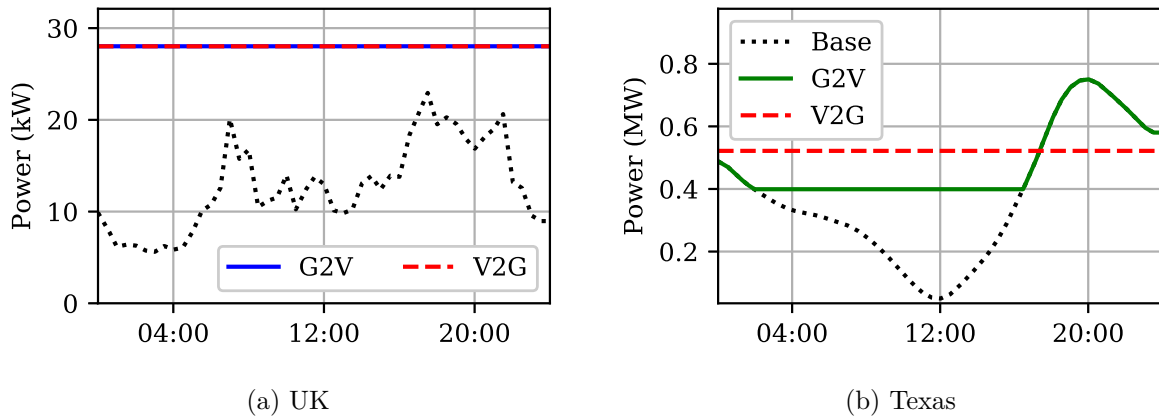


Figure 6.22: An example of total feeder load under both charging schemes. The dotted line shows the demand before EV charging was added, the solid line shows the total load with optimal G2V charging, and the dotted line shows optimal V2G charging.

Figure 6.23 shows the change in losses for the same set of simulations. Like the GB case, all simulations saw an increase in both charging and distribution losses, and the largest increase coincided with the greatest reduction in peak demand. The magnitude of the increase in total losses per household is similar to the GB case, however here the distribution losses made up a much more significant share. This makes sense, as the pre-existing load on the feeder is larger so the increase in load due to EV charging has a more significant effect. This difference is significant because the distribution losses represent a cost to all consumers on the network, while charging losses are incurred only by the households with participating EVs.

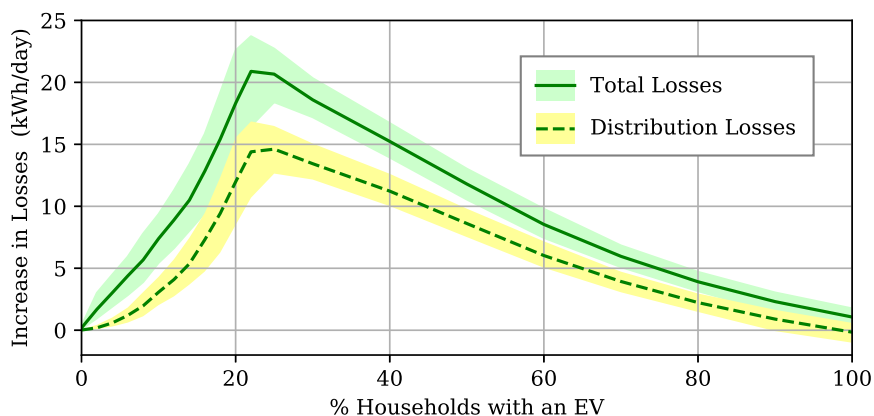


Figure 6.23: The increase in total losses and those just in the distribution system using bi-directional charging compared to uni-directional. The lines show the average values and the shaded areas cover the 90% confidence interval.

**Summary** Overall, this case study demonstrates how vastly different the impacts of EV charging on residential networks can be. While the GB network required controlled charging to avoid violating its transformer and voltage limits, this network could support uncontrolled charging without violating any constraints. Additionally, while bi-directional charging added no additional value at 100% penetration in the GB case, an additional 15% reduction in peak demand could be achieved in this case.

It is difficult to quantify how far these results can be extrapolated to represent Texas networks in general. For one thing, it is clear from the fuel mix analysis in Chapter 5 that the households in the trial used here had an above average penetration of solar panels, so there is danger to extrapolating even the loading. However, it is known that household demand in the US is much higher than in the UK, so it makes sense that the residential networks would be designed to tolerate larger loads. The test networks used were also very different, and it is hard to separate how much of this difference is due to variation between the countries, rather than variation in individual networks. Therefore, it is clear that more work needs to be done before a thorough assessment of the Texan distribution networks can be made. However, it is likely that the residential networks in Texas will be affected less severely in the UK, due to the proportionally smaller increase in loading.

## 6.5 Concluding Remarks

In this chapter the impact of electric vehicle charging on distribution systems was explored, using case studies from GB and Texas.

The impact of that EV charging has on distribution networks is likely to vary regionally, according to the local vehicle use, existing demand, and network structure. Distribution networks also have a smaller number of customers connected compared to transmission networks, so load tends to have a higher variability. The two potential problems considered here for distribution system operation are the overloading of transformers and the violation of voltage limits.

In the GB case, uncontrolled charging of 100% EVs would result in overloading of 20%

of transformers and under-voltages in 10% of networks. The worst affecting areas were commuter towns outside large cities, and urban areas with less public transport infrastructure. However, there were many areas that did not experience either violation due to oversized components. Flattening load in residential networks reduced the percentage of transformer overloads from 20% to 2% and under-voltages from 10% to 6%. Alternative smart charging strategies could reduce losses by an additional 2-5%, which would reduce the percentage of networks with under-voltages to 5-5.5%. With small numbers of EVs bi-directional charging could further reduce the network peak demand, but once 100% penetration is reached there is no additional benefit.

There was insufficient data to carry out a complete analysis of the Texas distribution system, but a single network case study was investigated. In Texas household loads were typically larger, due to air-conditioning loads and a larger proportion of households have electric heating. This meant that the addition of EV charging represented a much smaller proportional increase and in the network studies neither constraint was violated in any scenario. This case study included distributed solar generation, and it was shown that bi-directional charging could reduce the peak demand on a network further than uni-directional charging at any penetration level.

The following general conclusions can be drawn concerning the impact of EV charging on distribution networks. First, that uncontrolled charging of EVs will raise peak demand and reduce the lowest voltage in residential networks, which may result in a transformer overload or under-voltage. Second, smart charging can reduce both transformer overloads and under-voltages, although the latter with less success. Third, that bi-directional charging may be able to reduce the peak demand on the network further than uni-directional charging, but it will not further reduce the constraint violations – as the peak demand is reduced below that seen without electric vehicles. Finally, that distribution systems that were not built to tolerate electric heating or air conditioning are likely to be worse affected – as these household loads are comparable to EV chargers.

# Chapter 7

## Conflict Between System Levels

This chapter investigates the inherent conflict between the operation of the transmission level and distribution level system when it comes to optimising EV charging.

In Chapters 5 and 6 it was shown that using EV charging to flatten load can protect the operation of the power system at either the transmission level or the distribution level. However, it is not possible to flatten load in residential networks at the same as flattening load at the national level. This is because there is a large amount of high-power industrial load, which is connected directly to the medium-voltage network. Around 60% of GB's electricity demand is industrial, although this figure changes throughout the year. Although this load is flatter than residential demand, there is a significant overnight trough in power demand. This means that, when it comes to smart charging, there is a conflict between the interests of the national system and local networks. This chapter investigates the disparity between the optimal profiles for the distribution-level and transmission-level systems, and the potential trade-offs.

In Section 7.1 the costs of optimising for only one part of the system are investigated. First, the national power demand is estimated for the case where EV charging flattens loads in residential networks. Then, the impact of flattening load nationally on distribution system operation is investigated. This is done by repeating both the case study from Section 6.2.1 and the estimation of constraint violations with the alternative controlled charging scheme.

Section 7.2 investigates how a compromise between the two system levels can be found, by prioritising residential networks which are most heavily constrained. First, the transformer data is analysed to estimate the tolerable peak demand increase in over-specified networks. Then a novel heuristic strategy is proposed, which is shown to avoid constraint violations at both the transmission and distribution level.

## 7.1 Flattening at a Single Level

Comparing the analysis from Sections 5.1 and 6.2 it appears that the distribution systems is more likely to have its operating limits violated. Therefore it may make sense to focus smart charging on this level of the system. However, it is important to understand the effects this would have on the national demand (and hence the transmission level system).

Predicting this requires the national break down of industrial and residential demand. Although this precise information is not available, Elexon publish a set of standard industrial and domestic profiles for various times of year [250], and the UK government publishes the annual domestic and non-domestic electricity consumption in each area [249]. By scaling the Elexon profiles until the percentage of domestic electricity matches the true value, the national winter break-down of industrial and domestic load can be estimated. Note that sometimes commercial load is treated as distinct from industrial, but here industrial is defined as equivalent to non-domestic (i.e. it encompasses commercial load).

Figure 7.1 shows the national demand where charging is controlled to flatten load in residential networks, compared to uncontrolled charging. Under this control scheme, the national profile becomes a shifted version of the industrial load profile. This results in an increase in peak demand of up to 6 GW, which is almost as large as the one observed with uncontrolled charging. While this increase is within the UK's current generation limit, it does increase the minimum installed generation which is required; this is important when looking to the UK's future generation portfolio, as it aims to reduce carbon emissions.

Alternatively, load could be flattened at the national level, however this would require

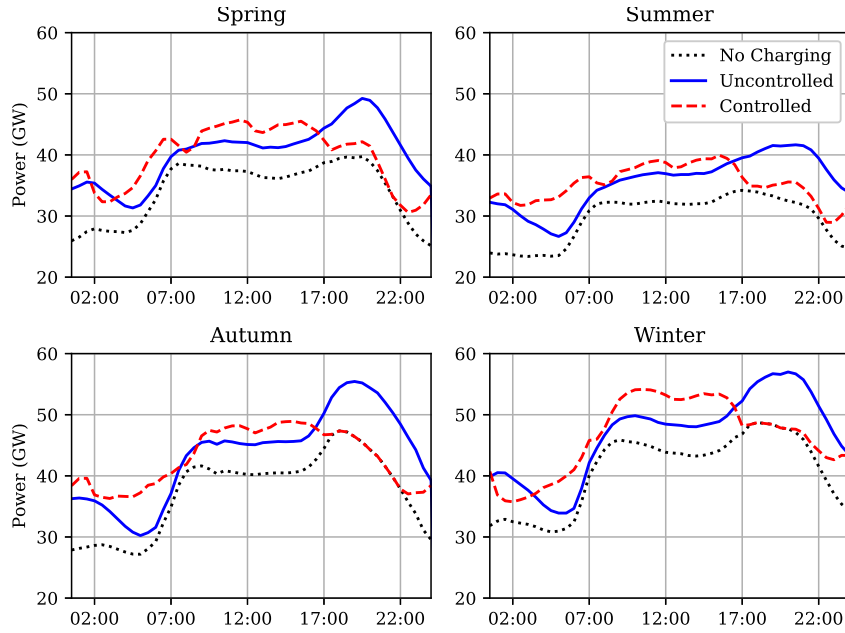


Figure 7.1: The GB national demand profile throughout the year with uncontrolled charging, and controlled charging if load is flattened in residential distribution networks.

distribution networks to offset the shape of the industrial load. Figure 7.2 shows the loading from the Rochdale case study, but where charging is controlled to flatten load nationally, at the transmission level. In the simulation from section 6.2.1, where charging was controlled to flatten load in the distribution network, controlled charging avoided violating the transformer limits in all cases. Whereas, in this case several of the Monte Carlo runs resulted in peak loads above the transformer limit. This is due to the overnight peak required to offset the industrial trough. Therefore, while controlling charging in this manner does significantly reduce the probability of a transformer overload compared to uncontrolled charging, this network would still require an upgrade.

More broadly, controlling charging in this way would significantly increase the number of networks with transformer constraint violations. Figure 7.3 shows the expected number of networks with violations, when EV charging is controlled to flatten the load at either the distribution or transmission level. Approximately 50% of the transformer overloads that are avoided by flattening the load at the distribution level are encountered if load is flattened at the transmission level. Voltage violations on the other hand are not significantly increased, possibly due to the individual vehicle charging profiles still being slow compared to the uncontrolled 3.5 kW loads, or due to the quadratic relationship

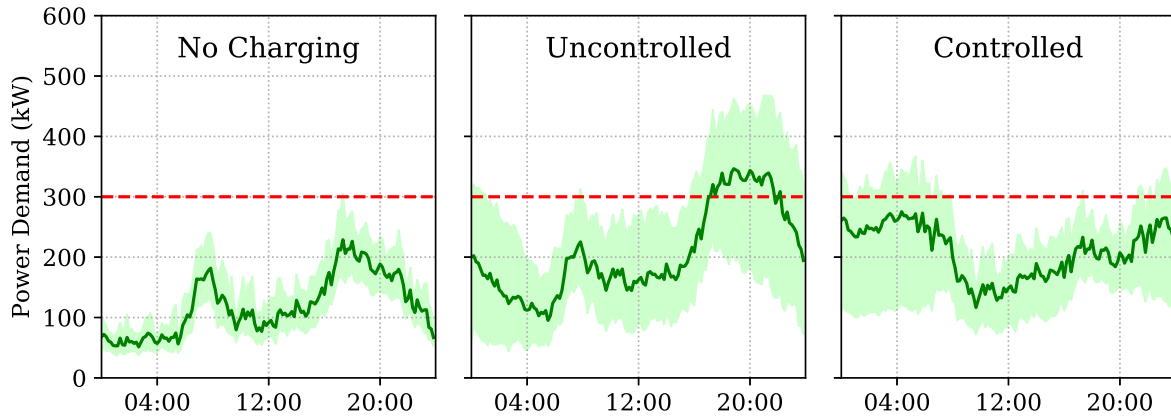


Figure 7.2: The LV network loading from the case study section 6.2.1, but where the controlled charging scenario represents flattening load at the transmission level.

between voltages and load.

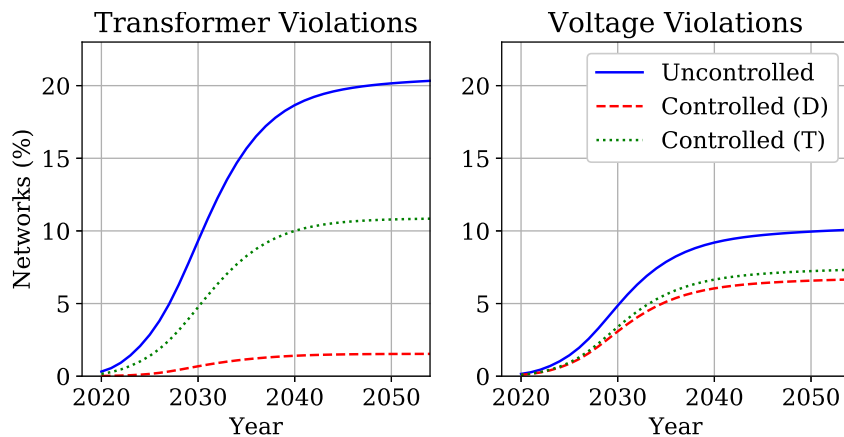


Figure 7.3: The expected number of distribution constraint violations with uncontrolled charging, and charging controlled at either the distribution (D) or transmission (T) level.

## 7.2 Multi-objective smart charging

It is clear that either a 6 GW increase in peak demand, or a 10% increase in network violations are undesirable. This section investigates whether it is possible to achieve both no increase in national peak demand, and no increase in LV network violations.

In Figure 6.6 from Chapter 6 it is shown that there are many areas that suffer no increase in network violations, even with uncontrolled charging of a 100% electric fleet. This is a result of many of the networks being fitted with oversized transformers. Over-specifying networks can be partly attributed to the small number of available transformer

sizes, but also to the difficulty in estimating network demand before the properties are connected. This means that some areas have some additional capacity which could be used to offset the flat load in constrained areas, maintaining a flat national load.

It has been shown that flattening load in all distribution networks results in a new peak in national demand during the late morning. In order to offset this, many local networks would need to reduce their load at this time of day, thereby increasing their peak demand (because the total energy demand is fixed, so a reduction at one time must result in an increase at another). The aggregated increase in residential peak demand that is possible without violating transformer limits can be estimated using the controlled charging Monte Carlo simulation results from Section 6.2. For each local authority, the distance between the transformer limit and the simulated peak load upper bound is calculated. If the distance is negative (i.e. the transformer limit is below the maximum demand) then that area is assumed to have zero flexibility. Otherwise, it is assumed that a network from the area can allow that increase in peak demand without violating its constraints. These results can be aggregated by scaling each area's allowable increase by the number of networks in that area.

Figure 7.4 shows the allowable cumulative increase in LV network peak demand as a percentage of networks. Networks are ordered from most to least flexible. The asymptote of the curve shows that 27% of networks have no allowable increase, however the rest of networks have at least some flexibility. Overall, around a 9 GW increase in residential peak demand is possible without increasing transformer violations, and 6 GW of this can be achieved using only the 30% least constrained networks. This demonstrates that there is a large amount of flexibility in some distribution networks, but does not prove that it is possible to flatten national load without violating constraints.

It may be possible to formulate a convex optimisation problem which optimises charging in each network and nationally simultaneously. However, the large number of necessary variables means that computational complexity is likely to be an issue. Therefore, developing a convex formulation which calculates a strategy that optimises national charging while minimising local network constraints is beyond the scope of this thesis.

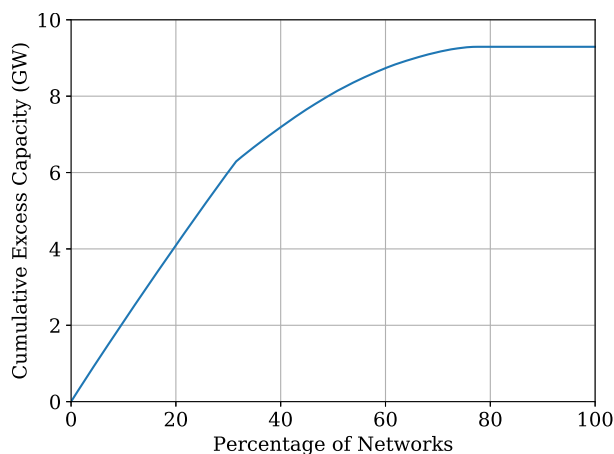


Figure 7.4: The cumulative allowable increase in LV network peak demand without transformer violations.

However, it is demonstrated that for the GB system a solution exists which minimises national peak demand and local network constraints.

In order to test the feasibility of achieving both goals, a heuristic algorithm is proposed to search for optimal charging profiles. The algorithm is described by the following steps:

1. Calculate the aggregate EV charging profile that would meet the total EV charging demand while flattening national load.
2. For a given area, scale the aggregate profile to the charging demand from that area.
3. Superimpose the charging profile on the existing demand.
4. Compare to the transformer demand limit; if necessary adjust charging to (if possible) prevent violation of the transformer limit.
5. Extract final charging profile.
6. Subtract the chosen charging profile from the required aggregate profile. Repeat 2-6 until charging for every area has been assigned.

The goal of this algorithm is to find a set of charging profiles that, where possible, avoids violating local constraints while maintaining a flat national demand. Figure 7.5 illustrates a single run through these steps for a single area. I should be noted that the order in which the areas' charging is calculated will have a significant affect on the result. In step 1

the optimal aggregated charging of the remaining EVs is calculated. For the first iteration this will be the inverse of the national demand profile (meaning that the load after EV charging would be completely flat). However, as charging is assigned to EVs this profile will be adjusted. In the second step this profile is scaled to meet the energy demand of the EV from a given network. Note that artificially inflated values for household and EV demand have been chosen for illustrative purposes - this does not correspond to an existing area. In step 3 this charging profile is superimposed onto the existing demand from that area and the transformer limit is shown as a red dotted line. In this case the proposed charging demand would violate the transformer limit, so in the 4th step the charging is adjusted until the transformer violation has been avoided. Step 5 shows the final charging profile for that area in blue, and the unadjusted profile from step 2 show with a dotted line. Finally, the assigned charging is removed from the aggregate profile in step 1, such that the areas whose charging has not been assigned can offset the adjustments required by this network.

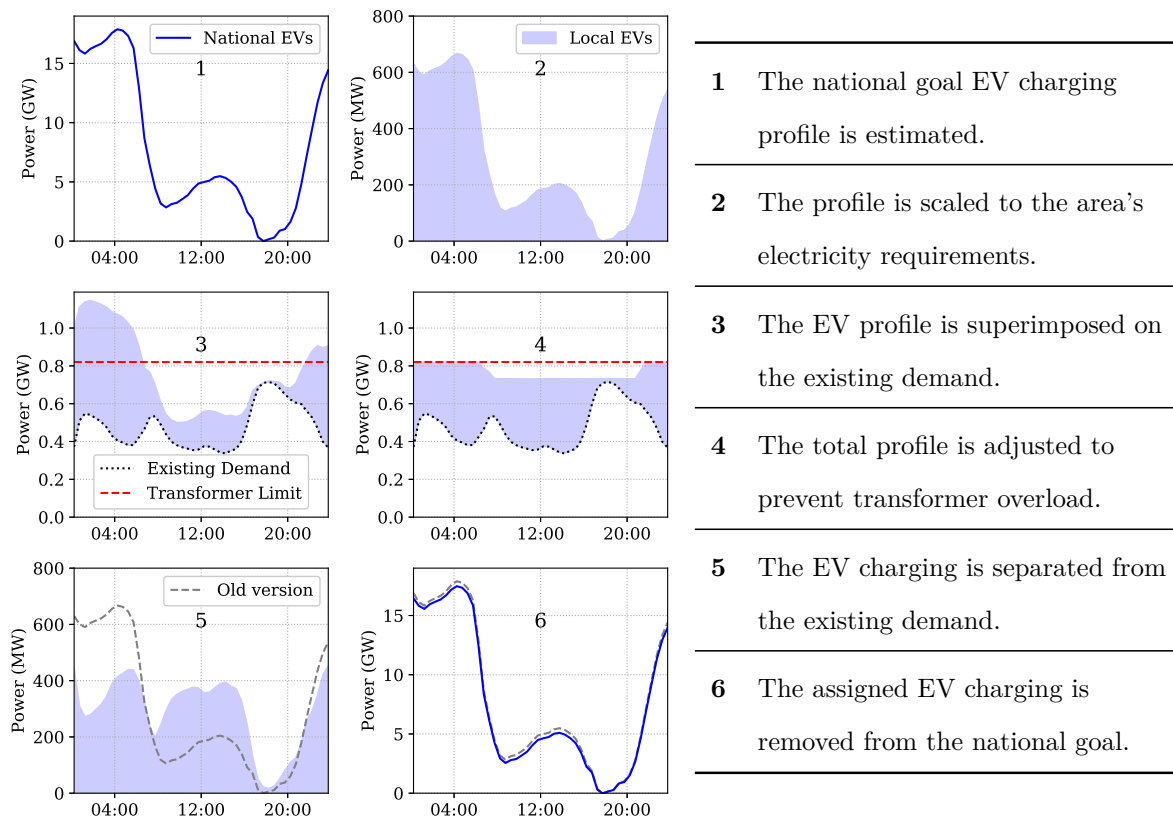


Figure 7.5: The heuristic algorithm steps.

The performance of this algorithm depends on the order that the areas' charging is assigned. If the final networks have very little flexibility they will not be able to meet

the goal profile; in order to perfectly meet the national goal profile, the final network must not require adjustments in step 4. To maximise the chances of success, the charging should be assigned to networks from most to least constrained. This means that the first networks will already be fully constrained, so the load will be completely flattened in these networks, while the last networks should have a large degree of flexibility.

To understand the reason this approximation works consider the following. If all networks' EV charging followed the goal aggregated profile (scaled to that networks energy demand) then the national aggregated load would equal the goal. However, some networks are not able to follow this profile and this will skew the national load. If we can anticipate this skew then the unconstrained networks can compensate by following an exaggerated version of the goal profile. The proposed algorithm constantly adjusts the goal profile to reflect the networks which have been unable to follow it. The larger the number of networks which have not been able to meet the goal profile, the more exaggerated the adjusted profile will become. By calculating the networks' charging in order from most to least constrained, there is the largest chance that the final network can meet the most exaggerated goal profile.

Figure 7.6 shows the charging profiles assigned to three areas with increasing amounts of flexibility. The allowable percentage increase in peak demand (from the perfect flattened scenario) is shown in brackets below the name of the area. Bracknell Forest is already at risk of overloading its transformer limit with perfectly controlled charging, so it is assigned a completely flat load. Whereas, Cheltenham and North Devon both have allowable increases in peak demand, so they are assigned charging profiles more similar to the aggregate goal profile from Figure 7.6. The peak demand increase is more substantial in the North Devon case because this is one of the least constrained networks, so its charging is assigned last, meaning its profile is offsetting the constrained networks that were unable to meet the overnight increase in peak demand.

Figure 7.7 shows the national load after this algorithm has been applied to charging in each distribution network, broken down into industrial, domestic and charging load. The addition of EV charging has not resulted in an increase in peak demand, suggesting that

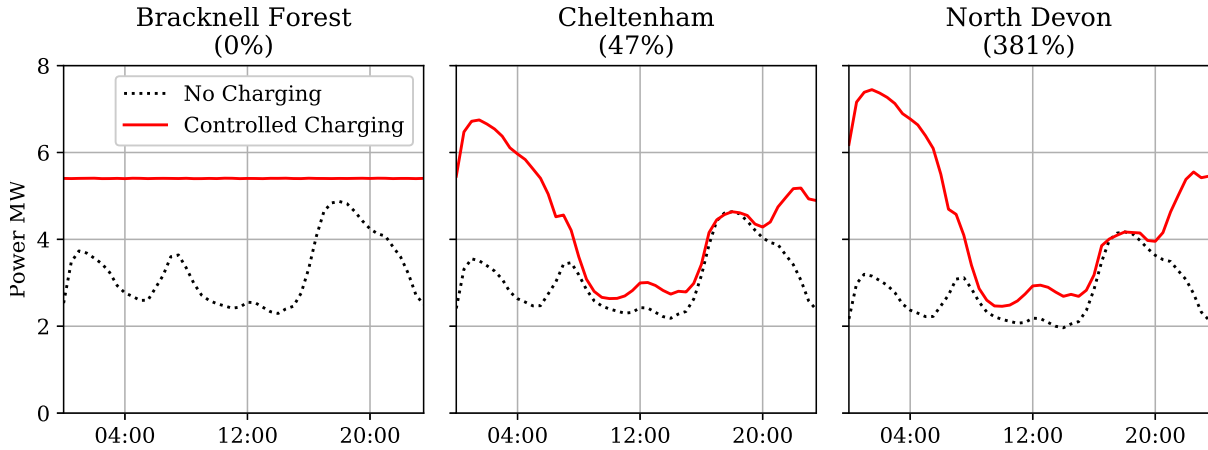


Figure 7.6: The total residential load in three example local authorities with and without the proposed controlled charging. The percentage of allowable overshoot in peak demand is shown in brackets in the title of each subfigure.

it is possible to avoid an increase in national peak demand without increasing constraint violations. The effectiveness of each of the considered charging strategies are summarised in Table 7.1.

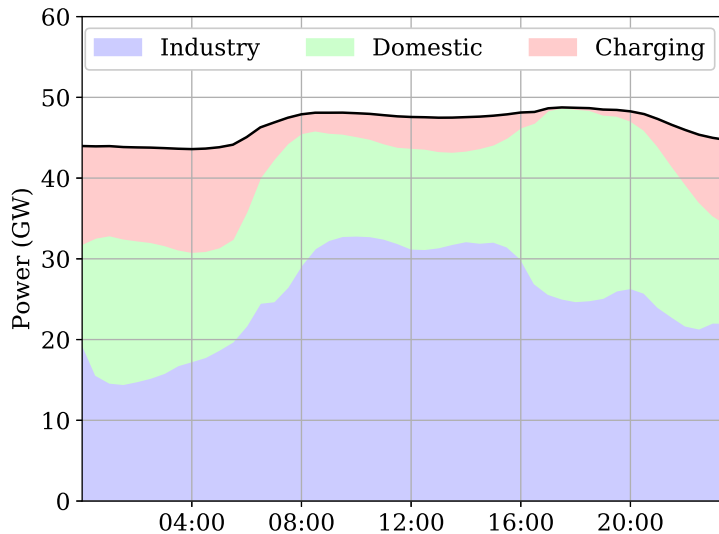


Figure 7.7: The national load profile under the proposed controlled charging scheme, broken down into domestic, industry, and charging load.

Note that deploying the multi-objective strategy does mean that no networks will require upgrades – in section 6.2.2 it is shown that many networks will require upgrades even with controlled charging, and this remains the case. However, the increase in constraint violations seen in Fig. 7.3 has been mitigated. It is also worth noting that the losses in the distribution networks with non-flat load will be increased, and this has not

	Peak Demand	Under-voltages	Transformer Overloads
Uncontrolled charging	+16%	+10%	+20%
Transmission level load flattening	+0%	+7%	+11%
Distribution level load flattening	+12%	+6%	+2%
Multi-objective smart charging	+0%	+6%	+2%

Table 7.1: A summary of the effects of each charging scheme assuming that all EV demand is met.

been considered here. However, it is likely that a more optimal set of charging profiles could be found using formal optimisation techniques – these results merely prove that a feasible solution exists.

### 7.3 Concluding Remarks

There is an inherent conflict between the optimal EV charging according to the transmission and distribution systems in GB; meaning that it is impossible to achieve optimal operation of both residential networks and the national system simultaneously. If charging is optimised at the distribution level, the national peak demand increases by up to 6 GW. On the other hand, if charging is optimised at the national level an additional 10% of networks will require reinforcement. However, oversized components mean that many residential networks are operating a large distance from their demand limits. If this additional flexibility is properly exploited, it is possible to find a compromise between the systems’ optimal charging profiles, avoiding both the increase in national peak demand and the increase in network upgrades.

For other power systems, if the industry load profile is not flat then it is impossible to flatten load in all residential networks and nationally. However, without analysing how close the distribution networks are to their operational constraints, it is not possible to say whether it is possible to avoid residential network constraint violations and an

increase in peak demand.

# Chapter 8

## Conclusions

This thesis has addressed the research question:

*As we move towards a 100% penetration of electric vehicles, how will this affect the steady state operation of the electricity network?*

Two components were identified to this question. First, what would be the impact of uncontrolled charging of a large fleet of electric vehicles on the electrical power system? Second, what would be an appropriate strategy to reduce this impact?

**The Impact of Uncontrolled Charging** In order to answer the first question, this thesis made two major contributions to the existing research. Firstly, spatial heterogeneity of EVs was incorporated into modelling of EV charging by using a large national travel survey that includes location data. Although travel survey data has been used previously in EV charging studies, few of these use the raw data, and none include the secure access version of the survey (which provides geographic information about participants). This new data source allows the regional impact of EV charging on the system to be evaluated nationally for the first time. Secondly, a stochastic modelling method for domestic uncontrolled charging was proposed which combines vehicle usage from travel survey data with charging data from an EV trial. Unlike existing strategies, this allows stochasticity in both vehicle use and charging to be incorporated simultaneously.

Uncontrolled charging simulations were then carried out using the Great Britain (GB) and Texas power systems as case studies. The impact on the generation, transmission, and distribution systems were considered simultaneously – allowing the relative severity of the impact of EV charging in these systems to be investigated. The generation system operation was quantified in terms of changes to the national demand profile, and the implications this has on maximising the use of renewables is discussed. For the transmission system, violations of line limits and increases in losses were investigated for both normal operation and in the N-1 case. For the distribution system, the percentage of residential networks experiencing transformer overheating and under-voltages was investigated.

The scope of this analysis is limited to the steady state operation of the system. Hence, system frequency and fault dynamics are not investigated. Additionally, all analysis is on the demand side and from the perspective of the network operator – meaning that, the implications on the electricity market, suppliers, and consumer are not included.

For the GB power system, uncontrolled residential charging of a 100% EV fleet would result in an 8 GW increase in peak demand, an increase in N-1 transmission violations, and 28% of low voltage distribution networks would require upgrades. Transformer overloads were twice as likely as under-voltages. The low voltage networks most likely to experience problems were those where private vehicles were the main form of commuting, vehicle ownership was above average, and existing electricity demand was high. With a 100% penetration of EVs the worst hit areas were commuting towns to the west of London, and cities in the north of England. However, in the 2030 projected scenario the local penetration of EVs had a much greater significance than the local travel behaviour.

For the Texas system, uncontrolled charging also resulted in an 8 GW increase in peak demand, although this represented a smaller percentage increase than in the GB case. Low voltage networks in Texas have a very different style compared to the GB case, and household demand is significantly larger (due to air-conditioning loads, and a more electrified heating system). This meant that in the distribution network simulations constructed, no network violations occurred – even with uncontrolled charging of a 100% EV fleet. This is particularly surprising, given that the vehicle usage in Texas is higher

than in the UK. It should be noted that far less information was available for the Texas case study, so rigorous conclusions can not be drawn. However, these results demonstrate the dependence on the impact of EV charging on the structure of the power system.

**Mitigation Strategies** The second component of the research question focuses on how smart charging can be used to reduce the impact of EV charging on the network. However, in order to answer this one must first consider what the optimal charging strategy for the system is. With this in mind, two further contributions were made.

First, the action of a variety of smart charging strategies were directly compared using stochastic simulations of residential charging. Specifically, loss minimisation was compared to load flattening, and bi-directional peak demand minimisation was compared to the uni-directional equivalent. These comparisons allow the relative performance of various smart charging strategies to be quantified. Secondly, the conflict between the interests of the distribution and transmission level systems in terms of EV smart charging are investigated. Existing literature predominately focuses on a single level of the system, and how its operation can be optimised, without considering the consequences to the rest of the system. Understanding the conflict between the levels of the system is important because a single optimisation strategy for smart charging needs to be selected.

A convex formulation for 3-phase loss minimisation was proposed such that loss minimisation and load flattening could be directly compared. Then, stochastic charging simulations for a variety of networks and loading conditions were carried out. Minimising losses directly minimises under-voltages, however it requires detailed modelling of the network impedances which may not be available.. The additional reduction in losses achieved compared with flattening load was only moderate (15-65 Wh per household per day, depending largely on the network structure). Furthermore, the direct loss minimisation resulted in an increase in peak demand – meaning the reduction in voltage violations may be offset by an increase in transformer overloading.

Based on these observations, a smart charging formulation is proposed which achieves some reduction in losses, without the increases in peak demand and modelling complexity. It is shown that reducing phase imbalance achieves approximately half of the reduction

in network losses, without the increase in peak demand.

The potential for AC bi-directional EV charging (V2G) to reduce peak demand in residential networks was quantified, compared to uni-directional smart charging. This is important because bi-directional charging requires additional infrastructure and market costs compared to uni-directional smart charging, so the additional value must be properly understood before the technology is pursued.

For the GB case, the benefit that this service provides compared to smart uni-directional charging is largely dependant on the number of EVs on the system; when the penetration is low a significant reduction in peak demand is possible, but as more EVs are added the feeder energy demand is increased, and at 100% penetration there is no additional benefit to bi-directional charging. There are also a number of additional costs incurred by providing this service. The throughput of EV batteries will be increased by up to 150%, likely accelerating their degradation. There will also be a small increase in the resistive losses in the network, and a large increase in the charger losses (meaning the user will see an increased electricity bill). Therefore, unless there are large financial incentives to reduce peak demand, the results do not present a strong argument for V2G in GB residential networks.

On the other hand, for the Texas case, an additional reduction in peak demand was possible with V2G regardless of the number of EVs on the network. This difference could largely be attributed to EV charging representing a smaller percentage of the total load on network in the Texas case. Similar to the GB case, the increase in battery throughput is closely linked to the amount of V2G provided. However, in this example the increase in losses was dominated by resistive losses in the network (meaning the increase will be funded by all users on the network, regardless of whether they own an EV or not).

Flattening load at the residential network level will not flatten it at the national level (and vice-versa), due to the non-flat industrial load that is connected to the higher voltage network; in the GB case flattening load locally would result in a 6 GW increase in national demand, while exclusively flattening load nationally would mean an additional 10% of networks require intervention.

It was noted that many residential networks have oversized transformers (due to limited sizes or difficulty in estimating demand). Therefore, a heuristic method was proposed which exploited the additional flexibility in over-specified networks to flatten load nationally without increasing constraint violations in residential networks. For the GB case, it was demonstrated that using appropriate smart charging it was possible to achieve both zero increase in peak demand and zero increase in constraint violations.

**General Remarks** Taking these two case studies into account, the following more general conclusions are made about the impact of EV charging on power systems. Residential chargers present a large load compared to typical household appliances and uncontrolled charging is likely to exacerbate the existing peak in demand.

Whether the additional load causes issues for the residential network to which the charger is connected, will depend on how far away from its voltage and thermal limits the network is operating. The distance of a network from its operational limits is determined by the structure of the network and the demand that it was designed to withstand; most notably, if there is electric heating already in the network then the addition of EV charging will not represent as large a proportional increase in demand.

At the transmission system level, there will also be an increase in peak demand. This means that the minimum generation capacity required to ensure demand is met increases. The maximum currents carried by the high voltage transmission system will also increase, in both the normal operation and N-1 scenarios.

Smart charging in residential networks offers a large amount of flexibility. EVs can be co-ordinated to optimise load at either the transmission level system, or the distribution level system. For the transmission level system, the optimal scenario is a flat national load profile.

In the distribution system, the optimal scenario for each network depends on the operating conditions of the network; flattening load will protect against transformer overload, while minimising losses will reduce under-voltages. However, in practice these schemes will produce very similar results. There is likely to be some conflict between the optimal scenarios at both the transmission and distribution levels, but (depending on the design

of the LV networks) it may be possible to compromise by flattening national load while ensuring no local constraints are violated – it is possible in the GB system.

Vehicle-to-grid may be able to further optimise the operation of the system, but this comes at the expense of additional losses in the charger and network, as well as a potentially accelerating the ageing of EVs batteries. If there is a large amount of renewable generation on the system, EV charging could also be used to offset uncertainty in generation. Ideally this would be done using real-time control, however reasonable performance can be achieved using stochastic optimisation on a day-ahead basis.

Overall it is shown that to understand the impact that EV charging will have on a specific power system, it is important to consider local travel behaviour, existing demand, and network structure in the analysis. This thesis has contributed new methods which allows this to be done, and has demonstrated these on the GB and Texas systems.

## 8.1 Future Work

The following areas have been identified as requiring further research:

(1) *Detailed analysis of other systems.* Network-specific analysis of other countries power systems must be done in order to compare the degree with which EV charging will affect the system. This would be especially useful to do for countries that share interconnections (e.g. the northwestern European counties connected to the GB system), so that the likelihood of these connections being available at peak times can be assessed.

(2) *Simultaneous analysis with electrified heating.* Electrified heating is going to present similar problems as EV charging to residential networks. Although this changes is likely to happen more slowly, meeting decarbonisation targets relies phasing out gas heating. It is therefore important to understand how heating and vehicle charging will interact, and the system reinforcements they will necessary. This is particularly important because much of the costs in upgrading the network is in labour and construction (not in materials) so if networks are to be upgraded it is preferable to only do it once.

(3) *Rapid public charging analysis.* This thesis has focused on only domestic charging

but, even rapid public charging will also play a role – at the least in motorway service stations. Therefore it is necessary to also analyse what a large rapid charging network would mean for the high voltage system, and how much it is likely to be used.

*(4) Smart charging implementation.* This research did not consider the implementation strategy of smart charging, only the benefit that it could achieve. There are two aspects which much be tackled before mass smart charging can be successfully implemented. Firstly, the technical co-ordination of EVs needs to be designed – this includes building communication infrastructure and designing a control architecture. Secondly, a social implementation strategy is needed – a way of incentivising consumers to adopt smart charging and rewarding them for participating.

# Appendix A

## Line Thermal Limits

In this thesis, thermal limits of lines in distribution networks were not considered as a failure mechanism, because in general under-voltages occur before thermal limits are violated. This appendix includes analysis supporting this hypothesis.

### A.1 Heating in overhead lines

Consider a overhead copper cable which runs from the substation of a network to the node that is the largest electrical distance away. The cable has length  $L$ , radius  $r$ , and temperature  $T_w$ . The node at the substation is at voltage  $V_0$  and the other end is at  $V_1$ , which should be the lowest voltage in the network. This arrangement is described in Figure A.1.

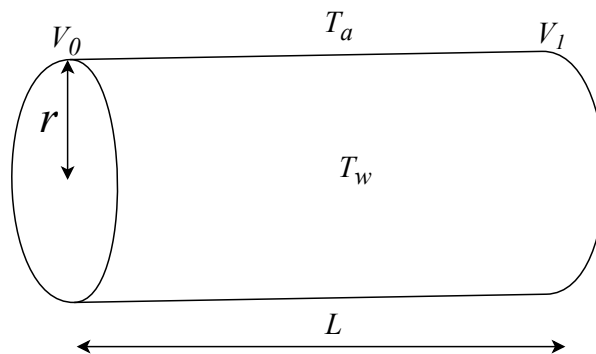


Figure A.1: A diagram of the idealised overhead line.

The resistive power dissipated in the cable can be described as:

$$P_{resistive} = I^2 R = \frac{(V_1 - V_0)^2}{R}, \quad (\text{A.1})$$

where  $I$  is the current through the line, and  $R$  is its resistance. The resistance of a conductor is a function of its geometry, such that:

$$R = \frac{\rho L}{A} = \frac{\rho L}{\pi r^2}, \quad (\text{A.2})$$

where  $\rho$  is the resistivity of the conductor, and  $A$  is the cross-sectional area. Assuming that most of the losses are dissipated as heat, at steady state there must be a balance between the resistive power lost and the thermal power leaving the wire. For the case of overhead lines, heat is predominately dissipated via convection, which can be described as:

$$P_{convection} = hA_s(T_w - T_a), \quad (\text{A.3})$$

where  $h$  is the thermal transfer coefficient,  $A_s$  is the surface area, and  $T_a$  is the ambient temperature. In this example the exposed surface area is the outer surface of the cylinder, such that:

$$A_s = 2\pi rL. \quad (\text{A.4})$$

By equating (A.1) and (A.3), and substituting (A.2) and (A.4), the following expression can be found:

$$\frac{(V_1 - V_0)^2 r}{\rho L} = 2hL(T_w - T_a). \quad (\text{A.5})$$

This can be rearranged to find an expression for the temperature of the wire in terms of

the voltage drop and cable parameters:

$$T_w = T_a + \frac{(V_1 - V_0)^2 r}{2\rho h L^2}. \quad (\text{A.6})$$

An under-voltage occurs when  $V_1$  falls below the voltage lower bound, so this expression can allow the temperature at this point to be estimated. If the temperature is within safe bounds, then the voltage limit is the constraining limit of the line, rather than the thermal limit.

Copper cables are rated to a temperature of at least 60°C. For a low voltage line at the point of an under-voltage it is assumed that  $V_0 = 240$  V and  $V_1 = 216$  V. The resistivity of copper is  $1.68 \times 10^{-8}$  Ωm, and an ambient temperature of  $T_a = 25^\circ\text{C}$  was assumed. The heat transfer coefficient will depend on whether there is wind or not, but a value of  $h = 60$  W/m<sup>2</sup>K was chosen [260]. Using this information it follows that the thermal and voltage limits will be coincident when the following equation is satisfied:

$$r = 1.2 \times 10^{-7} L^2. \quad (\text{A.7})$$

Figure A.2 shows the region of cable dimensions where an under-voltage occurs before a line limit, with cable diameter on the horizontal axis and length of the vertical. The range of cable diameters that are used for residential networks is shown by the red dashed lines, it can be seen that if the network length is over 150-220 m then an under-voltage will occur before a thermal overload. All of the test networks used in this analysis cover a greater distance than this (see Appendix B), therefore under-voltages will always be the limiting constraints.

It is possible that there are some networks for which this will not be true – particularly in the case of micro-grids. However no test low voltage distribution network was found which did not satisfy this inequality – including a set of 25 British distribution networks from [253].

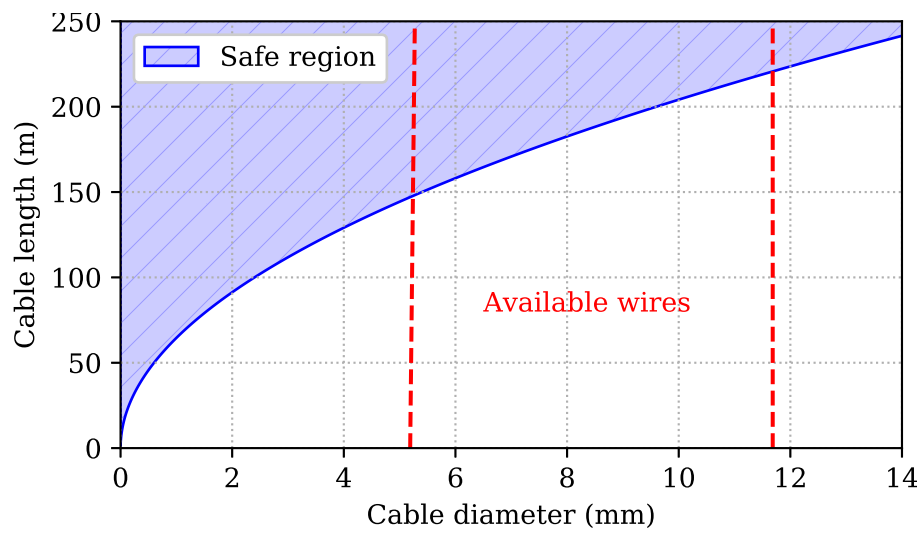


Figure A.2: The relationship between cable parameters that determines whether a voltage or thermal limit occurs first. The shaded area shows lines for which voltage limits are the constraints. The red dashed lines show the range of available cable diameters that are used in LV distribution networks.

# Appendix B

## Test Networks

Analysis of distribution system operation requires an electrical model of the network. Precise models of the GB and Texas networks were not available, so test networks had to be used to simulate behaviour. This section describes the networks used in the analysis in Chapter 6. The first section details the networks used in the GB wide analysis, while the second describes the smaller test feeders used to compare smart charging objectives.

### B.1 GB Representative Networks

Networks differ regionally in GB; in cities networks tend to connect a large number of homes densely, while rural areas are smaller but sparser. Here, three example 3-phase residential networks are used to quantify the effects of vehicle charging on distribution networks, each representing a different network style. The networks were taken from [253], and are shown in Figure B.1. They were purposefully selected to represent a typical network from rural, suburban, and urban areas respectively. The blue markers show the locations of households, and the black marker shows the substation location.

Unfortunately, these networks did not come with transformer ratings, so assumptions had to be made. Data describing transformer ratings from 32,854 LV circuits in GB was obtained from a DNO. Figure B.2 shows the distribution of transformer ratings for networks which had 50-80, 150-250, and 400-600 households respectively.

The most popular transformer size was 500 kVA in most areas. According to the



Figure B.1: The test networks used. Blue markers show the household locations and the black marker shows the substation position.

guidance in [248], networks with Economy 7 meters are designed to a higher limit than those with gas meters. Rural areas have a higher penetration of Economy 7 meters than suburban areas, so this might explain why 500 kVA transformers are more popular on the smaller networks. For the larger networks, 500 kVA was still the most popular, however, there was considerably less data available for these networks; while there were roughly 10,000 networks in the small and medium bracket, there were only around 100 in the largest group.

Based on this analysis, the following transformer sizes were assumed. For the rural

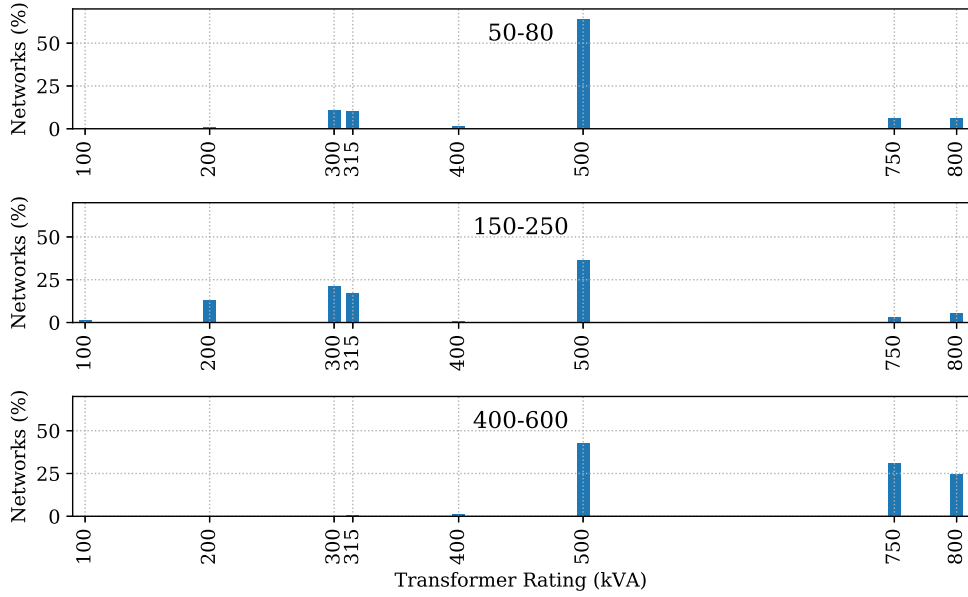


Figure B.2: The transformer ratings of networks with varying numbers of households..

and sub-urban networks: For the rural and suburban networks, local authorities with more than 10% of households had Economy 7 meters were given a 500 kVA transformer, while those with less were assumed to have a 315 kVA. The urban networks were all assumed to have 800 kVA transformers.

## B.2 Test Feeders

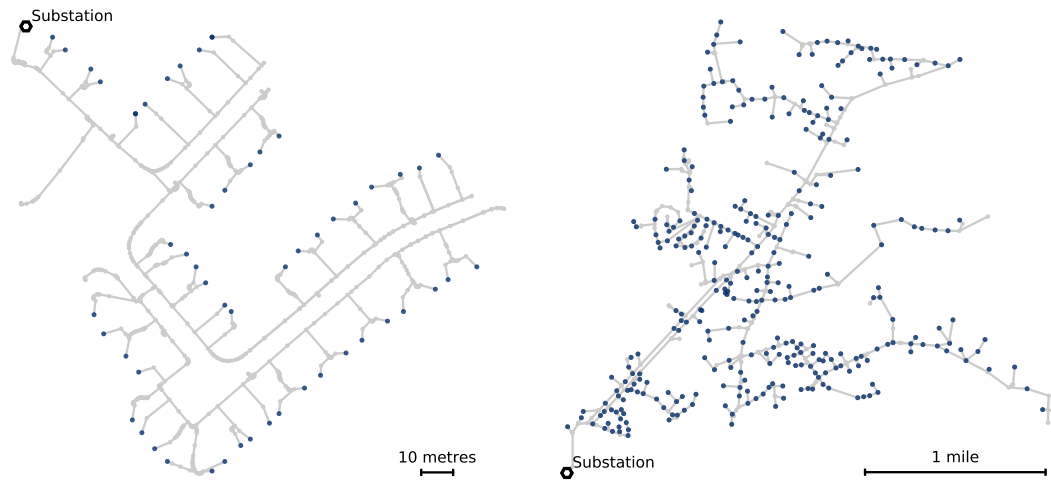
In order to compare the action of smart charging objectives in realistic loading conditions a test feeder was required. These simulations were not geographically specific, so the style of network is less important (providing it is realistic).

For both the UK and Texas case study popular open source test feeders were used to ease comparisons between existing literature. For the UK case, the IEEE European Low Voltage Test Feeder is used (see Fig. B.3a). There are 55 loads on the system, each of which represent a single residential household. The base voltage is at 230 V and the system frequency is 50 Hz.

For the Texas case study, Feeder K1 from the EPRI set of test networks is used [261]. This network (shown in Fig. B.3b) has 311 residential loads, and 13 industrial loads. It was assumed that the industrial loads were fixed and constant with time. The network

has base voltages of X and Y, and the system frequency is 60 Hz.

and the system frequency is 60 Hz.



(a) The IEEE European LV Test Feeder

(b) EPRI Network

Figure B.3: The test feeders considered. Blue markers show the household locations and the black marker shows the substation position.

As part of the sensitivity analysis in section 6.3.1.2, a selection of the other test feeders from [253] were used for comparison. The table below allows the reader to map the networks mentioned in that section to those from the paper:

#	1	2	3	4	5	6	7	8	9
<b>Network</b>	4	21	16	1	3	2	19	7	2
<b>Feeder</b>	1	3	2	1	1	1	3	4	4

# Bibliography

- [1] World Resources Institute. Climate analysis tool. <http://cait.wri.org/>, 2017.
- [2] Department for Business, energy & Industrial Strategy. Uk greenhouse gas emissions, provisional figures. Technical report, UK Government, 2018.
- [3] Paris agreement, 2015-12-12. u.n.t.c. XXVII 7.d.
- [4] Tyler A. Jacobson, Jasdeep S. Kler, Michael T. Hernke, Rudolf K. Braun, Keith C. Meyer, and William E. Funk. Direct human health risks of increased atmospheric carbon dioxide. *Nature Sustainability*, 2(8):691–701, 8 2019.
- [5] Ebrahim Saeidi Dehaghani. *Well-to-wheels energy efficiency analysis of plug-in electric vehicles including varying charging regimes*. PhD thesis, Concordia University, 2013.
- [6] Reed Doucette and Malcolm McCulloch. Modeling the co2 emissions from battery electric vehicles given the power generation mixes of different countries. *Energy Policy*, 39(1):803–811, 2011.
- [7] Society of Motor Manufacturers & Traders. Electric vehicle registration data. <https://www.smmt.co.uk/>. Accessed: 2019-08-11.
- [8] UK. Future energy scenarios. Technical report, National Grid, 2018.
- [9] Peter Campbell, Financial Times. Plug-in hybrid car sales fall after UK government cuts grants. <https://www.ft.com/content/e58b168c-70a4-11e9-bbfb-5c68069fbd15>, May 7th 2019.
- [10] World Energy Council. WORLD ENERGY TRILEMMA INDEX. <https://www.worldenergy.org/publications/entry/world-energy-trilemma-index-2019>, 2019.
- [11] Steven W. Blume. *Electric Power System Basics: For the Nonelectrical Professional*. Wiley, 2007.
- [12] University of Edinburgh. Matching renewable electricity generation with demand. Technical report, Scottish Executive, 2006.
- [13] International Electrotechnical Commission. Iec 60038, 1983.
- [14] National Electricity Transmission System. Security and quality of supply standard. Technical report, National Grid, 2019.
- [15] A. A. Sallam. *Electric distribution systems*. IEEE Press Wiley, Piscatawy, NJ Hoboken, New Jersey, 2011.
- [16] Zap-Map. Charging point statistics 2017.
- [17] Zap-Map. Guide to ev charging. <https://www.zap-map.com/charge-points/>.

- [18] Sheng Shui Zhang. The effect of the charging protocol on the cycle life of a Li-ion battery. *Journal of Power Sources*, 161(2):1385–1391, 2006.
- [19] Johannes Schäuble, Thomas Kaschub, Axel Ensslen, Patrick Jochem, and Wolf Fichtner. Generating electric vehicle load profiles from empirical data of three ev fleets in southwest germany. *Journal of Cleaner Production*, 150:253–266, 2017.
- [20] Andreas Thingvad, Charalampos Ziras, Junjie Hu, and Mattia Marinelli. Assessing the energy content of system frequency and electric vehicle charging efficiency for ancillary service provision. In *2017 52nd International Universities Power Engineering Conference, UPEC 2017*, volume 2017-Janua, pages 1–6, 2017.
- [21] UK Government Department for Business, Energy & Industrial Strategy. Government funded electric car chargepoints to be smart by july 2019. <https://www.gov.uk/government/news/government-funded-electric-car-chargepoints-to-be-smart-by-july-2019>. Accessed: 2019-04-16.
- [22] Electric Nation. The real-world smart charging trial - what we've learnt so far. Technical report, Western Power Distribution, 2019.
- [23] Nikos Hatziargyriou, Evangelos Karfopoulos, and Konstantinos Tsatsakis. *The Impact of EV Charging on the System Demand*, pages 57–85. Springer, 01 2013.
- [24] Dunbar P. Birnie. Solar-to-vehicle (S2V) systems for powering commuters of the future. *Journal of Power Sources*, 186(2):539–542, 2009.
- [25] R. Moghe, F. Kreikebaum, J. E. Hernandez, R. P. Kandula, and D. Divan. Mitigating distribution transformer lifetime degradation caused by grid-enabled vehicle (gev) charging. In *2011 IEEE Energy Conversion Congress and Exposition*, pages 835–842, 2011.
- [26] Eric Sortomme, Mohammad M. Hindi, S. D James MacPherson, and S. S. Venkata. Coordinated charging of plug-in hybrid electric vehicles to minimize distribution system losses. *IEEE Transactions on Smart Grid*, 2(1):186–193, 2011.
- [27] Regen. Market Insight Series: Harnessing the Electric Vehicle Revolution. Technical report, Regen, 2018.
- [28] National Grid. Forecourt thoughts: Mass fast charging of electric vehicles, August 2017.
- [29] Office for National Statistics. Census aggregate data. UK Data Service, 2011.
- [30] Energy & Industrial Strategy UK Department for Business. National statistics: Energy consumption in the uk. <https://www.gov.uk/government/statistics/energy-consumption-in-the-uk>, 2019.
- [31] UK Department of Business & Industry Strategy. Msoa estimates of households not connected to the gas network. <https://www.gov.uk/government/statistics/msoa-estimates-of-households-not-connected-to-the-gas-network>. Accessed: 2019-08-11.
- [32] Electrek. Texas brings back its \$2,500 electric vehicle incentives ? tesla is still out. <https://electrek.co/2018/06/05/texas-electric-vehicle-incentives-tesla/>. Accessed: 2019-04-05.
- [33] EV Adoption. Ev market share by us state. <https://evadoption.com/ev-market-share/ev-market-share-state/>. Accessed: 2019-04-11.

- [34] US Energy Information Administration. Among states, texas consumes the most energy, vermont the least, August 2017.
- [35] US Energy Information Administration. Household energy use in texas, 2009.
- [36] US Energy Information Administration. State profile: Texas. <https://www.eia.gov/state/data.php?sid=TX>, 2019.
- [37] G. T. Heydt. The impact of electric vehicle deployment on load management strategies. *IEEE Power Engineering Review*, 3(5), 1983.
- [38] Yijia Cao, Shengwei Tang, Canbing Li, Peng Zhang, Yi Tan, Zhikun Zhang, and Junxiong Li. An optimized EV charging model considering TOU price and SOC curve. *IEEE Transactions on Smart Grid*, 3(1):388–393, 2012.
- [39] Matthias D. Galus and Göran Andersson. Demand management of grid connected plug-in hybrid electric vehicles (PHEV). In *2008 IEEE Energy 2030 Conference, ENERGY 2008*, 2008.
- [40] Chris Hutson, Ganesh Kumar Venayagamoorthy, and Keith A. Corzine. Intelligent scheduling of hybrid and electric vehicle storage capacity in a parking lot for profit maximization in grid power transactions. In *2008 IEEE Energy 2030 Conference, ENERGY 2008*, 2008.
- [41] Liang Zhang, Vassilis Kekatos, and Georgios B. Giannakis. Scalable Electric Vehicle Charging Protocols. *Power Systems, IEEE Transactions on*, 32(2), 2017.
- [42] Lingwen Gan, Ufuk Topcu, and Steven H. Low. Optimal decentralized protocol for electric vehicle charging. *IEEE Transactions on Power Systems*, 28(2):940–951, 2013.
- [43] Stylianos I. Vagropoulos and Anastasios G. Bakirtzis. Optimal bidding strategy for electric vehicle aggregators in electricity markets. *IEEE Transactions on Power Systems*, 28(4):4031–4041, 2013.
- [44] Willem Leterme, Frederik Ruelens, Bert Claessens, and Ronnie Belmans. A flexible stochastic optimization method for wind power balancing with PHEVs. *IEEE Transactions on Smart Grid*, 5(3):1238–1245, 2014.
- [45] Jian Zhao, Can Wan, Zhao Xu, and Jianhui Wang. Risk-Based Day-Ahead Scheduling of Electric Vehicle Aggregator Using Information Gap Decision Theory. *IEEE Transactions on Smart Grid*, 8(4):1609–1618, 2017.
- [46] M. Kaleeswari and K. Lakshmi. Energy Management for Plug in Hybrid Electric Vehicles Using Stochastic Optimization. In *International Conference on Advanced Computing and Communication Systems*, 2015.
- [47] Junjie Hu, Shi You, Morten Lind, and Jacob Østergaard. Coordinated charging of electric vehicles for congestion prevention in the distribution grid. *IEEE Transactions on Smart Grid*, 5(2):703–711, 2014.
- [48] Faeza Hafiz, Anderson R. De Quieroz, Iqbal Husain, and Poria Fajri. Charge scheduling of a plug-in electric vehicle considering load demand uncertainty based on multi-stage stochastic optimization. In *2017 North American Power Symposium, NAPS 2017*, 2017.
- [49] Rakpong Kaewpuang and Dusit Niyato. An energy efficient solution: Integrating Plug-In Hybrid Electric Vehicle in smart grid with renewable energy. *2012 IEEE Conference on Computer Communications Workshops*, pages 73–78, 2012.

- [50] Caroline Le Floch, Emre Can Kara, and Scott Moura. PDE modeling and control of electric vehicle fleets for ancillary services: A discrete charging case. *IEEE Transactions on Smart Grid*, 9(2):573–581, 2018.
- [51] Chenrui Jin, Jian Tang, and P Ghosh. Optimizing electric vehicle charging with energy storage in the electricity market. *IEEE Transactions on Smart Grid*, 4(1):311–320, 2013.
- [52] Lucia Iguualada, Cristina Corchero, Miguel Cruz-Zambrano, and F. Javier Heredia. Optimal energy management for a residential microgrid including a vehicle-to-grid system. *IEEE Transactions on Smart Grid*, 5(4):2163–2172, 2014.
- [53] M. Hadi Amini, Amin Kargarian, and Orkun Karabasoglu. ARIMA-based decoupled time series forecasting of electric vehicle charging demand for stochastic power system operation. *Electric Power Systems Research*, 2016.
- [54] Ganesh K. Venayagamoorthy, Pinaki Mitra, Keith Corzine, and Chris Huston. Real-time modeling of distributed plug-in vehicles for V2G transactions. In *2009 IEEE Energy Conversion Congress and Exposition, ECCE 2009*, 2009.
- [55] Carl Binding, Dieter Gantenbein, Bernhard Jansen, Olle Sundström, Peter Bach Andersen, Francesco Marra, Bjarne Poulsen, and Chresten Træholt. Electric vehicle fleet integration in the Danish EDISON project - A virtual power plant on the island of Bornholm, 2010.
- [56] John Brady and Margaret O’Mahony. Modelling charging profiles of electric vehicles based on real-world electric vehicle charging data. *Sustainable Cities and Society*, 2016.
- [57] J Rolink and C Rehtanz. Large- Scale Modeling of Grid-Connected Electric Vehicles. *IEEE Trans. Power Deliv.*, 28(2):894–902, 2013.
- [58] Markus Godde, Tobias Findeisen, Torsten Sowa, and Phuong H. Nguyen. Modelling the charging probability of electric vehicles as a Gaussian mixture model for a convolution based power flow analysis. In *2015 IEEE Eindhoven PowerTech, PowerTech 2015*, 2015.
- [59] Qin Yan, Cheng Qian, Bei Zhang, and Mladen Kezunovic. Statistical analysis and modeling of plug-in electric vehicle charging demand in distribution systems. In *2017 19th International Conference on Intelligent System Application to Power Systems, ISAP 2017*, 2017.
- [60] Hao Liang, Isha Sharma, Weihua Zhuang, and Kankar Bhattacharya. Plug-in electric vehicle charging demand estimation based on queueing network analysis. In *IEEE Power and Energy Society General Meeting*, 2014.
- [61] Ali Ahmadian, Mahdi Sedghi, and Masoud Aliakbar-Golkar. Stochastic modeling of Plug-in Electric Vehicles load demand in residential grids considering nonlinear battery charge characteristic. In *20th Electrical Power Distribution Conference, EPDC 2015*, 2015.
- [62] M. Alizadeh, A. Scaglione, J. Davies, and K. S. Kurani. A scalable stochastic model for the electricity demand of electric and plug-in hybrid vehicles. *IEEE Transactions on Smart Grid*, 5(2), 2014.
- [63] S. Bae and A. Kwasinski. Spatial and temporal model of electric vehicle charging demand. *IEEE Transactions on Smart Grid*, 3(1):394–403, 2012.
- [64] Joakim Munkhammar, Joakim Widén, and Jesper Rydén. On a probability distribution model combining household power consumption, electric vehicle home-charging and photovoltaic power production. *Applied Energy*, 2015.

- [65] Nima H. Tehrani and Peng Wang. Probabilistic estimation of plug-in electric vehicles charging load profile. *Electric Power Systems Research*, 2015.
- [66] Ali Ashtari, Eric Bibeau, Soheil Shahidinejad, and Tom Molinski. PEV charging profile prediction and analysis based on vehicle usage data. *IEEE Transactions on Smart Grid*, 2012.
- [67] Stylianos I. Vagropoulos, Georgios A. Balaskas, and Anastasios G. Bakirtzis. An Investigation of Plug-In Electric Vehicle Charging Impact on Power Systems Scheduling and Energy Costs. *Power Systems, IEEE Transactions on*, 32(3), 2017.
- [68] Sinan Küfeoğlu and Michael G. Pollitt. The impact of PVs and EVs on domestic electricity network charges: A case study from Great Britain. *Energy Policy*, 2019.
- [69] P Denholm and W Short. An Evaluation of Utility System Impacts and Benefits of Optimally Dispatched Plug-In Hybrid Electric Vehicles. *NREL Report noTP-620*, 2006.
- [70] Michael Wolinetz, Jonn Axsen, Jotham Peters, and Curran Crawford. Simulating the value of electric-vehicle-grid integration using a behaviourally realistic model. *Nature Energy*, 2018.
- [71] Nick Kelly, Aizaz Samuel, and Jon Hand. Testing integrated electric vehicle charging and domestic heating strategies for future UK housing. *Energy and Buildings*, 2015.
- [72] Willett Kempton and Toru Kubo. Electric-drive vehicles for peak power in Japan. *Energy Policy*, 2000.
- [73] Jasna Tomić and Willett Kempton. Using fleets of electric-drive vehicles for grid support. *Journal of Power Sources*, 2007.
- [74] Roberto Moreira, Ladislav Ollagnier, Dimitrios Papadaskalopoulos, and Goran Strbac. Optimal multi-service business models for electric vehicles. In *2017 IEEE Manchester PowerTech*, 2017.
- [75] Willett Kempton and Jasna Tomić. Vehicle-to-grid power implementation: From stabilizing the grid to supporting large-scale renewable energy. *Journal of Power Sources*, 2005.
- [76] S.-L. Andersson, A.K. Elofsson, M.D. Galus, L. Goransson, S. Karlsson, and G. Andersson. Plug-in hybrid electric vehicles as regulating power providers: Case studies of Sweden and Germany. *Energy Policy*, 38(6):2751–2762, 2010.
- [77] W Short and P Denholm. A Preliminary Assessment of Plug-In Hybrid Electric Vehicles on Wind Energy Markets. Technical report, NREL, 2006.
- [78] Xin Li, Luiz A.C. Lopes, and Sheldon S. Williamson. On the suitability of plug-in hybrid electric vehicle (PHEV) charging infrastructures based on wind and solar energy. In *2009 IEEE Power and Energy Society General Meeting, PES '09*, 2009.
- [79] National Grid. Future Energy Scenarios, 2018.
- [80] Oscar Van Vliet, Anne Sjoerd Brouwer, Takeshi Kuramochi, MacHteld Van Den Broek, and André Faaij. Energy use, cost and CO2 emissions of electric cars. *Journal of Power Sources*, 196(4):2298–2310, 2011.
- [81] Stanton W Hadley. Impact of Plug-in Hybrid Vehicles on the Electric Grid. *Oak Ridge National Laboratory*, 2006.

- [82] Zahra Darabi and Mehdi Ferdowsi. Aggregated impact of plug-in hybrid electric vehicles on electricity demand profile. *IEEE Transactions on Sustainable Energy*, 2(4):501–508, 2011.
- [83] Xiaolong Yu. Impacts assessment of PHEV charge profiles on generation expansion using national energy modeling system. In *IEEE Power and Energy Society 2008 General Meeting: Conversion and Delivery of Electrical Energy in the 21st Century, PES*, 2008.
- [84] Ryan Liu, Luther Dow, and Edwin Liu. A survey of PEV impacts on electric utilities. In *IEEE PES Innovative Smart Grid Technologies Conference Europe, ISGT Europe*, 2011.
- [85] Soheil Shahidinejad, Shaahin Filizadeh, and Eric Bibeau. Profile of charging load on the grid due to plug-in vehicles. *IEEE Transactions on Smart Grid*, 3(1):135–141, 2012.
- [86] Joaquim Delgado, Ricardo Faria, Pedro Moura, and Aníbal T. de Almeida. Impacts of plug-in electric vehicles in the portuguese electrical grid. *Transportation Research Part D: Transport and Environment*, 2018.
- [87] Wolf Peter Schill and Clemens Gerbaulet. Power system impacts of electric vehicles in Germany: Charging with coal or renewables? *Applied Energy*, 2015.
- [88] Pia Grahn, K. Alvehag, and Lennart Soder. PHEV utilization model considering type-of-trip and recharging flexibility. *IEEE Transactions on Smart Grid*, 5(1):139–148, 2014.
- [89] Di Wu, Dionysios C. Aliprantis, and Konstanina Gkritza. Electric energy and power consumption by light-duty plug-in electric vehicles. *IEEE Transactions on Power Systems*, 26(2):738–746, 2011.
- [90] Jonn Axsen and Kenneth S. Kurani. Anticipating plug-in hybrid vehicle energy impacts in California: Constructing consumer-informed recharge profiles. *Transportation Research Part D: Transport and Environment*, 2010.
- [91] Dušan Božič and Miloš Pantoš. Impact of electric-drive vehicles on power system reliability. *Energy*, 2015.
- [92] Xue Wang and Rajesh Karki. Exploiting PHEV to Augment Power System Reliability. *IEEE Transactions on Smart Grid*, 2017.
- [93] Sang Keun Moon and Jin O. Kim. Balanced charging strategies for electric vehicles on power systems. *Applied Energy*, 2017.
- [94] David Dallinger and Martin Wietschel. Grid integration of intermittent renewable energy sources using price-responsive plug-in electric vehicles, 2012.
- [95] Wei Yang, Yue Xiang, Junyong Liu, and Chenghong Gu. v. *IEEE Transactions on Power Systems*, 33(2):1915–1925, 2018.
- [96] Pedro Sanchez-Martin, Sara Lumbreras, and Antonio Alberdi-Alen. Stochastic programming applied to ev charging points for energy and reserve service markets. *IEEE Transactions on Power Systems*, 31(1):198–205, 2016.
- [97] Fei Teng, Yunfei Mu, Hongjie Jia, Jianzhong Wu, Pingliang Zeng, and Goran Strbac. Challenges on primary frequency control and potential solution from EVs in the future GB electricity system. *Applied Energy*, 2016.
- [98] Bei Zhang and Mladen Kezunovic. Impact on Power System Flexibility by Electric Vehicle Participation in Ramp Market. *IEEE Transactions on Smart Grid*, 2016.

- [99] Yifeng He, B Venkatesh, and Ling Guan. Optimal Scheduling for Charging and Discharging of Electric Vehicles. *IEEE Transactions on Smart Grid*, 3(3):1095–1105, 2012.
- [100] Nicole Taheri, Robert Entriken, and Yinyu Ye. A dynamic algorithm for facilitated charging of plug-in electric vehicles. *IEEE Transactions on Smart Grid*, 4(4):1772–1779, 2013.
- [101] Trine Krogh Kristoffersen, Karsten Capion, and Peter Meibom. Optimal charging of electric drive vehicles in a market environment. *Applied Energy*, 2011.
- [102] Siyan Liu and Amir H. Etemadi. A Dynamic Stochastic Optimization for Recharging Plug-in Electric Vehicles. *Smart Grid IEEE Transactions on*, 2017.
- [103] Sikai Huang and D Infield. The impact of domestic Plug-in Hybrid Electric Vehicles on power distribution system loads. *POWERCON*, 2010.
- [104] Nima Ghiasnezhad Omran and Shaahin Filizadeh. Location-based forecasting of vehicular charging load on the distribution system. *IEEE Transactions on Smart Grid*, 5(2):632–641, 2014.
- [105] R. A. Verzijlbergh, Z. Lukszo, J. G. Slootweg, and M. D. Ilic. The impact of controlled electric vehicle charging on residential low voltage networks. In *2011 International Conference on Networking, Sensing and Control, ICNSC 2011*, pages 14–19, 2011.
- [106] S.A. Syed Mustafa, M.F. Mohd Yusoff, N. Baharin, and T.A.R Tuan Abdullah. Modeling the Impact of PHEV Penetration on the Residential Electrical Networks. *Applied Mechanics and Materials*, 2015.
- [107] S. Rahman and G. B. Shrestha. An investigation into the impact of electric vehicle load on the electric utility distribution system. *IEEE Transactions on Power Delivery*, 1993.
- [108] Joakim Munkhammar, Justin D.K. Bishop, Juan Jose Sarralde, Wei Tian, and Ruchi Choudhary. Household electricity use, electric vehicle home-charging and distributed photovoltaic power production in the city of Westminster. *Energy and Buildings*, 2015.
- [109] Matteo Muratori. Impact of uncoordinated plug-in electric vehicle charging on residential power demand. *Nature Energy*, 2018.
- [110] K Schneider. Impact assessment of plug-in hybrid vehicles on pacific northwest distribution systems. *Power and Energy Society General Meeting - Conversion and Delivery of Electrical Energy in the 21st Century*, pages 1–6, 2008.
- [111] Remco A. Verzijlbergh, Marinus O W Grond, Zofia Lukszo, Johannes G. Slootweg, and Marija D. Ilic. Network impacts and cost savings of controlled EV charging. *IEEE Transactions on Smart Grid*, 3(3):1203–1212, 2012.
- [112] Shengnan Shao, Manisa Pipattanasomporn, and Saifur Rahman. Challenges of PHEV penetration to the residential distribution network. In *2009 IEEE Power and Energy Society General Meeting, PES '09*, 2009.
- [113] J. Carlos Gómez and Medhat M. Morcos. Impact of EV battery chargers on the power quality of distribution systems. *IEEE Transactions on Power Delivery*, 18(3):975–981, 2003.
- [114] Radu Godina, Eduardo M.G. Rodrigues, João C.O. Matias, and João P.S. Catalão. Smart electric vehicle charging scheduler for overloading prevention of an industry client power distribution transformer. *Applied Energy*, 2016.

- [115] J. Taylor, A. Maitra, M> Alexander, D. Brppls, and M. Duvall. Evaluation of the Impact of Plug-in Electric Vehicle Loading on Distribution System Operations, 2009.
- [116] Kejun Qian, Chengke Zhou, and Yue Yuan. Impacts of high penetration level of fully electric vehicles charging loads on the thermal ageing of power transformers. *International Journal of Electrical Power and Energy Systems*, 2015.
- [117] Visvakumar Aravinthan and Ward Jewell. Controlled electric vehicle charging for mitigating impacts on distribution assets. *IEEE Transactions on Smart Grid*, 6(2):999–1009, 2015.
- [118] Chenglin Liao and Bing Yang. Phases-Controlled Coordinated Charging Method for Electric Vehicles. *CES Transactions on Electrical Machines and Systems*, 2(1), 2018.
- [119] H. S.V.S. Kumar Nunna, Swathi Battula, Suryanarayana Doolla, and Dipti Srinivasan. Energy Management in Smart Distribution Systems with Vehicle-To-Grid Integrated Microgrids. *IEEE Transactions on Smart Grid*, 9(5):4004–4016, 2018.
- [120] N. Z. Xu and C. Y. Chung. Reliability evaluation of distribution systems including vehicle-to-home and vehicle-to-grid. *IEEE Transactions on Power Systems*, 31(1):759–768, 2016.
- [121] Ahmad Karnama. *Analysis of Integration of Plug-in Hybrid Electric Vehicles in the Distribution Grid*. PhD thesis, KTH, 2009.
- [122] P. S. Moses, M. A. S. Masoum, and S. Hajforoosh. Overloading of distribution transformers in smart grid due to uncoordinated charging of plug-in electric vehicles. In *2012 IEEE PES Innovative Smart Grid Technologies (ISGT)*, pages 1–6, 2012.
- [123] C. H. Dharmakeerthi, N. Mithulanathan, and T. K. Saha. Impact of electric vehicle fast charging on power system voltage stability. *International Journal of Electrical Power and Energy Systems*, 2014.
- [124] Chenxi Wu, Fushuan Wen, Youlin Lou, and Feng Xin. Probabilistic load flow analysis of photovoltaic generation system with plug-in electric vehicles. *International Journal of Electrical Power and Energy Systems*, 2015.
- [125] S Shafiee, M Fotuhi-Firuzabad, and M Rastegar. Investigating the impacts of plug-in hybrid electric vehicles on power distribution systems. *Smart Grid, IEEE Transactions on*, 4(3):1351–1360, 2013.
- [126] Peter Richardson, Damian Flynn, and Andrew Keane. Impact assessment of varying penetrations of electric vehicles on low voltage distribution systems. In *IEEE PES General Meeting, PES 2010*, 2010.
- [127] Chin Ho Tie, Chin Kim Gan, and Khairul Anwar Ibrahim. The impact of electric vehicle charging on a residential low voltage distribution network in Malaysia. In *2014 IEEE Innovative Smart Grid Technologies - Asia, ISGT ASIA 2014*, 2014.
- [128] Kevin Mets, Tom Verschueren, Filip De Turck, and Chris Develder. Exploiting V2G to optimize residential energy consumption with electrical vehicle (dis)charging. In *2011 IEEE 1st International Workshop on Smart Grid Modeling and Simulation, SGMS 2011*, 2011.
- [129] AS Masoum, Sara Deilami, and PS Moses. Impact of plug-in electrical vehicles on voltage profile and losses of residential system. (*AUPEC*), *2010 20th*, 2010.

- [130] Andreas T. Procopiou, Jairo Quirós-Tortós, and Luis F. Ochoa. HPC-Based Probabilistic Analysis of LV Networks With EVs: Impacts and Control. *Smart Grid IEEE Transactions on*, 8(3), 2017.
- [131] Jairo Quirós-Tortós, Luis Ochoa, and Timothy Butler. How Electric Vehicles and the Grid Work Together: Lessons Learned from One of the Largest Electric Vehicle Trials in the World. *IEEE Access*, pages 64–76, 2018.
- [132] F. Geth, N. Leemput, J. Van Roy, J. Buscher, R. Ponnette, and J. Driesen. Voltage droop charging of electric vehicles in a residential distribution feeder. In *2012 3rd IEEE PES Innovative Smart Grid Technologies Europe (ISGT Europe)*, pages 1–8, 2012.
- [133] Kristien Clement-Nyns, Edwin Haesen, and Johan Driesen. The impact of vehicle-to-grid on the distribution grid. *Electric Power Systems Research*, 2011.
- [134] Yuchao Ma, Tom Houghton, Andrew Cruden, and David Infield. Modeling the benefits of vehicle-to-grid technology to a power system. *IEEE Transactions on Power Systems*, 27(2):1012–1020, 2012.
- [135] Niels Leemput, Frederik Geth, Juan Van Roy, Annelies Delnooz, Jeroen Buscher, and Johan Driesen. Impact of electric vehicle on-board single-phase charging strategies on a flemish residential grid. *IEEE Transactions on Smart Grid*, 2014.
- [136] L. Fernandez et al. Assessment of the Impact of Plug-in Electric Vehicles on Distribution Networks. *IEEE Transactions on Power Systems*, 26(1):206–213, 2011.
- [137] Omar Hafez and Kankar Bhattacharya. Queuing Analysis Based PEV Load Modeling Considering Battery Charging Behavior and Their Impact on Distribution System Operation. *Smart Grid, IEEE Transactions on*, 9(1):261–273, 2018.
- [138] Ahmed M.A. Haidar, Kashem M. Muttaqi, and Mohammed H. Haque. Multistage time-variant electric vehicle load modelling for capturing accurate electric vehicle behaviour and electric vehicle impact on electricity distribution grids. *IET Generation, Transmission & Distribution*, 9(16), 2015.
- [139] Li Pengcheng, Xiaoyu Duan, Jing Yang, Qiuyan Zhang, Yuanliang Zhao, and Zechun Hu. Coordinated EV charging and reactive power optimization for radial distribution network using mixed integer second-order cone programming. In *ITEC Asia-Pacific*, 2017.
- [140] A.S. Masoum, S. Deilami, P.S. Moses, M.A.S. Masoum, and A. Abu-Siada. Smart load management of plug-in electric vehicles in distribution and residential networks with charging stations for peak shaving and loss minimisation considering voltage regulation. *IET Generation, Transmission & Distribution*, 5(8):877, 2011.
- [141] Hamed Nafisi, Seyed Mohammad Mousavi Agah, Hossien Askarian Abyaneh, and Mehrdad Abedi. Two-Stage Optimization Method for Energy Loss Minimization in Microgrid Based on Smart Power Management Scheme of PHEVs. *IEEE Transactions on Smart Grid*, 7(3):1268–1276, 2016.
- [142] Jia Ying Yong, Vigna K. Ramachandaramurthy, Kang Miao Tan, and N. Mithulananthan. Bi-directional electric vehicle fast charging station with novel reactive power compensation for voltage regulation. *International Journal of Electrical Power and Energy Systems*, 2015.

- [143] Myriam Neaimeh, Robin Wardle, Andrew M. Jenkins, Jialiang Yi, Graeme Hill, Pdraig F. Lyons, Yvonne Hübner, Phil T. Blythe, and Phil C. Taylor. A probabilistic approach to combining smart meter and electric vehicle charging data to investigate distribution network impacts. *Applied Energy*, 2015.
- [144] P. Papadopoulos, S. Skarvelis-Kazakos, I. Grau, L.M. Cipcigan, and N. Jenkins. Electric vehicles' impact on British distribution networks. *IET Electrical Systems in Transportation*, 2012.
- [145] Kristien Clement-Nyns, Edwin Haesen, and Johan Driesen. The impact of Charging plug-in hybrid electric vehicles on a residential distribution grid. *IEEE Transactions on Power Systems*, 25(1):371–380, 2010.
- [146] Hamed Nafisi, Hossein Askarian Abyaneh, and Mehrdad Abedi. Energy loss minimization using PHEVs as distributed active and reactive power resources: a convex quadratic local optimal solution. *International Transactions on Electrical Energy Systems*, 26(6):1287–1302, 2016.
- [147] Rong Ceng Leou, Chun Lien Su, and Chan Nan Lu. Stochastic analyses of electric vehicle charging impacts on distribution network. *IEEE Transactions on Power Systems*, 29(3):1055–1063, 2014.
- [148] Kejun Qian, Chengke Zhou, Malcolm Allan, and Yue Yuan. Modeling of load demand due to EV battery charging in distribution systems. *IEEE Transactions on Power Systems*, 26(2):802–810, 2011.
- [149] P Papadopoulos, S Skarvelis-Kazakos, I Grau, B Awad, Liana Mirela Cipcigan, and Nicholas Jenkins. Impact of residential charging of electric vehicles on distribution networks, a probabilistic approach. *Universities Power Engineering Conference UPEC 2010 45th International*, pages 1–5, 2010.
- [150] A.a Bosovic, M.a Music, and S.b Sadovic. Analysis of the impacts of plug-in electric vehicle charging on the part of a real low voltage distribution network. In *2015 IEEE Eindhoven PowerTech, PowerTech 2015*, 2015.
- [151] Salvador Acha, Tim C. Green, and Nilay Shah. Effects of Optimised Plug-in Hybrid Vehicle Charging Strategies on Electric Distribution Network Losses. In *IEEE PES T&D*, 2010.
- [152] T. Klayklung, S. Dechanupaprittha, and P. Kongthong. Analysis of unbalance Plug-in Electric Vehicle home charging in PEA distribution network by stochastic load model. In *Proceedings - 2015 International Symposium on Smart Electric Distribution Systems and Technologies, EDST 2015*, 2015.
- [153] Fangjie Gou, Jianwei Yang, and Tianlei Zang. Ordered charging strategy for electric vehicles based on load balancing. In *2017 IEEE Conference on Energy Internet and Energy System Integration, EI2 2017 - Proceedings*, volume 2018-January, pages 1–5, 2018.
- [154] Sam Weckx and Johan Driesen. Load Balancing with EV Chargers and PV Inverters in Unbalanced Distribution Grids. *IEEE Transactions on Sustainable Energy*, 6(2):635–643, 2015.
- [155] Mohammad A.S. Masoum, Sara Deilami, and Syed Islam. Mitigation of harmonics in smart grids with high penetration of plug-in electric vehicles. In *IEEE PES General Meeting, PES 2010*, 2010.

- [156] G.a. Putrus, P. Suwanapingkarl, D. Johnston, E.C. Bentley, and M. Narayana. Impact of electric vehicles on power distribution networks. *2009 IEEE Vehicle Power and Propulsion Conference*, pages 827–831, 2009.
- [157] P. T. Staats, W. M. Grady, A. Arapostathis, and R. S. Thallam. A statistical analysis of the effect of electric vehicle battery charging on distribution system harmonic voltages. *IEEE Transactions on Power Delivery*, 1998.
- [158] E. C. Bentley, P. Suwanapingkarl, S. Weerasinghe, T. Jiang, G. A. Putrus, and D. Johnston. The interactive effects of multiple EV chargers within a distribution network. In *2010 IEEE Vehicle Power and Propulsion Conference, VPPC 2010*, 2010.
- [159] Chen Jiang, Ricardo Torquato, Diogo Salles, and Wilsun Xu. Method to assess the power quality impact of plug-in electric vehicles. In *Proceedings of International Conference on Harmonics and Quality of Power, ICHQP*, 2014.
- [160] Alexandre Lucas, Fausto Bonavitacola, Evangelos Kotsakis, and Gianluca Fulli. Grid harmonic impact of multiple electric vehicle fast charging. *Electric Power Systems Research*, 2015.
- [161] Sara Deilami, Amir S. Masoum, Paul S. Moses, and Mohammad A.S. Masoum. Voltage profile and THD distortion of residential network with high penetration of plug-in electrical vehicles. In *IEEE PES Innovative Smart Grid Technologies Conference Europe, ISGT Europe*, 2010.
- [162] Else Veldman and Remco A. Verzijlbergh. Distribution grid impacts of smart electric vehicle charging from different perspectives. *IEEE Transactions on Smart Grid*, 6(1):333–342, 2015.
- [163] Anamika Dubey and Surya Santoso. *Electric Vehicle Charging on Residential Distribution Systems: Impacts and Mitigations*, 2015.
- [164] Peter Richardson, Damian Flynn, and Andrew Keane. Optimal charging of electric vehicles in low-voltage distribution systems. *IEEE Transactions on Power Systems*, 27(1):268–279, 2012.
- [165] Peter Richardson, Damian Flynn, and Andrew Keane. Local versus centralized charging strategies for electric vehicles in low voltage distribution systems. *IEEE Transactions on Smart Grid*, 3(2):1020–1028, 2012.
- [166] E. Akhavan-Rezai, M. F. Shaaban, E. F. El-Saadany, and F. Karray. Incorporation of plug-in electric vehicles and solar panels in unbalanced mitigation of LV systems. In *IEEE Power and Energy Society General Meeting*, 2016.
- [167] Elham Akhavan-Rezai, Mostafa F. Shaaban, Ehab F. El-Saadany, and Fakhri Karray. Managing Demand for Plug-in Electric Vehicles in Unbalanced LV Systems with Photovoltaics. *IEEE Transactions on Industrial Informatics*, 2017.
- [168] Sara Deilami. Online Coordination of Plug-In Electric Vehicles Considering Grid Congestion and Smart Grid Power Quality. *Energies*, 2018.
- [169] Steven L. Judd and Thomas J. Overbye. An evaluation of PHEV contributions to power system disturbances and economics. In *40th North American Power Symposium, NAPS2008*, 2008.

- [170] Guido Benetti, Maurizio Delfanti, Tullio Facchinetti, Davide Falabretti, and Marco Merlo. Real-Time Modeling and Control of Electric Vehicles Charging Processes. *IEEE Transactions on Smart Grid*, 6(3):1375–1385, 2015.
- [171] M. J.E. Alam, Kashem M. Muttaqi, and Danny Sutanto. Effective Utilization of Available PEV Battery Capacity for Mitigation of Solar PV Impact and Grid Support with Integrated V2G Functionality. *IEEE Transactions on Smart Grid*, 7(3):1562–1571, 2016.
- [172] Pasqualino Lico, Mattia Marinelli, Katarina Knezović, and Samuele Grillo. Phase balancing by means of electric vehicles single-phase connection shifting in a low voltage Danish grid. In *Proceedings of the Universities Power Engineering Conference*, volume 2015-November, 2015.
- [173] Ying Li, Chris Davis, Zofia Lukszo, and Margot Weijnen. Electric vehicle charging in China’s power system: Energy, economic and environmental trade-offs and policy implications. *Applied Energy*, 2016.
- [174] Yanyan Xu, Serdar Çolak, Emre C. Kara, Scott J. Moura, and Marta C. González. Planning for electric vehicle needs by coupling charging profiles with urban mobility. *Nature Energy*, 2018.
- [175] Mengyu Li, Manfred Lenzen, Felix Keck, Bonnie McBain, Olivier Rey-Lescure, Bing Li, and Chaoyang Jiang. GIS-based probabilistic modeling of BEV charging load for Australia, 2018.
- [176] George Hilton, Mahdi Kiaee, Thomas Bryden, Borislav Dimitrov, Andrew Cruden, and Alan Mortimer. A Stochastic Method for Prediction of the Power Demand at High Rate EV Chargers. *IEEE Transactions on Transportation Electrification*, 4(3):744–756, 2018.
- [177] Erotokritos Xydias, Charalampos Marmaras, Liana M. Cipcigan, Nick Jenkins, Steve Carroll, and Myles Barker. A data-driven approach for characterising the charging demand of electric vehicles: A UK case study. *Applied Energy*, 162:763–771, 2016.
- [178] Wei Wei, Shengwei Mei, Lei Wu, Jianhui Wang, and Yujuan Fang. Robust Operation of Distribution Networks Coupled with Urban Transportation Infrastructures. *IEEE Transactions on Power Systems*, 32(3):2118–2130, 2017.
- [179] Yunfei Mu, Jianzhong Wu, Nick Jenkins, Hongjie Jia, and Chengshan Wang. A Spatial-Temporal model for grid impact analysis of plug-in electric vehicles. *Applied Energy*, 2014.
- [180] Difei Tang and Peng Wang. Nodal Impact Assessment and Alleviation of Moving Electric Vehicle Loads: From Traffic Flow to Power Flow, 2016.
- [181] Nick Storer. How will the growth of electric vehicles impact the grid? *Energy World*, 11:32–34, 2017.
- [182] Ofgem. Implications of the transition to Electric Vehicles. Technical report, Ofgem, 2018.
- [183] Olle Sundstrom and Carl Binding. Flexible charging optimization for electric vehicles considering distribution grid constraints. *IEEE Transactions on Smart Grid*, 3(1):26–37, 2012.
- [184] Michael Kintner-Meyer, Kevin Schneider, and Robert Pratt. Impacts Assessment of Plug-in Hybrid Vehicles on electric utilities and regional U.S. Power Grids. *Federal Energy Regulatory Commission*, pages 1–20, 2007.

- [185] Cedric De Cauwer, Joeri Van Mierlo, and Thierry Coosemans. Energy consumption prediction for electric vehicles based on real-world data. *Energies*, 8, 2015.
- [186] Kevin J. Dyke, Nigel Schofield, and Mike Barnes. The impact of transport electrification on electrical networks. *IEEE Transactions on Industrial Electronics*, 57(12):3917–3926, 2010.
- [187] Leandro Camacho Silva. *Modeling and Design of the Electric Drivetrain for the 2013 Research Concept Vehicle*. PhD thesis, KTH, 2013.
- [188] Saeedeh Barghi-Nia and Frederic Sirios. Development of Stochastic Models for Assessing the Impact of Electric Vehicles in Distribution Grids. In *IEEE Power & Energy Society General Meeting*, 2015.
- [189] Ehsan Pashajavid and Masoud Aliakbar Golkar. Charging of plug-in electric vehicles: Stochastic modelling of load demand within domestic grids. In *ICEE 2012 - 20th Iranian Conference on Electrical Engineering*, 2012.
- [190] Jairo Quirós-Tortós, Alejandro Navarro-Espinosa, Luis F. Ochoa, and Tim Butler. Statistical Representation of EV Charging: Real Data Analysis and Applications. In *20th Power Systems Computation Conference*, pages 1–7, 2018.
- [191] Kristien Clement-Nyns, Edwin Haesen, and Johan Driesen. Coordinated Charging of Multiple Plug-In Hybrid Electric Vehicles in Residential Distribution Grids. In *Power Systems Conference and Exposition*, 2009.
- [192] Pavan Balram, Le Anh Tuan, and Lina Bertling Tjernberg. Modeling of Regulating Power Market Based on AC Optimal Power Flow Considering Losses and Electric Vehicles. In *IEEE ISGT Asia*, 2013.
- [193] Shengnan Shao, Manisa Pipattanasomporn, and Saifur Rahman. Grid integration of electric vehicles and demand response with customer choice, 2012.
- [194] Qinglong Wang, Xue Liu, Jian Du, and Fanxin Kong. Smart Charging for Electric Vehicles: A Survey from the Algorithmic Perspective. *IEEE Communications Surveys and Tutorials*, 2016.
- [195] Thomas P. Lyon, Mark Michelin, Arie Jongejan, and Thomas Leahy. Is "smart charging" policy for electric vehicles worthwhile? *Energy Policy*, 41:259–268, 2012.
- [196] Michael J Fell, Moira Nicolson, Gesche M Huebner, and David Shipworth. Is it time? consumers and time of use tariffs. UCL Energy Institute, March 2015.
- [197] Joram H.M. Langbroeka, Joel P. Franklina, and Yusak O. Susiloa. When do you charge your electric vehicle? A stated adaptation approach. *Energy Policy*, 108:565–573, 2017.
- [198] Competition Commisison. Review of stated preference and willingness to pay methods. <https://webarchive.nationalarchives.gov.uk>, 2010.
- [199] Willett Kempton and Jasna Tomić. Vehicle-to-grid power fundamentals: Calculating capacity and net revenue. *Journal of Power Sources*, 144(1):268–279, 2005.
- [200] Alec Brooks, Tom Gage, and AC Propulsion. Integration of electric drive vehicles with the electric power grid? a new value stream. In *Proceedings of the 18th International Electric Vehicle Symposium and Exhibition*. Citeseer, 2001.

- [201] M. A. Mustafa, N. Zhang, G. Kalogridis, and Z. Fan. Smart electric vehicle charging: Security analysis. In *2013 IEEE PES Innovative Smart Grid Technologies Conference (ISGT)*, pages 1–6, Feb 2013.
- [202] Georgios Darivianakis, Angelos Georghiou, Annika Eichler, Roy S. Smith, and John Lygeros. Scalability through decentralization: A robust control approach for the energy management of a building community. *IFAC-PapersOnLine*, 50(1):14314 – 14319, 2017. 20th IFAC World Congress.
- [203] National Grid ESO. Short term operating reserve (stor): Technical requirements, 2019.
- [204] Northern Powergrid. Strategy for losses. Technical report, Northern Powergrid, 07 2015.
- [205] H M. Tawancy and M Hassan. On the degradation mechanism of low-voltage underground cable with poly(vinyl chloride) insulation. *Journal of Materials Engineering and Performance*, 25, 05 2016.
- [206] L. Ramesh, S.P. Chowdhury, S. Chowdhury, A.A. Natarajan, and C.T. Gaunt. Minimization of Power Loss in Distribution Networks by Different Techniques. *International Journal of Electrical and Electronics Engineering*, 2009.
- [207] Shilpa Kalambe and Ganga Agnihotri. Loss minimization techniques used in distribution network: Bibliographical survey. *Renewable and Sustainable Energy Reviews*, 2014.
- [208] Ali Nourai, V. I. Kogan, and Chris M. Schafer. Load leveling reduces T & D line losses. *IEEE Transactions on Power Delivery*, 2008.
- [209] Michiel van der Meulen, Wieb Bosma, Robin Hagemans, and Werner van Westering. *Reconfiguring Electricity Distribution Networks to Minimize Power Loss: NP-hardness and efficient approximation algorithms*. PhD thesis, Radboud University, 2015.
- [210] Mehdi Farasat and Amirsaman Arabali. Voltage and power control for minimising converter and distribution losses in autonomous microgrids. *IET Generation, Transmission & Distribution*, 9(13):1614–1620, 2015.
- [211] Anya Castillo and Dennice F. Gayme. Evaluating the Effects of Real Power Losses in Optimal Power Flow Based Storage Integration. *IEEE Transactions on Control of Network Systems*, 2017.
- [212] Arild Helseth. A Linear Optimal Power Flow Model Considering Nodal Distribution of Losses. In *9th International Conference on the European Energy Market (EEM)*, 2012.
- [213] W. Kong, K. Ma, and Q. Wu. Three-phase power imbalance decomposition into systematic imbalance and random imbalance. *IEEE Transactions on Power Systems*, 33(3):3001–3012, 2018.
- [214] Katriina Lapanjuuri, Peter Cornick, Christos Byron, Iain Templeton, and John Hurn. National travel survey: 2015 report. Technical report, Department for Transport, 2016.
- [215] Office for National Statistics. Urban and Rural Area Definitions for Policy Purposes in England and Wales: Methodology (v1.0). Technical report, UK Government Statistical Service, August 2013.
- [216] U.S. Department of Transportation. National household travel survey, 2009.
- [217] My electric avenue. <http://myelectricavenue.info/>.

- [218] Pecan Street inc. Spotlight, 2018.
- [219] Mary Inaba, Naoki Katoh, and Hiroshi Imai. Applications of weighted voronoi diagrams and randomization to variance-based k-clustering: (extended abstract). In *Proceedings of the Tenth Annual Symposium on Computational Geometry*, SCG '94, pages 332–339, New York, NY, USA, 1994. ACM.
- [220] David Arthur and Sergei Vassilvitskii. How slow is the k-means method? In *Proceedings of the Twenty-second Annual Symposium on Computational Geometry*, SCG '06, pages 144–153, New York, NY, USA, 2006. ACM.
- [221] Ulrike von Luxburg, Max Planck, and Robert C. Williamson. Clustering: Science or Art? In *27th Workshop on Unsupervised and Transfer Learning*, pages 65–79, 2012.
- [222] Ashish Agarwal. *A comparison of weekend and weekday travel behavior characteristics in urban areas*. PhD thesis, University of South Florida, Scholar Commons, 7 2004.
- [223] J. Paparrizos and L. Gravano. k-shape: Efficient and accurate clustering of time series. *Special Interest Group on Management of Data Rec.*, 45(1):69–76, 06 2016.
- [224] Purnima Bholowalia and Arvind Kumar. Ebk-means: A clustering technique based on elbow method and k-means in wsn. *International Journal of Computer Applications*, 2014.
- [225] María Insenser Nieto, Francisco Garrocho López, and Francisco Cruz. Performance analysis of technology using the s curve model: the case of digital signal processing (dsp) technologies, 1998.
- [226] William Guy Peck. *Elements of Mechanics: For the Use of Colleges, Academies, and High Schools*. A.S. Barnes & Burr, 1859.
- [227] David Eberly. Derivative approximation by finite differences, 2001.
- [228] Environmental Protection Agency. Data on cars used for testing fuel economy. Accessed: 2017-05-15.
- [229] R. A. White and H. H. Korst. The determination of vehicle drag contributions from coast-down tests. In *SAE Technical Paper*. SAE International, 1972.
- [230] Consumer Repots. Why You Might Not Be Getting the Efficiency Promised. <https://www.consumerreports.org>, August 2013.
- [231] M Andrè. The artemis european driving cycles for measuring car pollutant emissions. *Sci Total Environ*, 334-335:73–84, 2004.
- [232] Philip E. Gill and Elizabeth Wong. Methods for convex and general quadratic programming. *Mathematical Programming Computation*, 7(1):71–112, 2015.
- [233] L. Vandenberghe, M. Anderson, and J. Dahl. Cvxopt.
- [234] Andrey Bernstein, Cong Wang, Emiliano Dall’Anese, Jean-Yves Le Boudec, and Changhong Zhao. Load-flow in multiphase distribution networks: Existence, uniqueness, non-singularity, and linear models. *IEEE Transactions on Power Systems*, 2018.
- [235] Electric Power Research Institute. The open distribution system simulator (openss). <http://smartgrid.epri.com/SimulationTool.aspx>, 2018.
- [236] R Dungan, M. McGranaghan, S. Santoso, and H. Beaty. *Electrical Power Systems Quality*, chapter 2. MH Engineering, 1996.

- [237] J. Grainger and W. Stevenson. *Power System Analysis*, chapter 11. McGraw-Hill, 1994.
- [238] Ned Mohan. *Power Electronics: A First Course*. Wiley, 2012.
- [239] K. Nandha Kumar and K. J. Tseng. Efficiency evaluation of coordinated charging methods used for charging electric vehicles. In *IEEE PES Innovative Smart Grid Technologies Conference Europe*, pages 270–275, 2016.
- [240] IEEE Power and Energy Society. Distribution test feeders. <https://ewh.ieee.org/soc/pes/dsacom/testfeeders/>.
- [241] J. F. Franco, M. J. Rider, and R. Romero. A mixed-integer linear programming model for the electric vehicle charging coordination problem in unbalanced electrical distribution systems. *IEEE Transactions on Smart Grid*, 6(5):2200–2210, 2015.
- [242] Justine Sears, David Roberts, and Karen Glitman. A comparison of electric vehicle level 1 and level 2 charging efficiency. *SusTech*, 2014.
- [243] R Sevlian and R. Rajagopal. A Scaling Law for Short Term Load Forecasting on Varying Levels of Aggregation. *Science Direct*, 2017.
- [244] James W. Taylor, Lilian M. de Menezes, and Patrick E. McSharry. A comparison of univariate methods for forecasting electricity demand up to a day ahead. *International Journal of Forecasting*, 22(1):1 – 16, 2006.
- [245] W. A. Bukhsh and Ken McKinnon. Network data of real transmission networks. <https://www.maths.ed.ac.uk/optenergy/NetworkData/reducedGB/>, April 2013.
- [246] L. Thurner, A. Scheidler, F. Schäfer, J. Menke, J. Dollichon, F. Meier, S. Meinecke, and M. Braun. pandapower: An open-source python tool for convenient modeling, analysis, and optimization of electric power systems. *IEEE Transactions on Power Systems*, 33(6):6510–6521, Nov 2018.
- [247] Ofgem. Statutory security of supply report. Technical report, UK Department of Business, Energy, and Industrial Strategy, 2017.
- [248] Dave Croucher. Design and planning: Framework for underground networks in uk power networks. Technical report, UK Power Networks, 2011.
- [249] UK Govt. Department for Business, Energy & Industrial Strategy. Lsoa domestic electricity 2016. <https://www.gov.uk/government/statistics/lower-and-middle-super-output-areas-electricity-consumption>.
- [250] Elexon. Profile classes. <https://www.elexon.co.uk/operations-settlement/profiling/>.
- [251] Northern PowerGrid. Customer-led network revolution. <http://www.networkrevolution.co.uk/>, 2014.
- [252] British Standard Institute. Voltage characteristics of electricity supplied by public electricity networks, 2015.
- [253] Luis Ochoa. Dissemination document "low voltage networks models and low carbon technology profiles". Technical report, University of Manchester, 2015.
- [254] Fleet News. Ovo installs its first domestic vehicle-to-grid charger. <https://www.fleetnews.co.uk/news/fleet-industry-news/>, December 2018.

- [255] Murat Yilmaz and Philip T. Krein. Review of the impact of vehicle-to-grid technologies on distribution systems and utility interfaces, 2013.
- [256] Miguel A. Ortega-Vazquez. Optimal scheduling of electric vehicle charging and vehicle-to-grid services at household level including battery degradation and price uncertainty. *IET Generation, Transmission & Distribution*, 8(6):1007–1016, 2014.
- [257] Kotub Uddin, Tim Jackson, Widanalage D. Widanage, Gael Chouchelamane, Paul A. Jennings, and James Marco. On the possibility of extending the lifetime of lithium-ion batteries through optimal v2g facilitated by an integrated vehicle and smart-grid system. *Energy*, 133:710 – 722, 2017.
- [258] Anthony Barre, Benjamin Deguilhem, Sebastien Grolleau, Mathias Gerard, Frederic Suard, and Delphine Riu. A review on lithium-ion battery ageing mechanisms and estimations for automotive applications. *Journal of Power Sources*, 241:680 – 689, 2013.
- [259] IAECOM Building Engineering. Energy demand research project: Early smart meter trials, 2007-2010. UK Data Service.
- [260] Abdul Khalif and Israa Mousawi. Comparison of Heat Transfer Coefficients in Free and Forced Convection using Circular Annular Finned Tubes. *International Journal of Application or Innovation in Engineering & Management*, 5(4), 2016.
- [261] Electric Power Research Institute (EPRI). Hosting capacity feeders J1, K1, M1. [https://dpv.epri.com/feeder\\_models.html](https://dpv.epri.com/feeder_models.html), 2019. Accessed Apr. 19.